THE ROLE OF NRF2 ACTIVATION ON THE MURINE T CELL RESPONSE TO INFLUENZA INFECTION

By

Robert Arthur Freeborn, III

A DISSERTATION

Submitted to
Michigan State University
in partial fulfillment of the requirements
for the degree of

Pharmacology and Toxicology – Environmental Toxicology – Doctor of Philosophy

2020

ABSTRACT

THE ROLE OF NRF2 ACTIVATION ON THE MURINE T CELL RESPONSE TO INFLUENZA INFECTION

By

Robert Arthur Freeborn, III

Influenza infections cause millions of hospitalizations globally each year, resulting in hundreds of thousands of deaths and exacting a large toll on the economy. Accordingly, new interventions are highly desired including the elusive universal influenza vaccine capable of providing long-lasting immunity to all strains of influenza, including those which have not yet circulated in humans. It is vital to determine factors which suppress immunity to influenza infection and worsen host outcomes during infection. The food additive, *tert*-butylhydroquinone (tBHQ), was shown by our lab to modulate $CD4^+$ T cell activation and function in *ex vivo* analyses, in part by activating the stress-activated transcription factor, nuclear factor erythroid 2-related factor 2 (Nrf2). However, it was unknown if tBHQ hindered T cell function *in vivo*. To assess this, we fed mice diets with or without 0.0014% tBHQ and infected them with sublethal influenza A virus. Following primary infection, mice exposed to tBHQ had fewer $CD8^+$ T cells in the lungs, and these cells displayed a phenotype consistent with reduced effector function. Notably, these findings correlated with augmented viral RNA levels in the lungs. Following secondary infection with a heterosubtypic strain of influenza virus, mice on tBHQ-containing diets had exacerbated weight loss and delayed recovery compared to mice on control diets, indicating that tBHQ impaired heterosubtypic memory responses. It was further revealed that splenic memory T cell populations were diminished 28 days following primary infection in mice on the tBHQ diet, suggesting

failure to form a memory T cell population could be the cause for the diminished heterosubtypic immunity. To begin elucidating the molecular mechanism by which tBHQ suppressed the T cell response to influenza infection, two different models were utilized. The first model used adoptive transfer of wildtype or Nrf2-null T cells into T cell-deficient hosts prior to dietary exposure to tBHQ and infection with influenza virus. Interestingly, tBHQ had no effect on wildtype T cells in this model. However, this model demonstrated that Nrf2 in T cells contributes to influenza-associated morbidity, as mice with Nrf2-deficient T cells had reduced lung damage and ultimately lost less weight than their control counterparts. The other model exploited Cre/Lox technology to generate a conditional knockout mouse line with Nrf2-deficient T cells. In this model, the effects of tBHQ seen in wildtype mice during primary infection were shown to require Nrf2 in T cells. Additionally, this model also showed that mice with Nrf2-deficient T cells were protected from influenza-associated morbidity, though this only occurred in the presence of tBHQ. These studies collectively show that Nrf2 modulates the T cell response to influenza virus and contributes to host morbidity. Additionally, Nrf2 activation by tBHQ suppresses T cell responses to infection leading to failed memory responses. These are the first studies to investigate the role of tBHQ on T cell-mediated immunity *in vivo* in addition to interrogating the role of Nrf2 in T cell responses to influenza virus infection.

ACKNOWLEDGMENTS

I would like to thank Dr. Cheryl Rockwell for her professional and intellectual guidance during my time in her lab. She always kept my goals in mind as I continued my work and fostered my growth and independence to ensure I could succeed as an independent scientist. Also vital to my development were the members of my committee (Drs. Karen Liby, Jamie Bernard, and Elizabeth Gardner) as well as my unofficial mentor, Dr. James Luyendyk. This group of scientists ensured I thought broadly about my work and continuously challenged me to think bigger. I would also like to thank Drs. Joe Zagorski and Alex Turley who helped mentor me as I started in the lab and have continued to have fruitful discussions with me about the topics within this dissertation. Luca Kaiser, Allison Boss, Stephanie Brocke, and Dr. Yining Jin have all assisted in work within this dissertation, for which I will be forever grateful. In addition, Luca, Allison, and Stephanie have made late nights in the lab much more enjoyable with silly discussions and food deliveries. Most importantly, I have my family, friends, and girlfriend Jennifer Moore to thank for putting up with my insane schedule, lack of availability, and incessant talking about science. Without their support, I likely would have turned into a mad scientist, which while exciting, probably would not have been in my best interest.

TABLE OF CONTENTS

LIST OF TABLES

LIST OF FIGURES

KEY TO ABBREVIATIONS

15d-PGJ2 – 15-deoxy-$\Delta^{12,14}$-prostaglandin J_2

AAV – adeno-associated virus

ADI – allowable daily intake

AhR – aryl hydrocarbon receptor

APC – antigen-presenting cell

ARE – antioxidant response element

BALF – bronchoalveolar lavage fluid

BHT – butylated hydroxytoluene

bnAbs – broadly neutralizing antibodies

bZIP – basic leucine zipper

CM – central memory

CTL – cytotoxic T lymphocyte

DC – dendritic cell

DEM – diethyl maleate

dpi – day(s) post-infection

EFM – effector memory

ER – endoplasmic reticulum

FasL – Fas ligand

HA – Hemagglutinin

HMOX1 – heme oxygenase 1

HSPC – hematopoietic stem and progenitor cell

IAV – Influenza A Virus

IFN – interferon

IIV – inactivated influenza virus

IL – interleukin

LAIV – live attenuated influenza virus

M2 – Matrix protein 2

mLD_{50} – mouse lethal dose, 50%

MS – multiple sclerosis

MVA – Modified Vaccinia Ankara

NA – neuraminidase

NKT – natural killer T

NOAEL – no adverse effect level

NP – nucleoprotein

NRE – Nrf2-RPA1 element

Nrf2 – nuclear factor erythroid 2-related factor 2

OVA – ovalbumin

PA – acid polymerase

PB1 – basic polymerase 1

PB2 – basic polymerase 2

PGA1 – prostaglandin A_1

PGE2 – prostaglandin E_2

RNP – ribonucleoprotein

SFN – sulforaphane

tBHQ – *tert*-butylhydroquinone

TCDD – 2,3,7,8-tetrachlorodibenzo-*p*-dioxin

TCR – T cell receptor

T_{FH} – T follicular helper cell

T_H – helper T cell

TNFα – Tumor necrosis factor α

Treg – regulatory T cell

T_{RM} – resident memory T cell

CHAPTER 1

Literature Review

Influenza Virus

Background and Epidemiology

Influenza A Virus (IAV) is an enveloped, single-stranded RNA virus, which is made up of various proteins and a segmented negative-strand RNA genome.[1] Its genome encodes for numerous proteins, some with unknown function, but most of which aid in viral fusion and infection of host cells, genome replication, and virion release. Of particular importance to these processes are hemagglutinin (HA) which binds to sialic acid residues on the host cell membrane to begin the viral/host membrane fusion process; the proton pump Matrix protein 2 (M2), which leads to acidification of the endocytic vesicle containing the virus after initial binding of virus to host cell; acid polymerase (PA), basic polymerase 1 (PB1), and basic polymerase 2 (PB2), the virally encoded polymerases that contribute to viral genome replication; nucleoprotein (NP) which is an RNA-binding protein required for complete genome replication *in vivo*; and neuraminidase (NA), which similarly to HA, recognizes host sialic acid residues which it cleaves leading to the release of viral progeny from the host cell.[2–4]

IAVs are characterized by their hemagglutinin and neuraminidase residues, with there being 18 known HA subtypes and 11 known NA subtypes.[5–7] Importantly, only a distinct subset of these have been found to reliably cause human disease; HA 1, 2, and 3 and NA 1 and 2 are the primary types that infect humans, with other residues (i.e. H7N9, H5N1) only rarely causing human disease.[8] Following the pandemic of 2009, there have been two circulating strains: one H1N1 and one H3N2 virus. Each year, these circulating strains, in addition to influenza B, wreak havoc on both a national and

global level. Recent estimates suggest that up to 20% of the world's population gets infected annually, resulting in three to five million severe infections and roughly 400,000 respiratory deaths.[9–12] It should be noted that these numbers primarily correspond with high income countries, as disease diagnosis, surveillance, and reporting varies greatly country to country, resulting in a high degree of uncertainty how the viruses affect populations in middle-to-low income countries.[12,13] Other limitations to these estimates include underreporting of IAV infections due to not confirming the causative agent in patients with influenza-like illness and limiting mortality estimates to respiratory deaths. For instance, while the airway epithelium is the primary target of influenza viruses in mammals, the viruses also cause a considerable number of deaths due to causing or exacerbating cardiovascular events like heart failure and stroke, central nervous system disorders such as influenza-associated encephalitis, and musculoskeletal diseases – primarily rhabdomyolysis.[9]

One of the reasons influenza A viruses remain a persistent threat to society is the high frequency of mutations in the hemagglutinin residues on the circulating viruses. With hemagglutinin being a membrane spike protein, it is exposed to the extracellular environment and is thus targeted by host antibodies following infection. This exerts a selective pressure on the HA residues such that they undergo frequent mutation to evade the host immune response.[14] Consequently, the circulating IAV strains, currently H1 or H3 subtypes, can be drastically different at different times during the flu season; in fact, the amino acids within HA of a single subtype can vary extensively even within a single flu season.[15] This also makes current vaccine strategies difficult, as the currently

employed vaccine strategy aims to create sterile immunity by eliciting a host antibody response to predicted circulating strains.

Adaptive Immunity Against IAV

While cell types of the innate immune system are important in slowing early reproduction of the influenza A virus, viral clearance is ultimately attributed to an effective adaptive immune response in which both T and B cells play critical roles.[16,17] Cells of the adaptive immune response are unique because they launch highly specific attacks on the invading pathogen, resulting in effective clearance. More importantly, these cells develop memory to the pathogen so upon reinfection, a much more rapid and robust immune response can be launched.

Humoral Immunity to Primary Infection

B cells contribute to virus clearance through production of neutralizing antibodies. Primarily, these antibodies target HA and NA on the virus surface. In the context of primary IAV infection, three types of immunoglobulins are produced: IgM, IgG, and IgA; concentrations of these antibodies vary widely based on tissue distribution and day post-infection, with IgA being largely restricted to the upper airway and IgG and IgM being the dominant antibodies within the lung.[18] In serum, immunoglobulins spike at different days post infection (dpi), with IgM at day 7, IgG at day 14, and IgA at day 21; in the airways, the spikes in concentration are seen at day 8 (IgM), day 12 (IgG), and day 13 (IgA).[19] Notably, IAV infection is largely limited to the upper airway in humans and

thus IgA is thought to be the most critical antibody for viral neutralization during primary infection, and similar findings have been demonstrated in mice.[19–21]

Humoral Memory

B cells are also critical in developing memory against IAV so the virus can be rapidly eliminated following a subsequent infection. Often, memory responses are thought to be against the exact same pathogen as the first infection; however, because there are two circulating subtypes of IAV and HA residues mutate rapidly even within a single influenza season, the traditional memory response is rendered relatively ineffective. Instead, heterosubtypic immunity must be generated to provide the host with protection against subsequent infections. In humoral heterosubtypic immunity, antibodies are generated against epitopes that are conserved among many subtypes of the virus and are not prone to rapid mutation; unlike the antibodies that target the head region of HA, these broadly neutralizing antibodies (bnAbs) often target the conserved stem region of HA, but have also been found to target NP and NA .[22–26] Notably, recent evidence suggests that antibodies targeting the HA stem may contribute to a rise in viruses able to escape the antibodies.[27] B cells also produce non-neutralizing antibodies that contribute to heterosubtypic immunity by boosting the $CD8^+$ T cell memory response, discussed below.[17] Interestingly, there may be sex-differences in the humoral response leading to heterosubtypic immunity, as seen in mice in which females have higher antibody titers.[28]

Cell-mediated Immunity to Primary Infection

In conjunction with humoral immunity, the adaptive immune response also relies on cell-mediated immunity, or T cell-mediated immunity. In contrast to B cells, T cells do not produce antibodies. T cells are initially classified based on their T cell receptor (TCR) as either αβ T cells or γδ T cells. Currently, it is not thought that γδ T cells contribute much to the immune response to influenza, although emerging evidence suggests they may be important for protection that could potentially be exploited therapeutically, although this is still controversial.[29–32] The current dogma is that αβ T cells contribute more to immunity against IAV.

αβ T cells can be further divided into $CD4^+$ and $CD8^+$ T cells, also known as helper and cytotoxic T cells, respectively. As the names suggest, these two cell types play distinct roles in the immune response to influenza virus. The canonical role for $CD4^+$ T cells is orchestrating the immune response against IAV by secreting various cytokines; $CD8^+$ T cells, on the other hand, directly kill IAV-infected cells by triggering apoptosis through both the extrinsic and intrinsic pathways.[33]

Upon antigen presentation from antigen presenting cells (APCs), primarily dendritic cells, naïve $CD4^+$ T cells become activated and differentiate into effector subsets.[34] The cytokine environment during antigen presentation dictates which effector subset the naïve $CD4^+$ T cell becomes, with interleukin-12 (IL-12) and IFNγ programming T_H1 cells, IL-4 programming T_H2 cells, IL-6 and TGFβ programming T_H17 cells, and IL-6 and IL-21 programming T follicular helper (T_{FH}) cells.[34] In the context of influenza infections, these cell types have varying levels of importance. T_H1 cells respond to viral pathogens and also aid in anti-cancer immune responses.[35] T_H1 cells

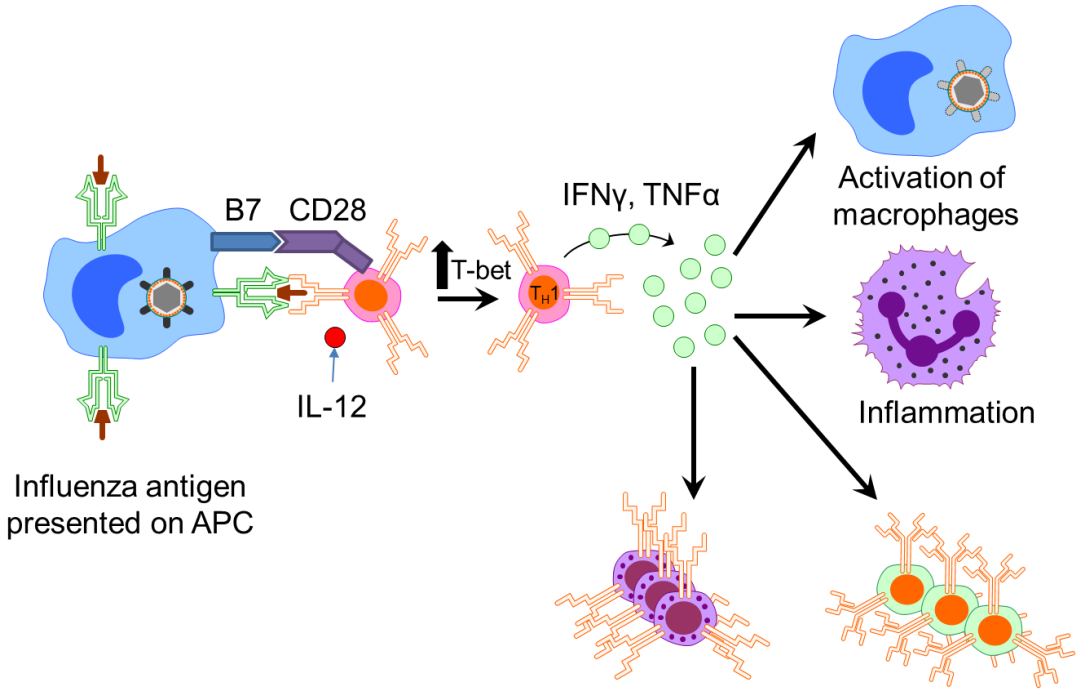

Figure 1: Schematic of helper CD4⁺ T cell function during influenza virus infection. Following presentation of virus-derived antigen to the CD4⁺ T cell by an antigen presenting cell, the T cell will then differentiate into a T_H1 cell. It will then secrete IFNγ and TNFα to induce anti-influenza immune responses by other immune cells. Figure created using illustrations from motifolio.com.

guide various parts of the immune system, both innate and adaptive, launching a concerted effort to clear the virus. They do this by secreting the cytokines IFNγ and tumor necrosis factor α (TNFα) which go on to cause immunoglobulin class-switching in B cells, classical activation of macrophages, generalized inflammatory responses, and stimulation of effector CD8⁺ T cells.[36–40] While T_H1 cells are the predominant CD4⁺ T cell in the response to IAV infection, emerging studies are revealing a role for T_H17 cells, however it is unclear whether their responses are beneficial or detrimental and this appears to differ largely with different experimental conditions.[41–44] One possible advantage of T_H17 cells during IAV infection is their protection against bacterial co-infections and secondary infections.[45] Contrary to T_H1 and T_H17 cells, T_H2 cells have

no documented beneficial role during IAV infection, and have in fact been shown to be detrimental to the host.[46]

While $CD4^+$ T cells coordinate the anti-influenza response amongst various cell types, $CD8^+$ T cells play an indispensable role in halting viral replication. Like $CD4^+$ T cells, $CD8^+$ T cells copiously secrete IFNγ.[47] However, the primary method $CD8^+$ T cells contribute to viral clearance is through triggering apoptosis within infected cells, and this occurs via two distinct pathways.[33] The first pathway $CD8^+$ T cells induce apoptosis is through signaling via the Fas/Fas-ligand (FasL) pathway. Upon $CD8^+$ T cell activation, cell surface expression of FasL is enhanced.[48] When the activated $CD8^+$ T cells reach the infected cells, FasL interacts with Fas expressed on the infected cells, which then leads to activation of caspases and apoptosis via the extrinsic pathway.[33,49] The other pathway by which $CD8^+$ T cells induce apoptosis is the release of granules containing cytolytic mediators, namely perforins and granzymes.[33,50] Production of these mediators begins in the draining lymph nodes during infection, when T cells become activated following antigen presentation; however, the vast majority of perforin/granzyme-containing $CD8^+$ T cells are found in the lungs.[51] In this method of killing, the aptly-named perforins perforate the infected cell's membrane by forming pores; following this, granzymes enter the cell and enter the mitochondria to trigger the intrinsic pathway for apoptosis.[52,53] Interestingly, both of these pathways appear to be sufficient to eliminate influenza-infected cells, as genetic ablation of Fas or perforin did not impact cytotoxicity of $CD8^+$ T cells.[33]

Two other types of $CD4^+$ T cells are important but often overlooked in the immune response to IAV infection: regulatory T cells (Tregs) and cytotoxic $CD4^+$ T

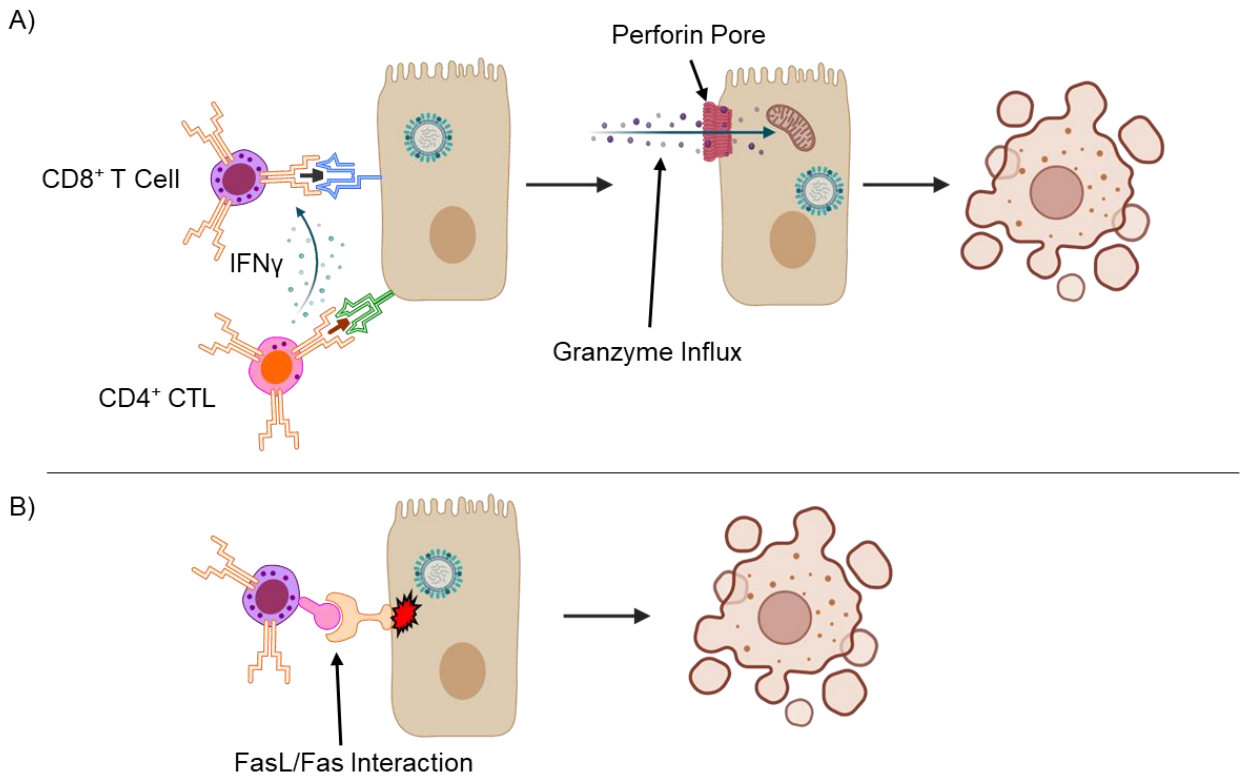

Figure 2: Schematic of cytotoxic T cell function. (A) Upon recognition of infected target cells through MHC/TCR interactions, cytotoxic $CD8^+$ and $CD4^+$ T cells release perforin to form a pore in the infected cell. Cytotoxic granules containing granzymes then enter the cell, triggering the intrinsic pathway of apoptosis. (B) $CD8^+$ T cells also kill infected cells through upregulation of FasL. The interaction between Fas on infected cells and FasL on the T cell result in downstream caspase activation and apoptosis. Created with motifolio.com and BioRender.com.

lymphocytes. Tregs serve many purposes during primary IAV infection. The most widely recognized role for these cells is limiting inflammation within the lungs and airways during infection. Various groups have shown that Treg numbers are enhanced in lungs and airways during IAV infection.[54–56] Other studies that utilized antibody depletion of Tregs, NOD2 receptor activation, and antigen-specific Treg adoptive transfer have shown that Tregs impair $CD4^+$ and $CD8^+$ T cell proliferation and effector

function in what appears to be antigen-dependent mechanisms.[54,55,57,58] While it was originally thought that Tregs didn't respond to virus-associated antigen and instead were activated by APCs presenting self-antigen associated with damage, influenza virus-pulsed dendritic cells were able to activate regulatory T cells *ex vivo*.[54] While Tregs are able to diminish the influenza-specific T cell population and limit immunopathology, their effects on viral clearance remain poorly characterized. One group recently found that depletion of Tregs at different stages of infection could result in enhanced or reduced viral titers, while Treg depletion for the entire course of infection augmented viral load.[59] Of note, this group used a genetic mouse model and diphtheria toxin to deplete Tregs, and it is possible that the diphtheria toxin had effects as controls were not implemented to detect toxin-specific effects. Another group found that antibody-mediated depletion of Tregs did not affect viral titer during infection, so it remains to be seen how Tregs ultimately affect antiviral immunity.[60] In addition to restricting immunopathology, Tregs aid in recovery and tissue regeneration which may have to do with their ability to prevent epithelial cell growth within the alveolar space following infection.[61–63] However, how Tregs promote recovery still remains a mystery.

An important but often overlooked cell type are the so-called cytotoxic $CD4^+$ T cells, or $CD4^+$ CTL, which were first described in 1985.[64] Since their discovery, these cells have been found *in situ* under various pathological conditions such as HIV, cytomegalovirus infection, rheumatoid arthritis, multiple sclerosis (MS), West Nile virus infection, gammaherpesvirus infection, melanoma, Dengue virus, and influenza virus.[64–73] Similar to $CD8^+$ T cells, these cells cause infected cells to undergo apoptosis primarily through IL-2-driven perforin-dependent mechanisms, and this has been

observed in both mice and humans.[73–77] Notably, these specialized $CD4^+$ CTLs are able to kill infected cells with similar potency, specificity, and kinetic profiles as $CD8^+$ CTLs, and adoptive transfer of perforin-deficient $CD4^+$ T cells reduces host survival to IAV infection compared to transfer of in-tact $CD4^+$ T cells.[73,78] Interestingly, the vast majority of these cells are found in the lungs, with little to no $CD4^+$ CTLs found in secondary lymphoid organs.[76,79,80] In contrast to $CD8^+$ T cells, cytotoxic $CD4^+$ T cells operate through MHC-II-restricted mechanisms similar to canonical $CD4^+$ T cells.[64,81] While dogma holds that MHC-II is typically only expressed on APCs, evidence suggests that influenza-infected epithelial cells within the airways and lung parenchyma express MHC-II, and $CD4^+$ CTLs have been found in close proximity to these MHC-II-expressing epithelial cells.[79] Moreover, MHC-II expression was upregulated in influenza-infected explanted human lung and primary bronchial epithelial cells.[74] Another whodunit is what factors drive the differentiation of these cells. Use of IFNAR1-null and IL2Rα-null mice revealed roles for both IFNα and IL-2 in promoting granzyme B and perforin expression in $CD4^+$ T cells, and these cytokines act synergistically in driving the differentiation of $CD4^+$ CTLs.[76,77] Additionally, numerous transcription factors have been implicated in the generation of these cells. Mice lacking STAT2 had a reduction in T-bet within lung $CD4^+$ T cells during IAV infection, and an associated loss of granzyme B production; moreover, cells from Tbx21-deficient mice (Tbx21 being the gene that encodes T-bet) had substantially lower granzyme B and perforin expression compared to wild-type counterparts.[76] Blimp-1 was also found to be crucial for the differentiation of these cells, and mice which received Blimp-1-deficient $CD4^+$ T cells responded as poorly to infection as mice which received no adoptive transfer; notably, Blimp-1 and T-bet act

synergistically, with Blimp-1 promoting the binding of T-bet to cytolytic genes to drive their transcription.[76] In addition to Blimp-1, Hobit – a homolog of Blimp-1 – has also been shown to be highly upregulated in $CD4^+$ CTLs.[82] Other proteins that seem to be associated with these cells, although unrelated to their differentiation, are class I-restricted T cell-associated molecule (CRTAM) and NKG2C/E.[80,83] Ultimately, these cells act as a complement to $CD8^+$ T cells; they are less abundant, but act in a very similar manner by secreting IFNγ and inducing apoptosis of infected cells.[79,83]

Cell-mediated Memory

Like with B cells, T cells develop memory to homologous and heterologous influenza viruses; this has been observed in numerous animal models as well as indirectly in humans.[74,84–92] It has been hotly debated whether B cells or T cells are more important for heterosubtypic immunity, with several lines of evidence supporting each cell type.[24,93] Interestingly, numerous reports demonstrated that $CD4^+$ T cells seem to be more vital in heterosubtypic responses than $CD8^+$ T cells; in these studies, genetic ablation or antibody depletion of $CD8^+$ T cells had minimal effects on host survival and viral clearance, but depletion of $CD4^+$ T cells during secondary challenge led to poor immunity against the virus.[25,94] One possible reason $CD8^+$ T cells could be dispensable for heterosubtypic immunity is the ability for $CD4^+$ CTLs to compensate for $CD8^+$ T cells, as has been demonstrated in several heterosubtypic models.[25,74] Additionally, several studies show that $CD4^+$ T cells are critical for the ability of $CD8^+$ T cells to form memory, and the $CD8^+$ T cell response to heterologous challenge is abrogated in the absence of $CD4^+$ T cells.[37,38,95–97] Other studies show that lack of

$CD8^+$ T cells results in failure to generate complete protection against heterologous challenge, further obfuscating the importance of each cell type in this enigma; instead, it seems likely that these cell types all cooperate to mediate protection, possibly in conjunction with the innate immune system.[98–102] Importantly, both $CD4^+$ and $CD8^+$ T cells recognize epitopes from internal influenza proteins – especially NP – which are highly conserved between subtypes, thus providing a strong rationale for why T cells provide heterosubtypic immunity.[74,88,90–92,103,104]

How T cells mediate rapid protection during heterologous challenge is a matter of great interest. As with primary infections, $CD8^+$ T cells mediate lysis of infected cells through perforin/granzyme and Fas/FasL interactions.[87,95] However, one thing that distinguishes the memory response of $CD8^+$ T cells from the primary response is the polyfunctional nature of the memory cells and their rapid production of IFNγ upon reinfection.[47,105] While IFNγ is not required for heterosubtypic immunity, mice lacking IFNγ have prolonged time to recovery, slightly reduced cytolytic function, and increased IgG1:IgG2a ratios.[106,107] Another interesting finding is that several subsets of memory $CD8^+$ T cells are able to protect the host without clonally expanding upon reinfection, unlike primary infections which require clonal expansion of influenza-specific $CD8^+$ T cells to provide protection.[47,108] One of the reasons for this is that following primary infection, a portion of the $CD8^+$ T cells become resident memory T cells (T_{RM}), and remain present in the lung parenchyma and airways after the contraction phase of the immune response.[109–113] T_{RM} cells are indispensable in defense against heterosubtypic infection, while central memory T cells in circulation seem to be expendable.[114] While it remains unclear how these cells arise, recent evidence suggests the importance of

chemokine signaling in recruiting memory cells to the lung parenchyma and airways.[115] Notably, the number of T_{RM} cells increases with repeated influenza exposures, and memory T cells appear to traffic to the lungs faster than non-memory T cells.[102,116] Moreover, memory T cells are more sensitive to antigenic stimuli and are critical for rapidly responding to heterosubtypic influenza infections.[115,117–120] As noted above, $CD8^+$ T cell memory cannot be formed without $CD4^+$ T cell help.[37,38] A recent study suggests that $CD4^+$ T cells help establish $CD8^+$ T cell memory through regulation of metabolic pathways, with unhelped $CD8^+$ T cells exhibiting phenotypes more similar to exhausted T cells.[97] This provides a likely mechanism by which $CD4^+$ T cells regulate formation of $CD8^+$ T cell memory, as $CD8^+$ T cells undergo metabolic shifts during memory formation in which they start as rapidly proliferating cells but transition to be slow-cycling once acquiring a memory phenotype.[121]

In addition to guiding formation of the memory $CD8^+$ T cell pool, $CD4^+$ T cells provide heterosubtypic immunity via several mechanisms, and a reduced $CD4^+$ T cell response enhances morbidity and mortality upon secondary challenge.[24,25] As mentioned above, B cells produce antibodies against conserved epitopes in the virus proteome, including NP. Depletion of $CD4^+$ T cells reduces antibody titers against these conserved residues, providing a key mechanism by which $CD4^+$ T cells mediate heterosubtypic immunity.[24,122] Memory $CD4^+$ T cells have also been shown to produce high amounts of IFNγ, which is known to be protective in heterosubtypic challenges.[91,96,123] Further evidence demonstrated that heterosubtypic immunity mediated by $CD4^+$ T cells is dependent on IFNγ production.[94] Memory $CD4^+$ T cells also rapidly accumulate in the lungs during infection to a greater degree than naïve

$CD4^+$ T cells, and memory $CD4^+$ T cell responses are enhanced with repeated antigen challenge.[86,94] In addition to the traditional helper roles of $CD4^+$ T cells, memory $CD4^+$ T cells have some cytotoxic capacity, however they primarily promote memory by synergizing with B cells and $CD8^+$ T cells.[98]

Little is known about the role of Tregs in the memory response to influenza. It appears that these cells are required for memory formation, however their activity can also limit memory formation and mechanisms are in place, such as IL-6 production, to limit the role of Tregs during memory formation.[124–127] Despite their suppressive role, evidence suggests that memory Tregs, which do respond in an antigen-specific manner, are necessary for preventing $CD8^+$ T cell-mediated immunopathology during secondary challenge.[56] More work ultimately needs to be completed to determine how Tregs influence memory formation without impairing the secondary immune response while also limiting immunopathology.

Therapeutics for Prevention and Treatment

FDA-Approved Pharmacological Agents

Anti-influenza agents target various proteins important to the viral life cycle. Among the first influenza-specific drugs to be used in the clinic are amantadine and rimantadine which inhibit M2, the virus' proton pump required for acidification leading to release of viral ribonucleoprotein (RNP) from M1.[128,129] However, many influenza viruses are resistant to this class of drugs, and these are no longer recommended for use as anti-influenza therapeutics.[130,131]

The next promising class of agents are neuraminidase inhibitors. These act by preventing release of newly-formed virions from cells, thus limiting the spread of the virus in the respiratory tract.[132] The FDA-approved NA inhibitors are oseltamivir, peramivir, and zanamivir.[133] These drugs have a favorable safety profile and can even be used in pregnant women.[134] Studies suggest that when administered within 48 hours of the onset of symptoms, these drugs can drastically shorten the duration infection, potentially up to 3 days.[135] However, this is problematic since only an estimated 52% of patients with influenza-like illness seek treatment.[136] Moreover, evidence continues to arise suggesting the emergence of resistant viral variants, although fortunately the proportion of resistant strains in circulation remains low.[132,137–140]

While the markets were dominated by M2 and NA inhibtors for decades, an anti-influenza drug with a novel target won FDA approval in 2018.[141] Baloxavir marboxil (Xofluza) is a novel drug targeting influenza PA.[142] This is another drug meant to be taken within 48 hours of symptom onset, but has increased antiviral potency compared to oseltamivir.[143] Baloxavir also showed prophylactic efficacy in a phase III clinical trial, in which household members (noninfected) took the drug prophylactically when someone in the house was confirmed to be influenza-infected: baloxavir treatment prevented 86% of infections compared to placebo.[144] Notably, there is evidence that baloxavir has broad-spectrum influenza activity, as it can provide protection against avian strains as well as seasonal strains, and may even protect against influenza B and C viruses.[145,146] However, resistant strains of the virus again arose, with an I38T

mutation in PA being the resistant mutation which does not alter fitness of the virus.[143,147–149]

Promising Experimental Therapeutics

In addition to the FDA-approved drugs, several novel therapeutics have been explored pre-clinically, some of which have begun early clinical trials. Many of these therapeutics target HA, but instead of targeting the mutation-prone globular head like endogenous antibodies do, these therapeutics target the conserved stem of HA. Broadly neutralizing antibodies (bnAbs) are one example of this type of therapeutic, and one example – VIR-2482 – is currently undergoing a phase 1/2 clinical trial to assess safety and efficacy in preventing influenza infection in healthy volunteers.[150–152] Notably, these have the potential to be used prophylactically, but may not be long-lived and would therefore require multiple administrations in a given flu season.[153] Another group produced a novel adeno-associated virus (AAV) vector delivering multidomain llama antibodies to the upper airway; this resulted in complete protection against multiple strains of influenza in mice even after 35 days of AAV vector delivery, suggesting this method produces bnAbs yielding potentially universal protection with enhanced longevity compared to normal bnAb infusion.[154] The same group also created cyclized peptides based on the antigen-binding region of bnAbs against group 1 HA molecules; the cyclized peptides were shown to have an IC_{50} in the high nanomolar range, but only provide protection against group 1 HA molecules and have a short half-life of 2.7 hours suggesting these could be used as an antiviral but provide no practical

prophylactic use.[155] In addition, they identified a small molecule capable of binding to the conserved HA stem which could provide insights to inform drug discovery efforts.[156]

In addition to binding the conserved HA stem, other novel methods are being investigated to develop therapeutics. A recent report demonstrated that influenza infection altered the metabolism of infected cells, and using a PI3K/mTOR inhibitor reverted these changes, promoted host survival, and reduced lung viral titers.[157] Perhaps the most promising therapeutic in development is EIDD-2801, which is orally available in cynomolgus macaques and prevented influenza infection *in vitro* and in ferrets.[158] Notably, this was shown to be more efficacious than prophylactic oseltamivir, works at low micromolar doses, and has a high barrier to resistance.[158] This compound received IND approval to begin clinical trials for the ongoing COVID-19 pandemic, as it has also been shown to be efficacious in preventing viral infection by SARS-CoV-2 in addition to other viruses like Ebola, chikungunya, and equine encephalitis.[159]

Vaccines

A large problem with the current pharmacologic interventions is that they require rapid use after onset of symptoms to be effective, and viral shedding can occur before symptoms show.[160] Additionally, influenza infections are frequently followed by secondary bacterial infections, likely due to alterations in epithelial layer integrity and alterations in receptor expression.[161] In the cases of severe infection, patient conditions can be worsened by cytokine storm.[162,163] Several strategies have been employed to curtail this immune response, but evidence of clinical efficacy is lacking with the exception of intravenous immunoglobulin treatment.[163] All of these problems can be

mitigated through prevention of influenza infection, for which the primary method is vaccination.

Currently, seasonal influenza vaccines are designed to trigger antibody production, specifically IgG, against predicted HA epitopes for circulating strains of IAV and consequently allowing for rapid elimination of IAV upon infection.[25,164,165] In the United States, inactivated influenza virus (IIV), recombinant hemagglutinin, and live attenuated influenza viruses (LAIV) are used for vaccination.[166] As the humoral response is largely generated against HA epitopes, the vaccine doses are standardized to HA content.[164,166] These vaccines are currently recommended for all people over the age of 6 months, including pregnant individuals (though the LAIV vaccine is not recommended for pregnant women) and the elderly.[166]

IIV vaccines contain a chemically inactivated virus which then gets disturbed with detergents to remove contaminants to reduce unwanted reactions.[164,167] These vaccines are either trivalent or quadrivalent, meaning they protect against H1N1, H3N2, and either one or two strains of influenza B virus – quadrivalent vaccines are more efficacious than trivalent vaccines in seasons when influenza B viruses are more active than normal.[168] IIV vaccines are currently given by route of intramuscular injection.[166] The only licensed recombinant HA vaccine is also quadrivalent and administered through intramuscular injection, but is produced from insect cells.[164,166] The currently licensed LAIV vaccine contains a cold-adapted virus which is able to infect the upper airways but cannot effectively replicate in warm environments; it is also quadrivalent, but administered intranasally as a mist.[164,166] IIV and LAIV vaccine candidates are grown in embryonated chicken eggs – or in one case, a mammalian cell line – which

allows for production of large quantities of virus to be produced, but introduces complications.[166] Production of influenza vaccines requires informed predictions on which strains will be in circulation during the upcoming influenza season, as these vaccines do not efficiently generate cross-protective immunity, although even in the cases of mismatching a small degree of protection is conferred.[169–172] Even when virus strains are correctly matched, propagation of the selected virus in embryonated chicken eggs can produce detrimental mutations within the HA molecule such that it no longer elicits an immune response against the epitopes on circulating strains, as was recently demonstrated.[173,174] These mutations are unlikely to develop when generating recombinant HA, which is a benefit for the recombinant HA vaccines which produce similar antibody responses to IIV vaccines.[173] Despite the fact that IIV vaccines generate a 4-fold increase in anti-HA antibody titers, the antibody responses generated are short-lived, and are only slightly longer with LAIV vaccines which are shorter than responses elicited to live virus.[175,176]

The Need for a Universal Vaccine

The need to generate new vaccines annually, the associated costs, the lack of efficacy, and the failure to induce long-lived immunity are all problems with current influenza vaccines. Therefore, there exists a need to develop a vaccine providing broad, long-lasting coverage among many – or ideally, all – influenza strains including those with pandemic potential. A notable pitfall of current vaccines is their inability to induce T cell responses against influenza virus, with the exception of the intranasal LAIV vaccine which can induce virus-specific T cells.[88,177] This difference could likely be

due to the route of administration since local immunization is important for generation of influenza-specific T cell memory, and IIV vaccines delivered intranasally in animal models and humans elicited influenza-specific T cells.[85,178–181] Expanding on this, a recent report suggests that lung-resident memory B cells are more effective than systemic B cells at eliciting a rapid antibody response following infection, and establishment of resident memory B cells requires antigen delivery to the lungs during vaccination.[182] These findings suggest intranasal influenza vaccinations could be critical in providing more diverse and long-lived immunity.

Currently, there are 683 reports on vaccines being developed for universal protection.[183] As of 2018, this number was 569, with only 73 having the potential to activate T cells.[184] Using the same criteria to identify T cell-activating vaccines (live attenuated, live Modified Vaccinia Ankara (MVA)-vectored, simian adenovirus vectored, virus-like particle, DNA vaccine, live adenovirus vectored, non-replicating adenovirus vectored, or T cell peptide based) suggests only 83 of the current studies involve potentially T cell-activating vaccines. Of these, 52 are for phase 1 or phase 1/2 clinical trials, 18 are for phase 2 or phase 2/3 clinical trials, one is for a phase 3 clinical trial, and 12 are for phase 4 clinical trials (all of these were LAIV vaccines for the 2009 pandemic and completed between 2010-2011).[183]

While some of the vaccines and novel vaccine strategies being tested may be effective in eliciting broad protection against influenza viruses through both humoral and cell-mediated immune responses, other challenges still exist for developing a universal vaccine to provide life-long immunity.[119,185–187] Similar to how antibody responses against seasonal influenza vaccines are short-lived, evidence from animal studies

suggests that the longevity of lung-resident memory T cells – paramount to the rapid protection desired for heterosubtypic immunity – may also be severely limited.[114,120,188] Conversely, T_{RM} restricted to the nasal passages in mice are long-lived compared to their lung-resident counterparts; if consistent in humans, this cell population could be a critical target for vaccine development as influenza is largely limited to the upper respiratory tract in humans, compared to the lower respiratory tract in mice.[189] However, there is limited evidence on the longevity of lung T_{RM} cells in humans; some studies have been done on the longevity of memory T cells in general, but not on resident memory T cells.[190,191]

Ultimately, generating a universal vaccine to provide life-long protection against all influenza strains, including those of pandemic potential, is the holy grail of the influenza world. To come up with such a vaccine, many hurdles must be overcome including how to generate the humoral and cell-mediated responses necessary to protect against all strains and how to prevent waning of these responses, if possible.

Nrf2

Discovery of Nrf2

Nuclear factor erythroid 2-related factor 2 (Nrf2) is a basic leucine zipper (bZIP) Cap'n'collar (CNC) stress-activated transcription factor that was discovered in 1994.[192] Nrf2 is ubiquitously expressed in various tissues and highly conserved among various animal species.[192–194] While ubiquitous, the total amounts of Nrf2 and its repressor protein, Kelch ECH-associated protein 1 (Keap1), as well as the ratio between the two, varies among cell types.[195] Though Nrf2 was originally discovered binding to the locus

control region of β-globin, the first use of Nrf2-null mice demonstrated that Nrf2 was not essential for erythropoiesis, nor was it essential for growth or development of mice.[193] Nrf2 canonically acts by heterodimerizing with small Maf proteins and subsequently upregulating NQO1 and other phase II detoxifying enzymes' expression through the antioxidant response element (ARE) – a *cis*-acting element with the sequence "TGACnnnGC" in the regulatory region of various stress-responsive genes.[196–203] Nrf2 has also been shown to heterodimerize with Jun proteins to upregulate ARE-dependent genes.[204] Several polymorphisms of the Nrf2 gene have been reported in humans.[205]

Structure and Regulation of Nrf2

Nrf2 contains six evolutionarily conserved regions that have been termed Neh1-Neh6.[206] Under homeostatic conditions, Nrf2 is tethered to the actin cytoskeleton by its repressor protein, Kelch ECH-associated protein 1 (Keap1).[206] The interaction between dimerized Keap1 and the N-terminal Neh2 region of Nrf2 results in degradation of Nrf2 via the 26S proteasome, as Keap1 acts as an adaptor for the E3 ubiquitin ligase.[207–212] In the presence of oxidative and/or electrophilic stress, Nrf2 becomes activated and induces transcription of cytoprotective genes.[213] Many chemical inducers of Nrf2 modulate one of various cysteine residues on Keap1.[214] Through these modifications, Nrf2 may either dissociate from Keap1 and travel to the nucleus, or Nrf2 will remain bound but in an altered configuration no longer conducive for proteasomal degradation thus allowing *de novo* synthesized Nrf2 to accumulate in the nucleus; this altered state is referred to as the hinge-latch hypothesis.[215,216] Another similar model showed that Keap1 undergoes a conformational change upon modification with Nrf2 activators, thus

uncoupling Keap1/Nrf2 from the ubiquitination complex, allowing newly synthesized Nrf2 to evade proteasomal degradation.[217] In addition to Nrf2 activation by oxidative and electrophilic stress, it was shown that p62 could induce ARE activity through nuclear accumulation of Nrf2.[218] Further studies revealed that p62-mediated induction of Nrf2 occurs as a result of autophagy deficiency in which p62 forms aggregates with Keap1 to prevent Nrf2 ubiquitination.[219–221] Furthermore, free Nrf2 binds to an ARE within the p62 promoter to create a positive feedback loop of Nrf2 activation to resolve oxidative stress.[222] This has also been shown to occur following TLR agonism with various ligands.[223,224]

Post-translational modifications have also been shown to drive ARE-mediated transcription. In one instance, protein kinase C (PKC) phosphorylates Nrf2 at S40 which results in poor interaction between Keap1 and Nrf2.[225,226] Casein kinase 2 has also been shown to phosphorylate Nrf2 within the Neh4 and Neh5 domains contributing to *tert*-butylhydroquinone-mediated Nrf2 activation.[227] Further phosphorylation of Nrf2 by casein kinase 2 has also been postulated to facilitate degradation of Nrf2.[228] Nrf2 is similarly activated following phosphorylation by PERK with involvement of AMPK under conditions of endoplasmic reticulum (ER) stress.[229,230] Acetylation/deacetylation of Nrf2 has also been shown to be important, as deacetylation of Nrf2 was also shown to reduce its activity as a transcription factor.[231]

In addition to Keap1-facilitated degradation of Nrf2, a redox-insensitive pathway for Nrf2 degradation was also identified, dependent on the Neh6 domain of Nrf2.[210] The degron within Neh6 was shown to be essential for efficient turnover of Nrf2 in oxidatively stressed cells. It was later discovered that GSK-3β phosphorylates serine residues

within the Neh6 degron to facilitate binding of β-TrCP.[232,233] This leads to subsequent ubiquitination and degradation of Nrf2. Notably, this pathway for degradation can be suppressed by Nrf2 activators via PI3K-Akt-mediated phosphorylation of GSK-3β.[234]

The C-terminal Neh3 domain was shown to be important for transcriptional activity following Nrf2 binding; deletion of the C-terminal 16 amino acids within Neh3 of Nrf2 yielded a protein which still heterodimerized with small Maf proteins and bound to the ARE, but failed to induce Nrf2 target genes, possibly due to failure to interact with transcriptional machinery.[235] The conserved Neh4 and Neh5 domains have also been found to be important in driving transcription by serving as transactivators via synergistic cooperative binding to CREB binding protein.[236] It was later shown that this interaction results in the acetylation of Nrf2 by CREB binding protein which enhances the DNA binding ability of Nrf2, though this appears to be dependent on the particular ARE, as DNA binding was not enhanced within the heme oxygenase 1 (HMOX1) gene.[231,237]

Beyond the canonical pathways for Nrf2 activation and degradation, numerous proteins are emerging as novel regulators of Nrf2. Jun dimerization protein 2 interaction with Nrf2/Maf heterodimers was shown to be critical to mediate ARE-driven gene expression and resolve oxidative insults.[238] Poly(ADP-riboe) polymerase-1 has also been shown to enhance Nrf2 binding to the ARE by binding MafG and the ARE, thus facilitating favorable conditions for Nrf2 binding to the ARE.[239] During hypoxia, Nrf2 was shown to be suppressed independently of Keap1 through binding with the hypoxia-induced protein, seven in absentia homolog 2.[240] Another protein, WDR23, facilitates Nrf2 degradation in a similar manner as Keap1 but occurs in the absence of Keap1 including in species completely lacking Keap1.[241] The oncogene RAC3 was also shown

to interact with Neh4/Neh5 to induce ARE-mediated gene expression.[242] The Golgi apparatus-associated protein, PAQR3, has also been shown to facilitate degradation of Nrf2 by promoting the interaction of Nrf2 and Keap1.[243] Hrd1 was identified in cirrhotic human liver and confirmed using a liver cirrhosis model in wildtype, Nrf2-null mice, and conditional Hrd1-null mice.[244] Hrd1 was found to bind the Neh4/Neh5 domains of Nrf2. In addition to ubiquitination, Nrf2 can also be degraded via SUMOylation in a Keap1-independent process.[245] In this process, nuclear Nrf2 gets poly-SUMOylated and then polyubiquitinated by RING finger protein 4. While this pathway of degradation has not been thoroughly explored, recent evidence suggests some viral infections can reduce Nrf2 stores via SUMOylation.[246]

Nrf2 Activators

Heavy metals such as cadmium and arsenic, reactive electrophiles such as diethyl maleate (DEM) and *tert*-butylhydroquinone (tBHQ), endogenous ligands such as prostaglandins, and other xenobiotics activate Nrf2 through various mechanisms.[247] These different activators can be grouped into various classes based on their mechanism of activation, such as inducing oxidative stress, modifying reactive cysteines within Keap1, or facilitating phosphorylation of Nrf2.[248,249] Arsenic was shown to cause a robust and durable induction of Nrf2 and downstream target genes in various cell types in a manner partially dependent on the production of H_2O_2.[213,250–252] It was further shown that, unlike other metals that act independently of the reactive cysteine sensors on Keap1, Nrf2 activation by arsenic requires the presence of C151, C273, and C288 in Keap1.[249] Like arsenic, reactive electrophiles including the widely used Nrf2

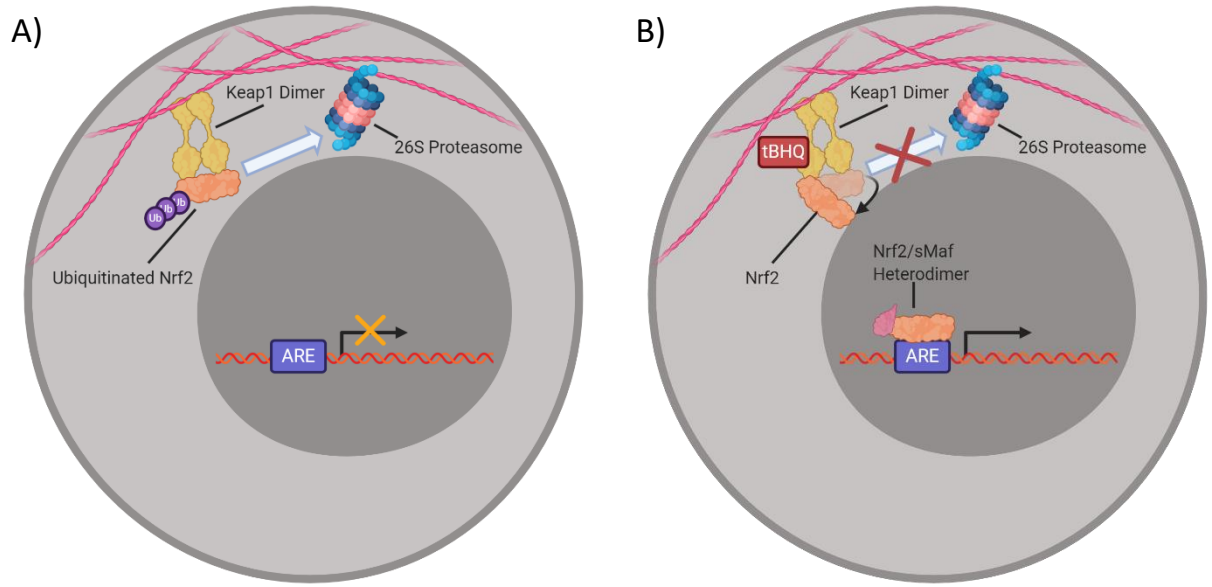

Figure 3: Schematic of Nrf2 activation by *tert*-butylhydroquinone (tBHQ). (A) Under basal conditions, Nrf2 is tethered in the cytosol by the repressor protein Keap1. This interaction results in polyubiquitination of Nrf2 and subsequent degradation via the 26S proteasome. (B) Following the introduction of cell stress, such as electrophilic stress caused by tBHQ, the association between Nrf2 and Keap1 is altered such that Nrf2 is no longer ubiquitinated. This allows newly synthesized Nrf2 to accumulate in the nucleus where it heterodimerizes with small Maf (sMaf) proteins to drive ARE-mediated transcription of target genes. Created with BioRender.com.

activators tBHQ, DEM, sulforaphane (SFN), and triterpenoids are known to interact with reactive cysteine residues on Keap1, such as C151.[248] Notably, it was shown that hydroquinones, including tBHQ, require *in-situ* copper-mediated oxidation to interact with this cysteine residue and exert biological activity.[253] In addition to modifying C151 on Keap1, tBHQ has also been shown to activate Nrf2 through inducing mitochondrial stress.[254]

In macrophages, 15-deoxy-$\Delta^{12,14}$-prostaglandin J_2 (15d-PGJ2) was shown to be an endogenous Nrf2 activator by modifying C288 within Keap1.[249,255] In peritoneal macrophages, low micromolar concentrations of exogenous 15d-PGJ2 activated Nrf2 target genes in wild-type but not Nrf2-null cells. Exogenous prostaglandin A_1 (PGA1),

but not prostaglandin E_2, was also shown to induce nuclearization of Nrf2. Nrf2-null mice also had persistent inflammatory immune cells in carrageenan-induced pleurisy in which 15d-PGJ2 is highly upregulated during the resolution phase, suggesting a potential role of Nrf2 in mediating the anti-inflammatory effects of 15d-PGJ2. In addition to anti-inflammatory prostaglandins, it was also recently demonstrated that Keap1 could sense endogenous Zn^{2+} – proposed to be released by damaged proteins within a cell – and thus undergo a conformational change preventing the degradation of Nrf2.[256]

Importantly, the longevity and sensitivity of the Nrf2/antioxidant response following chemical activation has not been well characterized. Many questions exist about whether recurrent exposure to Nrf2 activators led to altered antioxidant responses due to increased metabolism of the xenobiotic(s), desensitization of the pathway, or some other mechanism. One study in astrocytes revealed that heme oxygenase 1 protein levels peaked twelve hours after the removal of SFN from the culture media.[257] Notably, this study also showed that constant SFN exposure led to drastically higher HMOX1 protein levels, but mRNA expression peaked after twelve hours of stimulation. In contrast to HMOX1, four hours of SFN treatment led to increased NQO1 protein expression that continued to increase for at least 44 hours following removal of SFN from the culture media, suggesting some Nrf2 target genes might have long-lived induction following Nrf2 activation. Perhaps most interesting from this study was the finding that HMOX1 protein was not inducible following daily stimulation with SFN; a single administration of SFN resulted in increased HMOX1 production, but as few as 2 stimulations of 4 hours per day resulted in no HMOX1 upregulation at the protein level, despite being upregulated at the transcript level. This was not the case for NQO1 which

accumulated with repeated SFN treatments. Another study using a similar treatment scheme (one four hour treatment or three days with four hour SFN exposure per day) in human fibroblasts showed that repeated SFN exposure induces Nrf2 target gene expression and protects the cells against ionizing radiation in a Nrf2-dependent manner.[258] These studies provide some insight that the antioxidant response is dynamically regulated and is capable of reshaping following multiple exposures to a single Nrf2 activator. Another study demonstrated that chronic exposure (5 hrs/day for 3 days/week for 10 weeks) to nanoparticulate matter resulted in upregulation of Nrf2 mRNA and downstream target genes in cerebellum, liver, and lung, but this did not occur in aged mice.[259] This was likely due to increased c-Myc and Bach1, another CNC transcription factor, suppressing ARE-driven gene expression in the aged mice. A more recent study examined the dynamics of repeat exposure of reporter HepG2 cells to the two electrophilic compounds, DEM and tBHQ.[260] This study revealed that in each case, repeated exposure to the xenobiotics led to a reduced number of cells devoted to the Nrf2 activation pathway, and the cells which showed activated Nrf2 remained activated for a shorter time compared to the original exposure. However, the downstream response seemed to be poised to be more sensitive to toxic insult, as a reduced number of cells activating Nrf2 still led to a heightened induction of the Nrf2 target gene, sulfiredoxin 1. Ultimately, many questions remain about the duration and magnitude of Nrf2-mediated gene induction following continued exposure to reactive xenobiotics, especially in the context of *in vivo* exposures where compounds are actively metabolized and excreted.

Direct Evidence of Nrf2 as a Transcriptional Repressor

While Nrf2 is typically thought of as a transcriptional activator, new lines of evidence suggest that Nrf2 can directly repress genes through multiple distinct mechanisms. One example of this was shown in macrophages in which Nrf2 bound directly to the promoters of IL-6 and IL-1β and prevented binding of RNA polymerase II.[261] Another recent study utilizing wildtype and Nrf2-null A549 cells identified an inhibitory motif located adjacent to the ARE in 55 genes; this was termed the NRE, or Nrf2-RPA1 element.[262] It was demonstrated that the protein RPA1 was capable of binding to Nrf2 within the Neh1 region and consequently prevented Nrf2 heterodimerization with small Maf proteins. As a proof-of-concept of Nrf2/RPA1-mediated gene repression, MYLK – the gene encoding non-muscle myosin light chain kinase – was targeted in the lung. Nrf2 and RPA1 were shown to bind the NRE within the MYLK promoter to suppress nmMLCK expression in A549 cells. Furthermore, using mice lacking Nrf2, MYLK, both, or neither, it was shown that Nrf2 suppressed MYLK gene expression and prevented lung injury and inflammation in an acute lung injury model, suggesting Nrf2/RPA1-mediated gene suppression occurs *in vivo*. Several other genes were also verified to be inhibited through an NRE. Emerging studies continue to build evidence that Nrf2 can bind genes with AREs in their promoters but repress instead of drive transcription, though at this point the breadth of Nrf2-mediated gene repression remains largely uncharacterized.[263–265]

Crosstalk Between Nrf2 and Other Notable Pathways

The Nrf2 pathway has significant overlap with many other pathways related to xenobiotic metabolism and cell stress. For instance, the potent aryl hydrocarbon receptor (AhR) ligand, 2,3,7,8-tetrachlorodibenzo-p-dioxin (TCDD), was shown to induce the Nrf2 target gene, NQO1, in a Nrf2-dependent manner.[266] Moreover, the induction of NQO1 by TCDD also required Arnt and AhR. While this was not true for induction of NQO1 by tBHQ, it suggests that in some instances Nrf2 coordinates with other transcriptional activators to induce downstream targets. Nrf2 has also been shown to interact with NFκB and AP-1 family members. Various members of each protein family are differentially regulated in fibroblasts lacking Nrf2.[267] Additionally, Nrf2 was shown to induce rat glutamate-cysteine ligase catalytic subunit expression indirectly through the regulation of c-Jun, c-Fos, and Fra-1. Another study similarly showed that Nrf2 and c-Jun heterodimerized to induce ARE-driven expression of NQO1.[204] In the absence of Fra1, Nrf2 has an extended half-life and readily accumulates in the nucleus in response to oxidants.[268] Nrf2, NFκB, and AP-1 also have overlap in gene regulation independent from each other; under various cell stresses, each of these transcription factors can regulate expression of HMOX1 without relying on interactions with the other transcription factors.[269] In contrast with their ability to interact to drive gene expression, Nrf2 and NFκB have also been shown to repress one another's expression.[270] Notably, the crosstalk between these various pathways often depends on the type of cell stress driving the stress response.[271] Additionally, it was shown that c-Myc formed complexes with Nrf2 and phosphorylated c-Jun which destabilizes Nrf2 and dampens ARE-mediated gene expression.[272]

Effects of Nrf2 in Immune Cell Populations

Hematopoietic Stem and Progenitor Cells

Nrf2 regulates hematopoietic stem and progenitor cell (HSPC) populations. Nrf2-null mice possessed elevated common myeloid progenitor, granulocyte-macrophage progenitor, megakaryocyte-erythroid progenitor, lymphoid-primed multipotent progenitor, and common lymphoid progenitor populations within the bone marrow.[273] This study also revealed that HSPCs lacking Nrf2 proliferated and differentiated into T cells more rapidly than wildtype cells *in vitro*, but hyperproliferation was not observed following bone marrow transplantation suggesting Nrf2 can extrinsically suppress the proliferation of Nrf2-deficient HSPCs. Notably, Nrf2 was shown to maintain quiescence and self-renewal of the HSPCs by preventing cells from entering the G1 phase of the cell cycle. It was also revealed that Nrf2-null cells have impaired homing to the bone marrow, evidenced by increased HSPC populations within spleens in Nrf2-null mice and a reduction in bone marrow engraftment with Nrf2-null bone marrow due to diminished CXCR4 expression on the HSPCs. A follow-up study showed that Nrf2 mRNA was highly expressed in granulocytes and monocytes and was only lowly expressed in B cells.[274] Genetic activation of Nrf2 by conditional knockout of Keap1 in bone marrow cells led to an increased proportion of monocytes and granulocytes in the bone marrow with concurrent reductions in the proportions of erythrocytes, B cells, and T cells. Tracing these changes upstream revealed the percentage of granulocyte-monocyte progenitor cells was similarly increased within the bone marrow.

Macrophages

Nrf2 activates antioxidant genes in macrophages and Nrf2-null macrophages are more sensitive to cell stress due to reduced antioxidant gene expression.[213,275] TLR4 agonism with LPS activates Nrf2 in a manner dependent on MyD88 signaling with and without the involvement of ROS.[223,276] Bone marrow transplant of Nrf2-deficient bone marrow into LDLR-null mice on a high-fat diet results in increased atherosclerotic vessel injury associated with an inflammatory macrophage phenotype.[277] In a co-culture system of wildtype or Nrf2-null bone marrow-derived macrophages with OT-I $CD8^+$ T cells, it was found that Nrf2-null macrophages had increased expression of co-stimulatory molecules CD80 and CD86.[278] However, the Nrf2-null macrophages failed to activate the antigen-specific T cells as evidenced by reduced proliferation, surface expression of CD25 and CD69, and intracellular perforin and granzyme B within the T cells. It was found that this was due to impaired cysteine export by the macrophages which is needed in the early stages of T cell activation. Nrf2 activation and resolution of oxidative stress has also been shown to enhance phagocytosis of bacteria by macrophages.[279–281]

Dendritic Cells

Nrf2-null bone marrow-derived dendritic cells (DCs) have enhanced expression of MHC-II and CD86 compared to wildtype dendritic cells.[282,283] The DCs also have a more pro-inflammatory response to ambient particulate matter compared to wildtype DCs, which was partially ameliorated with NAC. In a DC/OT-II coculture system, ovalbumin (OVA) treatment led to higher IL-13 and IL-5 production and moderate

increases in IL-12p70 and IFNγ production with Nrf2-null DCs than WT DCs. Endocytic activity was reduced in particulate-matter-exposed Nrf2-deficient DCs. For these studies, DCs were from CD1:ICR mice (T_H2-biased). Nrf2-null dendritic cells were also more sensitive to ultrafine particles as an adjuvant to OVA-induced airway allergy.[284] In similar experiments using wildtype or Nrf2-null bone marrow-derived DCs, it was shown that Ragweed extract induced oxidative stress in Nrf2-deficient dendritic cells but not wildtype dendritic cells.[285] NAC reduced expression of CD80 and MHC-II in wildtype but not Nrf2-null Ragweed extract-exposed DCs, and CD86 in both genotypes. Nrf2-null bone marrow-derived DCs and lung DCs exposed to Ragweed extract produced substantially more IL-6 and TNFα compared to wildtype DCs. Nrf2-null bone marrow-derived DCs also produced more IL-12 in response to Ragweed extract or LPS stimulation, but Ragweed extract reduced IL-12 production in wildtype DCs. Similarly, IL-12 production was suppressed by arsenic in a Nrf2-dependent manner in human dendritic cells.[286] In contrast to Nrf2-null macrophages which failed to induce antigen-specific T cell activation, human dendritic cells with siRNA-mediated knockdown of Nrf2 were shown to induce stronger T cell responses to tumor-conditioned media, evidenced by enhanced T cell proliferation, IFNγ secretion, and target cell lysis by T cells in a co-culture system.[287] Nrf2-null bone marrow-derived DCs were also shown to proliferate more in response to antigen and cause a robust $IFN\gamma^+$ $CD8^+$ T cell response.[283] Histone deacetylase activity was required for these effects in Nrf2-null DCs. Notably, LPS-stimulated Nrf2-null dendritic cells were also shown to produce more IFNγ than wildtype dendritic cells.[288] In this instance, expression of TNFα, IFNγ, and IL-12 was reduced in a Nrf2-dependent manner with the triterpenoid CDDO-DFPA while IL-10

expression was conversely augmented by CDDO-DFPA. Expanding on previous findings, this study also revealed that pharmacological activation of Nrf2 maintained dendritic cells in a tolerogenic state by enhancing their use of oxidative phosphorylation as an energy source, while Nrf2-null dendritic cells completely shifted away from oxidative phosphorylation.

Natural Killer Cells and Natural Killer T Cells

The role of Nrf2 activation on natural killer (NK) cells is largely unknown. One study demonstrated that topical tBHQ treatment of Rag2-knockout mice impaired tumor growth and this was associated with increased NK cell infiltration in the tumors.[289] This effect was diminished in the absence of Nrf2. Notably, this study showed that Nrf2 drove IL-17D expression, and knockout of IL-17D in tumors also failed to elicit an NK cell response. While a Nrf2-dependence wasn't shown in the context of viral infection, tBHQ did enhance Nrf2 expression and IL-17D expression in response to vaccinia virus scarification, and a follow-up study revealed that the NK cell response to cytomegalovirus infection was abrogated in the absence of Nrf2.[290] Conversely, treatment of murine splenocytes with tBHQ showed reduced activation and cytotoxic potential within the NK cell population.[291] Ultimately, more studies are warranted to determine the role of Nrf2 in NK cells. In NK/T cells which basally have high ROS, it was shown that constitutive Nrf2 activity altered the metabolism, proliferation, maturation, and death of NK/T cells; these effects were rescued with knockout of Nrf2.[292]

B Cells

Like NK cells, B cells are largely understudied in the context of Nrf2. A recent study from our lab demonstrated that tBHQ impaired murine B cell activation but increased IgM production in a Nrf2-dependent manner.[293] During *in vivo* infection with *Haemophilus influenzae*, higher antigen-specific IgG titers were found in Nrf2-null mice, suggesting humoral immunity was enhanced in the absence of Nrf2.[294] More evidence is still needed to clarify the role of Nrf2 in B cell development and function.

T Cells

Over the past ten years, several groups have been investigating the role of Nrf2 in murine and human T cells. One group demonstrated that T cells in Nrf2-null mice were skewed toward an inflammatory T_H2 subtype within the lungs following bleomycin-induced pulmonary fibrosis.[295] In stark contrast, analysis of wildtype and Nrf2-null T cells *ex vivo* showed that activation of Nrf2 promoted a T_H2 immune response, and Nrf2-null T cells exhibited T_H1 phenotypes.[296] In this study, Nrf2 activation was shown to induce Gata3 DNA binding activity while reducing T-bet DNA binding activity. Similarly, it was shown in 3T3-L1 adipocytes that Nrf2 activation with SFN substantially upregulated Gata3 mRNA expression.[297] In addition to the *ex vivo* results, similar findings were also observed *in vivo* in mice with T cell-specific constitutive Nrf2 activity, in which Nrf2 activity suppressed the proportion of $IFN\gamma^+$ and $TNF\alpha^+$ $CD4^+$ T cells.[298] These mice also had an increase in the percentage of $FoxP3^+$ Tregs and IL-17-producing T cells following ischemia-reperfusion injury in kidneys. These results suggest that Nrf2 is capable of altering helper T cell populations even outside the

context of an immune response. In unstimulated primary human $CD4^+$ T cells which had Keap1 knocked down via CRISPR/Cas9 gene editing, a significant reduction in IL-17^+ cells was observed.[299] When Keap1 was knocked down specifically in regulatory T cells, CD69 and IL-10 were significantly upregulated, suggesting Nrf2 may promote the rise of immunosuppressive T cells. Notably, this study did not utilize naïve T cells prior to assessing cytokines indicative of helper T cell subtypes, so the role of Nrf2 on human T cell differentiation remains unknown. In addition to the potential role of Nrf2 on $CD4^+$ T cell differentiation, Nrf2 activation with tBHQ and the triterpenoid CDDO-Im was shown to impair activation of Jurkat T cells, and this was at least partially dependent on Nrf2.[300] tBHQ was also shown to impair primary human $CD4^+$ T cell activation, although this has not been shown to require Nrf2.[301] Interestingly, mice heterozygous for Keap1 deletion within $FoxP3^+$ cells, and thus increased basal Nrf2 activation within these cells, had reduced Treg populations.[302] Furthermore, mice harboring this mutation had a reduced number of naïve T cells within the spleen with compensatory increases in $CD4^+$ T cells with effector/memory and central memory phenotypes. These mice also had dysregulated inflammatory T cell responses in the lung and liver in the absence of infection, suggesting Nrf2 overexpression limited to regulatory T cells can drive autoimmunity.

Pathologies Associated with Nrf2 Polymorphisms in Humans

Two polymorphisms (-617 C/A and -617 A/A) in humans were shown to reduce Nrf2 gene expression and are associated with increased risk of acute lung injury and non-small-cell lung cancers, respectively.[303,304] Another single nucleotide polymorphism

(-653 G/A) was studied in cohort of Mexican children with systemic lupus erythematosus (SLE).[305] It was found that while the polymorphism did not increase the risk of developing SLE, it did increase the odds of female patients developing SLE-associated nephritis. Conversely, four human patients were also recently described with gain-of-function mutations found within the Nrf2 gene allowing constitutive Nrf2 activity.[306] These patients (aged 1.8-14 years old) had dystrophy, mild developmental delay, learning disabilities, and recurring lung and skin infections. Three of the four patients had reduced IgA, IgM, and IgG antibody titers in addition to a reduction in class-switched memory B cells. These patients also failed to produce positive antibody responses to pneumococcal vaccine, suggesting hyperactive Nrf2 impairs the formation of lasting immunity to pathogens. Ultimately, these studies reveal the importance of Nrf2 in maintaining cellular homeostasis and that perturbations of this system, whether positive or negative, can lead to severe clinical outcomes.

Nrf2 in Autoimmunity

When Nrf2-null mice were developed, it was noted that the females were prone to developing autoimmune-like pathologies leading to premature death compared to wildtype littermates.[307] The first well-described pathology in Nrf2-null mice was systemic lupus erythematosus with accompanying nephritis; the pathology was characterized by the presence of dsDNA antibodies and antibody deposits within glomeruli, inflammation within the liver and kidneys, increased oxidative stress, reduced creatinine clearance, and splenomegaly with alterations of immune cell populations.[307–311] These findings correspond well with the finding in a human cohort in which a single

nucleotide polymorphism that reduced Nrf2 expression increased the risk of developing autoimmune nephritis in systemic lupus erythematosus patients.[305] Subsequent studies have revealed a role for Nrf2 in protection again myriad autoimmune diseases such as psoriasis, multiple sclerosis, acute graft versus host disease, rheumatoid arthritis, type 1 diabetes, scleroderma, polymyositis, and dermatomyositis.[312,313,322–331,314–321] Notably, many of these pathologies are driven by pathogenic T_H1 and T_H17 cells. Nrf2 activation within T cells was shown to ameliorate multiorgan autoimmune pathologies in mice lacking Tregs, suggesting Nrf2 can intrinsically suppress T cell activation and effector function.[329]

Nrf2 in the Lung

In the highly oxidative microenvironment within the lung, Nrf2 is vital for preventing oxidative and inflammatory injuries. Nrf2-null mice have increased susceptibility to lung injury following exposure to butylated hydroxytoluene (BHT) or hyperoxia.[275,332] Following hyperoxic insult, Nrf2 is highly upregulated in the airway epithelium and alveoli.[333] This upregulation of Nrf2 contributes to upregulation of antioxidant genes within the lung which are not upregulated in the lungs of Nrf2-deficient mice which have inflammatory macrophage infiltration in the lungs.[275,333] It was also shown that other stress-responsive proteins like heat shock proteins likely aid in resolving hyperoxic injury in the absence of Nrf2. Another study revealed that Nrf2-null mice fail to upregulate peroxisome proliferator activated receptor γ (PPARγ) in the lungs following hyperoxic insult.[334] A functional ARE was identified within the PPARγ gene, and 15d-PGJ2 was shown to increase nuclear accumulation of PPARγ in a Nrf2-

dependent manner leading to the resolution of inflammation following hyperoxic insult. Mice with a conditional deletion of Nrf2 in club cells show enhanced protein in bronchoalveolar lavage fluid (BALF) following hyperoxic insult.[335] This was associated with increased cell death in the airway epithelium and corresponding macrophage infiltration. These effects were long lived in the lungs of mice with Nrf2-deficient club cells, with inflammation still apparent 72 hours into the recovery phase at which point mice with in-tact Nrf2 had recovered to baseline. Nrf2-null mice also exhibit enhanced inflammation and emphysema in an elastase-induced emphysema model.[336] This is associated with augmented neutrophilia and macrophage infiltration in the lungs, as well as hemoglobin and albumin content in bronchoalveolar lavage fluids. These effects seemed to be due to defects within immune cells, especially defects in antioxidant and antiprotease pathways, as bone marrow transplantation with wildtype bone marrow rescued the effects seen in Nrf2-null mice.

Nrf2 has also been shown to be critical in suppressing pathogenic immune responses in the lung. Nrf2-null mice have exaggerated cellularity within the airways following OVA challenge, driven by neutrophils, eosinophils, lymphocytes, and epithelial cells.[337] Neutrophilia was largely reduced by NAC administration, but other cellular abnormalities were unaffected by NAC. Lack of Nrf2 led to thickening of the airway epithelial layer and widespread eosinophilia in the interstitium. Nrf2-null mice also had increased evidence of oxidative damage in their lungs and increased NFκB activity. Nrf2-null mice also had exacerbated mucus cell hyperplasia compared to wildtype mice. The Nrf2-null mice also had a T_H2 skew based on BALF cytokines. Notably, the mice in these studies were on a CD1:ICR background which has a T_H2-biased immune

response.[338] Notably, C57BL/6 mice harboring a club-cell dependent knockout of Keap1 had a diminished inflammatory response following OVA challenge suggesting Nrf2 in the airway epithelium is vital for limiting allergic inflammation.[339] Similarly, Nrf2-null mice on a C57BL/6 background have reduced survival in a bleomycin-induced pulmonary fibrosis model.[295] This phenotype is driven by an early neutrophilic inflammatory response that led to enhanced lung edema and LDH within bronchoalveolar lavage fluid. This was accompanied by increased TNFα and MIP-2 in the airways and enhanced NFκB activation. Nrf2-null mice had substantially more alveolitis than wildtype mice. Nrf2-null mice had a stronger T_H2 phenotype, evidenced by reduced $IFN\gamma^+$ $CD4^+$ T cells, enhanced $IL\text{-}4^+$ T cells, and enhanced mRNA expression of Gata3, IL-4, and IL-13. SFN and Nrf2 promote airway epithelial barrier integrity independently of antioxidant gene induction.[340] Nrf2-null lungs were also more sensitive to irradiation, showing marked fibrosis and depletion of alveolar type II cells 250 days after the toxic insult.[341] Notably, Nrf2 deficiency specific to alveolar type II cells was not sufficient to cause this effect. In various models of sepsis, Nrf2-null mice have exacerbated inflammatory responses within the lung resulting in exacerbated alveolar destruction and mortality.[342–345] Similar inflammatory responses were seen during lung infections with *Staphylococcus aureus*, *Streptococcus pneumoniae*, and *Haemophilus influenzae*.[294,346,347] These studies collectively demonstrate that Nrf2 is necessary for redox and immune homeostasis within the lungs.

Disparate Roles of Nrf2 in Antiviral Immunity

Nrf2 has been studied in a variety of viral infection models *in vitro* and *in vivo* and has benefits for both hosts and viruses depending on the infectious agent. For instance, several viruses utilize the Nrf2 pathway to inhibit antiviral and apoptotic pathways, thus permitting extensive viral replication.[348–353] In some instances, Nrf2 induction by viruses is ROS-dependent. However, some virus proteins are able to directly bind Keap1 to activate Nrf2 to confer a survival advantage to the virus, as is the case with the hemorrhagic fever-inducing Marburg virus.[354] Notably, Nrf2-null mice have improved survival rates and reduced viral titers following infection with Marburg virus. In complete opposition, Nrf2 activation has also been shown to limit viral replication by several viruses and promote viral clearance *in vivo*.[290,355–362] In the context of influenza virus, Nrf2 was also shown the prevent viral entry in human nasal epithelial cells, likely due to alterations of protease expression needed to cleave hemagglutinin on the virus.[363]

In addition to the dual roles of Nrf2 on viral replication in various systems, disparate effects of Nrf2 on the innate antiviral immune response have also been reported. Chemical Nrf2 activation in nasal epithelial cells was shown to induce antiviral gene expression in a Nrf2-dependent manner, but this was not observed in a model of Nrf2 overexpression in airway epithelial cells.[357,363] In Dengue virus infected-mice, Nrf2 activation upregulated the proinflammatory protein CLEC5A which led to downstream inflammation, and Nrf2-null mice were protected from this inflammatory response.[364] In human cells and in *in vivo* infection of mice, Nrf2 was shown to impair innate antiviral immune responses against two herpesviruses, though the mechanism varied between

species.[352,353] Nrf2 was also shown to limit inflammation during influenza infection, but this had no effect on viral clearance.[365,366]

Toxicological Importance of the Nrf2 Activator, *tert*-butylhydroquinone

tBHQ, a potent Nrf2 activator, was first introduced into the global food supply in 1972 to prevent spoilage of fats in food products ranging from vegetable oils to frozen meats/fish to processed foods like crackers.[367] Following evaluation of standard toxicity tests, an allowable daily intake of tBHQ was established by the World Health Organization's and United Nations' Food and Agriculture Organization's Joint Expert Committee on Food Additives (JECFA). It was found that in dogs, dietary exposures above 72 mg/kg/day caused significant reductions in hematocrit so the allowable daily intake (ADI) was established as 0.7 mg/kg/day utilizing a 100-fold safety factor.[368] While solid exposure data for tBHQ is largely nonexistent, expert estimates suggest consumers in various countries, including the United States, China, and New Zealand/Australia, among others, are capable of exceeding the ADI.[369] Immunotoxicological assessment of chemicals was not performed prior to the late 1970's, many years after the approval and evaluation of tBHQ, and formal guidelines by the FDA for immunotoxicity testing of food additives were not drafted until 1993.[370] At the time of writing, no formal immunotoxicity testing of tBHQ has been published.

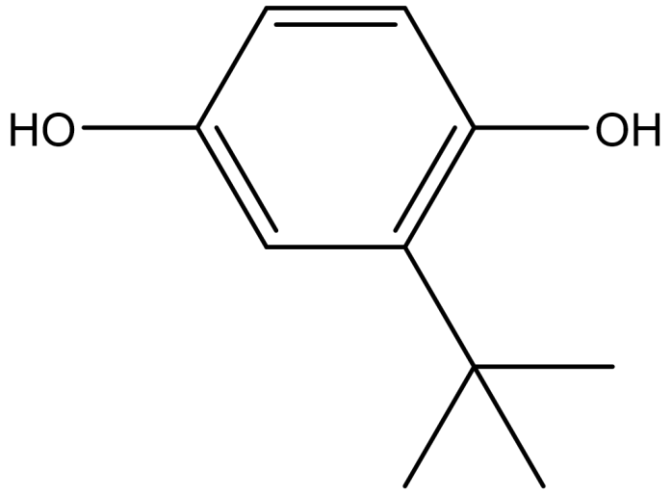

Figure 4: The structure of tBHQ. tBHQ is a phenolic antioxidant used widely in human food products and is also present in many rodent diets.

Rationale for the Presented Studies

Previous studies from our lab have revealed a role of tBHQ in modulating $CD4^+$ T cell activation and differentiation.[301,371,372] Of particular interest, tBHQ skewed $CD4^+$ T cells toward a T_H2 phenotype and suppressed expression of T_H1 cytokines.[296] Additionally, Nrf2 activation within $CD4^+$ T cells showed similar suppression of T_H1 activity *in vivo* in a model of acute kidney injury.[298] Given the importance of T_H1 cells in the development of immunological memory to viral infections, the studies described in these chapters aimed to answer the question of whether dietary tBHQ exposure at doses relevant to human exposure would impair the immune response to influenza virus *in vivo* in a manner dependent on Nrf2.

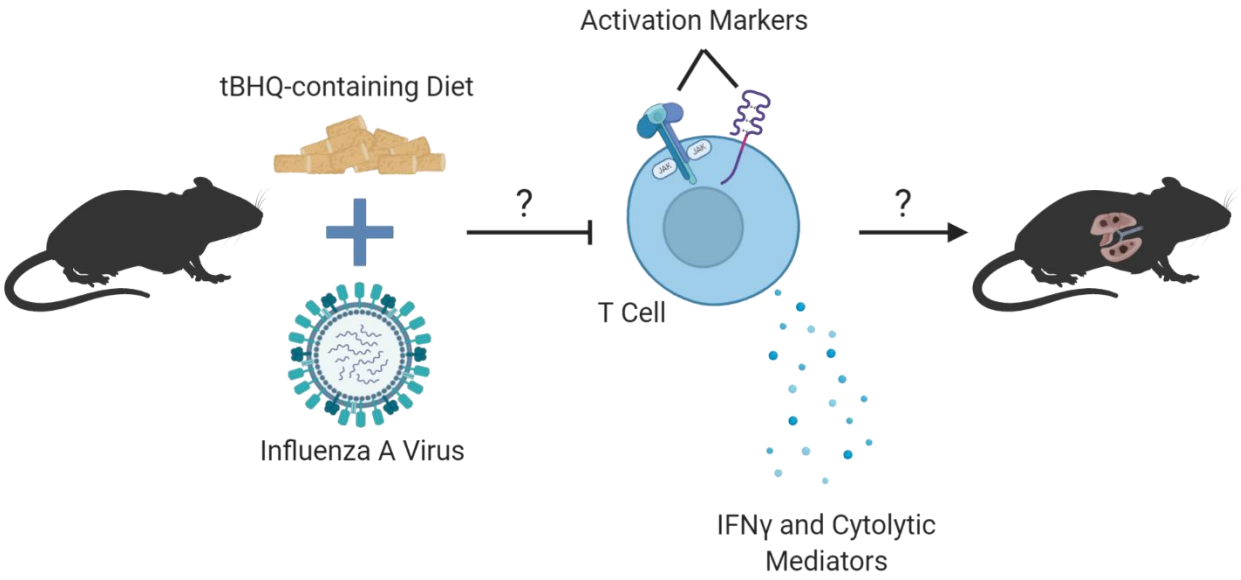

Figure 5: The central hypothesis for the presented studies. Based on our findings of tBHQ effects on T cells *ex vivo*, we hypothesized that dietary exposure to tBHQ would impair the T cell response to influenza infection through modulation of cell activation and downstream effector function. Created with BioRender.com.

CHAPTER 2

The synthetic food additive, *tert*-butylhydroquinone, impairs the primary immune response to influenza virus infection in mice.

Abstract

Tert-butylhydroquinone (tBHQ) is a food additive widely used to prevent rancidification of fats in human food products. It is also found in some commonly used rodent diets, including many in the AIN series of diets. This product was approved for use in food and the allowable daily intake was established in the 1970's before immunotoxicity guidelines were established for food additive testing. Previous studies from our lab have shown immunomodulatory effects of tBHQ at low micromolar levels *ex vivo*, including skewing murine $CD4^+$ T cell polarization toward a T_H2 phenotype and impairing primary and Jurkat human T cell differentiation. We have also shown that tBHQ modulates primary murine NK cell and B cell activation. However, it remains unknown if tBHQ consumed through the diet at doses relevant to human exposure produces immunotoxic effects. To begin answering this question, we fed mice standard AIN-93G diet which is 0.0014% tBHQ or AIN-93G with the tBHQ removed and then infected the mice with a sublethal titer of influenza A/PR/8/34 (H1N1). Ten days later, various parameters associated with the T cell response to influenza infection were assessed. It was found that mice on the tBHQ diet had fewer $CD8^+$ T cells in the lungs as well as delayed activation of both $CD4^+$ and $CD8^+$ T cells. Additionally, these mice had fewer influenza-specific T cells detected in the draining lymph nodes. Similar to our *ex vivo* results which showed tBHQ promoted $CD4^+$ T cell polarization to a T_H2 phenotype, we observed several phenomena of a type 2 immune response with tBHQ exposure including mucus hypersecretion and eosinophilic inflammation within the lungs. Notably, the dietary intake of tBHQ in this model equated to 1-2 mg/kg, far lower than the previously reported no adverse effect level (NOAEL) of 72 mg/kg/day.

Introduction

Influenza virus infections are a persistent threat to society, causing hundreds of thousands of hospitalizations annually in the United States and putting considerable strain on the economy.[373,374] The primary medical intervention for influenza is annual vaccination to prevent infection and reduce symptom severity. However, despite increased vaccination uptake in recent years, the number and severity of reported influenza cases has not improved.[373,375,376] Therefore, there has been considerable interest in identifying factors that contribute to susceptibility to influenza virus infections and/or reduce vaccine efficacy.

Influenza infection causes a robust immune response, involving many cell types of both the innate and adaptive branches of immunity. T cell-mediated immunity is a critical component of the anti-viral response, in which $CD8^+$ T cells directly lyse virus-infected cells while $CD4^+$ T cells, primarily T_H1 cells, promote viral clearance by secreting cytokines, namely IFNγ and TNFα, which cause activation of macrophages and cytotoxic T cells as well as induction of immunoglobulin class-switching in B cells.[36–40] Additionally, a small subset of $CD4^+$ T cells have cytolytic capacity and aid in the clearance of virus-infected cells.[73,79] $CD4^+$ and $CD8^+$ T cells are also necessary in establishing memory cell populations to quickly and effectively respond to secondary influenza infections.[37,38,95,98]

Published studies from our lab suggest that the synthetic food additive, *tert*-butylhydroquinone (tBHQ), negatively impacts $CD4^+$ T cell activation and differentiation. tBHQ is widely used to prevent rancidification of fats and oils and can be found in many products including cooking oils, frozen fish products, and crackers among others.[367]

The allowable daily intake (ADI) of tBHQ was established as 0.7 mg/kg/day based on studies performed in dogs which demonstrated doses above 72 mg/kg/day resulted in reduced hemoglobin and hematocrit levels.[368] However, some estimates based on model diets suggest that high consumers of tBHQ could regularly consume up to 1100% of the ADI, equivalent to 7.7 mg/kg/day.[369] We previously showed that tBHQ has immunomodulatory effects. Specifically, we showed that tBHQ – through activation of the transcription factor, nuclear factor erythroid 2-related factor 2 (Nrf2) – impaired human $CD4^+$ T cell activation and murine $CD4^+$ Th1 polarization while promoting Th2 polarization.[296,300,301,371,372] This could negatively impact host defense against influenza, as adoptive transfer of Th2 populations during secondary influenza challenge was shown to dramatically increase mortality, while transfer of Th1 populations completely prevented death from infection with lethal influenza titers.[46] In addition to our studies in T cells, we also recently showed that tBHQ impairs primary murine NK cell and B cell activation *ex vivo.*[291,293]

As mentioned above, one way tBHQ exerts immunomodulatory effects is through Nrf2 activation. Nrf2 is a stress-activated transcription factor and helps maintain cellular homeostasis by upregulating cytoprotective genes [377]. Under basal conditions, Nrf2 remains tethered to the cytoskeleton by its repressor protein, Kelch-like ECH-associated protein 1 (Keap1).[206] The introduction of cell stress, including oxidative and electrophilic stresses, results in modification of cysteine residues on Keap1 which then permits *de novo* synthesized Nrf2 to accumulate in the nucleus where it upregulates its target genes through binding to antioxidant response elements.[197,204,214] tBHQ is an electrophilic compound that modifies cysteine residues on Keap1 and is a potent

activator of Nrf2 [253]. In addition to our findings in T cells, other Nrf2 activators and genetic models have also revealed that activation of Nrf2 impairs the ability of dendritic cells to effectively present antigen and stimulate T cells, suppresses the expression of inflammatory cytokines in macrophages, and dampens the immune response in various inflammatory disease models.[261,283,286,294,298] Often, the reduced immune response caused by Nrf2 activation results in improved host outcomes likely due to reduced immunopathology and resolution of oxidative stress associated with inflammatory diseases.

Our previous studies examining the effects of Nrf2 activation by tBHQ in T cells were all conducted using *in vitro* or *ex vivo* systems, and no investigation has been performed on the effects of Nrf2 activation or tBHQ exposure on the T cell response to influenza virus infection. Accordingly, the purpose of the present study was to determine if low, physiologically relevant doses of tBHQ consumed through the diet would impair the T cell-mediated immune response to influenza infection *in vivo*.

Materials and Methods

Animals, Diets, and Virus

An aliquot of influenza A/PR/8/34 (H1N1) was generously gifted by Dr. Kymberly Gowdy at East Carolina University in Greenville, North Carolina. The virus was then propagated and quantified following a published protocol.[378] Briefly, the virus was injected into the allantoic fluid of specific pathogen-free, embryonated chicken eggs (Charles River Laboratories, Wilmington, MA). The infected eggs were incubated for 48 hours at 37.5 ˚C, followed by another 24 hours at 4 ˚C. Following incubation, allantoic

fluid was collected, centrifuged, and supernatant was divided into single-use aliquots. Aliquots were stored at -80 ˚C until used for experiments. The propagated virus stock was quantified by tissue culture infectious dose 50 ($TCID_{50}$) and hemagglutination methods. For the $TCID_{50}$, the virus was serially diluted across a 96-well plate containing confluent monolayers of MDCK cells (ATCC, Manassas, VA). Cells were observed daily for cytopathic effect, at which point the titer was determined using the Reed-Muench method.[379] The hemagglutination assay was performed by serially diluting the virus across a 96 well plate containing 0.5% chicken red blood cells and incubating the cells for 30 minutes at room temperature, at which point agglutination was recorded. The virus stock was determined to be 2.5×10^5 $TCID_{50}$/mL and 7260 HAU/mL.

Female C57BL/6J mice (12 weeks old) were purchased from Jackson Laboratories (Bar Harbor, Maine). Upon arrival, mice were housed in cages in groups of 3-4 animals per cage and given AIN-93G purified rodent diet containing 0 or 0.0014% tBHQ (Dyets, Inc, Bethlehem, PA) and water *ad libitum*. Food consumption was monitored daily. After 2 weeks of acclimation to the diets, mice were anesthetized with 2,2,2-tribromoethanol (avertin; Alfa Aesar, Ward Hill, MA) via intraperitoneal injection. For studies on the immune response to primary infection, mice were intranasally instilled with 30 µL of influenza A/PR/8/34 (H1N1) at a titer of 7.5 $TCID_{50}$/mL (0.22 HAU/mL). This resulted in a total amount of 0.23 $TCID_{50}$ per mouse (0.0066 HAU per mouse). Upon recovery from anesthesia, mice were returned to their cages and monitored daily for changes in food consumption and body weight. Three mice on each diet were intranasally instilled with 30 µL of sterile saline instead of virus as experimental controls. The timeline for this experiment can be seen in Figure 6. All

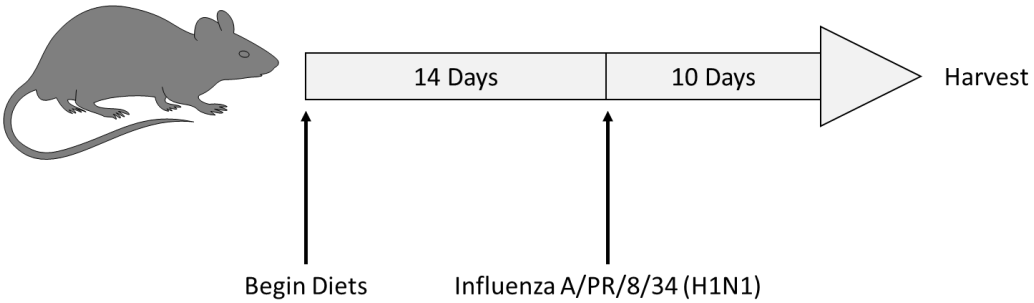

Figure 6: Experimental Timeline. Mice arrived at Michigan State University from Jackson Laboratories. Upon arrival, mice were placed on their diets and were allowed a 14-day acclimation period. Mice were then infected with influenza A/PR/8/34 (H1N1) and tissues were collected 10 days later.

animal studies were conducted in accordance with the Guide for Care and Use of Animals as adopted by the National Institutes of Health and were approved by the Institutional Animal Care and Use Committee at Michigan State University.

Tissue Collection and Cell Separation

Ten days after primary infection, mice were anesthetized with avertin and euthanized via cardiac puncture. Blood was collected into heparinized tubes, and lungs and mediastinal lymph nodes (MLN) were removed. Lungs were placed in 5 mL of DMEM containing 1 mg/mL collagenase D and subsequently dissociated with the gentleMACS dissociator (Miltenyi Biotec, Auburn, CA). After dissociation, 1 mL of lung homogenate was centrifuged and resuspended in TRIzol reagent RNA analysis. The remaining lung homogenate was used for FACS analysis. Cells from the MLNs were isolated by grinding the MLN between the frosted ends of two microscope slides and resuspending in DMEM. For lungs used for histology, bronchoalveolar lavage fluid (BALF) was first collected by cannulating the trachea and flushing the lungs with 1 mL of sterile saline.

Immunophenotyping

Lung cells were washed in FACS buffer (1% FBS in dPBS). Cells were incubated with Fc block (BD Pharmingen, San Diego, CA) prior to labeling with antibodies against CD4, CD8α, CD25, CD69, CD44, CD62L, FasL, and CD107a (Table 1). Cells were fixed with 4% formaldehyde fixative prior to FACS analysis on the Attune NxT (Thermo Scientific, Waltham, MA). Cell viability was assessed by labeling cells with the Zombie Aqua Fixable Viability Kit (BioLegend, San Diego, CA) prior to labeling with antibodies, per the manufacturer's protocol.

Table 1: Flow Cytometry Antibodies

Antibody Target	Fluorochrome	Source
CD4	FITC	eBioscience
CD8a	PerCP-Cy5.5	BioLegend
CD25	APC	BioLegend
CD69	Alexa Fluor700	BioLegend
CD44	APC-Cy7	BioLegend
FasL	PE	BioLegend
CD107a	PE-Cy7	BD Pharmingen
IFNγ	APC	BioLegend
T-bet	PE	eBioscience
CD19	FITC	BioLegend
CD8a	PE	BioLegend
CD4	AF647	BioLegend

Ex Vivo Stimulation and Intracellular Labeling

24 hours before collection, splenic $CD11c^+$ dendritic cells were isolated from untreated C57BL/6J mice using positive selection (Miltenyi Biotec, Auburn, CA). Dendritic cells were plated at a density of 4×10^5 cells/mL in RPMI 1640 supplemented with 10% fetal bovine serum, 25 mM HEPES, 1 mM sodium pyruvate, 1x nonessential amino acids, and 100 U/mL penicillin and streptomycin. Influenza A $NP_{366-374}$ (ASNENMETM) and influenza A $NP_{311-325}$ (QVYSLIRPNENPAHK) peptides were synthesized (New England Peptide, Inc., Gardner, MA) and added to dendritic cells at a concentration of 1 μM. 24 hours later, single-cell suspensions from the lungs of infected mice were co-cultured with the dendritic cells for 5 hours in the presence of monensin (BioLegend). Cells were labeled with the Zombie Aqua kit prior to being labeled for surface markers (CD4 and CD8α) and permeabilized with the FoxP3/transcription factor staining buffer set (eBioscience). After permeabilization, cells were labeled with antibodies against IFNγ and T-bet (Table 1). After labelling, cells were fixed with 1% formaldehyde fixative prior to FACS analysis on the Attune NxT.

Tetramer Labeling

To identify influenza-specific $CD8^+$ and $CD4^+$ T cells within the MLNs, the H-2D(b) Influenza A $PA_{224-233}$ SSLENFRAYV (Alexa 647-Labeled MHC-I Tetramer) and I-A(b) Influenza A $NP_{311-325}$ QVYSLIRPNENPAHK (PE-labeled MHC-II Tetramer) tetramers were used. The tetramers were prepared by the NIH Tetramer Core Facility (Atlanta, GA). To identify influenza-specific $CD4^+$ T cells, MLN cells were labeled with CD4 (AF647) and the NP tetramer. For influenza-specific $CD8^+$ T cells, MLN cells were

labeled with CD19, CD8α (PE), and the PA tetramer; influenza-specific $CD8^+$ T cells were identified as viable $CD8\alpha^+$ $CD19^-$ $PA\text{-}tetramer^+$ cells. Both panels were also labeled for viability with the Zombie Aqua kit, as above. Cells were fixed with a 4% formaldehyde solution prior to analysis on the Attune NxT.

Detection of Influenza-specific Antibodies

Influenza-specific IgG2c ELISAs were performed following a previously published protocol.[380] Briefly, high-binding plates (Corning, Inc., Kennebunk, ME) were coated with 40 HAU of influenza A/PR/8/34 (H1N1) diluted in 1x coating buffer. Plates were blocked with 10% BSA, and plasma was diluted and added to the wells. Influenza-specific IgG2c was quantified using an HRP-conjugated antibody against IgG2c (Abcam, Cambridge, MA) followed by the addition of TMB substrate. Absorbance was quantified at 450 nm on a Tecan Infinite M1000 Pro Microplate Reader (Tecan, San Jose, CA).

RNA Isolation and Quantitative PCR

RNA was isolated from lung homogenate using TRIzol reagent per the manufacturer's protocol (Life Technologies, Grand Island, NY). RNA was quantified with the Nanodrop 2000c spectrophotometer (Thermo Fisher Scientific, Waltham, MA). Following reverse transcription, cDNA was quantified with real-time PCR SYBR green analysis using the QuantStudio 7 Flex Real-Time PCR System (Applied Biosystems, Foster City, CA). Ribosomal protein L13A (RPL13A) served as the endogenous control

Table 2: Primer Sequences

Gene	Forward Primer Sequence	Reverse Primer Sequence
Influenza M1	CAAAGCGTCTACGCTGCAGTCC	AAGACCAATCCTGTCACCTCTGA
CTLA-4	CATGTACCCACCGCCATACT	CCAAGCTAACTGCGACAAGG
IL-10	ACCAGCTGGACAACATACTGC	ATTTCTGGGCCATGCTTCTCT
RPL13a	GTTGATGCCTTCACAGCGTA	AGATGGCGGAGGTGCAG

and relative mRNA expression was calculated using the ΔΔCt method. Primer sequences are listed in Table 2.

Histology and Immunohistochemistry

After collecting BALF from animals, lungs were inflated with 500 µL of 10% neutral buffered formalin purchased from Thermo Scientific (Waltham, MA). After sitting in formalin for 24 hours, lungs were transferred to 30% ethanol until further processing, at which point 2 mm sections were dissected at airway generations 5 and 11. These sections were then paraffin-embedded and sectioned by the Michigan State University histology laboratory. Sections were loaded onto glass slides and stained with hematoxylin and eosin, Alcian Blue (pH 2.5)/Periodic Acid Schiff (AB/PAS), or immunohistochemically stained for major basic protein.

Statistical Analysis

The mean ± SEM was determined for each treatment group in individual experiments. The virus-infected VEH and tBHQ groups were compared against each other using two-tailed T-tests with Sigma-Plot 12.3 software (Systat Software, San Jose, CA). For parameters with unequal variances, Welch's t-tests were performed. Animals

which showed no signs of infection (no weight loss and no detectable viral RNA) were excluded from statistical analyses. Additionally, saline-instilled animals were not used for statistical analyses as their role in the present study was to provide context about the magnitude of the T cell response during influenza infection.

Results

tBHQ Diet Impaired $CD8^+$ T cell Infiltration to the Lungs of Infected Mice

Ten days following infection, lungs were removed and homogenized. A single-cell suspension from lung homogenate was labeled with antibodies against CD8α and CD4. Viable $CD4^+$ and $CD8^+$ T cells were detected via flow cytometry (Figure 7A). The number of $CD4^+$ T cells in the lungs was increased with viral infection, as expected, but was not affected by tBHQ consumption (Figure 7B). Conversely, $CD8^+$ T cell infiltration to the lungs during infection was blunted in mice fed a diet containing tBHQ, suggesting that tBHQ inhibits $CD8^+$ T cell trafficking to the lungs of infected mice (Figure 7C).

tBHQ Reduced the Number of Influenza-specific T Cells in Mediastinal Lymph Nodes of Infected Mice

We next sought to determine whether the number of influenza-specific T cells was diminished by tBHQ in mice infected with influenza. To test this, we quantified the number of influenza-specific $CD4^+$ (Figure 8A, B) and $CD8^+$ (Figure 8C, D) T cells from the mediastinal lymph nodes using tetramers expressing MHC-I-restricted ($PA_{224-223}$) or MHC-II-restricted ($NP_{311-325}$) influenza peptides. Influenza-specific $CD8^+$ T cells were identified as viable, $CD19^-$ $CD8^+$ PA^+ cells. Our results demonstrate that tBHQ

consumption reduces the number of influenza-specific $CD4^+$ (Figure 8B) and $CD8^+$ T cells (Figure 8D) in the draining lymph nodes.

tBHQ Delayed Activation of T Cells in Lungs

To assess T cell activation status, we quantified the surface expression of CD25 and CD69 on $CD4^+$ (Figure 9A, B) and $CD8^+$ (Figure 9C, D) T cells, which are rapidly upregulated following T cell activation. In both $CD4^+$ (Figure 9B) and $CD8^+$ (Figure 9D) T cells, tBHQ altered the kinetics of activation, as the number of $CD25^-CD69^+$ cells (early activation phenotype) was enhanced by tBHQ, while the number of $CD25^+CD69^-$ cells (late activation phenotype) was blunted by tBHQ. The numbers of $CD25^+CD69^+$ T cells (intermediate activation phenotype) were differentially affected within the $CD4^+$ and $CD8^+$ T cell populations, suggesting different sensitivities to tBHQ within these cell types.

tBHQ Reduced the Number of Cells with an Effector Phenotype and Suppressed Effector Function of Cytolytic $CD4^+$ and $CD8^+$ T Cells

In addition to activation, we also investigated whether tBHQ would affect the population of effector T cells during primary influenza infection. CD44 is upregulated after activation and remains highly expressed on effector T cells.[381] Accordingly, we quantified the number of $CD44^{hi}$ $CD4^+$ (Figure 10A) and $CD8^+$ T cells (Figure 10B). We also quantified the number of cells expressing CD107a (Figure 11A, B) and FasL (Figure 11E, F), as these are two markers of cytotoxic effector function. tBHQ substantially reduced the number of $CD4^+$ (Figure 10C) and $CD8^+$ T cells (Figure 10D) expressing CD44. Additionally, the number of $CD8^+$ T cells expressing CD107a was

markedly decreased in the lungs of mice on the tBHQ diet (Figure 11D). Interestingly, this effect was not seen in $CD4^+$ T cells (Figure 11C). Mice on the tBHQ diet also had reduced the numbers of $CD4^+$ and $CD8^+$ T cells expressing FasL (Figure 11G, H). Taken together, these results suggest tBHQ impairs T cell cytotoxic function during primary influenza challenge. Like the effect on $CD25^+CD69^+$ T cells, the effect on $CD107a^+$ cells hints that $CD4^+$ and $CD8^+$ T cells differ in sensitivity to tBHQ.

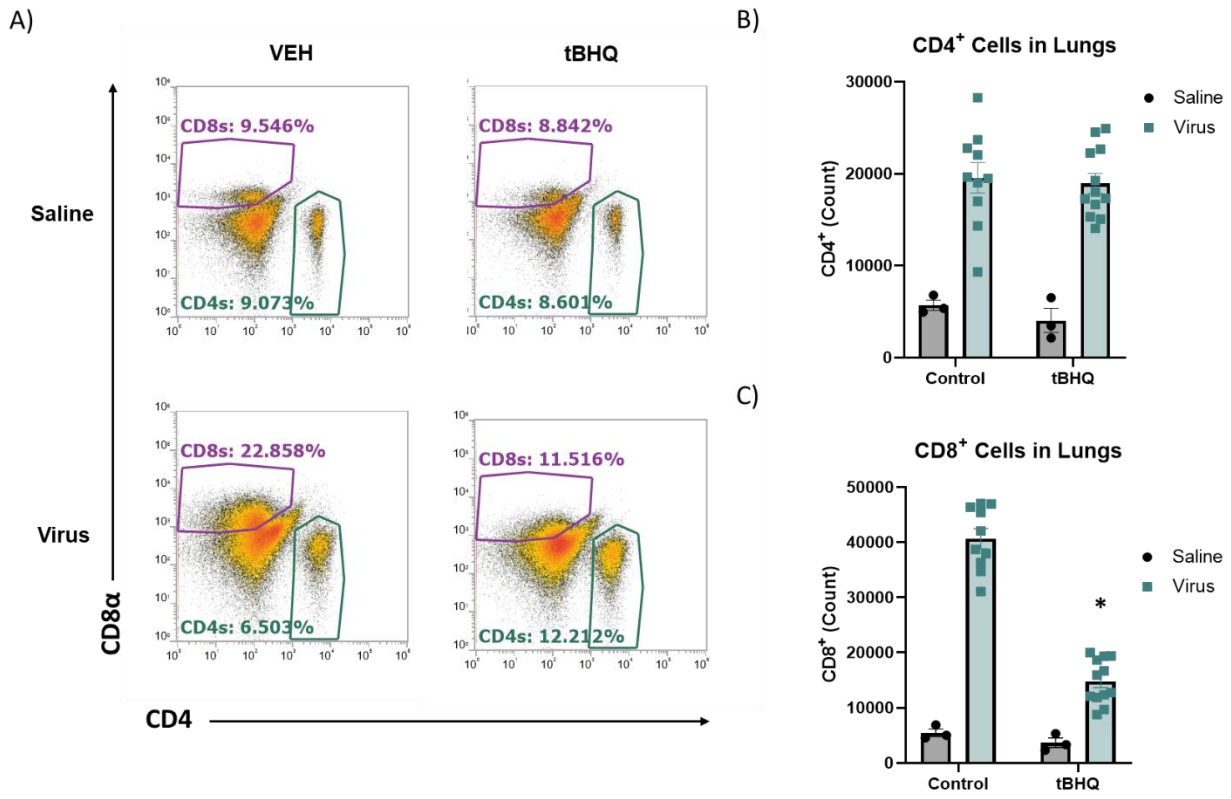

Figure 7: Consumption of a low dose of tBHQ impairs CD8⁺ T cell infiltration to the lung during primary influenza infection. Mice were put on a diet with or without 0.0014% tBHQ 14 days prior to intranasal instillation with either sterile saline or influenza A/PR/8/34 (H1N1). Ten days post-infection, lungs were removed and homogenized. Lung homogenates were labeled with fluorescent antibodies against CD4 and CD8α. Cells were quantified via flow cytometry. (A) Representative dot plots of CD4 and CD8 surface expression in lung homogenates from each treatment group. (B) Quantification of $CD4^+$ cells expressed as count. (C) Quantification of $CD8^+$ cells expressed as count. * $p < 0.05$ (Student's t-test) between VEH and tBHQ treatments within the infected mice. VEH/Saline n = 3; tBHQ/Saline n = 3; VEH/Virus n = 10; tBHQ/Virus n = 12

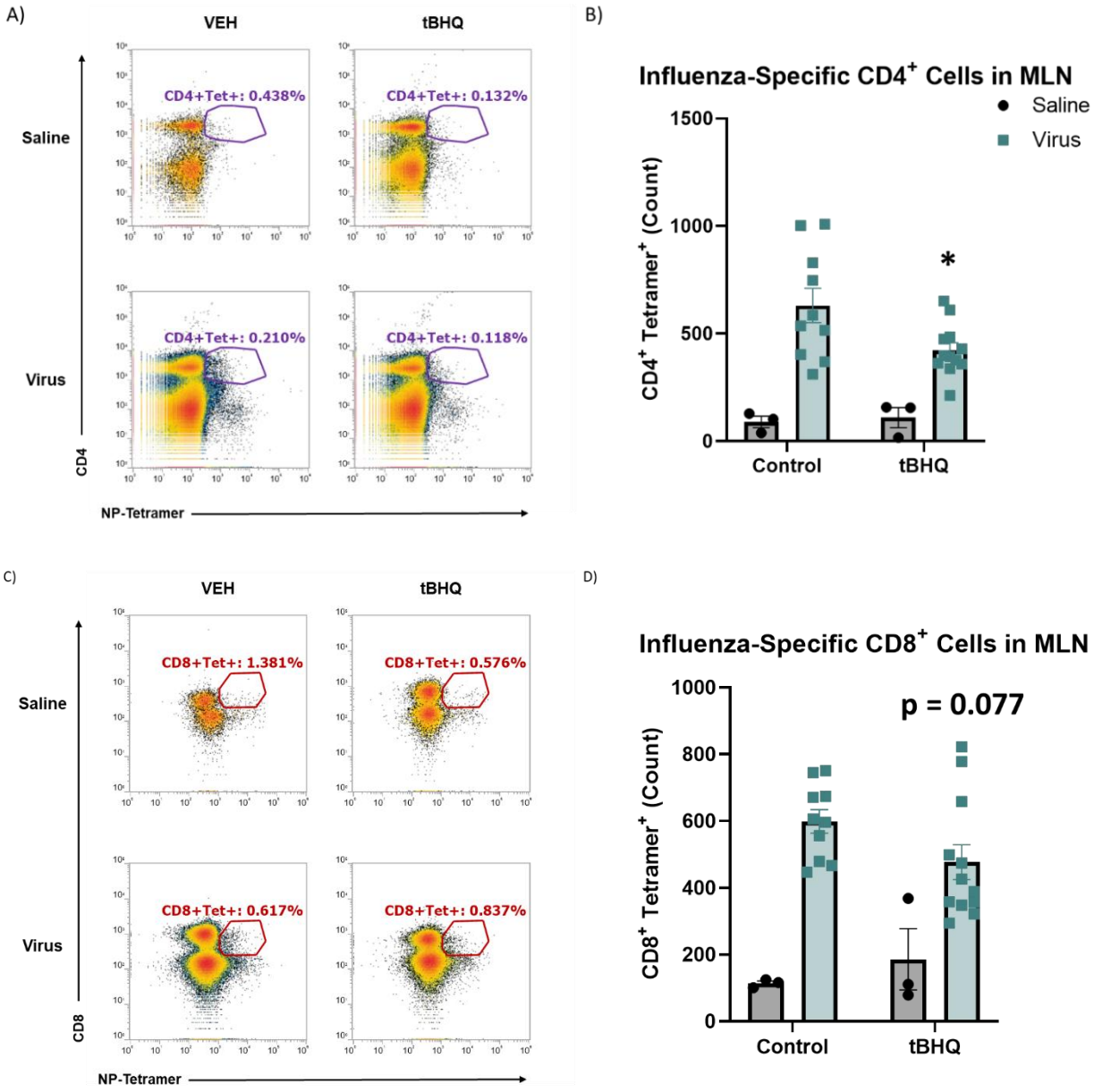

<u>Figure 8: tBHQ reduces the number of influenza-specific T cells in the mediastinal lymph nodes of infected mice. tBHQ reduced the number of influenza-specific T cells in the mediastinal lymph nodes of infected mice.</u> Mice were put on a diet with or without 0.0014% tBHQ 2 weeks prior to intranasal instillation with either sterile saline or influenza A/PR/8/34 (H1N1). Ten days post-infection, cells from the mediastinal lymph nodes were labeled with I-A(b) Influenza A $NP_{311-325}$ (PE-labeled MHC-II Tetramer) and a fluorescent antibody against CD4, or H-2D(b) Influenza A $PA_{224-233}$ (Alexa 647-Labeled MHC-I Tetramer) and antibodies against CD19 and CD8α. Cells were quantified via flow cytometry. (A) Representative dot plots for each treatment group demonstrating influenza-specific $CD4^+$ T cells. (B) Quantification of influenza-specific $CD4^+$ T cells expressed as count. (C) Representative dot plots for each treatment group demonstrating influenza-specific $CD8^+$ T cells. (D) Number of

Figure 8: (cont'd) influenza-specific $CD8^+$ T cells expressed as count. * $p < 0.05$ (Welch's t-test) between VEH and tBHQ treatments within the infected mice. p value for influenza-specific $CD8^+$ T cells derived from Student's t-test. VEH/Saline n = 3; tBHQ/Saline n = 3; VEH/Virus n = 10; tBHQ/Virus n = 12

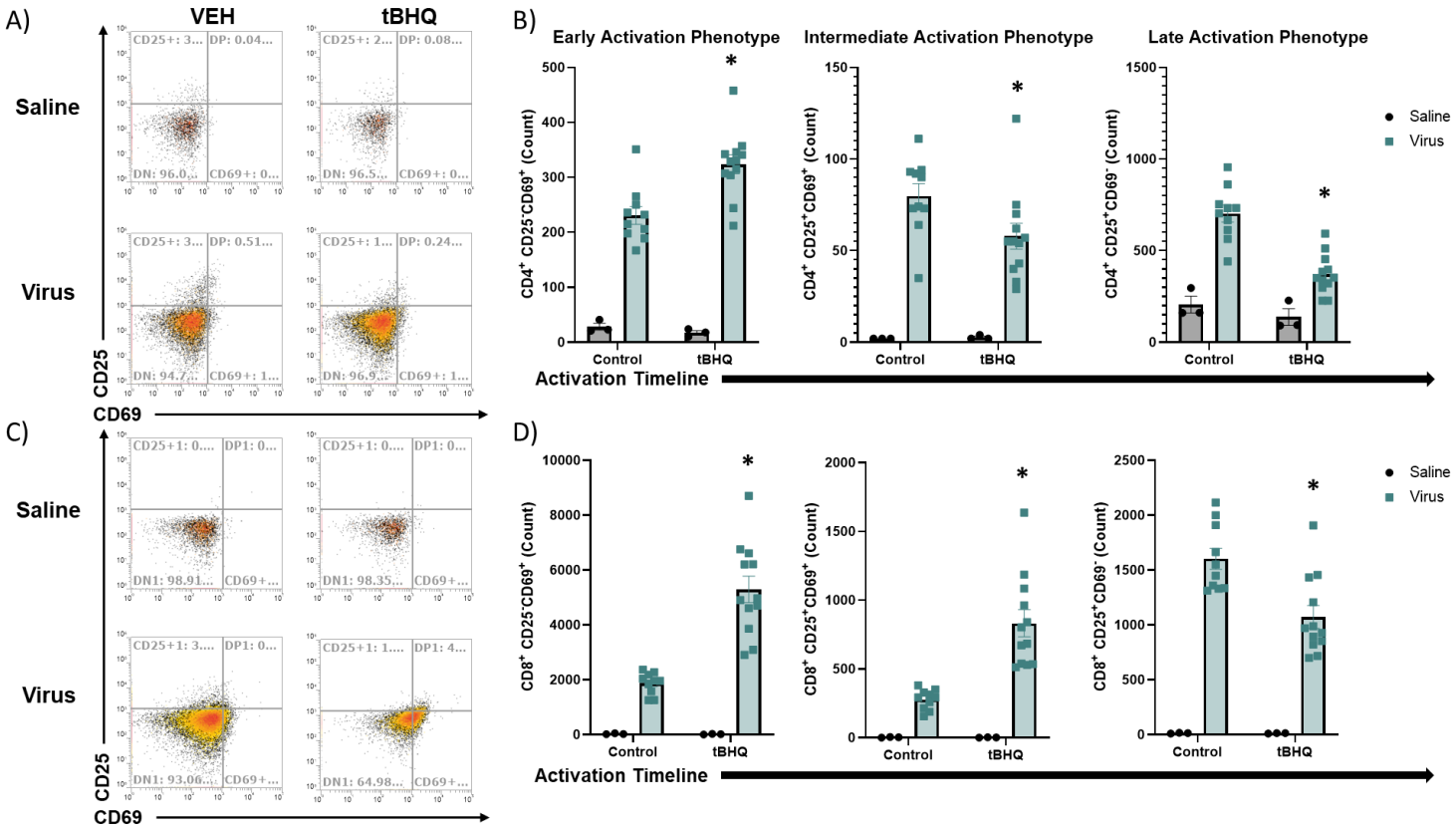

Figure 9: tBHQ delayed activation of T cells in the lungs of infected mice. Mice were put on a diet with or without 0.0014% tBHQ 2 weeks prior to intranasal instillation with either sterile saline or 0.23 $TCID_{50}$ of influenza A/PR/8/34 (H1N1). Ten days post-infection, lungs were removed and homogenized. Lung homogenates were labeled with fluorescent antibodies against CD4, CD8α, CD25 and CD69. Fluorescence was detected and quantified via flow cytometry. (A) Representative dot plots for each treatment group demonstrating CD25 and CD69 expression on $CD4^+$ T cells from lung homogenates. (B) Number of $CD4^+$ T cells expressing CD69, CD25 and CD69, or CD25 alone expressed as count. (C) Representative dot plots for each treatment group demonstrating CD25 and CD69 expression on $CD8^+$ T cells from lung homogenates. (D) Number of $CD8^+$ T cells expressing CD69, CD25 and CD69, or CD25 alone expressed as count. * $p < 0.05$ (Student's t-test) between VEH and tBHQ treatments within the infected mice. VEH/Saline n = 3; tBHQ/Saline n = 3; VEH/Virus n = 10; tBHQ/Virus n = 12

tBHQ Did not Alter the Number of IFNγ$^+$ or T-bet$^+$ T Cells

Based upon our previously published studies, we hypothesized that tBHQ would impair Th1 polarization and similarly suppress IFNγ and T-bet expression in CD8$^+$ T cells. Therefore, we quantified the number of IFNγ$^+$ and T-bet$^+$ CD4$^+$ T cells and CD8$^+$ T cells within the lungs. Our results suggest that consumption of a low dose of tBHQ had little effect on the number of IFNγ$^+$ and T-bet$^+$ T cells at this timepoint, both in the CD4$^+$ and CD8$^+$ populations (Figure 12).

tBHQ did not Alter Secretion of Influenza-specific IgG2c in Plasma

A downstream effect of IFNγ secretion by T cells is immunoglobulin class-switching of IgM to IgG2c, an antiviral immunoglobulin.[36] Since we hypothesized that Th1 polarization and subsequent IFNγ production would be impaired, we also hypothesized that influenza-specific IgG2c secretion would be reduced. Analysis of influenza-specific IgG2c in plasma by ELISA showed no statistical difference between the VEH and tBHQ-exposed animals (Figure 13), consistent with our findings for IFNγ in T cells.

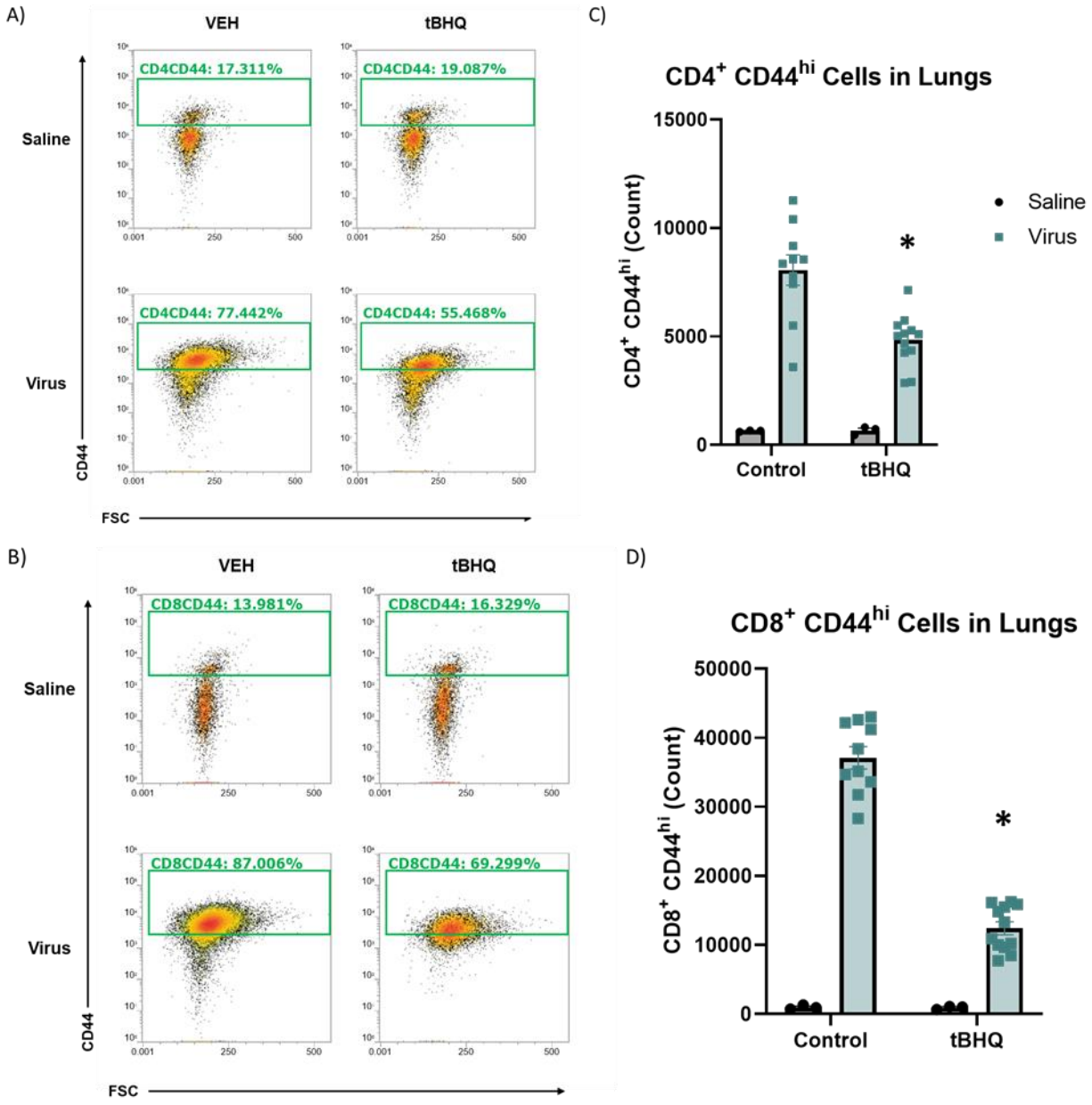

Figure 10: tBHQ modulates expression of CD44 in T cells in the lungs of infected mice. Mice were fed diets with or without 0.0014% tBHQ 2 weeks prior to intranasal instillation with either saline or influenza A/PR/8/34 (H1N1). Ten days post-infection, lungs were removed and homogenized and labeled with fluorescent antibodies against CD4, CD8α, and CD44. (A) Representative density plots for each treatment group demonstrating CD44 expression on $CD4^+$ T cells from lung homogenates. (B) Representative dot plots for each treatment group demonstrating CD44 expression on $CD8^+$ T cells from lung homogenates. (C) Number of $CD4^+$ T cells with an effector ($CD44^{hi}$) phenotype expressed as count. (D) Number of $CD8^+$ T cells with an effector phenotype expressed as count. * $p < 0.05$ (Student's t-test) between VEH and tBHQ treatments within the infected mice. VEH/Saline n = 3; tBHQ/Saline n = 3; VEH/Virus n = 10; tBHQ/Virus n = 12

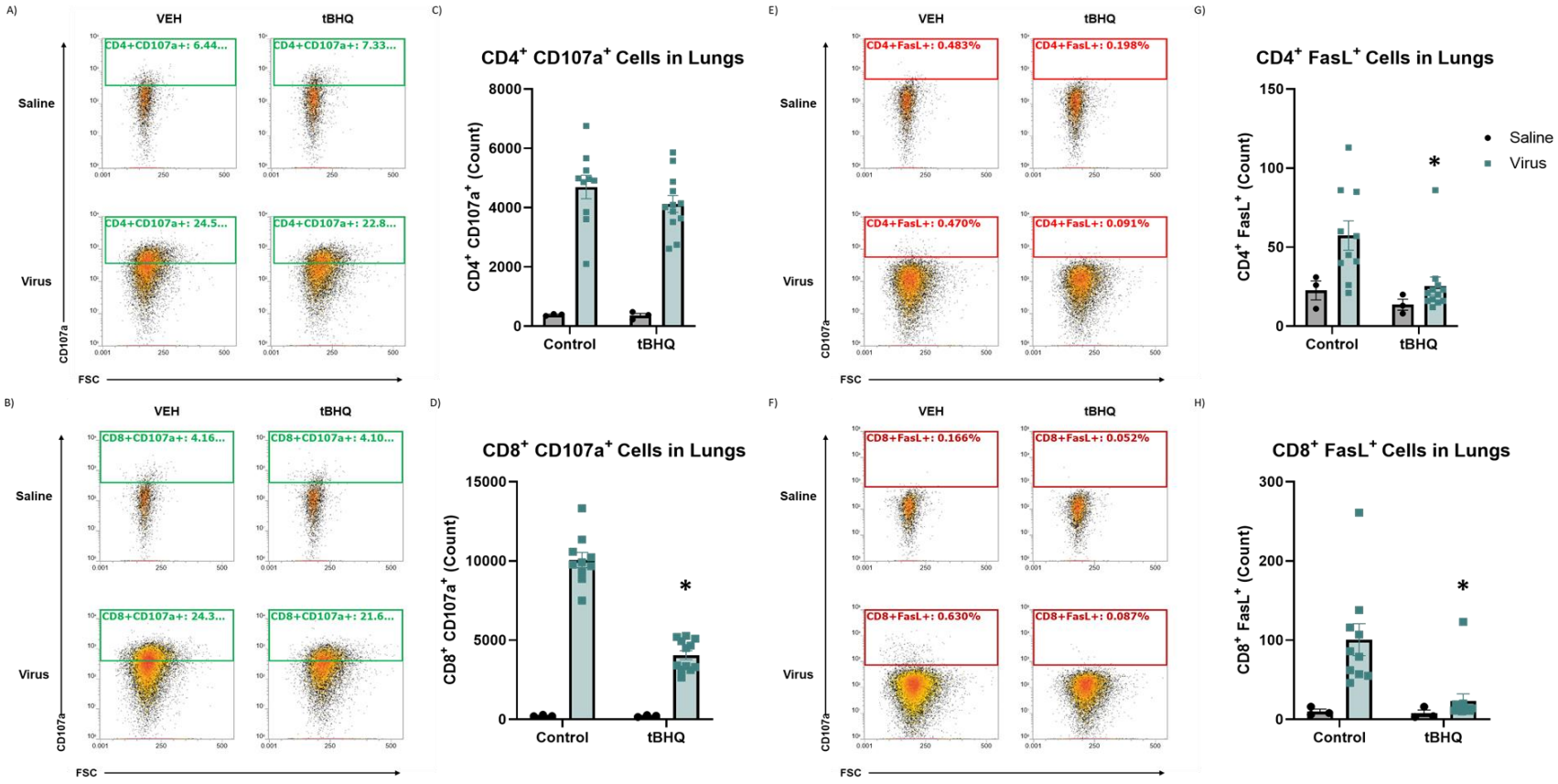

Figure 11: tBHQ modulates the expression of CD107a and FasL in $CD4^+$ and $CD8^+$ T cells in the lungs of infected mice. Mice were fed diets with or without 0.0014% tBHQ 14 days prior to intranasal instillation with either saline or influenza A/PR/8/34 (H1N1). Ten days post-infection, lungs were removed and homogenized and labeled with fluorescent antibodies against CD4, CD8α, CD107a, and FasL. (A,B) Representative density plots for each treatment group demonstrating CD107a expression on $CD4^+$ or $CD8^+$ T cells. (C) Number of $CD4^+$ T cells expressing CD107a expressed as count. (D) Number of $CD8^+$ T cells expressing CD107a expressed as count. (E,F) Representative density plots for each treatment group demonstrating FasL expression on $CD4^+$ or $CD8^+$ T cells from lung homogenates. (G) Quantification of $FasL^+$ $CD4^+$ cells expressed as count. (H) Quantification of $FasL^+$ $CD8^+$ cells expressed as count. * $p < 0.05$ (Student's t-test) between VEH and tBHQ treatments within the infected mice.

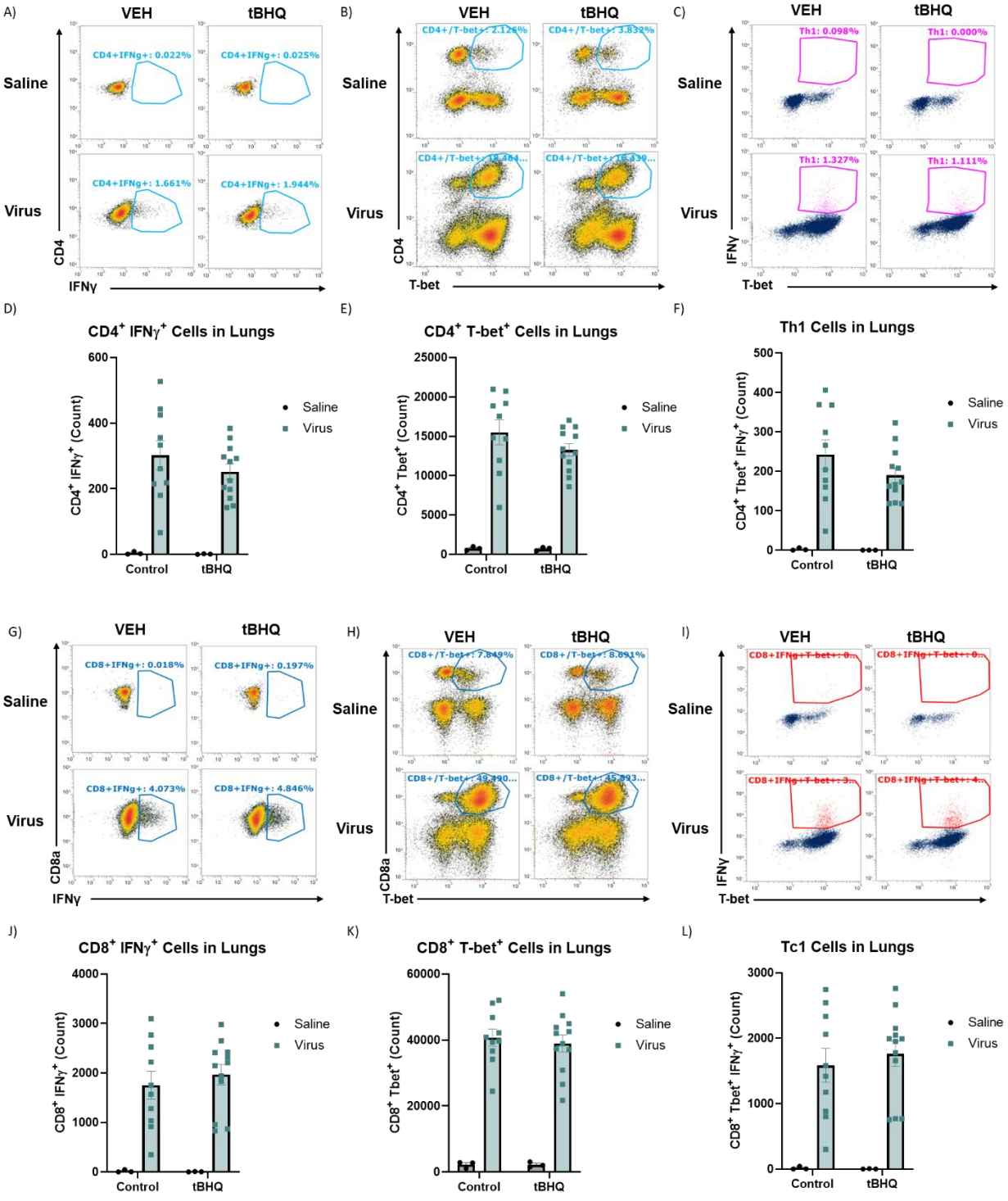

Figure 12: tBHQ had no discernible effect on the number of IFNγ⁺ or T-bet⁺ T cells in the lungs of infected mice. Mice were put on a diet with or without 0.0014% tBHQ 2 weeks prior to intranasal instillation with either sterile saline or influenza A/PR/8/34

Figure 12: (cont'd) (H1N1). Ten days post-infection, lungs were removed and homogenized. The resulting single-cell suspension was co-cultured with influenza-peptide-pulsed dendritic cells in the presence of monensin. 5 hours later, cells were labeled with antibodies against CD4, CD8α, IFNγ, and T-bet. Cells were quantified by flow cytometry. (A-C) Representative dot plots showing the number of $CD4^+$ T cells with intracellular IFNγ, T-bet, or both. (D-F) Number of $CD4^+$ T cells with intracellular IFNγ, T-bet, or both expressed as count. (G-I) Representative dot plots showing the number of $CD8^+$ T cells with intracellular IFNγ, T-bet, or both. (J-L) Number of $CD8^+$ T cells with intracellular IFNγ, T-bet, or both expressed as count. VEH/Saline n = 3; tBHQ/Saline n = 3; VEH/Virus n = 10; tBHQ/Virus n = 12

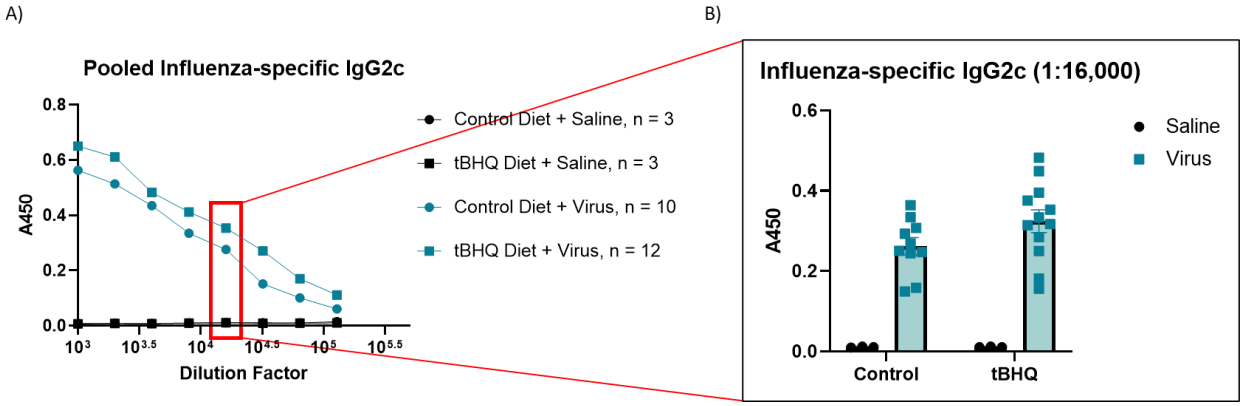

Figure 13: tBHQ did not alter secretion of influenza-specific IgG2c in plasma. Mice were put on a diet with or without 0.0014% tBHQ 2 weeks prior to intranasal instillation with either sterile saline or influenza A/PR/8/34 (H1N1). Ten days post-infection, blood was collected via cardiac puncture and plasma was collected. (A) Serial dilutions of pooled plasma were added to a 96-well plate coated with influenza virus. IgG2c was detected using an HRP-conjugated antibody and quantified using absorbance at 450 nm after addition of TMB substrate. (B) Relative influenza-specific IgG2c levels in individual plasma samples were determined as in (A) at a dilution of 1:16000. VEH/Saline n = 3; tBHQ/Saline n = 3; VEH/Virus n = 10; tBHQ/Virus n = 12

tBHQ Correlated with Increased Expression of CTLA-4 and IL-10 in Lungs of Infected Animals

In addition to activation and effector molecules, we also considered immunoinhibitory mechanisms by which tBHQ could impair the immune response to influenza. We chose CTLA-4 and IL-10 as targets of interest since it is known that they

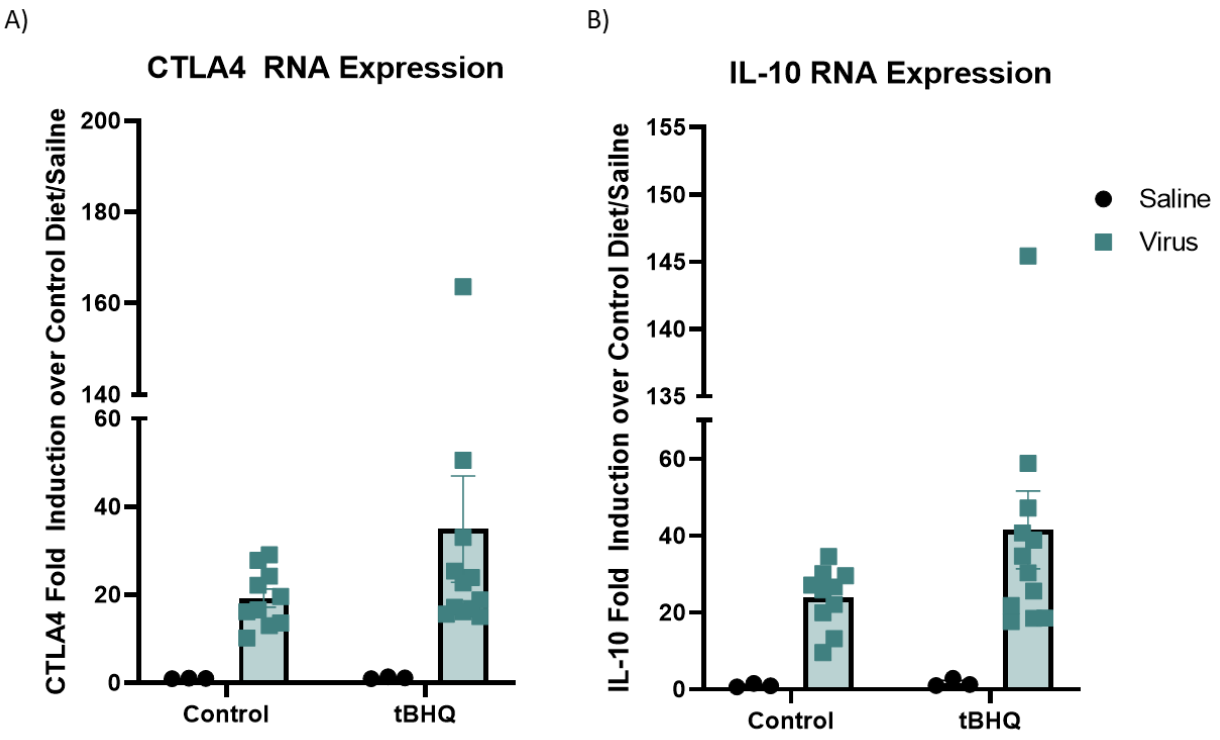

Figure 14: Mice on a low-dose tBHQ diet exhibited elevated mRNA expression of CTLA4 and IL-10 in lungs. Mice were put on a diet with or without 0.0014% tBHQ 2 weeks prior to intranasal instillation with either sterile saline or of influenza A/PR/8/34 (H1N1). Ten days post-infection, lungs were removed and homogenized. Real-time PCR was used to quantify CTLA4 and IL-10 mRNA from the lung homogenate. VEH/Saline n = 3; tBHQ/Saline n = 3; VEH/Virus n = 10; tBHQ/Virus n = 12

can impair T cell activation and have demonstrated immunosuppressive roles during influenza infection.[382,383] mRNA analysis revealed a trend toward enhanced expression of CTLA-4 (Figure 14A) and IL-10 (Figure 14B) in whole lung RNA from animals on the tBHQ diet, suggesting tBHQ may inhibit T cell activation through enhancement of immunosuppressive pathways.

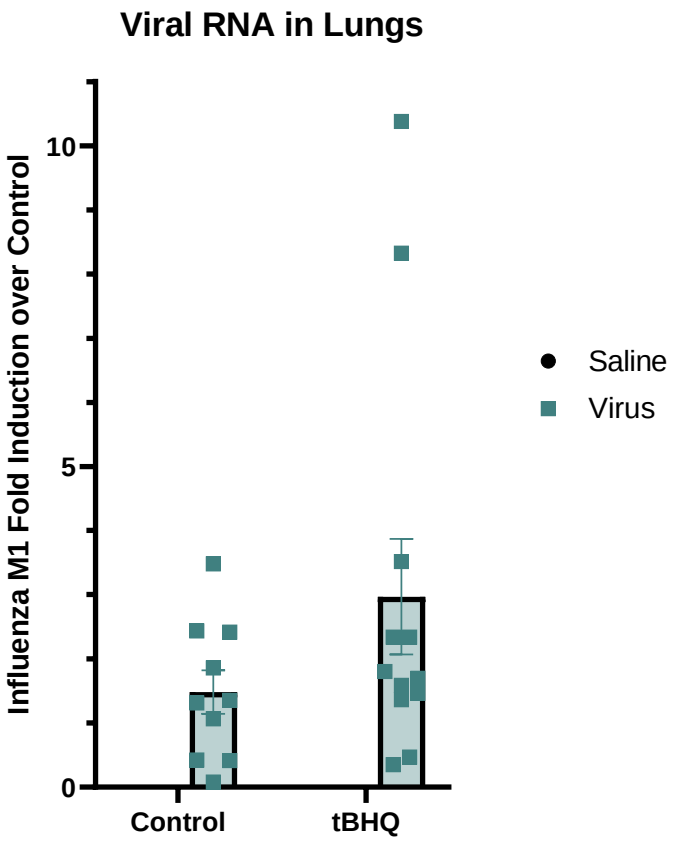

Figure 15: tBHQ associated with increased viral titer in the lungs of infected mice. Mice were put on a diet with or without 0.0014% tBHQ 2 weeks prior to intranasal instillation with either sterile saline or influenza A/PR/8/34 (H1N1). Ten days post-infection, lungs were removed and homogenized. Real-time PCR was used to quantify viral RNA from the lung homogenate. The viral matrix protein, M1, was used for viral quantification and was normalized to the housekeeper gene RPL13a. VEH/Saline n = 3; tBHQ/Saline n = 3; VEH/Virus n = 10; tBHQ/Virus n = 12

tBHQ Exposure Correlated with Slow Viral Clearance

We next assessed viral clearance. Ten days post-infection, we analyzed viral RNA levels in the lung using primers to amplify viral M1 RNA. We saw a 2-fold increase in viral RNA in animals fed tBHQ, though there was a lot of variability in response and therefore the effect was not statistically significant (Figure 15).

Dietary tBHQ caused Enhanced Lymphocytic Infiltration that Penetrated Deeper in the Lungs of Infected Mice

Hematoxylin and eosin staining of the left lung revealed that mice on the tBHQ diet had more pronounced lymphocytic infiltration at both proximal (Figure 16C) and distal (Figure 16F) sites within the lung compared to mice on a control diet (Figure 16B, D). Additionally, mice on the tBHQ diet had more severe virus-induced alveolitis in the proximal section (Figure 16C) compared with mice on the control diet (Figure 16B). All mice on the tBHQ diet had marked bronchointerstitial pneumonia while mice on the control diet all had moderate bronchointerstitial pneumonia (Figure 16G).

tBHQ Enhanced Virus-induced Mucous Cell Metaplasia

Staining of neutral and acidic mucus proteins with AB/PAS revealed the enhanced presence of mucosubstances in the airways of mice on the tBHQ diet (Figure 17). Notably, the mucous cell metaplasia spread deeper into the airways of mice on the tBHQ diet, as evidenced by the positive staining in the 11th airway generation in mice on the tBHQ diet (Figure 17F) but not in mice on the control diet (Figure 17E).

tBHQ Exacerbated Perivascular Eosinophilia in the Lungs of Infected Mice

Immunohistochemical staining for major basic protein allowed detection of eosinophils within the lungs. While influenza infection caused a modest increase in perivascular eosinophilic inflammation in the lungs (Figure 18B,E), tBHQ exacerbated this effect, resulting in substantial eosinophilic inflammation around the pulmonary arteries and alveolar parenchyma in mice on the tBHQ diet (Figure 18C,F).

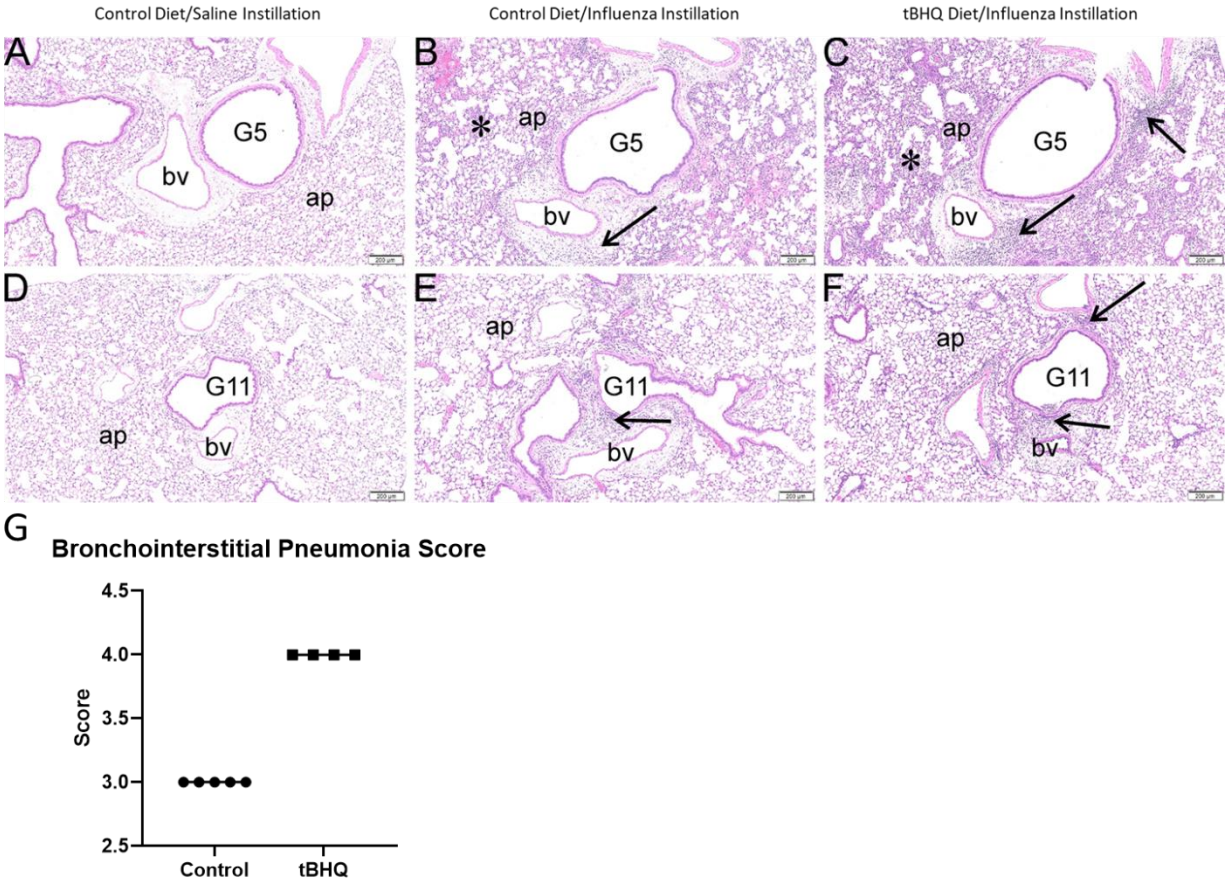

Figure 16: Dietary tBHQ caused enhanced lymphocytic infiltration that penetrated deeper in the lungs of infected mice. Mice were put on a diet with or without 0.0014% tBHQ 2 weeks prior to intranasal instillation with either sterile saline or influenza A/PR/8/34 (H1N1). Ten days post-infection, lungs were removed and formalin-fixed. Lungs were then sectioned at the 5th and 11th airway generations prior to sectioning and paraffin-embedding. Paraffin-embedded sections were stained with hematoxylin and eosin. Pictured are light photomicrographs of transverse tissue sections at the level of the proximal (generation 5, G5; A, B, C) and distal (generation 11, G11; D, E, F) axial airways in the left lung lobe of mice instilled with saline (vehicle control; A,D; n = 3), virus (B, E; n = 5), or virus + tBHQ diet (C, F; n = 4). bv, blood vessel; ap, alveolar parenchyma; asterisks, virus-induced alveolitis; arrows, virus-induced peri-vascular and peri-airway lymphocytic inflammation. Scale bar = 200 μm. (G) Scores of bronchointerstitial pneumonia, with 3 being moderate and 4 being marked.

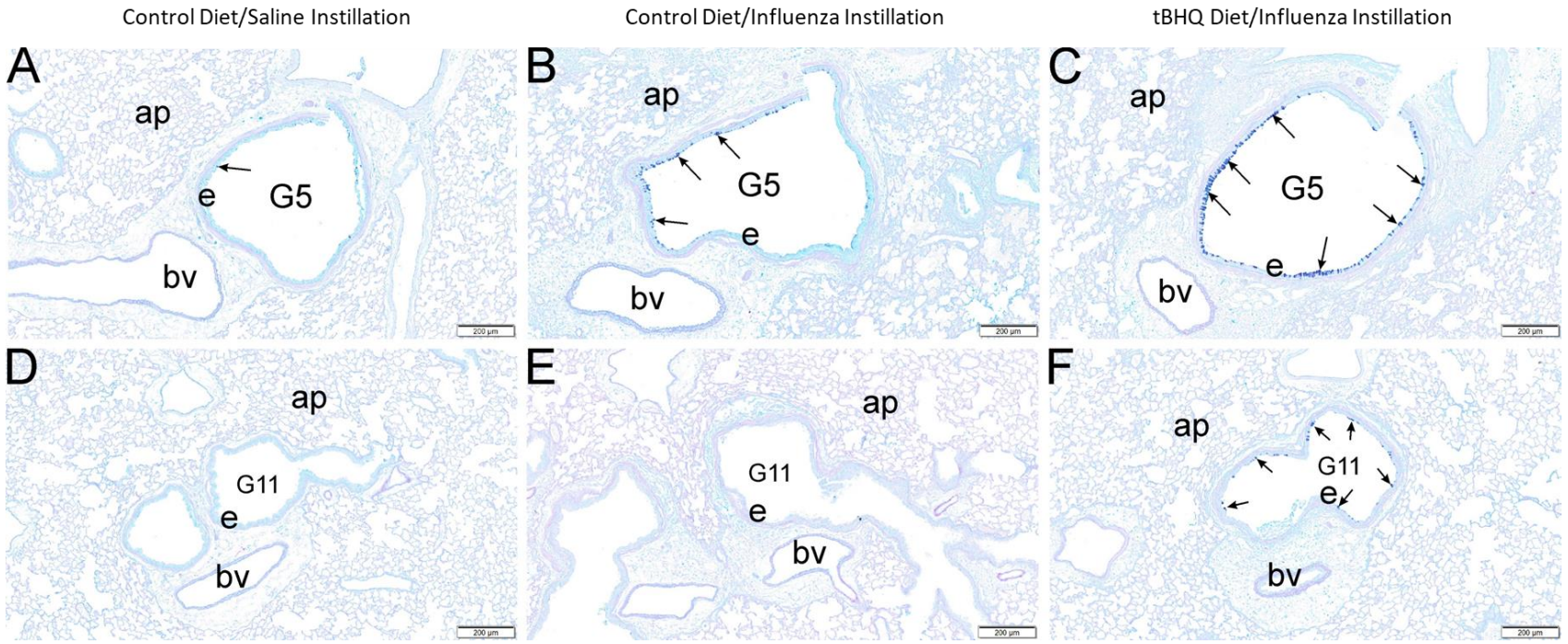

Figure 17: tBHQ enhanced virus-induced mucous cell metaplasia. Mice were put on a diet with or without 0.0014% tBHQ 2 weeks prior to intranasal instillation with either sterile saline or influenza A/PR/8/34 (H1N1). Ten days post-infection, lungs were removed and formalin-fixed. Lungs were later sectioned at the 5th and 11th airway generations. Tissue sections stained with Alcian Blue (pH 2.5)/Periodic Acid Schiff (AB/PAS) to identify acidic and neutral mucosubstances in mucous (goblet) cells (arrows) of airway epithelium (e). Pictured are light photomicrographs of transverse tissue sections of the proximal (generation 5, G5; A, B, C) and distal (generation 11, G11; D, E, F) axial airways in the left lung lobe from mice instilled with saline (vehicle controls; A,D; n = 3), virus (B, E; n = 5),or virus + tBHQ diet (C, F; n = 4). bv, blood vessel; ap, alveolar parenchyma. Little or no AB/PAS-stained mucosubstances in airway epithelium of control mouse (A, D). Conspicuous mucous cells (mucous cell metaplasia) in virus-instilled airways (B, C, F). Scale bar = 200 µm

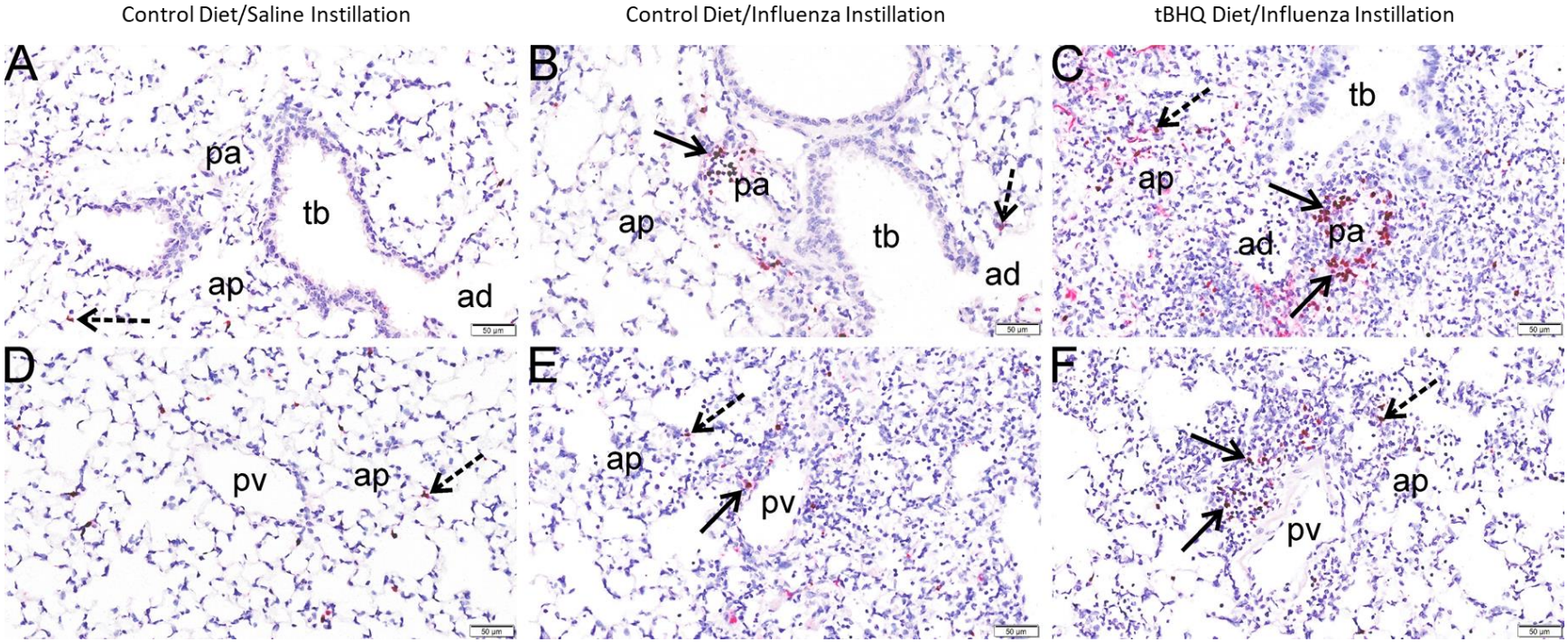

Figure 18: tBHQ exacerbated perivascular eosinophilia in the lungs of infected mice. Mice were put on a diet with or without 0.0014% tBHQ 2 weeks prior to intranasal instillation with either sterile saline or influenza A/PR/8/34 (H1N1). Ten days post-infection, lungs were removed and formalin-fixed. Lungs were later sectioned at the 5th and 11th airway generations. Tissues were immunohistochemically stained for major basic protein-positive eosinophils (red chromagen) and counterstained with hematoxylin. Light photomicrographs of pulmonary arteries (pa; A,B,C) and veins (pv; D,E,F) in the lungs of mice exposed to control diet and saline (A,D), control diet and influenza virus (B,E), or tBHQ diet and influenza virus (C,F). Marked perivascular eosinophilic inflammation after influenza virus + tBHQ exposure (C,F) and similar but less severe influx of eosinophils in the interstitial tissue around pulmonary arteries and veins with virus exposure alone (B,E). No perivascular inflammation was present in saline control mice (A,D). Stippled arrows, eosinophils in alveolar parenchyma (ap); tb, terminal bronchioles; ad, alveolar ducts. Scale bar = 50 μm

tBHQ did not Affect Weight Loss

Common symptoms of influenza infection in mice include loss of appetite accompanied by weight loss. Food consumption for each cage of mice (3 mice per saline cage, 4 mice per virus cage) was monitored from 2 weeks prior to infection up through collection (Figure 19A). However, because not all mice in the virus cages showed signs of infection and mice were not singly-housed, it was impossible to determine the exact amount of food consumed by each mouse. Accordingly, averages were generated which did not account for mice which did not get infected and therefore these data were not used for statistical comparisons, but rather are included to provide an idea of how much tBHQ mice were exposed to during the study. Estimated daily tBHQ consumption was calculated per mouse (Table 3) according to Equation 1, and the daily average was compared against estimates of human exposure in various countries (Figure 19C).[369] Notably, mice in this study were exposed to doses of tBHQ relevant to human exposure according to conservative estimates.[369] Additionally, the calculation relied on the amount of diet consumed by saline-instilled mice over the ten-day period post-instillation. It is important to note that mice infected with influenza stopped eating several days before terminal collection, and it's likely that tBHQ was excreted by day 10 post-infection as tBHQ is readily excreted from the body by phase II conjugation within 1-3 days.[384,385] Additionally, while this study was performed in female mice, it was shown in rats that males more readily absorb tBHQ from the diet than females, suggesting males might be more sensitive to the same dose.[386] Conversely, individual animal weight was monitored daily following infection (Figure 19B). Weight loss during infection was not significantly impacted by dietary tBHQ.

Equation 1: Calculation of Daily tBHQ Intake per Mouse

$$\frac{\text{Food eaten per cage (g)}}{\text{3 mice per cage}} \times \frac{\text{0.014 mg tBHQ}}{\text{1 g food}} \times \frac{\text{1 mouse}}{\text{Average weight of mice in cage (g)}} \times \frac{\text{1000 g}}{\text{1 kg}} = \frac{\text{mg tBHQ}}{\text{kg bodyweight}}$$

Table 3: tBHQ Consumption during Primary Infection (mg/kg)

Primary Exposure with H1N1	Day 0	Day 1	Day 2	Day 3	Day 4	Day 5	Day 6	Day 7	Day 8	Day 9	Day 10
tBHQ Saline	1.54	1.42	1.48	1.61	1.81	1.23	1.92	1.65	1.64	1.89	1.26
tBHQ Virus	1.37	1.35	1.37	1.51	1.31	0.73	0.53	-0.01*	-0.01*	0.16	0.16

* negative values due to error inherent to the scale used for measuring food mass.

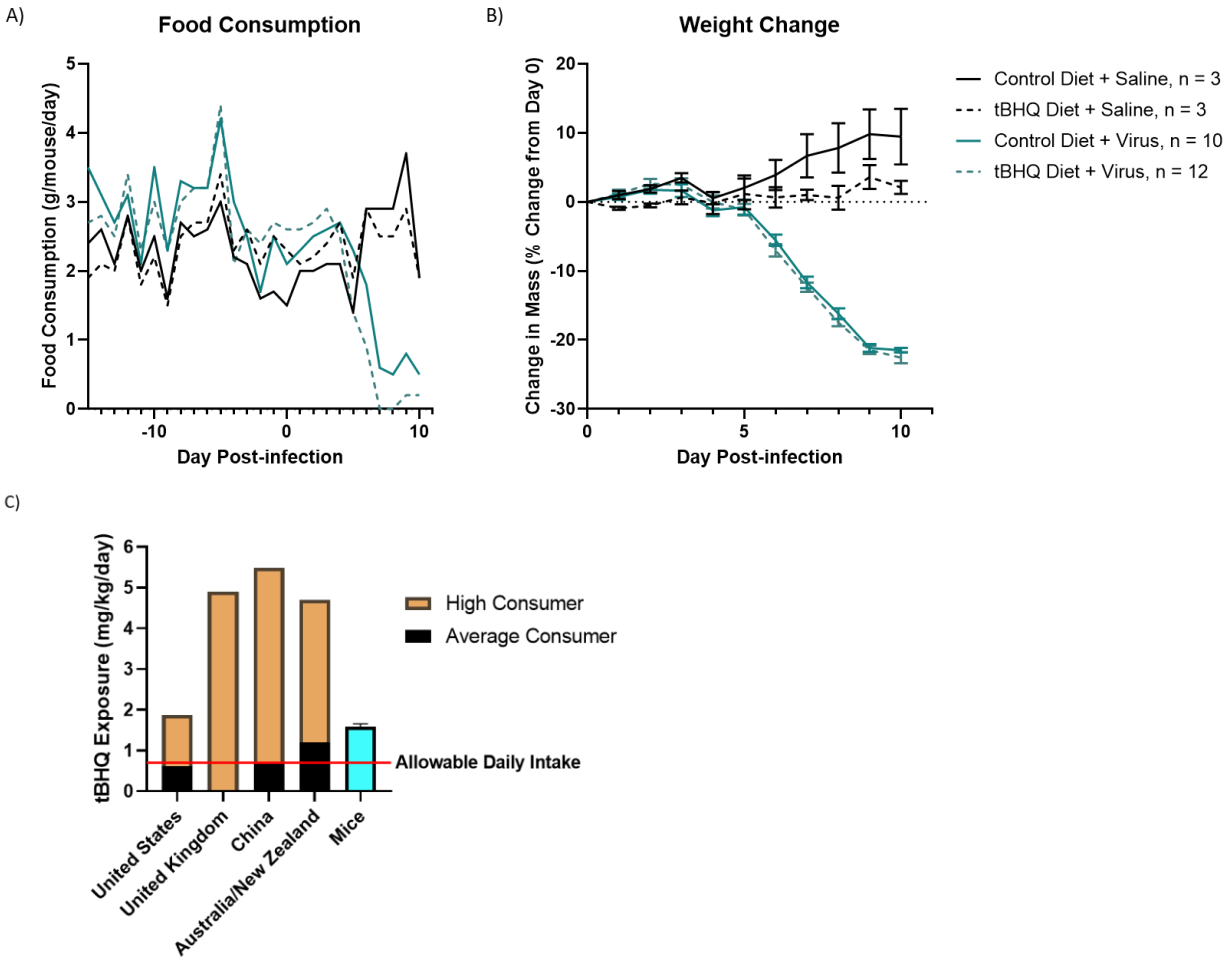

Figure 19: A low concentration of tBHQ in the diet did not affect food consumption or weight change during primary influenza infection. Mice were put on a diet with or without 0.0014% tBHQ 2 weeks prior to intranasal instillation with

Figure 19: (cont'd) sterile saline or influenza A/PR/8/34 (H1N1). Food consumption (A) and body weight (B) were monitored daily up to 10 days post-infection. (C) Average tBHQ intake (mg tBHQ/kg bodyweight/day) of saline-instilled mice was compared against estimates of human tBHQ exposures in various countries.[369]

Discussion

This study is the first to our knowledge to examine the effects of the food additive tBHQ on the T cell response to influenza virus infection *in vivo*. A low, physiologically relevant dose of tBHQ decreased $CD8^+$ T cell infiltration to the lungs and reduced the number of $CD4^+$ and $CD8^+$ T cells with effector phenotype and function in response to influenza infection in mice. Additionally, tBHQ reduced the number of influenza-specific T cells in the draining lymph nodes of infected animals. These effects correlated with a trend in increased viral burden in the lungs of infected animals. While we hypothesized that tBHQ would impair the immune response to influenza infection through inhibition of Th1 cell polarization, that at least at this time point, this was not the case. Interestingly, tBHQ exposure correlated with elevated gene expression of the immunosuppressive proteins, CTLA-4 and IL-10, which may contribute to the suppression of the cytotoxic function of the cytolytic $CD4^+$ and $CD8^+$ T cells. To our knowledge, this is the first study to show CTLA-4 induction by tBHQ, and corroborates *ex vivo* findings showing an increase of IL-10 mRNA in astroglia following tBHQ treatment.[387] Whether this occurs at the protein level and within T cells remains to be seen. Chemical Nrf2 activation of RAW264.7 cells and primary murine dendritic cells enhanced IL-10 production in a Nrf2-dependent manner, and it is likely tBHQ acts on lung macrophages and dendritic cells in this model.[323,388] Notably, these findings correlated with more widespread lymphocytic infiltration, eosinophilia, and mucous cell metaplasia in mice on the tBHQ diet.

In our previous studies, we observed that treatment of Jurkat T cells with tBHQ reduced CD25 surface expression, *ex vivo* treatment of primary human $CD4^+$ T cells with tBHQ decreased CD25 and CD69 expression, and *ex vivo* treatment of murine $CD4^+$ T cells with tBHQ slightly reduced CD69 expression.[300,301,371,372] Consequently, we sought to determine if tBHQ would diminish the surface expression of these activation markers in the context of an acute infection at a dose relevant to human exposure. Consistent with our previous findings in human $CD4^+$ T cells, CD25 surface expression was abrogated in infected mice fed a tBHQ-containing diet. However, CD69 expression was enhanced with tBHQ consumption, especially on $CD8^+$ T cells. Since CD69 is an earlier marker of activation than CD25, these results suggest that tBHQ may be delaying, rather than diminishing, T cell activation in this model.[389]

Another marker of T cell activation which is also used to identify antigen-experienced T cells is the adhesion protein CD44.[381] Like CD25, surface expression of CD44 on $CD4^+$ and $CD8^+$ T cells was substantially reduced in lungs of infected mice exposed to tBHQ. To determine if effector function was likewise suppressed, we looked at surface expression of CD107a, a lysosomal-associated protein which integrates into the plasma membrane upon cytolytic degranulation, and FasL which induces apoptosis in infected cells expressing Fas on their surfaces.[33,390] Surface expression of CD107a was blunted on $CD8^+$ T cells in tBHQ-exposed mice, suggesting that tBHQ not only delays T cell activation, but also suppresses effector function of $CD8^+$ T cells. Furthermore, the numbers of $CD4^+$ and $CD8^+$ T cells expressing FasL on their surfaces were decreased in mice on the tBHQ diet. Taken together, these data suggest that tBHQ impairs the ability of cytotoxic $CD8^+$ and cytolytic $CD4^+$ T cells to clear virus-

infected cells using both cytotoxic granules and Fas/FasL interactions. One recent study showed that siRNA knockdown of Nrf2 in dendritic cells enhanced cytotoxic capacity of T cells; logically, this suggests that activation of Nrf2 would lead to impaired cytotoxic capacity.[287] Therefore, activation of Nrf2 by tBHQ in dendritic cells could contribute to the reduced effector function seen here.

Many published studies using Nrf2 activators, including tBHQ, and genetic modulation of Nrf2 expression suggest that activation of Nrf2 inhibits IFNγ production and Th1 polarization.[287,296,298,301,371,372,391] Therefore, we quantified the number of IFNγ$^+$ and T-bet$^+$ CD4$^+$ T cells in the lungs of infected mice. Unexpectedly, we observed little effect by tBHQ on the numbers of IFNγ$^+$ and T-bet$^+$ CD4$^+$ T cells in the lungs at this timepoint (10 days post-infection). While we did not directly observe evidence of reduced T_H1 polarization, several indicators of a tBHQ-induced type 2 immune response were observed, including mucus hypersecretion in the airways and perivascular eosinophilia. Moreover, a number of other immune parameters were affected by tBHQ, including decreased CD8$^+$ T cell infiltration into the lung, reduced influenza-specific CD4$^+$ and CD8$^+$ T cells in the draining lymph nodes, diminished expression of the activation markers, CD25 and CD44, and lower expression of the cytotoxicity-associated molecules, CD107a and FasL. In addition to these findings, tBHQ was associated with increased expression of CTLA-4 and IL-10 which are known to suppress the immune response to influenza infection.[382,383,392] These findings are consistent with a report that showed tBHQ and another Nrf2 activator, dimethyl fumarate, induced IL-10 in astroglia.[387] Another study showed constitutive activation of Nrf2 by CRISPR/Cas9-mediated knockdown of Keap1 in Jurkat T cells led to

augmented IL-10 production.[299] Additionally, IL-10 is a cytokine secreted by regulatory T cells which are known modulators of cytotoxic T cells during influenza infection.[54,57] In fact, it was previously shown that influenza-specific regulatory T cells prevented the expansion of influenza-specific $CD8^+$ T cells, resulting in impaired effector function without affecting IFNγ production.[57] Additionally, in contrast to the dogmatic role for IL-10 in impairing Th1 polarization, a recent study demonstrated that IL-10 expression by $CD4^+$ T cells impairs the ability of influenza's neuraminidase protein to activate TGF-β early during the immune response, resulting in enhanced T_H1 polarization.[393] Thus, the increased IL-10 expression in mice on the tBHQ diet may also explain why there was no observed difference in $IFN\gamma^+$ $CD4^+$ T cell numbers. While we previously showed that tBHQ suppresses T_H1 polarization, this effect may be offset by the effects of IL-10 and other factors in the context of influenza infection.

Despite the effects noted above, there were no apparent effects of tBHQ on weight loss during infection. This is in agreement with a published study in which mice lacking Nrf2 lost the same amount of weight as wild-type mice upon influenza infection, despite the Nrf2-null mice having a more severe inflammatory response.[365] Despite this, we observed a trend consistent with reduced viral clearance in tBHQ-exposed animals. Additionally, we noted increased lymphocytic infiltration, eosinophilia, and mucous cell metaplasia with tBHQ exposure which penetrated further into the lung, indicative of a type 2 inflammatory response. It's previously been shown that influenza infection can lead to the development of asthma and airway allergies, conditions that are characterized by mucous cell metaplasia and eosinophilia like that seen in our model.[394] In support of this, we have seen that the dose of tBHQ used in the current

study exacerbates anaphylaxis in a murine model of food allergy, a T_H2-predominant model (Jin et. al., unpublished data).

Of paramount importance, the dose of tBHQ used in this study equates to roughly 1-2 mg/kg/day (Table 3) which is far below the reported NOAEL (72 mg/kg/day) used to establish the current ADI. Moreover, the dose used in this study is well within the estimated range of human exposures which suggest high consumers of tBHQ could be exposed to 1100% of the ADI, or 7.7 mg/kg/day.[369] Moreover, consumption of tBHQ by mice drops below the ADI during infection, suggesting tBHQ may cause immunotoxic effects at doses below the ADI. Our studies showed that tBHQ consumption at a dose relevant to human exposure diminished $CD8^+$ T cell infiltration to the lung and reduced T cell activation and effector function while promoting eosinophilia and mucous cell metaplasia. These effects correlated with increased viral titer in the lungs of infected animals. It is possible that upregulation of CTLA-4 and IL-10 contribute to the impaired immune response to influenza caused by tBHQ, though further studies are warranted to clarify the role of these proteins in this context. Overall, these studies show that doses of tBHQ relevant to human exposure impair the immune response to primary influenza virus infection.

CHAPTER 3

Dietary *tert*-Butylhydroquinone Impairs the Memory T Cell Response to Heterosubtypic Infection

Abstract

Current seasonal influenza vaccines often exhibit poor efficacy for a variety of reasons and must be administered annually to match circulating influenza strains. Consequently, a universal vaccine providing lasting immunity to a broad range of diverse influenza viruses is highly sought after. Such a vaccine would rely heavily on T cell-mediated heterosubtypic immunity. In our previous works, we demonstrated that the food additive *tert*-butylhydroquinone (tBHQ) impairs human T cell activation, suppresses murine T_H1 $CD4^+$ T cell polarization *ex vivo*, and abrogates the T cell response to primary influenza infection. Accordingly, we hypothesized that tBHQ would impair heterosubtypic immunity to influenza virus infection as T cell activation during primary infection is critical to memory formation. In this study, mice that were exposed to a low dose of tBHQ through the diet lost more weight and recovered more slowly than mice on a control diet following heterosubtypic influenza infection. This delay was associated with an increased number of $FoxP3^+$ $CD4^+$ T cells in the lungs post-infection. Additionally, tBHQ-exposed mice had a reduced number of splenic effector memory cells and influenza-specific T cells 28 days following primary infection, suggesting memory formation was impaired by tBHQ. Ultimately, these studies suggest tBHQ impairs heterosubtypic immunity mediated by T cells which could result in blunted immune responses to universal vaccine candidates.

Introduction

Influenza virus infections have been and continue to be a persistent threat to society, causing hundreds of thousands of hospitalizations and tens of thousands of deaths annually in the United States.[373] Starting in 2010, vaccination against influenza became recommended in the US for all people over the age of 6 months. Following these recommendations, there has been an increase in influenza vaccine coverage of approximately 1.5% per year from 2011-2016.[376] However, the numbers of hospitalizations and deaths have not improved, as just in the 2017/8 season there were 959,000 hospitalizations and 79,400 deaths in the United States.[395] This trend in morbidity translates to the global population as well, with influenza claiming 300,000 - 650,000 lives annually.[11] This suggests that although vaccination coverage is improving, patient outcomes don't necessarily correlate with improved vaccination rates. This warrants further research into what other factors may be contributing to influenza infections/outcomes and factors which may be diminishing vaccine efficacy.

Influenza A virus subtypes are classified by their hemagglutinin (HA) and neuraminidase (NA) residues, of which there are 18 known HA types and 11 known NA types.[7] Current vaccines generate potent antibodies against HA and NA residues on predicted circulating strains of H1N1 and H3N2 which prevent the viruses from infecting host cells. However, these vaccines have limited efficacy due to antigenic drift in the HA and NA residues.[396,397] Additionally, these viruses elicit short-lived memory B cell responses due to their inability to produce long-lived bone marrow plasma cells which were recently shown in a first of its kind study to dwindle within a year of vaccination.[398] Therefore, the ideal vaccine for influenza would provide long-lived immunity against all

drift variants of influenza as well as novel strains arising from antigenic shift.[399] Such a vaccine would rely on the host's ability to recognize and defend against influenza strains which the body has not encountered; this type of memory response is termed heterosubtypic immunity. Heterosubtypic immunity prevents severe infection upon infection with a heterologous strain of virus after immunization in many animal models, and several studies provide evidence to suggest that this phenomenon exists in humans.[74,89,95,179,400] It's currently thought that one of the key cell types behind heterosubtypic immunity are cross-reactive T cells, of both the $CD4^+$ and $CD8^+$ lineage, which recognize epitopes from conserved internal proteins in the influenza viruses.[93,119,120,122] Accordingly, if something were to interfere with the function of these T cells, it would follow that heterosubtypic memory would be impaired.

Our lab has demonstrated that the widely-used food additive, *tert*-butylhydroquinone (tBHQ), affects T cell function. Specifically, we have shown that tBHQ impairs the differentiation of murine $CD4^+$ T cells into T_H1 cells while promoting T_H2 polarization, and tBHQ impairs activation and subsequent cytokine secretion in both primary human and Jurkat T cells.[296,300,301,371,372] Notably, these effects were largely dependent on the ability of tBHQ to activate the stress-activated transcription factor, nuclear factor erythroid 2-related factor 2 (Nrf2). Under basal conditions, Nrf2 undergoes rapid degradation via the 26S proteasome due to repression via its repressor protein, Kelch-like ECH-associated Protein 1 (Keap1), an adaptor protein for an E3 ubiquitin ligase.[206,208,209,211] tBHQ is a potent activator of Nrf2, and acts through modifying cysteine residues on Keap1.[253] These interactions result in a conformational change in Keap1 that prevents degradation of Nrf2 and thus allow Nrf2 to accumulate in

the nucleus of the cell, where it enhances the transcription of antioxidant and phase II metabolism genes that contain an antioxidant response element (ARE) within their regulatory regions.[204] Typically, activation of Nrf2 is considered beneficial to the host, as it results in detoxification of xenobiotics, resolves oxidative stress, and ameliorates inflammation.[401] Indeed, modulation of Nrf2 through chemical and genetic means yields favorable outcomes in many disease models, including intestinal and pulmonary fibrosis, allergic asthma, liver injury, and multiple autoimmune disorders.[295,307,403,404,308,309,314,339,343–345,402] However, the prominent role of $CD4^+$ T cells, specifically T_H1 cells, in promoting memory to influenza and our data suggesting tBHQ impairs T_H1 polarization led us to hypothesize that exposure to tBHQ would impair the immune response to heterosubtypic influenza infection. In this study, we aimed to address the effects of low-dose tBHQ consumed through the diet on the immune response to heterosubtypic influenza infection.

Materials and Methods

Materials

Unless otherwise stated, all materials were purchased from Sigma Aldrich (St. Louis, MO).

Animals, Diets, and Viruses

12-week-old female C57BL/6J mice were purchased from Jackson Laboratories (Bar Harbor, ME). Upon arrival, mice were housed in groups of 3-4 mice per cage and fed AIN-93G purified rodent diets containing 0 or 0.0014% tBHQ (Dyets Inc.,

Bethlehem,PA) and water *ad libitum.* After 2 weeks of acclimatization to the diets, mice were anesthetized with an intraperitoneal injection of avertin (2,2,2-tribromethanol). After anesthesia was achieved, mice were intranasally instilled with 30 µL of Kilbourne F108: Influenza A/Aichi/2/68 (HA, NA) x A/Puerto Rico/8/34(H3N2), Reassortant X-31(Derived from Mouse-adapted X-31b), NR-3483 (NIH Biodefense and Emerging Infections Research Resources Repository, NIAID, NIH), hereon referred to as x31, at a titer of 9.3×10^3 EID_{50}/mL. This resulted in a total amount of 280 EID_{50} per mouse. Upon recovery from anesthesia, mice were returned to their cages and monitored daily for changes in food consumption and body weight for the duration of the study. 28 days following primary infection, mice were again anesthetized via intraperitoneal injection of avertin. Mice were then infected with 30 µL of influenza A/PR/8/34 (H1N1) at a titer of 2.5×10^2 $TCID_{50}$/mL (7.26 HAU/mL), resulting in a final amount of 7.5 $TCID_{50}$ (0.218 HAU) per mouse. 7.5 $TCID_{50}$ was used as this was previously determined to be 5x the mouse lethal dose, 50% (mLD_{50}) in naïve mice (data not shown). For all instillations, small groups of mice on each diet were intranasally instilled with 30 µL of sterile saline instead of virus as experimental controls. To assess memory cell populations without reinfection, mice were infected with x31 as above. 28 days post-infection, spleens, lungs, and mediastinal lymph nodes were collected for analysis. Schematics for the two experiments are shown in Figure 20. All animal studies were conducted in accordance with the Guide for Care and Use of Animals as adopted by the National Institutes of Health and were approved by the Institutional Animal Care and Use Committee at Michigan State University.

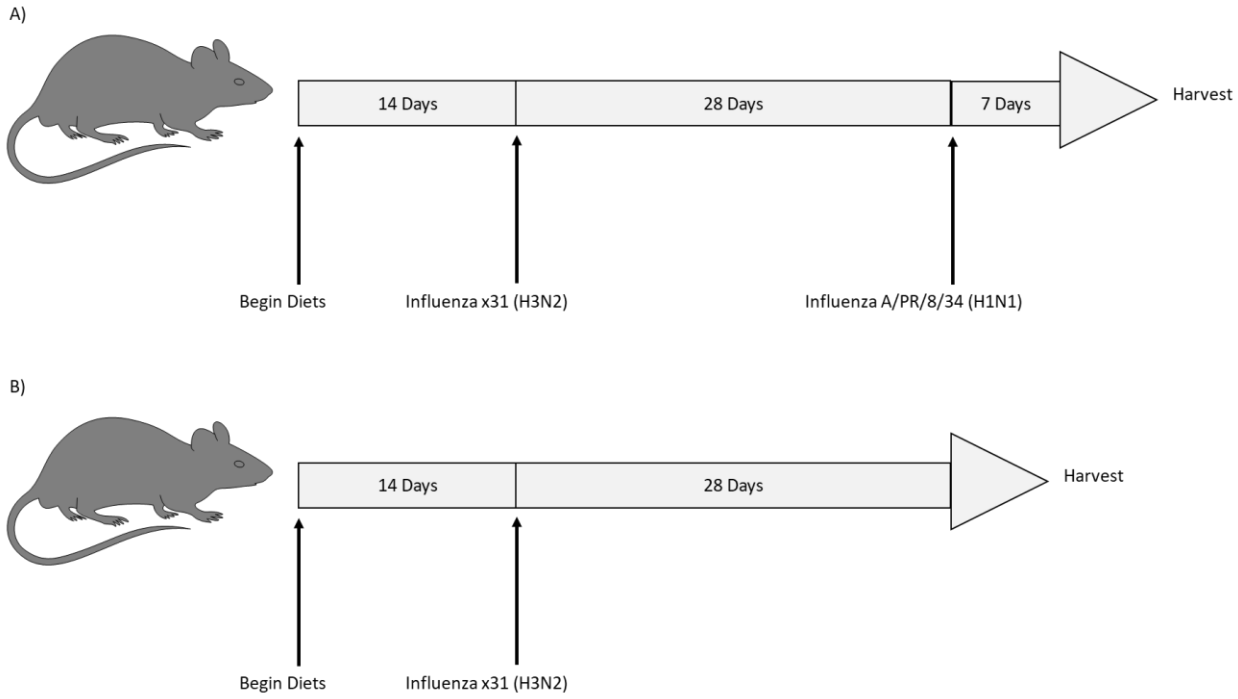

Figure 20: Timelines of heterosubtypic infection model and memory model without reinfection. Mice were received from Jackson Laboratories and fed diets with or without tBHQ for 14 days prior to infection with influenza x31 (H3N2). 28 days later, mice were infected with a high titer of influenza A/PR/8/34 (H1N1) (A) or tissues were collected for analysis of memory T cell populations (B). 7 days following secondary infection, tissues were collected for downstream analyses.

Tissue Collection and Cell Separation

Seven days following secondary infection, mice were anesthetized via intraperitoneal injection of avertin. Mice were then euthanized by cardiac puncture and plasma was collected. Following euthanasia, bronchoalveolar lavage fluid (BALF) was collected by cannulating the trachea and flushing the lungs with 1 mL of sterile saline. Subsequently, mediastinal lymph nodes (MLN) and lungs were collected. For assessment of memory cell populations without reinfection, mice were euthanized via exsanguination from the inferior vena cava. Lungs, spleens, and mediastinal lymph nodes were removed for processing.

Lungs were placed in 5 mL of DMEM containing 1 mg/mL collagenase D and subsequently dissociated with the gentleMACS dissociator (Miltenyi Biotec, Auburn, CA). After dissociation, 1 mL of lung homogenate centrifuged and resuspended in TRIzol reagent RNA analysis. The red blood cells were lysed in the remaining lung homogenate with ACK lysis medium (Lonza, Morristown, NJ) and the remaining cells were used for FACS analysis. Cells from the MLN were isolated by grinding the MLN between the frosted ends of two microscope slides, and subsequently used for FACS analysis. BALF and plasma were centrifuged, and supernatants were stored at -80 °C to await further use. Spleens were place in culture dishes with 10 mL of DMEM and mashed with the plungers of 10 mL syringes. The remaining cell suspension was transferred through a 40 μm strainer, then the culture dish was washed with another 5 mL of DMEM and this was transferred through the strainer as well. Cells were washed twice, and red blood cells were lysed with ACK lysis medium prior to staining cells in tandem with lung and lymph node cells.

Immunophenotyping

Following collagenase digestion and dissociation with the gentleMACS dissociator, lung cells were washed in PBS. Cells were stained with the Zombie Aqua Fixable Viability Kit (BioLegend, San Diego, CA) per the manufacturer's protocol, then washed with FACS buffer (1% FBS in PBS). Cells were then incubated with Fc block (BD Pharmingen, San Diego, CA) for 10 minutes prior to labeling with antibodies against CD4, CD8α, CD25, CD69, CD44, CD62L, CD107a, and FasL (Table 4). Cells were then fixed with a 4% formaldehyde fixative. FACS analysis was conducted on the

Attune NxT (Thermo Scientific, Waltham, MA). For assessment of memory populations without reinfection, cells from spleens, lungs, and mediastinal lymph nodes were incubated with Fc block prior to staining with fluorescent antibodies against CD4, CD8α, CD44, CD62L, CD127 (IL-7Rα), KLRG1, and CX3CR1 in conjunction with tetramers to identify influenza-specific $CD4^+$ and $CD8^+$ T cells. Cells were then permeabilized with the FoxP3/transcription factor staining buffer set (eBioscience) and labeled with antibodies against T-bet and FoxP3 (Table 4). Cells were fixed prior to FACS analysis on the Attune NxT.

Table 4: Flow Cytometry Antibodies for Memory Response Analyses

Antibody Target	Fluorochrome	Source
CD4	FITC	eBioscience
CD4	AF647	BioLegend
CD4	PE/Cy7	eBioscience
CD8a	PerCP/Cy5.5	BioLegend
CD8a	PE	BioLegend
CD8a	PE/Cy5.5	eBioscience
CD19	FITC	BioLegend
CD25	APC	BioLegend
CD44	APC/Cy7	BioLegend
CD44	BV605	BioLegend
CD62L	Pacific Blue	BioLegend
CD69	AF700	BioLegend
CD107a	PE/Cy7	BD Pharmingen
CD127 (IL-7Ra)	APC/Cy7	BioLegend
CX3CR1	PerCP/Cy5.5	BioLegend
FasL	PE	BioLegend
FoxP3	AF647	BioLegend
FoxP3	AF700	BioLegend
Granzyme B	FITC	eBioscience
IFNγ	APC	BioLegend
KLRG1	PE/eFluor610	eBioscience
T-bet	PE	eBioscience
T-bet	BV711	BioLegend
CD4 Tetramer	PE	NIH Tetramer Core
CD8 Tetramer	AF647	NIH Tetramer Core

Ex Vivo Stimulation and Intracellular Labeling following Heterosubtypic Infection

24 hours before the collection, $CD11c^+$ dendritic cells were isolated from the spleens of untreated C57BL/6J mice using positive selection (Miltenyi Biotec). Dendritic cells were plated at a density of 4×10^5 cells/mL in RPMI 1640 supplemented with 10% fetal bovine serum, 25 mM HEPES, 1 mM sodium pyruvate, 1x nonessential amino acids, and 100 U/mL penicillin and streptomycin. Influenza A $NP_{366-374}$ (ASNENMETM) and influenza A $NP_{311-325}$ (QVYSLIRPNENPAHK) peptides were synthesized (New England Peptide, Inc., Gardner, MA) and added to the dendritic cells at a concentration of 1 μM. 24 hours later, single-cell suspensions from the lungs of infected mice were co-cultured with the dendritic cells for 5 hours in the presence of monensin (BioLegend). Cells were labeled with the Zombie Aqua kit prior to being labeled for surface markers (CD4 and CD8α) and permeabilized with the FoxP3/transcription factor staining buffer set. After permeabilization, cells were labeled with antibodies against IFNγ, T-bet, Granzyme B, and FoxP3 (Table 4). After labelling, cells were fixed with 1% formaldehyde fixative prior to FACS analysis on the Attune NxT.

Tetramer Labeling of Mediastinal Lymph Node Cells following Heterosubtypic Infection

To identify influenza-specific $CD8^+$ and $CD4^+$ T cells, the H-2D(b) Influenza A $PA_{224-233}$ SSLENFRAYV (Alexa 647-Labeled MHC-I Tetramer) and I-A(b) Influenza A $NP_{311-325}$ QVYSLIRPNENPAHK (PE-labeled MHC-II Tetramer) tetramers were used. The tetramers were prepared by the NIH Tetramer Core Facility (Atlanta, GA). To identify influenza-specific $CD4^+$ T cells, MLN cells were labeled with CD4 (AF647) and the NP tetramer. For influenza-specific $CD8^+$ T cells, MLN cells were labeled with

CD19, CD8α (PE), and the PA tetramer; influenza-specific $CD8^+$ T cells were identified as viable $CD8\alpha^+$ $CD19^-$ PA-$tetramer^+$ cells. Both panels were also labeled for viability with the Zombie Aqua kit, as above. Cells were fixed with a 4% formalin solution prior to analysis on the Attune NxT.

Detection of Influenza-specific Antibodies

Influenza-specific IgG2c ELISAs were performed following a previously published protocol.[380] Briefly, high-binding plates (Corning, Inc., Kennebunk, ME) were coated with 40 HAU of influenza A/PR/8/34 (H1N1) diluted in 1x coating buffer. Plates were blocked with 10% BSA, and plasma was diluted 1:16000 and added to the wells. Influenza-specific IgG2c was quantified using an HRP-conjugated antibody against IgG2c (Abcam, Cambridge, MA) followed by the addition of TMB substrate. Absorbance was quantified at 450 nm on a Tecan Infinite M1000 Pro Microplate Reader (Tecan, San Jose, CA).

RNA Isolation and Quantitative PCR

RNA was isolated from lung homogenate using TRIzol reagent per the manufacturer's protocol (Life Technologies, Grand Island, NY). RNA was quantified with the Nanodrop 2000c spectrophotometer (Thermo Fisher Scientific, Waltham, MA). Following reverse transcription, cDNA was quantified with real-time PCR SYBR green analysis using the QuantStudio 7 Flex Real-Time PCR System (Applied Biosystems, Foster City, CA). Ribosomal protein L13A (RPL13A) served as the endogenous control

and relative mRNA expression was calculated using the ΔΔCt method. Primer sequences are listed in Table 5.

Table 5: CTLA-4 and RPL13a Primer Sequences

Gene	Forward Primer Sequence	Reverse Primer Sequence
CTLA-4	CATGTACCCACCGCCATACT	CCAAGCTAACTGCGACAAGG
RPL13a	GTTGATGCCTTCACAGCGTA	AGATGGCGGAGGTGCAG

Statistical Analysis

The mean ± SEM was determined for each treatment group in individual experiments. The virus-infected VEH and tBHQ groups were compared against each other using two-tailed Student's T-tests with Sigma-Plot 12.3 software (Systat Software, San Jose, CA). Animals which showed no signs of infection were excluded from statistical analyses. Additionally, saline-instilled animals were not used for statistical analyses as their role in the present study was to provide context about the magnitude of the T cell response during influenza infection.

Results

Mice on a tBHQ Diet Suffered More Severe Weight-loss Following Heterosubtypic Challenge

Following heterosubtypic challenge with a lethal titer of influenza A/PR/8/34 (H1N1), mice were weighed daily. Mice on the tBHQ diet had more severe weight loss and took several days longer to begin recovering from the infection compared to mice on a control diet (Figure 21).

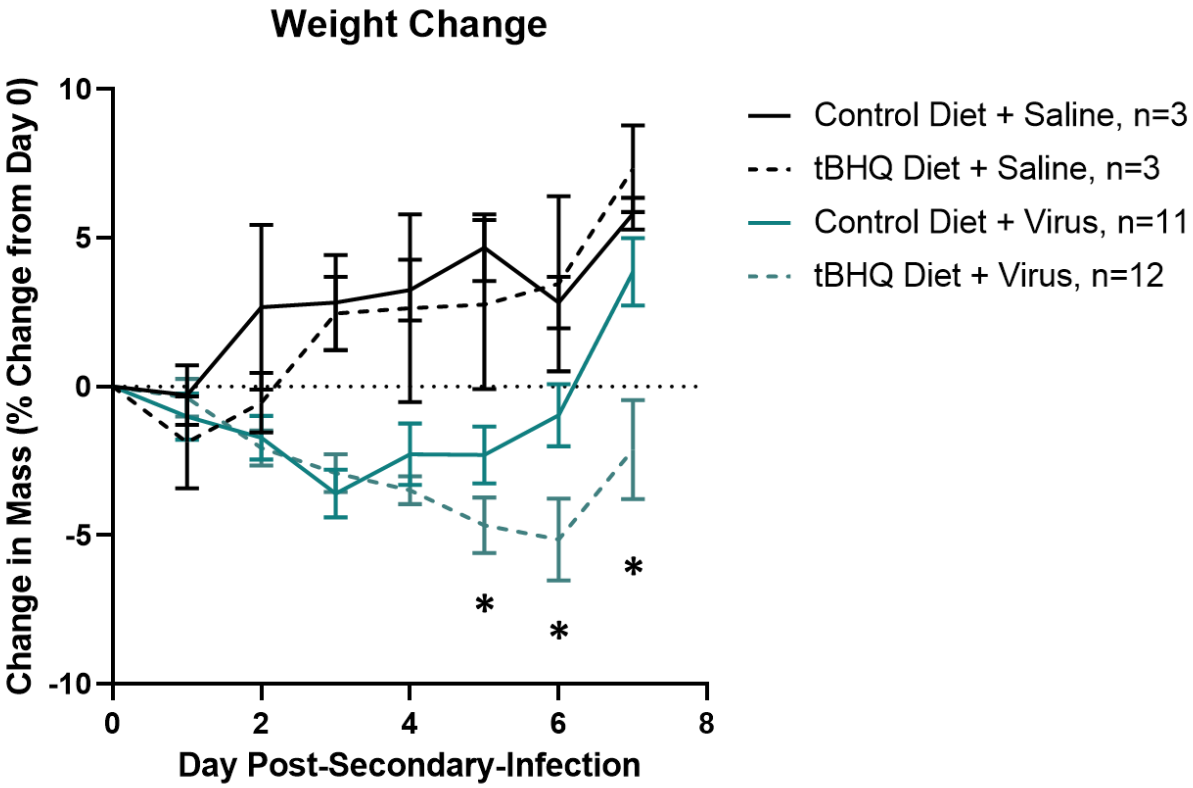

Figure 21: tBHQ exposure caused in a delayed recovery following heterosubtypic infection. Mice were fed diets with or without 0.0014% tBHQ prior to sublethal infection with influenza x31 (H3N2). 28 days post-infection, mice were infected again with 5 mLD_{50} of influenza A/PR/8/34 (H1N1) and body weight was recorded over the following 7 days. * $p < 0.05$ (Student's t-test) between control and tBHQ treatments within virus-infected mice.

tBHQ did not Affect T Cell Infiltration in the Lungs of Infected Mice

Seven days following secondary infection with influenza A/PR/8/34 (H1N1), lungs were collected and dissociated for immunophenotyping. The resulting single-cell suspension was labeled with fluorescent antibodies against CD4 and CD8α, and cells were quantified via flow cytometry. No significant differences were observed between the number of $CD4^+$ or $CD8^+$ cells within the lungs (Figure 22).

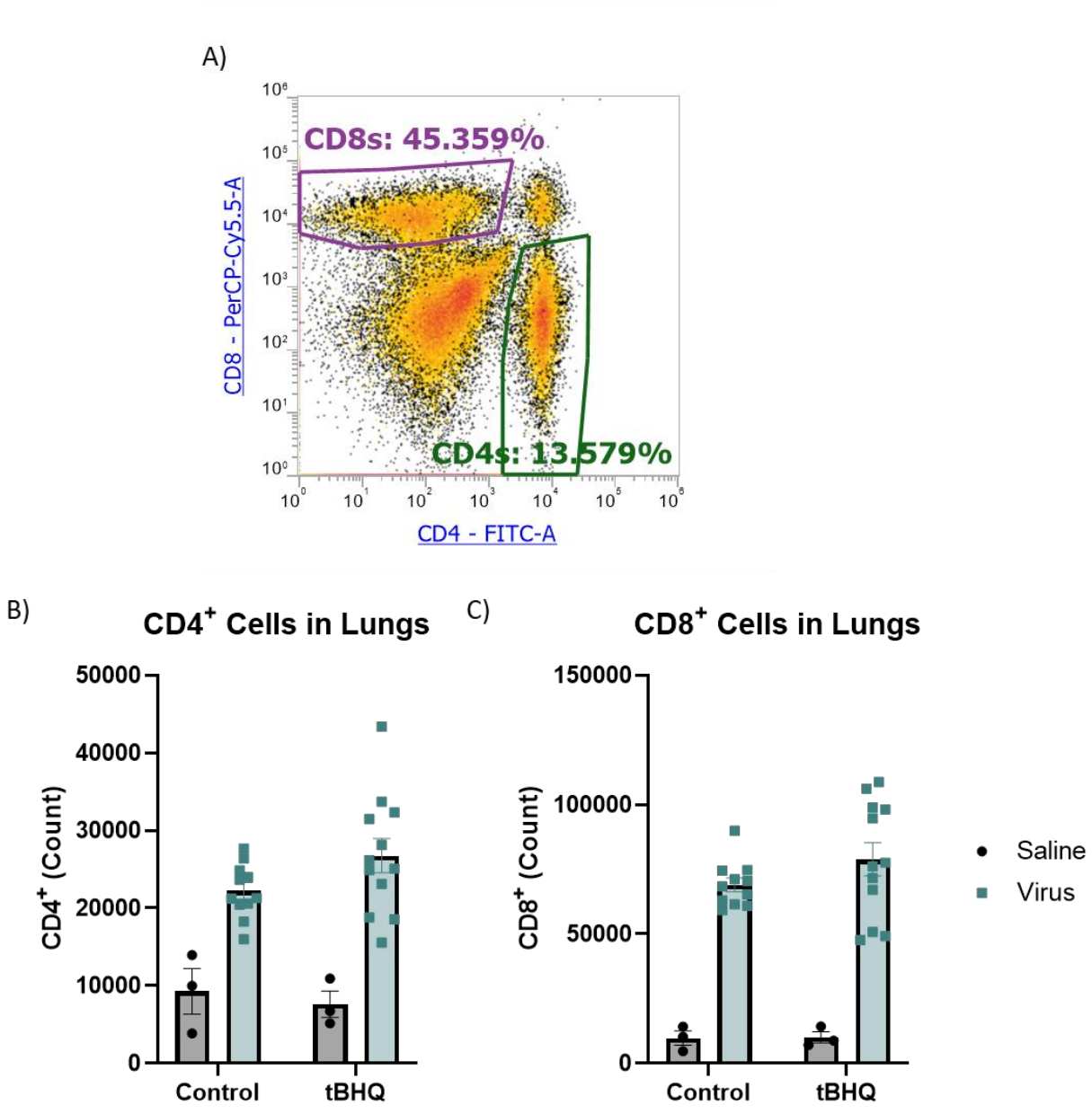

Figure 22: tBHQ exposure did not alter CD4⁺ or CD8⁺ numbers in the lungs after heterosubtypic infection. Mice were fed diets with or without 0.0014% tBHQ prior to sublethal infection with influenza x31 (H3N2). 28 days post-infection, mice were infected again with 5 mLD_{50} of influenza A/PR/8/34 (H1N1). Seven days post-infection, lungs were removed and homogenized. Lung homogenates were labeled with fluorescent antibodies against CD4, CD8α, and CD44. Cells were quantified via flow cytometry. (A) Representative density plot demonstrating CD8α and CD4 populations. (B) Quantification of $CD4^+$ cells. (C) Quantification of $CD8^+$ cells.

tBHQ Exposure was Associated with a Decrease in the Number of Influenza-Specific T Cells in the Lymph Nodes of Infected Mice

In addition to T cells within the lung, we used fluorescent peptide-loaded MHC-I and MHC-II tetramers in addition to antibodies against CD4 and CD8α to identify influenza-specific T cells from the MLNs of infected mice. While not statistically significant, tBHQ-exposed animals showed a trend toward decreased influenza-specific T cells, especially within the $CD4^+$ population (Figure 23) which was consistent with what we previously observed during primary infection.

tBHQ did not Reduce the Number of IFNγ$^+$ or T-bet$^+$ T Cells or Downstream Production of IgG2c

Seven days after heterosubtypic challenge, single-cell suspensions from lung homogenates were co-cultured with peptide-pulsed dendritic cells for five hours in the presence of monensin. Following restimulation, the cells were labeled with fluorescent antibodies against CD4, CD8α, IFNγ, and T-bet (Figure 24A-C). No significant differences were detected in the number of $IFN\gamma^+$, $T\text{-}bet^+$, or $IFN\gamma^+T\text{-}bet^+$ $CD4^+$ or $CD8^+$ T cells (Figure 24D-F). Additionally, plasma was collected from mice and influenza-specific IgG2c was quantified by ELISA. tBHQ had no effect on the amount of influenza-specific IgG2c in plasma (Figure 24G, H).

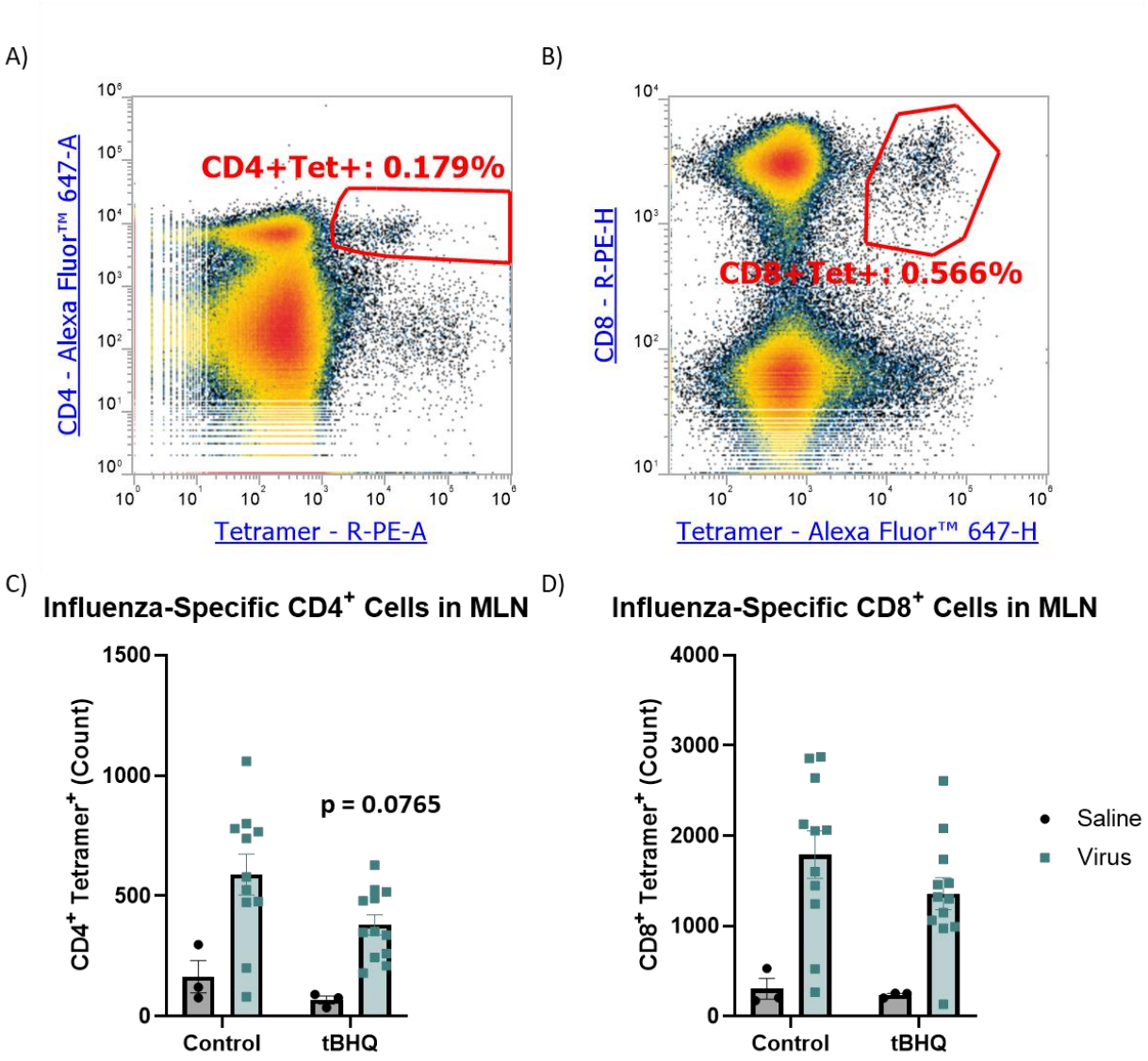

Figure 23: tBHQ exposure was associated with lower frequencies of influenza-specific T cells in mediastinal lymph nodes. Mice were fed diets with or without 0.0014% tBHQ prior to sublethal infection with influenza x31 (H3N2). 28 days post-infection, mice were infected again with 5 mLD_{50} of influenza A/PR/8/34 (H1N1). Seven days post-infection, cells from the mediastinal lymph nodes were labeled with I-A(b) Influenza A $NP_{311-325}$ (PE-labeled MHC-II Tetramer) and a fluorescent antibody against CD4, or H-2D(b) Influenza A $PA_{224-233}$ (Alexa 647-Labeled MHC-I Tetramer) and antibodies against CD19 and CD8α. Cells were quantified via flow cytometry. (A, B) Representative dot plots for each treatment group demonstrating influenza-specific $CD4^+$ or $CD8^+$ T cells. (C) Quantification of influenza-specific $CD4^+$ T cells. (D) Quantification of influenza-specific $CD8^+$ T cells.

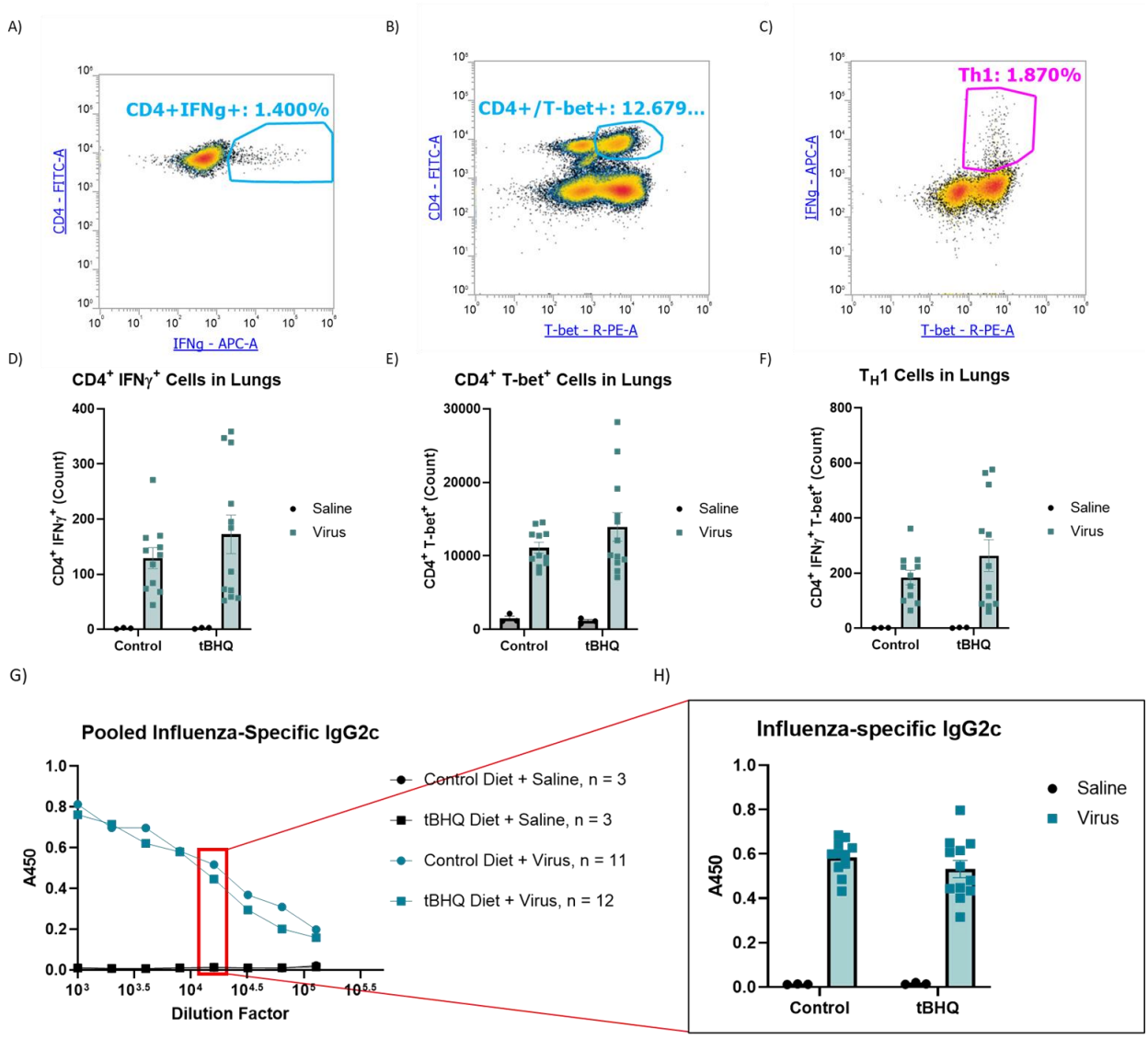

Figure 24: tBHQ exposure had no discernible effect on T_H1 cell polarization or function. Mice were fed diets with or without 0.0014% tBHQ prior to sublethal infection with influenza x31 (H3N2). 28 days post-infection, mice were infected again with 5 mLD_{50} of influenza A/PR/8/34 (H1N1). Seven days post-infection, lungs were removed and homogenized. The resulting single-cell suspension was co-cultured with influenza-peptide-pulsed dendritic cells in the presence of monensin. 5 hours later, cells were labeled with antibodies against CD4, CD8α, IFNγ, and T-bet. Cells were quantified by flow cytometry. Plasma was also collected and influenza-specific IgG2c was measured via ELISA. (A-C) Representative dot plots showing the number of $CD4^+$ T cells with intracellular IFNγ, T-bet, or both. (D-F) Number of $CD4^+$ T cells with intracellular IFNγ, T-bet, or both. (G) Serial dilutions of pooled plasma were added to a 96-well plate coated with influenza virus. IgG2c was detected using an HRP-conjugated antibody and quantified using absorbance at 450 nm after addition of TMB substrate. (H) Relative influenza-specific IgG2c levels in individual plasma samples were determined as in (G) at a dilution of 1:16000.

tBHQ Augmented the Number of FoxP3$^+$ Regulatory CD4$^+$ T Cells and Gene Expression of Immunosuppressive Proteins in the Lungs of Infected Mice

Cells from the lungs were labeled with a fluorescent antibody against CD4 and were then permeabilized and stained with an antibody against FoxP3. Mice exposed to tBHQ had a greater number of regulatory CD4$^+$ T cells, identified as CD4$^+$ FoxP3$^+$ cells (Figure 25A), in the lungs during heterosubtypic infection compared to mice on a control diet (Figure 25B). Additionally, expression of CTLA-4 mRNA was upregulated in the lungs of infected mice on the tBHQ diet (Figure 25C), but expression of IL-10 mRNA was not significantly enhanced with tBHQ in this model (data not shown).

tBHQ Led to a Reduction in Splenic Influenza-specific T Cells 28 Days After Primary Infection with x31

Analysis of T cells within the lungs 7 days after heterosubtypic challenge revealed no substantial differences in T cell activation or cytotoxic effector function (data not shown). However, this likely could have been due to kinetic differences between the immune responses by control- or tBHQ-fed mice, as mice on the control diet began recovering from infection several days earlier than mice exposed to tBHQ. Therefore, memory T cell populations were assessed within the lungs, mediastinal lymph nodes, and spleens 28 days after primary infection with influenza x31 (H3N2). The first striking difference between the groups was a marked reduction in viable splenocytes in tBHQ-exposed mice (Figure 26A). This finding translated to reductions in the numbers of memory (CD127$^+$) influenza-specific CD4$^+$ T cells (Figure 26D) and CD8$^+$ T cells (Figure 26E), as well. Notably, the percentages of influenza-specific T cells did not vary

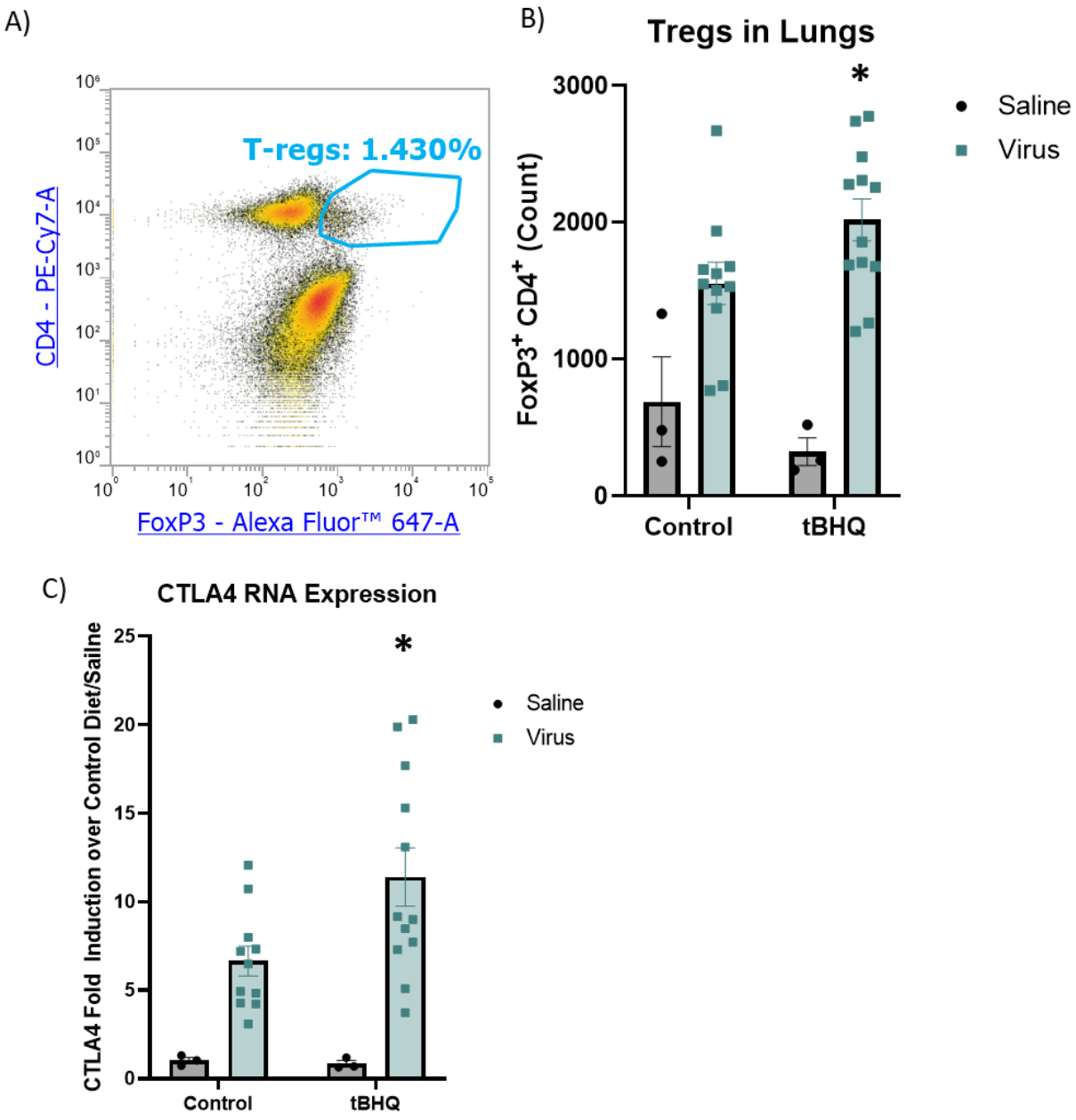

Figure 25: tBHQ enhanced markers of immune suppression within the lungs of mice during heterosubtypic infection. Mice were fed diets with or without 0.0014% tBHQ prior to sublethal infection with influenza x31 (H3N2). 28 days post-infection, mice were infected again with 5 mLD_{50} of influenza A/PR/8/34 (H1N1). Seven days post-infection, lungs were removed and homogenized. The resulting single-cell suspension was co-cultured with influenza-peptide-pulsed dendritic cells in the presence of monensin. 5 hours later, cells were labeled with antibodies against CD4 and FoxP3. Cells were quantified by flow cytometry. Real-time PCR was used to quantify CTLA-4 and IL-10 mRNA from the lung homogenate. * $p < 0.05$ (Student's t-test) between control and tBHQ treatments within virus-infected mice.

between groups (data not shown), suggesting the difference here is due to the generalized depletion of splenocytes and not specific death or lack of differentiation of the memory cell population.

tBHQ Reduced the Splenic Memory Cell Population with the Effector Memory Population Being Most Affected

To determine if memory cell populations were altered, effector memory (EFM) and central memory (CM) cells within the lungs, mediastinal lymph nodes, and spleens were quantified by flow cytometry. It was found that spleens of tBHQ-fed mice were home to fewer effector memory $CD4^+$ (Figure 27D) and $CD8^+$ T cells (Figure 27B) and central memory $CD8^+$ T cells (Figure 27F). Notably, the percentage of effector memory cells compared to total memory $CD8^+$ cells (Figure 27C) was also reduced while the proportion of central memory $CD8^+$ cells was increased (Figure 27G), suggesting tBHQ promotes the generation of central memory cells instead of effector memory cells. Notably, an increase in the proportion of central memory $CD8^+$ T cells was also observed within the lungs (Figure 27G) and the proportion of central memory $CD4^+$ cells was also slightly elevated in the spleens of tBHQ-exposed mice (Figure 27I).

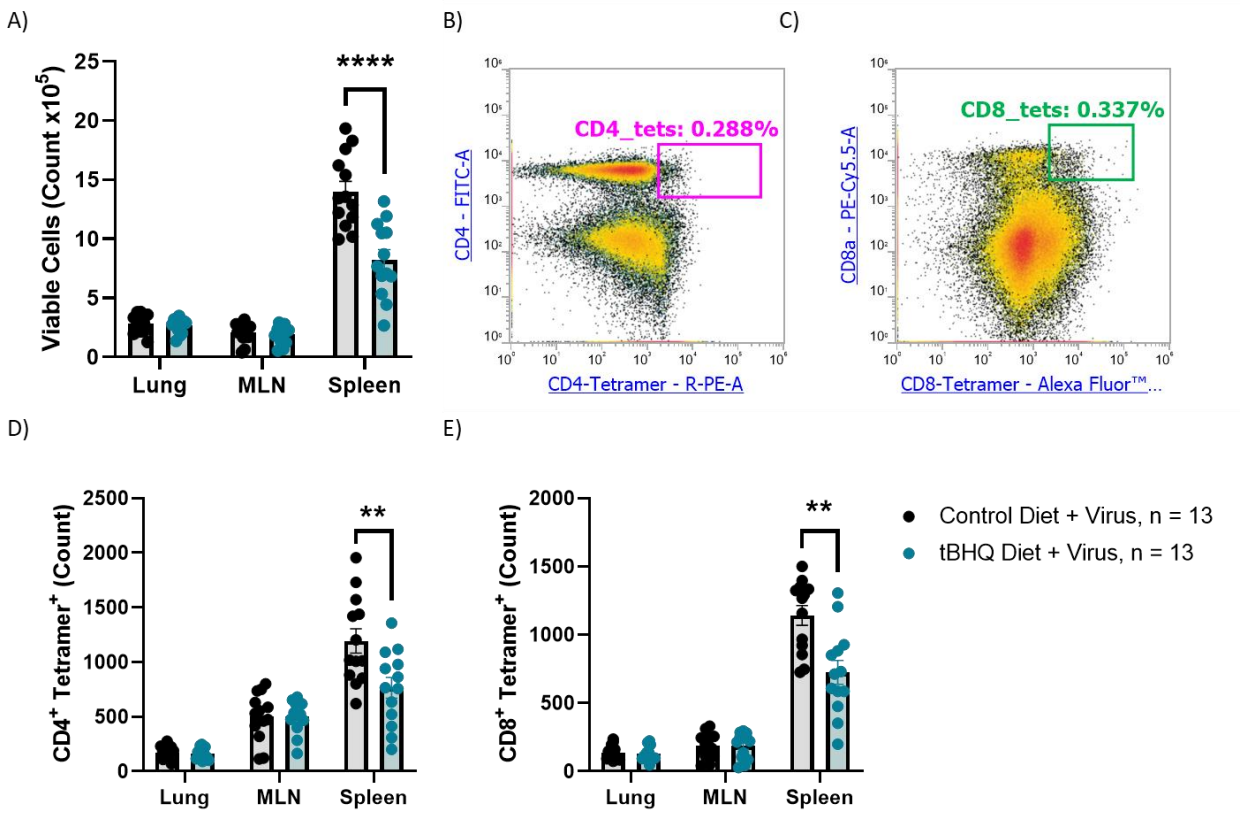

Figure 26: Mice exposed to dietary tBHQ during primary infection with influenza x31 had fewer splenocytes and splenic influenza-specific T cells than control counterparts. Mice were fed diets with or without 0.0014% tBHQ prior to sublethal infection with influenza x31 (H3N2). 28 days post-infection, cells from the lungs, mediastinal lymph nodes, and spleens were labeled with I-A(b) Influenza A $NP_{311-325}$ (PE-labeled MHC-II Tetramer), Influenza A $PA_{224-233}$ (Alexa 647-Labeled MHC-I Tetramer), and antibodies against CD4, CD8α, and CD127. Viable cells (Zombie Aqua-negative) were quantified via flow cytometry. (B, C) Representative dot plots demonstrating influenza-specific $CD4^+$ or $CD8^+$ T cells within the splenic population. Cells were first gated on viability and $CD127^+$ expression. (D) Quantification of influenza-specific $CD4^+$ T cells. (E) Quantification of influenza-specific $CD8^+$ T cells.

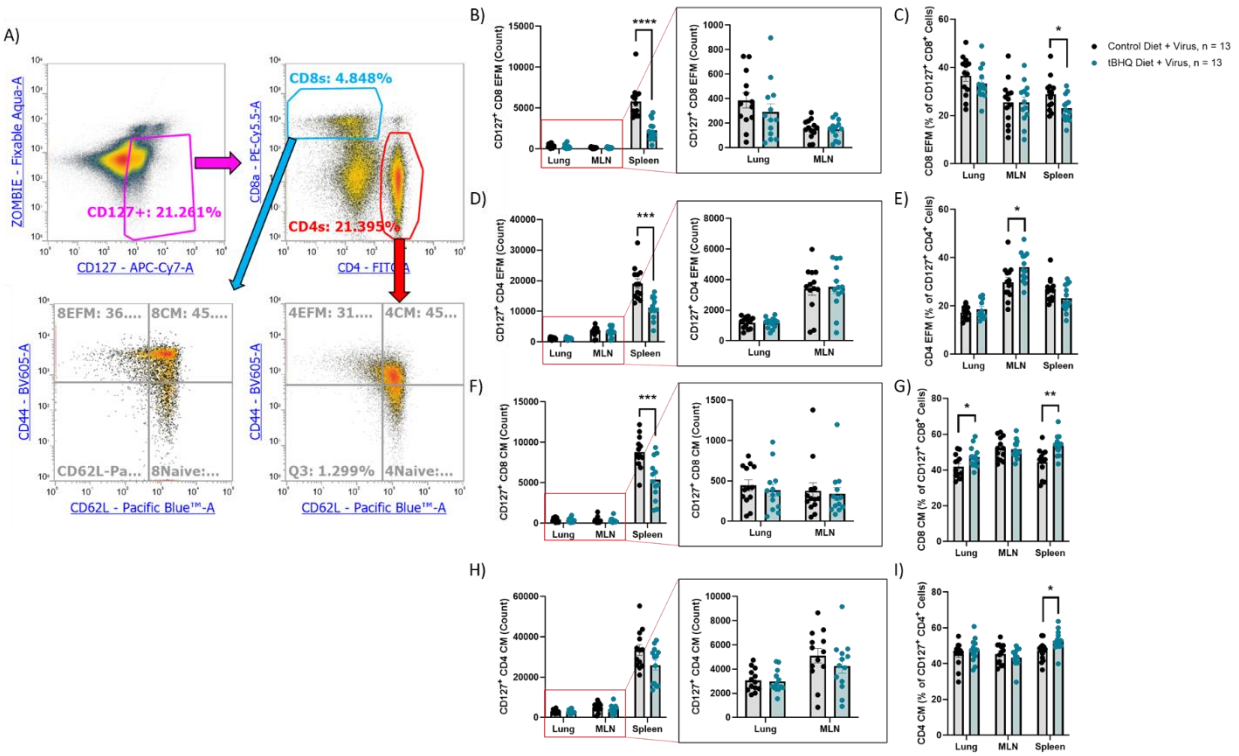

Figure 27: tBHQ altered the frequencies of effector memory and central memory cells following influenza infection. Mice were fed diets with or without 0.0014% tBHQ prior to sublethal infection with influenza x31 (H3N2). 28 days post-infection, cells from the lungs, mediastinal lymph nodes, and spleens were labeled with I-A(b) Influenza A $NP_{311-325}$ (PE-labeled MHC-II Tetramer), Influenza A $PA_{224-233}$ (Alexa 647-Labeled MHC-I Tetramer), and antibodies against CD4, CD8α, CD127, CD44, and CD62L. (A) Gating strategy to identify effector memory ($CD44^{hi}/CD62^{lo}$) and central memory ($CD44^{hi}/CD62L^{hi}$) cells within the $CD4^+$ and $CD8^+$ populations. Standard lymphocyte gating and doublet exclusion was performed prior to generating these plots. (B) Quantification of effector memory $CD8^+$ cells. (C) Effector memory cells expressed as a percentage of $CD127^+$ $CD8^+$ cells. (D) Quantification of effector memory $CD4^+$ T cells. (E) Effector memory cells expressed as a percentage of $CD127^+$ $CD4^+$ cells. (E) Quantification of central memory $CD8^+$ cells. (F) Central memory cells expressed as a percentage of $CD127^+$ $CD8^+$ cells. (G) Quantification of central memory $CD4^+$ T cells. (H) Central memory cells expressed as a percentage of $CD127^+$ $CD4^+$ cells.

Discussion

Previously, we showed that dietary exposure to human-relevant doses of tBHQ led to an impaired T cell response to influenza infection in female C57BL/6J mice. While that study revealed no overt effects on morbidity, we hypothesized that the impaired T cell response would result in the inability to launch an effective memory response to infection with a heterosubtypic strain of influenza virus since $CD4^+$ T cells are vital in formation of heterosubtypic immunity.[37,38,95,122] Accordingly, we fed mice diets with or without tBHQ prior to infection with an H3N2 influenza virus. After recovery, mice were infected with 5 mLD_{50} of an H1N1 virus. Consistent with our hypothesis, mice on the tBHQ diet had a diminished memory response to heterosubtypic infection evidenced by more severe weight loss and delayed recovery following secondary infection.

In contrast with what was seen in our previous study on the effects of tBHQ on the primary immune response to influenza infection, the number of $CD8^+$ cells in the lung was not affected by tBHQ during heterosubtypic infection. In contrast, the trend in influenza-specific T cells in the draining lymph node was consistent in both studies where tBHQ exposure correlated with reduced influenza-specific T cells. Despite several studies suggesting Nrf2 activation suppresses T_H1 polarization, we saw no tBHQ-dependent effect on the number of T_H1 cells or on the amount of influenza-specific IgG2c produced by mice in this study.[287,296,298] However, we did not assess IFNγ or T-bet expression strictly in influenza-specific T cells which could have drastically different phenotypes than bystander T cells. Nevertheless, it is possible that Nrf2 activation does not alter T_H1 cell polarization in this model. In bleomycin-induced

pulmonary fibrosis models, Nrf2 presence was associated with an augmented T_H1:T_H2 ratio compared to Nrf2-null mice which exhibited strong T_H2 inflammatory phenotypes.[295,337] Moreover, Nrf2 may be differentially activated by tBHQ in a heterogenous cell population such as the lung, as the amount of Nrf2 is variable among cell types.[195] Additionally, it is unknown if repeated exposure to tBHQ results in continued Nrf2 activation or if adaptive mechanisms exist that modify the stress response to tBHQ. We were unable to detect upregulation of the Nrf2 target genes NQO1, HMOX1, and GCLC in RNA isolated from whole lung homogenate of tBHQ-exposed saline-instilled animals; however, we frequently observe modulation of immune endpoints *ex vivo* using concentrations of tBHQ below those required to induce canonical Nrf2 target genes (data not shown). Accordingly, further work is required to determine the role of Nrf2 on T_H1 cell polarization and function during influenza infection.

A notable finding of this study was that tBHQ increased the frequency of regulatory T cells (Tregs) within the lung which was accompanied by enhanced expression of the coinhibitory molecule, CTLA4. In an investigation of acute graft-vs-host disease, the Nrf2 activating compound dimethyl fumarate caused a similar induction of Tregs.[391] Genetic activation of Nrf2 restricted to T cells also promoted the development of Tregs.[298] Interestingly, a recent study demonstrated that genetic activation of Nrf2 restricted to Tregs impaired Treg function through metabolic perturbations and promoted inflammation.[302] The role of Nrf2 activation on the development and function Tregs remains largely unexplored, and to our knowledge this is the first study to show tBHQ augments Treg numbers. While Tregs suppress T cell

responses to influenza infection to limit immunopathology, it was also recently shown that memory Tregs promoted efficient clearance of viral infection.[405] Accordingly, more studies are required to determine the role of tBHQ-enhanced Treg accumulation in this model.

The last notable finding of this study was that tBHQ reduced the number of splenic EFM cells following primary infection, which could explain the diminished memory immune response seen with heterosubtypic infection. Notably, in a model of primary infection we showed that tBHQ suppressed the T cell response and was associated with upregulation of anti-inflammatory cytokine expression. Evidence suggests that the formation of effective memory T cell responses relies on inflammatory responses, so the lack of an inflammatory environment during primary infection could likely explain the lack of memory formation seen here.[406] Effector memory cells are well known for being able to rapidly respond to secondary infection through rapid upregulation of cytotoxic effector functions.[117] Consequently, reductions in poised effector memory cells leave the host susceptible to secondary infection with slower memory responses. It must be noted that it was not directly established in these studies that the reduced EFM population was responsible for the weakened memory response observed, as tBHQ was administered for the duration of the secondary infection and could have had direct effects on the T cells during the memory response. Further studies are warranted to determine if tBHQ causes lasting effects on memory cells that persist in the absence of tBHQ exposure.

Overall, these studies demonstrated that tBHQ impaired the memory response to heterosubtypic infection, potentially due to the increased abundance of Tregs and

reduction of splenic effector memory cells. In the search for a universal influenza vaccine, it has been widely acknowledged that the generation of long-term T cell memory is highly desirable.[407] In this context, dietary exposure to tBHQ at doses achievable in the human diet pose an interesting problem, as these data suggest that heterosubtypic immunity is impaired by tBHQ which could potentially translate to immunity elicited by a universal influenza vaccine.

CHAPTER 4

Nrf2 Exacerbates Lung Damage and Morbidity in a T Cell-dependent Manner During Primary Influenza Infection

Abstract

One of the best tools to fight against pandemic influenza viruses is T cell-mediated immunity. We previously demonstrated that Nrf2 activator, *tert*-butylhydroquinone (tBHQ), suppressed the T cell response to both primary and heterosubtypic infection. However, it was unclear if the effects elicited by tBHQ occurred through Nrf2 or a different pathway. Accordingly, we sought to determine the effects of Nrf2 on the T cell response to influenza virus infection. We utilized a model of adoptive transfer whereby we injected T cells from wildtype or Nrf2-null animals into T cell-deficient hosts. Recipient mice were then exposed to tBHQ and infected with influenza virus. This study revealed that Nrf2 in T cells contributed to influenza-associated morbidity, as mice with Nrf2-deficient T cells lost significantly less weight than mice with wildtype T cells. This seemed to be due to T cell-associated immunopathology, as Nrf2-deficient T cells had reduced cytotoxic effector function which correlated with less LDH activity in bronchoalveolar lavage fluid. In contrast, mice with Nrf2-deficient T cells had an increased abundance of influenza-specific $CD4^+$ and $CD8^+$ T cells, and Nrf2-deficient T cells produced more IFNγ than wildtype T cells, consistent with our previously published findings from *ex vivo* functional studies. Despite the reduced effector function, mice with Nrf2-null T cells were able to clear influenza virus as efficiently as mice with wildtype T cells, suggesting Nrf2 in T cells is not critical for resolving influenza infection. In contrast to our previous studies, the Nrf2 activator, tBHQ, had no effect on T cell function in this model. It is likely that this is an artifact generated by using SCID mice which lack functional intrathymic T cells and natural killer T cells, though further studies are warranted to determine why tBHQ did not affect wildtype T cells in this context.

Introduction

The stress-activated transcription factor, nuclear factor erythroid 2-related factor 2 (Nrf2), has both antiviral and proviral effects depending on the infectious agent. For instance, Nrf2 activation was shown to suppress replication of human immunodeficiency virus, respiratory syncytial virus, hepatitis viruses, and dengue virus.[355,356,359,360,408,409] Conversely, Nrf2 activation was shown to be detrimental to the host in infections with Marburg virus or herpesviruses.[265,352–354] In the context of influenza, Nrf2 was shown to prevent viral entry and damage to airway epithelial cells *ex vivo*.[357,363] However, the role of Nrf2 on influenza virus infection *in vivo* remains poorly characterized. Two studies demonstrated that Nrf2-null mice had exacerbated inflammatory responses to influenza virus and Nrf2 activation with carbocisteine ameliorates influenza virus-induced inflammation in a Nrf2-dependent manner.[365,366] However, these studies were primarily directed at targeting Nrf2 as a therapeutic for viral exacerbations of COPD, and therefore did not assess immunity to influenza infection beyond generalized inflammation during primary exposure.

Nrf2 is a transcription factor that under homeostatic conditions remains repressed in the cytosol by the E3 ubiquitin ligase adaptor protein, Kelch ECH-associated protein 1 (Keap1).[206,209] Upon oxidative or electrophilic cell stress, the interaction between Keap1 and Nrf2 becomes disrupted and allows nuclear accumulation of Nrf2 where it drives the expression of stress-responsive genes encoding antioxidant and phase II metabolic enzymes.[196,197,204,213] The widely used food additive, *tert*-butylhydroquinone (tBHQ), is a potent activator of Nrf2 and acts by modifying C151 within Keap1 as well as inducing mitochondrial oxidative stress.[248,254]

Pervious studies from our lab showed that tBHQ impaired human $CD4^+$ T cell activation and murine T_H1 cell polarization *ex vivo*.[296,301,371,372] Additionally, we showed that dietary tBHQ at doses relevant to human exposure impaired the primary and memory responses to influenza A virus infection. However, it was not determined if tBHQ impaired antiviral immunity through Nrf2-mediated effects.

As we previously saw that tBHQ suppressed the primary immune response to influenza virus and impaired memory formation, we sought to determine if Nrf2 was responsible for these effects in a T cell-intrinsic manner. Since Nrf2 was ubiquitously expressed and affects so many cell types involved in the immune response to influenza virus, we decided to use an adoptive transfer model with B6 SCID mice to determine the role of Nrf2 in T cells during primary infection with influenza virus. B6 SCID mice lack functional T and B lymphocytes due to defects in VDJ recombination, thus providing a good model to study the effects of genetic effects in a T cell-specific manner.[410,411] Utilizing this model, we observed that Nrf2-null T cells contributed to a less inflammatory immune response, characterized by augmented numbers of $CD4^+$ T cells and influenza-specific $CD4^+$ and $CD8^+$ T cells in the lungs but reduced activation and effector function within the T cells. Notably, the Nrf2-null T cells had higher intracellular IFNγ, but produced substantially less granzyme B. These effects were associated with less severe lung damage and reduced morbidity. Notably, no differences in viral RNA in the lungs were detected.

Materials and Methods

Animals and Viruses

Nrf2-null mice on a C57BL/6 background were maintained under specific pathogen-free conditions as previously described.[371] Age-matched female C57BL/6J mice were purchased from Jackson Laboratories (Bar Harbor, Maine) and housed under the same conditions as Nrf2-null mice. Three-week-old B6.Cg-Prkdc$_{SCID}$SzJ mice were purchased from Jackson Laboratories and housed under specific pathogen-free conditions for two weeks prior to adoptive transfer. All animal studies were conducted in accordance with the Guide for Care and Use of Animals as adopted by the National Institutes of Health and were approved by the Institutional Animal Care and Use Committee at Michigan State University.

An aliquot of influenza A/PR/8/34 (H1N1) was generously gifted by Dr. Kymberly Gowdy at East Carolina University in Greenville, North Carolina. The virus was then propagated and quantified following a published protocol.[378] Briefly, the virus was injected into the allantoic fluid of specific pathogen-free, embryonated chicken eggs (Charles River Laboratories, Wilmington, MA). The infected eggs were incubated for 48 hours at 37.5 ˚C, followed by another 24 hours at 4 ˚C. Following incubation, allantoic fluid was collected, centrifuged, and supernatant was divided into single-use aliquots. Aliquots were stored at -80 ˚C until used for experiments. The propagated virus stock was quantified by tissue culture infectious dose 50 ($TCID_{50}$) and hemagglutination methods. For the $TCID_{50}$, the virus was serially diluted across a 96-well plate containing confluent monolayers of MDCK cells (ATCC, Manassas, VA). Cells were observed daily for cytopathic effect, at which point the titer was determined using the Reed-

Muench method.[379] The hemagglutination assay was performed by serially diluting the virus across a 96 well plate containing 0.5% chicken red blood cells and incubating the cells for 30 minutes at room temperature, at which point agglutination was recorded. The virus stock was determined to be 2.5 x 10^5 $TCID_{50}$/mL and 7260 HAU/mL.

Adoptive Transfer of T and B Cells

$CD4^+$ and $CD8^+$ T cells were isolated with a Pan T Cell negative selection kit (Miltenyi Biotec, Auburn, CA) from age-matched female wildtype and Nrf2-null mice between five to eight weeks of age. Similarly, B cells were isolated with a Pan B Cell negative selection kit (Miltenyi Biotec) from wildtype female mice that were six weeks old. Live T cells were counted using Trypan blue and resuspended to a concentration of 20 x 10^6 cells/mL in RPMI 1640. B cells were counted similarly and resuspended to a concentration of 10 x 10^6 cells/mL in RPMI 1640. T cell and B cell purity were tested by labeling cells with fluorescent antibodies against CD3, CD4, CD8α, and CD19 (Table 6). Adoptive transfer was performed by intraperitoneally injecting 200 µL of the T cell suspension (either wildtype or Nrf2-null T cells) and 200 µL of the B cell suspension into each mouse, resulting in 4 million T cells and 2 million B cells injected per mouse. Mice were then rested for 16 weeks to allow lymphocyte reconstitution prior to initiating influenza studies.

Table 6: Flow Cytometry Antibodies used for Surface Labeling and Intracellular Staining

Antibody Target	Fluorochrome	Source
CD3	AF647	BioLegend
CD4	FITC	eBioscience
CD4	PE/Cy7	eBioscience
CD8a	PE/Cy5.5	eBioscience
CD8a	PerCP/Cy5.5	BioLegend
CD19	FITC	BioLegend
CD25	BV711	BioLegend
CD44	BV605	BioLegend
CD62L	Pacific Blue	BioLegend
CD69	AF700	BioLegend
CD107a	PE/Cy7	BD Pharmingen
Granzyme B	Pacific Blue	BioLegend
IFNγ	AF700	BioLegend
CD4 Tetramer	PE	NIH Tetramer Core
CD8 Tetramer	AF647	NIH Tetramer Core

Diets and Influenza Infection

16 weeks after adoptive transfer, mice were housed in cages in groups of 5 animals per cage and given AIN-93G purified rodent diet containing 0 or 0.0014% tBHQ (Dyets, Inc, Bethlehem, PA) and water *ad libitum*. Food consumption was monitored daily. After 2 weeks of acclimation to the diets, mice were anesthetized with 2,2,2-tribromoethanol (avertin; Alfa Aesar, Ward Hill, MA) via intraperitoneal injection. In previous studies in our lab, we utilized intranasal instillation to infect animals. However, in an effort to reduce variability and reduce the number of mice required, we opted to

utilize intrapharyngeal installation. In this method, anesthetized mice were hung by their incisors on a thin wire. The tongue was gently rolled out of the mouth with a cotton swab and held out of the way. A wide-bored pipet tip pre-filled with 23 µL of influenza virus was then placed into the mouth, and the virus was inhaled. To determine the titer to be used with this method that would result in similar weight loss as intranasal instillation in wildtype mice, the virus was titrated. Based on the results, a total of 0.17 $TCID_{50}$ of influenza A/PR/8/34 (H1N1) was administered in a volume of 23 µL. Upon recovery from anesthesia, mice were returned to their cages and monitored daily for changes in food consumption and body weight. The timeline for this experiment can be seen in Figure 28.

Blinding

Prior to sample collection, a blinding key was established whereby each mouse was de-identified and given a number 1 through 40. All assays besides weight loss utilized the blinding system with the only identifying information on tubes being the assigned number. When assays were completed, samples were re-identified using the key (Table 7).

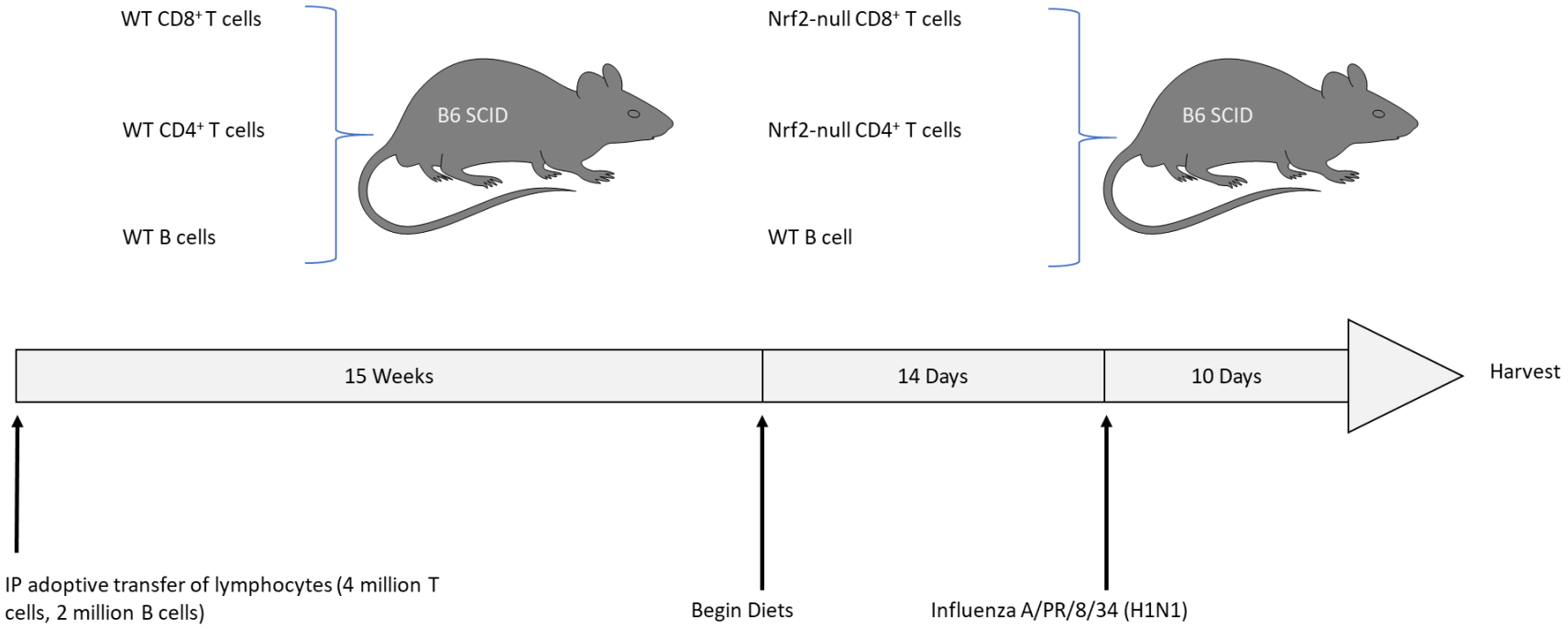

Figure 28: Adoptive transfer scheme and experiment timeline. 5-week-old B6 SCID mice from Jackson were reconstituted with either wildtype or Nrf2-null T cells, and wildtype B cells. 15 weeks later, mice were placed on diets with or without 0.0014% tBHQ. 2 weeks later, mice were challenged with sublethal influenza, and tissues were collected 10 days post-infection.

Table 7: Blinding Key

Cage #	T Cell Genotype	Diet	Tail Marking	Blinding Number
1	Wildtype	Control	Red	3
1	Wildtype	Control	Blue	20
1	Wildtype	Control	Green	32
1	Wildtype	Control	Black	19
1	Wildtype	Control	None	17
2	Nrf2-null	Control	Red	35
2	Nrf2-null	Control	Blue	14
2	Nrf2-null	Control	Green	30
2	Nrf2-null	Control	Black	12
2	Nrf2-null	Control	None	26
3	Wildtype	Control	Red	8
3	Wildtype	Control	Blue	22
3	Wildtype	Control	Green	27
3	Wildtype	Control	Black	38
3	Wildtype	Control	None	7
4	Nrf2-null	Control	Red	18
4	Nrf2-null	Control	Blue	2
4	Nrf2-null	Control	Green	1
4	Nrf2-null	Control	Black	36
4	Nrf2-null	Control	None	4
5	Wildtype	0.0014% tBHQ	Red	5
5	Wildtype	0.0014% tBHQ	Blue	23
5	Wildtype	0.0014% tBHQ	Green	25
5	Wildtype	0.0014% tBHQ	Black	29
5	Wildtype	0.0014% tBHQ	None	37
6	Nrf2-null	0.0014% tBHQ	Red	21
6	Nrf2-null	0.0014% tBHQ	Blue	16

Table 7: (cont'd)

Cage #	T Cell Genotype	Diet	Tail Marking	Blinding Number
6	Nrf2-null	0.0014% tBHQ	Green	28
6	Nrf2-null	0.0014% tBHQ	Black	31
6	Nrf2-null	0.0014% tBHQ	None	9
7	Wildtype	0.0014% tBHQ	Red	10
7	Wildtype	0.0014% tBHQ	Blue	33
7	Wildtype	0.0014% tBHQ	Green	24
7	Wildtype	0.0014% tBHQ	Black	11
7	Wildtype	0.0014% tBHQ	None	34
8	Nrf2-null	0.0014% tBHQ	Red	6
8	Nrf2-null	0.0014% tBHQ	Blue	40
8	Nrf2-null	0.0014% tBHQ	Green	15
8	Nrf2-null	0.0014% tBHQ	Black	13
8	Nrf2-null	0.0014% tBHQ	None	39

Tissue Collection and Cell Separation

Ten days after primary infection, mice were anesthetized with avertin and euthanized via cardiac puncture. Mice were euthanized via cardiac puncture, at which point blood was collected into heparinized tubes. Bronchoalveolar lavage fluid (BALF) was collected by cannulating the trachea and flushing the lungs with 1 mL of sterile saline. Lungs were excised and placed in 5 mL of DMEM containing 1 mg/mL collagenase D and subsequently dissociated with the gentleMACS dissociator (Miltenyi Biotec, Auburn, CA). After dissociation, 1 mL of lung homogenate was centrifuged and resuspended in TRIzol reagent RNA analysis. The remaining lung homogenate was used for FACS analysis. Mediastinal lymph nodes (MLN) were removed and cells from

the MLNs were isolated by grinding the MLN between the frosted ends of two microscope slides and resuspending in DMEM.

Lactate Dehydrogenase (LDH) Activity Assay

After collection, BALF was centrifuged and supernatants were transferred to fresh tubes. As LDH activity dramatically decreases following a single freeze-thaw, BALF was stored on ice and used in an LDH activity assay within hours of collection.[412] A commercial LDH activity kit was used following the manufacturer's protocol (Abcam PLC, Cambridge, MA).

Immunophenotyping

After dissociation, lung cells were washed in FACS buffer (1% FBS in dPBS). Cells were incubated with Fc block (BD Pharmingen, San Diego, CA) prior to labeling with antibodies against CD4, CD8α, CD25, CD69, CD44, CD62L, FasL, CD107a, IL-12 receptor β2, CTLA4, and the H-2D(b) Influenza A $PA_{224-233}$ SSLENFRAYV (Alexa 647-Labeled MHC-I Tetramer) and I-A(b) Influenza A $NP_{311-325}$ QVYSLIRPNENPAHK (PE-labeled MHC-II Tetramer) tetramers (Table 6). Cell viability was assessed by labeling cells with the Zombie Aqua Fixable Viability Kit (BioLegend, San Diego, CA) prior to labeling with antibodies, per the manufacturer's protocol. Lymph nodes were similarly stained with tetramers and antibodies against CD4, CD8α, CD69, IL-12 receptor β2, CD101, CD11c, I-A(b), CTLA4, CD86, and intracellular FoxP3.

Ex Vivo Stimulation and Intracellular Labeling

24 hours before collection, splenic $CD11c^+$ dendritic cells were isolated from untreated C57BL/6J mice using positive selection (Miltenyi Biotec, Auburn, CA). Dendritic cells were plated at a density of 4×10^5 cells/mL in RPMI 1640 supplemented with 10% fetal bovine serum, 25 mM HEPES, 1 mM sodium pyruvate, 1x nonessential amino acids, and 100 U/mL penicillin and streptomycin. Influenza A $NP_{366-374}$ (ASNENMETM) and influenza A $NP_{311-325}$ (QVYSLIRPNENPAHK) peptides were synthesized (New England Peptide, Inc., Gardner, MA) and added to dendritic cells at a concentration of 10 μM. 24 hours later, single-cell suspensions from the lungs of infected mice were co-cultured with the dendritic cells for 5 hours in the presence of monensin (BioLegend). Cells were labeled with the Zombie Aqua kit prior to Fc blocking and labeling with fluorescent antibodies against CD4, CD8α, IL-12 receptor β2, FasL, CD107a, and the H-2D(b)-restricted and I-A(b)-restricted influenza A tetramers. After surface labeling, cells were permeabilized with the FoxP3/transcription factor staining buffer set (eBioscience). After permeabilization, cells were labeled with antibodies against IFNγ, T-bet, and Granzyme B (GZMB) (Table 6). After labelling, cells were immediately analyzed on the Attune NxT.

RNA Isolation and Quantitative PCR

RNA was isolated from lung homogenate using TRIzol reagent per the manufacturer's protocol (Life Technologies, Grand Island, NY). RNA was quantified with the Nanodrop 2000c spectrophotometer (Thermo Fisher Scientific, Waltham, MA). Following reverse transcription, cDNA was quantified with real-time PCR SYBR green

analysis using the QuantStudio 7 Flex Real-Time PCR System (Applied Biosystems, Foster City, CA). Ribosomal protein L13A (RPL13A) served as the endogenous control and relative mRNA expression was calculated using the ΔΔCt method. Primer sequences are listed in Table 8.

Table 8: Influenza M1 and RPL13a Primer Sequences

Gene	Forward Primer Sequence	Reverse Primer Sequence
Influenza M1	CAAAGCGTCTACGCTGCAGTCC	AAGACCAATCCTGTCACCTCTGA
RPL13a	GTTGATGCCTTCACAGCGTA	AGATGGCGGAGGTGCAG

Statistical Analysis

The mean ± SEM was determined for each treatment group in individual experiments. Homogenous data were analyzed by two-way parametric ANOVA with Prism8 (GraphPad Software, San Diego, CA). When significant differences were observed, Tukey's post-hoc analysis was used to compare treatment groups. Animals which showed no signs of infection were excluded from statistical analyses.

Results

Purity of Isolated T and B Cells

Following magnetic isolation of splenic T cells and B cells by negative selection, the T cell suspensions and B cell suspension were labeled with fluorescent antibodies against CD3, CD4, CD8α, and CD19 (Figure 29A, B). These results showed the T cell population was ~97% pure (Figure 29C) and the B cell population was ~96% pure

(Figure 29D). Additionally, CD4:CD8 ratios were not significantly different between the isolated wildtype and Nrf2-null (KO) T cells (Figure 29E, F).

Comparison of Intrapharyngeal Influenza Instillation to Intranasal Instillation

In previous studies, we utilized intranasal administration of virus to cause infection. However, intranasal instillation can result in experimental variability due to varied inhalation of the instilled material; several studies have demonstrated that intranasal instillation leaves a significant portion of the administered dose in the nasal passages, and some of the dose also reaches the gastrointestinal tract.[413,414] Evidence suggests that using intratracheal administration of influenza virus results in less variability in delivered viral titers and subsequent inflammation and immune responses.[415] While intratracheal administration is attractive, it must be performed by skilled personnel. An alternative route of administration which still bypasses the nasal cavity and esophagus is intrapharyngeal instillation. This technique reliably dispersed nanomaterials and bacteria in the lungs of mice.[416,417] In the method we used here, influenza virus was pre-loaded into a wide-bored pipet tip. Surface tension keeps the virus inoculum in the tip until the force of aspiration draws the inoculum into the trachea. Since this can result in a higher delivered viral titer to the lungs, we performed a titration of the virus using 1x, 0.1x, and 0.05x compared to 1x intranasal infection (1x = 0.23 $TCID_{50}$ delivered). As expected, 1x delivered intrapharyngeally caused more severe weight loss than 1x intranasal infection (Figure 30A). On the contrary, 0.1x and 0.05x instillations resulted in significantly reduced weight loss compared to 1x intranasal instillation. Beyond weight loss, $CD4^+$ and $CD8^+$ T cell infiltration to the lung was

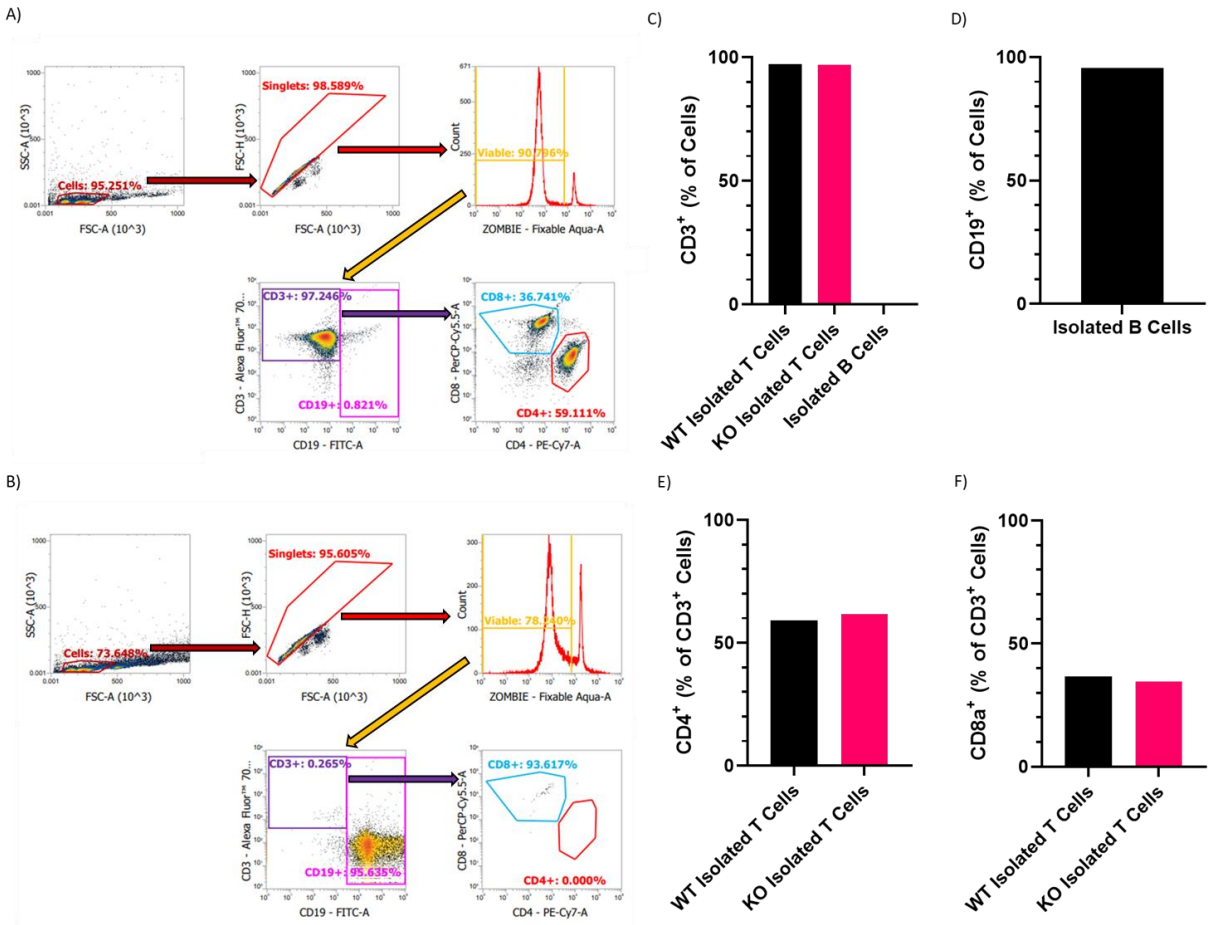

Figure 29: Isolated T and B cells were of high purity and not substantially different between genotypes. T cells were magnetically isolated from wildtype and Nrf2-null (KO) mice to be used for adoptive transfer. B cells from wildtype mice were similarly isolated. The resulting cells were labeled with fluorescent antibodies against CD3, CD4, CD8α, and CD19 along with Zombie Aqua viability dye. Cells were quantified on the Attune NxT flow cytometer. (A) Gating strategy to determine purity of T cells as well as $CD4^+$ and $CD8^+$ T cell percentages within the total T cell pool. (B) Gating strategy to determine the purity of isolated B cells. (C) Purity of isolated T cells. (D) Purity of isolated T cells from wildtype and Nrf2-null mice. (E) Percentages of $CD4^+$ T cells within the total T cell pools. (F) Percentages of $CD8^+$ T cells within the total T cell pools.

also assessed. 0.1x and 0.05x instillations resulted in minute T cell responses compared to 1x intrapharyngeal administration (Figure 30B, C), and a reduced frequency of effector $CD8^+$ T cells, denoted by high CD44 and low CD62L expression (Figure 30C). As 1x was too high but 0.1x and 0.05x were too low, 0.75x was used in subsequent studies.

The Absence of Nrf2 in T Cells Ameliorated Weight Loss During Influenza Infection

Following sublethal infection with influenza A virus, body weight was monitored daily (Figure 31B). Mice lacking Nrf2 in the T cell compartment showed substantially lower morbidity during infection compared to mice with wildtype T cells. Notably, food consumption data (Figure 31A) matched the weight loss data, but no differences in food consumption were detected in the two weeks leading up to infection suggesting the difference is due to the infection and associated immune response.

Lack of Nrf2 in T Cells was also Associated with Less Lung Damage Following Infection

To assess lung damage, lactate dehydrogenase (LDH) activity was measured in the BALF of infected animals (Figure 32). Regardless of diet, the presence of Nrf2 in T cells was associated with elevated LDH activity which suggests increased Nrf2 in T cells promoted lung damage. Surprisingly, the amount of total protein in the BALF was not different among groups (data not shown).

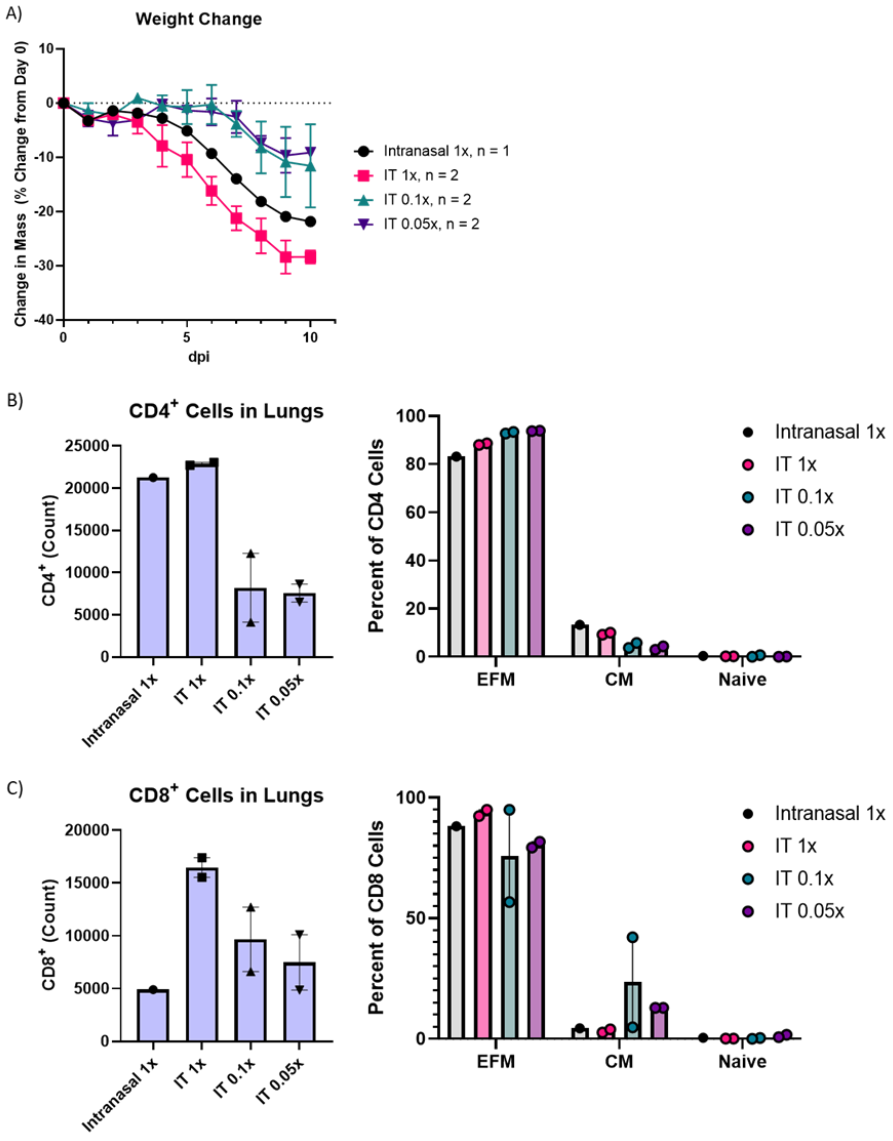

Figure 30: Comparison of intrapharyngeal influenza instillation to intranasal instillation. B6 SCID mice which were reconstituted with wildtype T cells and B cells were anesthetized with avertin and infected with 1x (0.23 $TCID_{50}$), 0.1x (0.023 $TCID_{50}$), or 0.05x (0.0115 $TCID_{50}$) of influenza A/PR/8/34 (H1N1). Ten days post-infection, lungs were removed and dissociated for flow cytometric analysis of $CD4^+$ and $CD8^+$ T cells within. (A) Weight loss was monitored for 10 days post-infection. (B) Quantitation of $CD4^+$ cells within the lungs and distribution of effector/memory (EFM), central memory (CM), or naïve cells. (C) Quantitation of $CD8^+$ cells within the lungs and distribution of effector/memory (EFM, $CD44^{hi}CD62L^{lo}$), central memory (CM, $CD44^{hi}CD62L^{hi}$), or naïve cells ($CD44^{lo}CD62L^{hi}$).

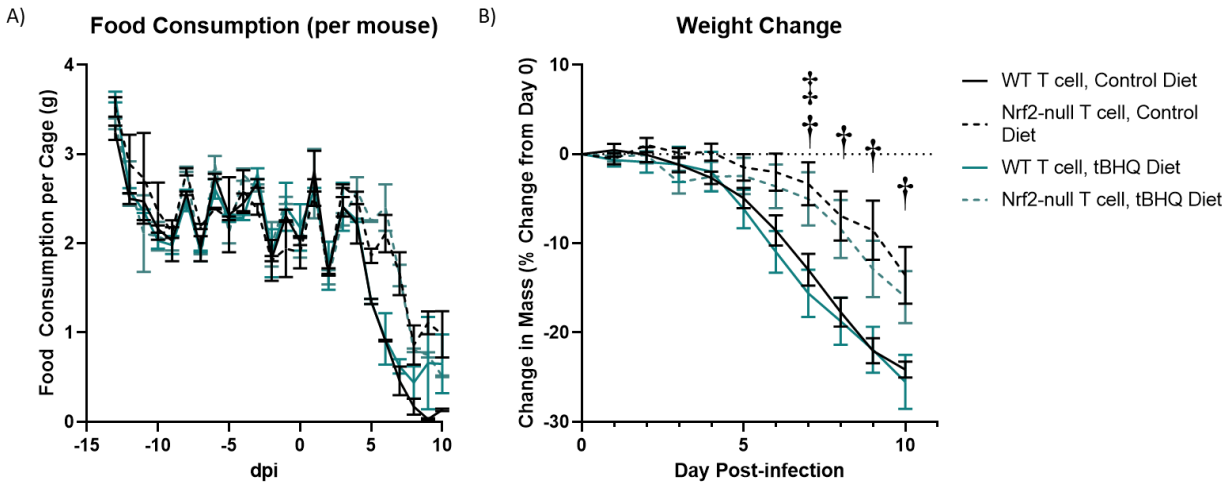

Figure 31: The absence of Nrf2 in T cells protected mice against influenza-associated weight loss. B6 SCID mice were reconstituted with T cells from either wildtype or Nrf2-null mice. 15 weeks later, mice were placed on diets with or without 0.0014% tBHQ. 2 weeks after starting the diets, mice were infected with 0.17 $TCID_{50}$ of influenza A/PR/8/34 (H1N1) and their body weights were monitored daily. (A) Daily food consumption estimates. (B) Change in body weight from the day of infection. † denotes $p < 0.05$ between wildtype and Nrf2-null reconstituted animals on control diet. ‡ denotes $p < 0.05$ between wildtype and Nrf2-null reconstituted animals on tBHQ diet.

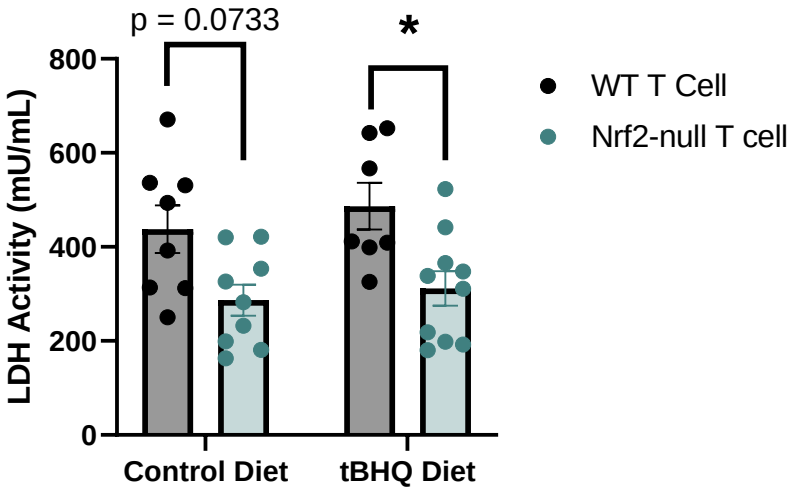

Figure 32: The presence of Nrf2 in T cells was associated with exacerbated lung injury during influenza infection. Ten days post-infection, bronchoalveolar lavage fluid was collected and LDH activity was measured. * $p < 0.05$ between indicated groups.

Nrf2-null T Cells were Found More Frequently in the Lungs of Infected Mice

Following infection, single cell suspensions from dissociated lungs were labeled with MHC-I- and MHC-II-restricted tetramers loaded with influenza peptides in addition to fluorescent antibodies against CD4 and CD8α (Figure 33A-C). Mice with Nrf2-deficient T cells had enhanced $CD4^+$ T cell counts in the lung (Figure 33D) in addition to an increased abundance of influenza-specific $CD4^+$ and $CD8^+$ T cells (Figure 33F, G). Interestingly, no differences in $CD8^+$ T cells within the lung were detected between groups, in stark contrast to our previous work that showed a staunch reduction in lung $CD8^+$ T cells following tBHQ exposure. Another interesting phenomenon was that the noted increases were suppressed by tBHQ, and these reductions were limited to mice lacking Nrf2 in T cells.

Lack of Nrf2 in T Cells Altered the Frequency of Effector T Cells within the Lungs of Infected Mice

Following infection, single cell suspensions from dissociated lungs were labeled with fluorescent antibodies against CD4, CD8α, CD44, and CD62L to identify effector cells ($CD44^{hi}CD62L^{lo}$). As expected, the majority of $CD4^+$and $CD8^+$ cells in the lung at this time were effector cells (Figure 34A, B). Consistent with the increase in total $CD4^+$ cells within the lung, the number of effector $CD4^+$ cells was also increased (Figure 34C). Notably, this difference appeared to be due to the total increase in $CD4^+$ T cells as there was no difference in the ratio of effector $CD4^+$ cells to total $CD4^+$ cells (Figure

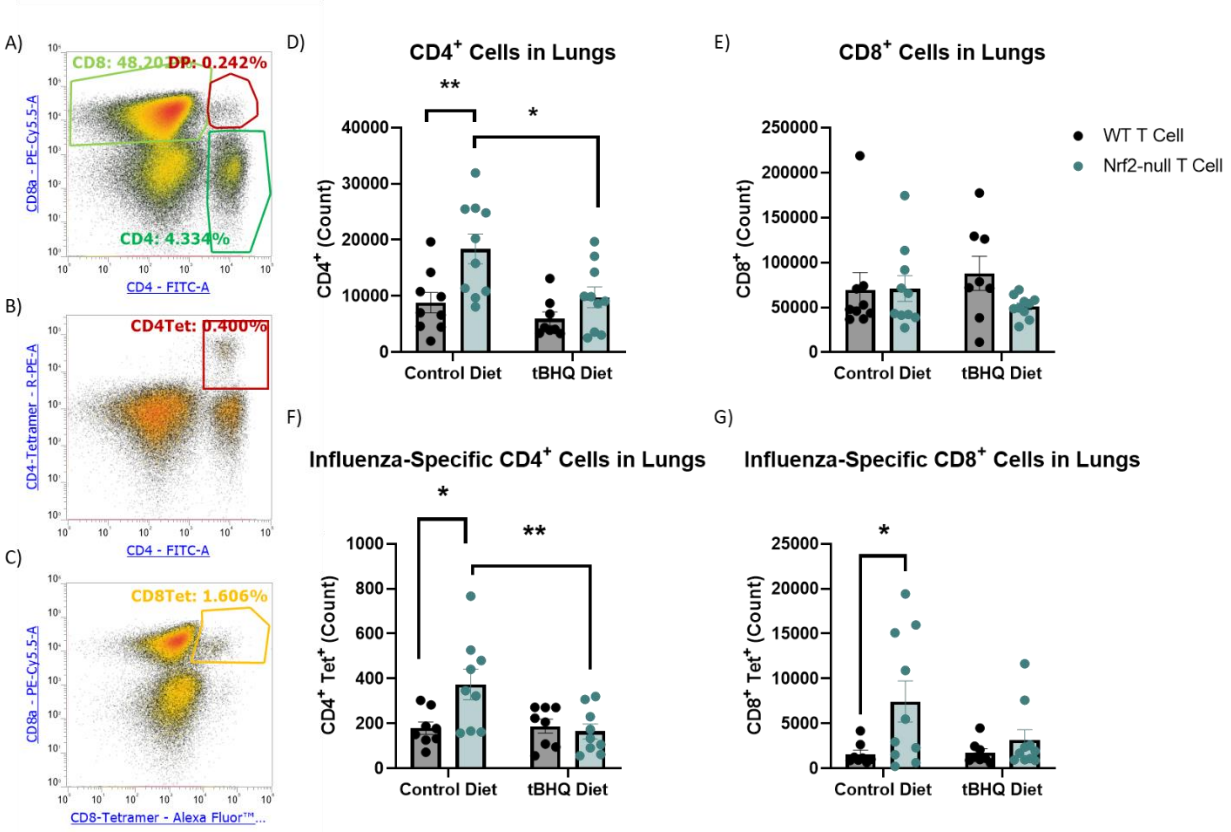

Figure 33: Nrf2 intrinsically suppresses influenza-specific T cell accumulation in the lungs during infection. B6 SCID mice were reconstituted with T cells from either wildtype or Nrf2-null mice. 15 weeks later, mice were placed on diets with or without 0.0014% tBHQ. 2 weeks after starting the diets, mice were infected with 0.17 $TCID_{50}$ of influenza A/PR/8/34 (H1N1). Ten days later, their lungs were removed and dissociated into single cell suspensions which were labeled with influenza peptide-loaded tetramers and fluorescent antibodies against CD4 and CD8α. (A) Representative density plot showing CD4 and CD8 populations within the lungs, gated first on viable lymphocytes. (B) Density plot showing positive MHC-II-restricted tetramer binding. (C) Density plot showing positive MHC-I-restricted tetramer binding. (D) Quantification of $CD4^+$ cells within the lung. (E) Quantification of $CD8^+$ cells within the lung. (F) Quantification of influenza-specific $CD4^+$ cells in the lung. (G) Quantification of influenza-specific $CD8^+$ cells in the lung. * $p < 0.05$ between indicated groups. ** $p < 0.01$ between indicated groups.

34D). However, this was not the case for effector $CD8^+$ cells, in which Nrf2-null $CD8^+$ T cells were shown to be reduced in counts as well as frequency within the total $CD8^+$ T cell pool (Figure 34E, F).

Absence of Nrf2 in T Cells Led to Dysregulated T Cell Activation

Following infection, single cell suspensions from dissociated lungs were labeled with fluorescent antibodies against CD4, CD8α, CD25, and CD69 to identify T cells in various stages of activation (Figure 35A, B). Notably, Nrf2-null $CD4^+$ T cells were found in each stage of activation assessed based on variable expression of CD69 and CD25 (Figure 35C). In contrast, Nrf2-null $CD8^+$ T cells displayed a reduction in activation markers compared to wildtype T cells (Figure 35D). Consistent with our previous study in wildtype animals, exposure to tBHQ reduced $CD4^+$ T cell activation. While this was only statistically significant among Nrf2-null T cells, the trend persisted within the wildtype $CD4^+$ T cell population as well.

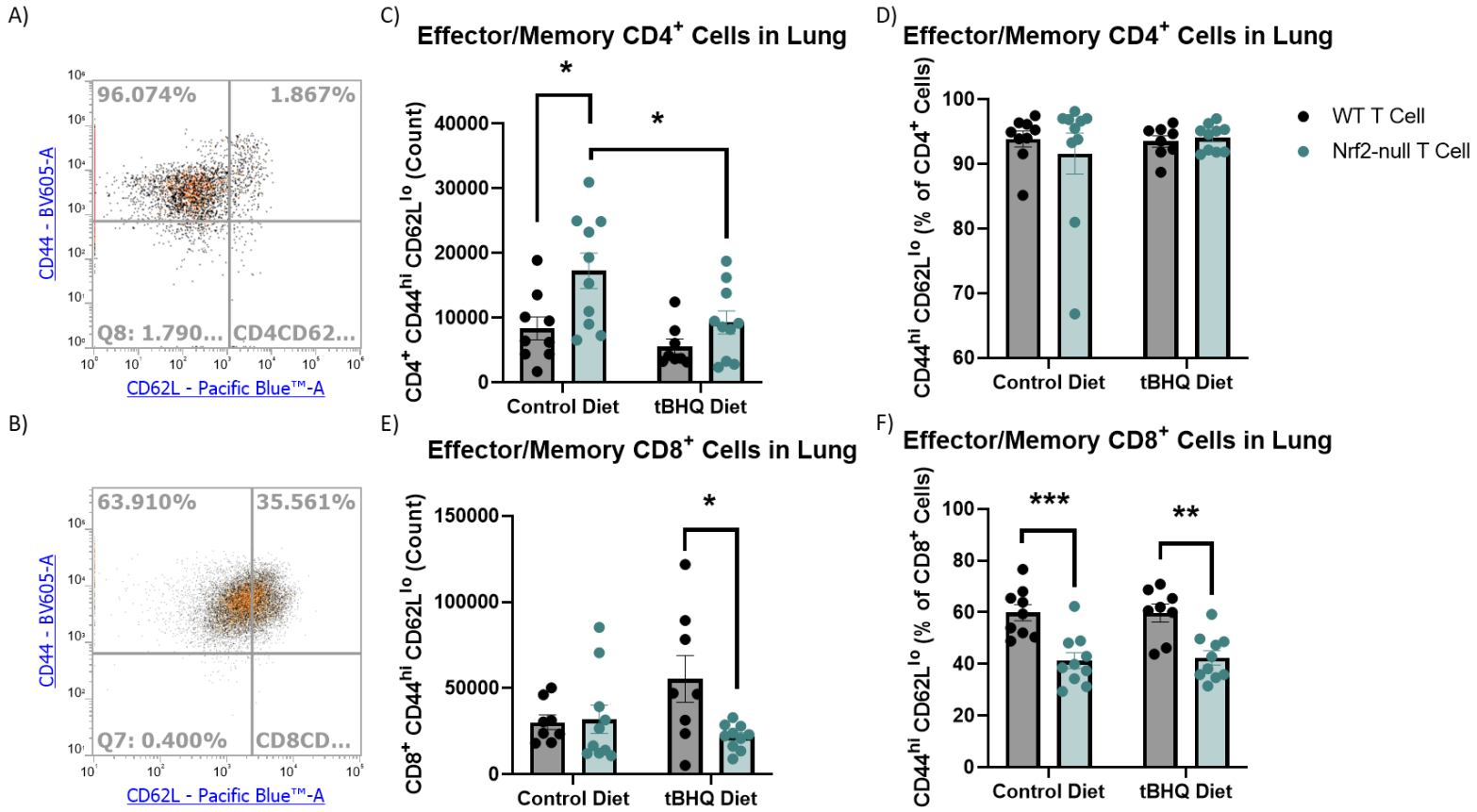

Figure 34: Lack of Nrf2 in T cells enhanced the presence of effector CD4⁺ T cells but diminished the frequency of effector CD8⁺ T cells in the lungs during infection. B6 SCID mice were reconstituted with T cells from either wildtype or Nrf2-null mice. 15 weeks later, mice were placed on diets with or without 0.0014% tBHQ. 2 weeks after starting the diets, mice were infected with 0.17 $TCID_{50}$ of influenza A/PR/8/34 (H1N1). Ten days later, their lungs were removed and dissociated into single cell suspensions which were labeled with fluorescent antibodies against CD4, CD8α, CD44, and CD62L. (A) Representative density plot of CD44/CD62L-stained $CD4^+$ cells. (B) Representative density plot of CD44/CD62L-stained $CD8^+$ cells. (C) Quantification of effector $CD4^+$ cells in lung. (D) Effector $CD4^+$ cells expressed as a percentage of total $CD4^+$ cells. (E) Quantification of effector $CD8^+$ cells in lung. (F) Effector $CD8^+$ cells expressed as a percentage of total $CD8^+$ cells.

Nrf2-null T Cells Produced More IFNγ than Wildtype T Cells During Infection

Ten days post-infection, single-cell suspensions from lung homogenates were co-cultured with peptide-pulsed dendritic cells for five hours in the presence of monensin. Following restimulation, the cells were labeled with fluorescent antibodies against CD4, CD8α, and intracellularly stained with an antibody against IFNγ (Figure 36A, D). Notably, the percentage of IFNγ $CD4^+$ T cells (Figure 36C) was enhanced by the T cell-specific absence of Nrf2 in mice on the control diet and a similar trend was observed in influenza-specific $CD8^+$ T cells (Figure 36F). The abundance of $IFN\gamma^+$ $CD4^+$ and $CD8^+$ T cells was similarly elevated in lungs with Nrf2-null T cells (Figure 36B, E). The majority of these cells were influenza-specific T cells, and the ratio of influenza-specific to total T cells producing IFNγ were not different between groups (data not shown). The mean fluorescent intensity of IFNγ was also elevated in Nrf2-deficient T cells (data not shown). Additionally, tBHQ exposure diminished this effect on IFNγ production.

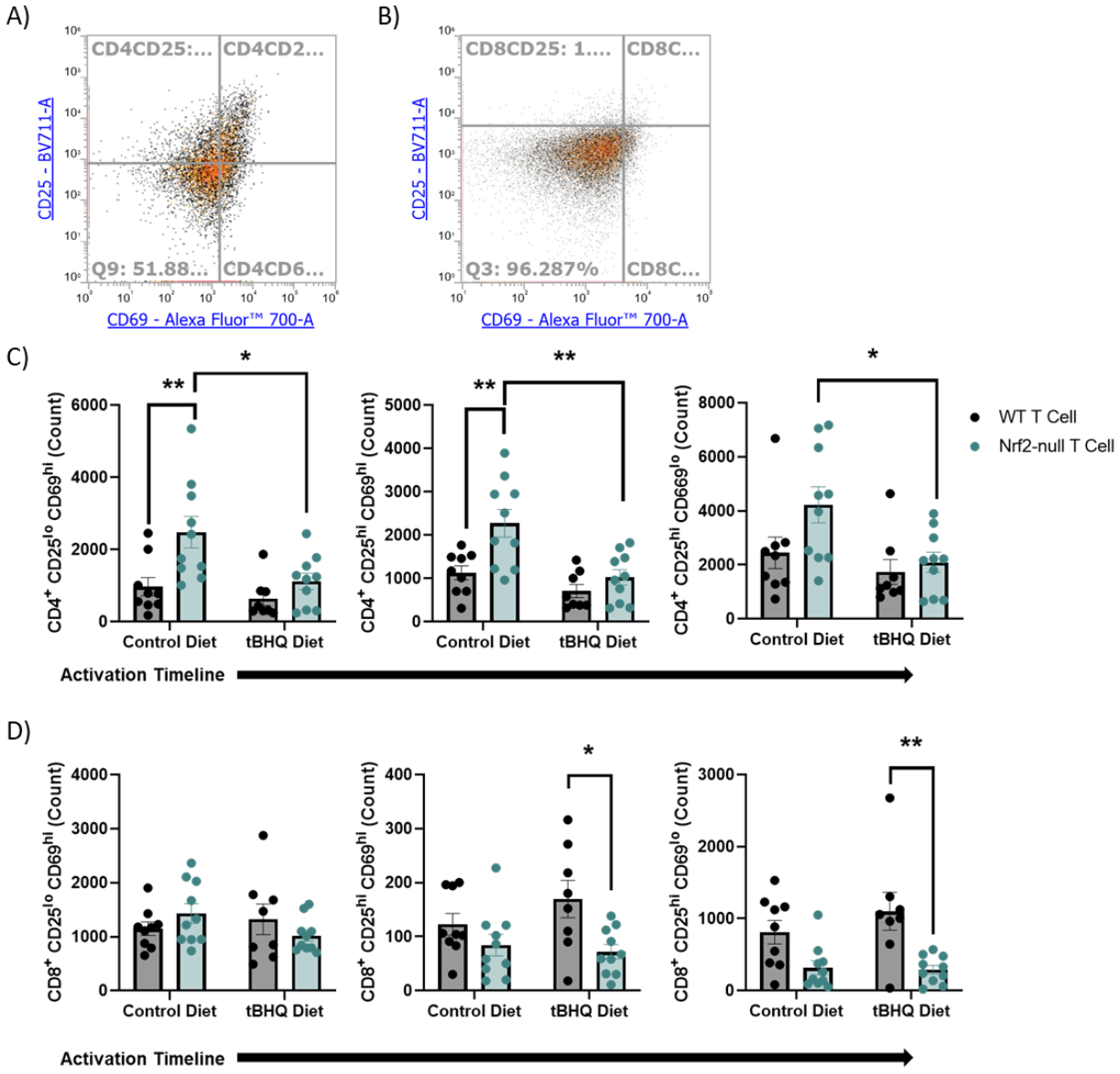

Figure 35: Nrf2-null T Cells Exhibit Altered Activation Profiles During Influenza Infection. B6 SCID mice were reconstituted with T cells from either wildtype or Nrf2-null mice. 15 weeks later, mice were placed on diets with or without 0.0014% tBHQ. 2 weeks after starting the diets, mice were infected with 0.17 $TCID_{50}$ of influenza A/PR/8/34 (H1N1). Ten days later, their lungs were removed and dissociated into single cell suspensions which were labeled with fluorescent antibodies against CD4, CD8α, CD25, and CD69. (A) Representative density plot of CD25/CD69-stained $CD4^+$ cells. (B) Representative density plot of CD25/CD69-stained $CD8^+$ cells. (C) Quantification of $CD4^+$ cells in lung expressing CD69, CD69 and CD25, or CD25. (D) Quantification of $CD8^+$ cells in lung expressing CD69, CD69 and CD25, or CD25.

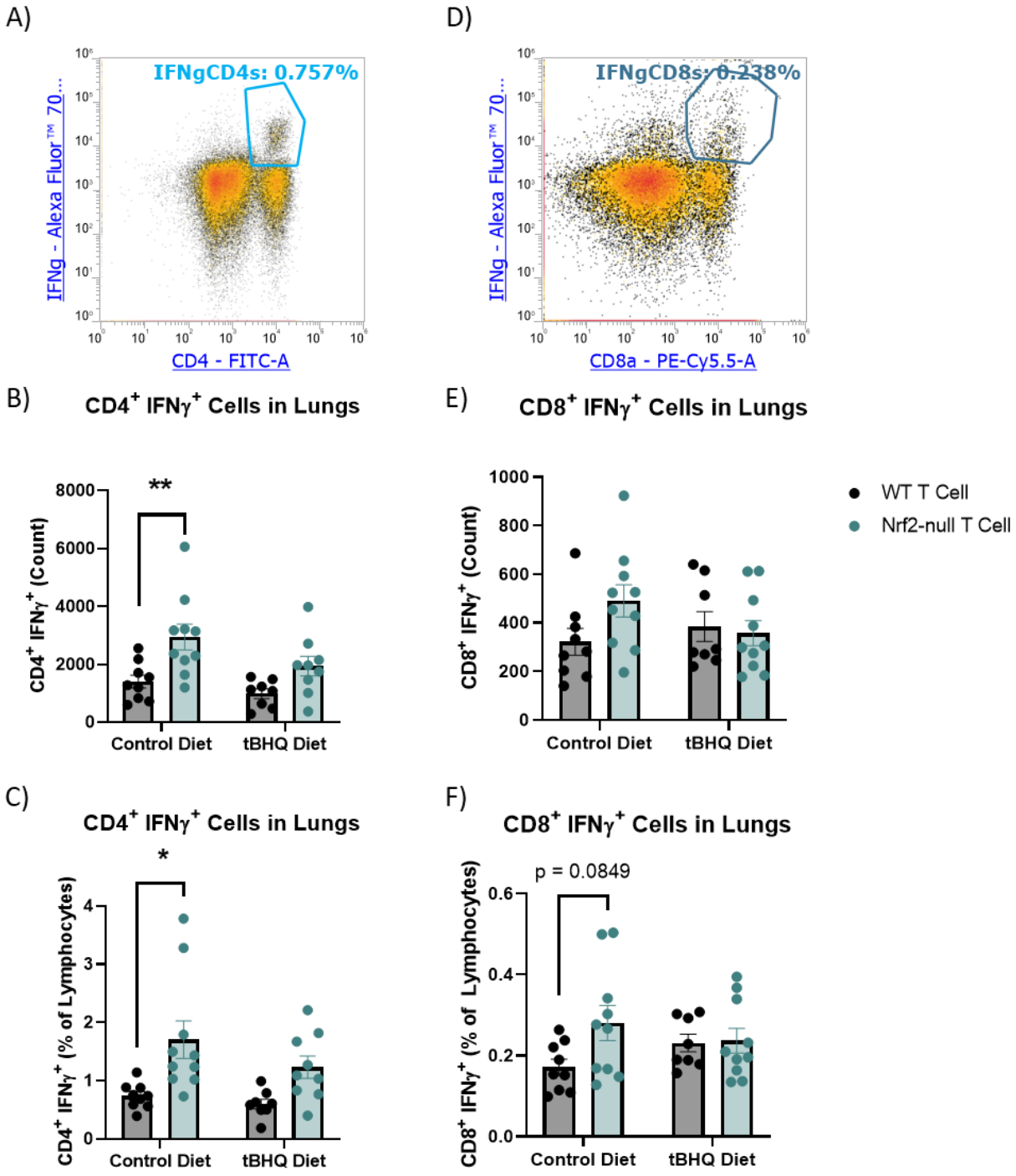

Figure 36: T cells lacking Nrf2 have augmented IFNγ production in response to influenza infection. B6 SCID mice were reconstituted with T cells from either wildtype or Nrf2-null mice. 15 weeks later, mice were placed on diets with or without 0.0014% tBHQ. 2 weeks after starting the diets, mice were infected with 0.17 $TCID_{50}$ of influenza A/PR/8/34 (H1N1). Ten days later, their lungs were removed and homogenized. The resulting single-cell suspension was co-cultured with influenza-peptide-pulsed dendritic cells in the presence of monensin. 5 hours later, cells were labeled with antibodies

Figure 36: (cont'd) against CD4, CD8α, and IFNγ. Cells were quantified by flow cytometry. (A) Density plot showing positive IFNγ staining within $CD4^+$ T cells. (B) Quantification of $IFN\gamma^+$ $CD4^+$ T cells. (C) $IFN\gamma^+$ $CD4^+$ cells expressed as a percentage of viable lymphocytes. (D) Density plot showing positive IFNγ staining within $CD8^+$ T cells. (B) Quantification of $IFN\gamma^+$ $CD8^+$ T cells. (C) $IFN\gamma^+$ $CD8^+$ cells expressed as a percentage of viable lymphocytes. * $p < 0.05$ between indicated groups. ** $p < 0.01$ between indicated groups.

Nrf2-deficient T Cells Display Reduced Effector Function Upon Stimulation with Viral Antigen

Ten days post-infection, single-cell suspensions from lung homogenates were co-cultured with peptide-pulsed dendritic cells for five hours in the presence of monensin. Following restimulation, the cells were labeled with fluorescent antibodies against CD4, CD8α, CD107a, and intracellularly stained with an antibody against granzyme B (GZMB, Figure 37A). Not only was the number of $GZMB^+$ $CD8^+$ T cells reduced overall in the absence of Nrf2 (Figure 37B), but the lack of Nrf2 also reduced the percentage of $CD8^+$ T cells producing GZMB (Figure 37C). Consistent with this finding, the overall amount of GZMB production was reduced as evidenced by a reduction in median fluorescence intensity (Figure 37D), and this finding was consistent within influenza-specific $CD8^+$ T cells (Figure 37E) as well as in $GZMB^+$ $CD107a^+$ $CD8^+$ T cells (data not shown).

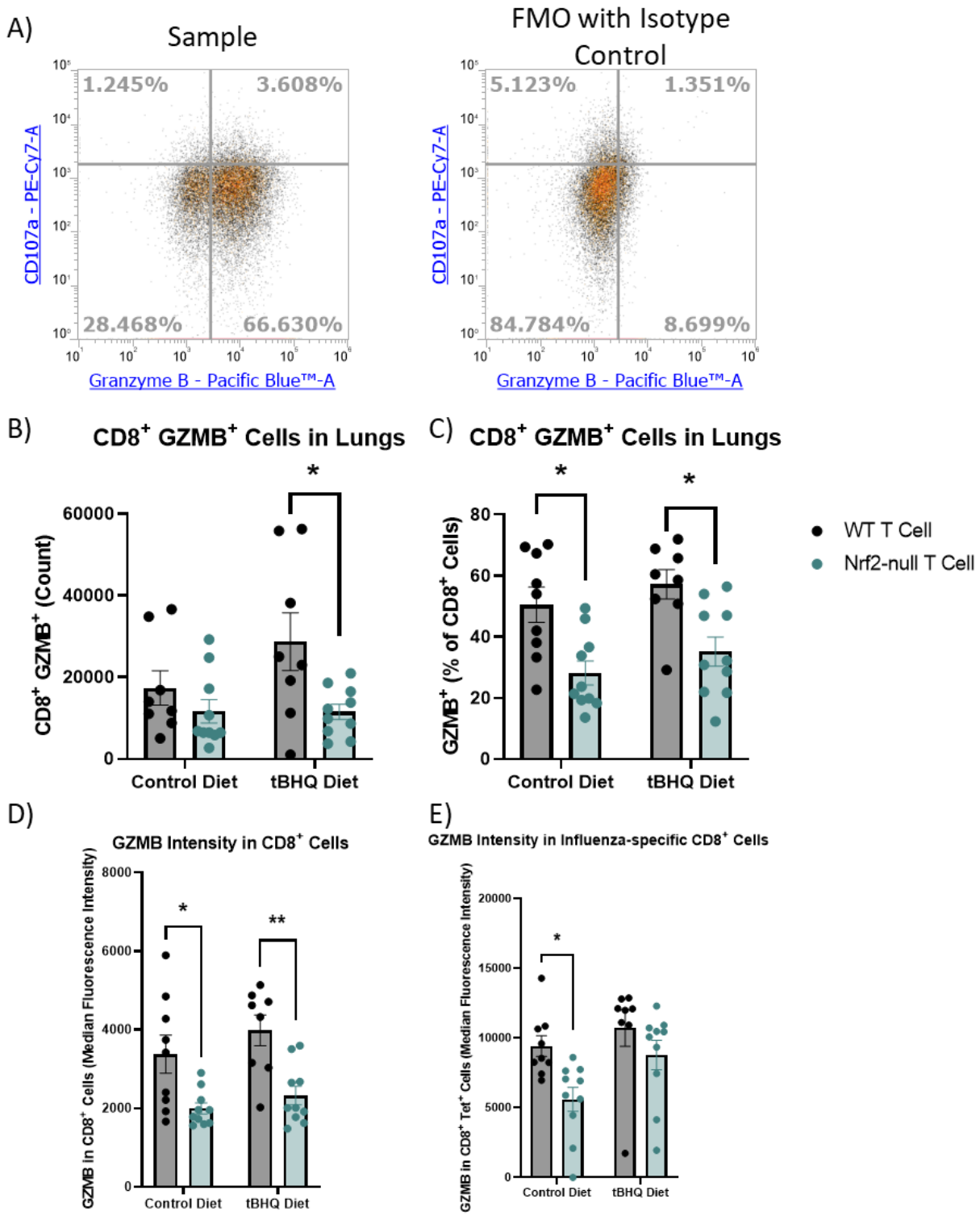

Figure 37: Nrf2-deficient CD8+ T cells have reduced effector function during influenza infection. B6 SCID mice were reconstituted with T cells from either wildtype or Nrf2-null mice. 15 weeks later, mice were placed on diets with or without 0.0014% tBHQ. 2 weeks after starting the diets, mice were infected with 0.17 $TCID_{50}$ of influenza

Figure 37: (cont'd) A/PR/8/34 (H1N1). Ten days later, their lungs were removed and homogenized. The resulting single-cell suspension was co-cultured with influenza-peptide-pulsed dendritic cells in the presence of monensin. 5 hours later, cells were labeled with antibodies against CD4, CD8α, CD107a, and granzyme B (GZMB). Cells were quantified with the Attune NxT flow cytometer. (A) Density plots showing positive staining of GZMB with a targeted antibody (left) compared to an fluorescence minus one with isotype control. (B) Quantification of $GZMB^+$ cells. (C) Percentage of $GZMB^+$ cells within the total $CD8^+$ population. (D) Median GZMB fluorescence intensity within $CD8^+$ cells. (E) Median GZMB fluorescence intensity within influenza-specific $CD8^+$ cells. * $p < 0.05$ between the indicated groups. ** $p < 0.01$ between the indicated groups.

Nrf2 Status of T Cells did not Affect Viral Load

We next analyzed viral titer by determining relative viral mRNA levels with qRT-PCR. Following amplification of influenza M1 no overt differences were detected between groups (Figure 38).

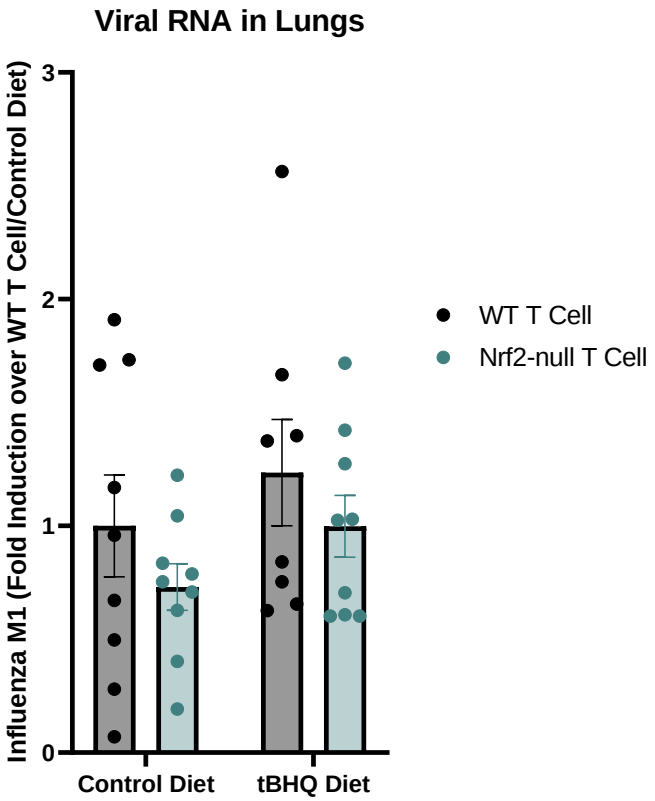

Figure 38: No differences detected in viral RNA within the lungs of infected mice. B6 SCID mice were reconstituted with T cells from either wildtype or Nrf2-null mice. 15 weeks later, mice were placed on diets with or without 0.0014% tBHQ. 2 weeks after starting the diets, mice were infected with 0.17 $TCID_{50}$ of influenza A/PR/8/34 (H1N1). Ten days later, their lungs were removed and homogenized. Real-time PCR was used to quantify viral RNA from the lung homogenate. The viral matrix protein, M1, was used for viral quantification and was normalized to the housekeeper gene RPL13a.

Discussion

Nrf2 has been postulated to be a potential antiviral target and prevented viral entry and inflammation in influenza models.[357,363,365,366] However, our understanding of how Nrf2 acts during viral infections at a cellular level remains poorly characterized. We previously showed *ex vivo* that treatment of murine $CD4^+$ T cells with the Nrf2 activator tBHQ caused a Nrf2-dependent polarization toward a T_H2 phenotype and away from a T_H1 phenotype.[296] Given that the T_H1-associated cytokine, IFNγ, has important roles in

the immune response to influenza virus infection, we sought to determine the role of Nrf2 on the antiviral immune response *in vivo*. By reconstituting B6 SCID mice with T cells from wildtype or Nrf2-null animals, we showed that Nrf2 exacerbated $CD8^+$ T cell-driven morbidity, evidenced by enhanced $CD8^+$ T cell activation and effector function that resulted in elevated LDH activity and weight loss compared to mice with Nrf2-deficient T cells.

A notable finding in this study was the increase in $CD4^+$ T cells in the lungs of mice with Nrf2-null T cells compared to mice with wildtype T cells. Interestingly, this effect was not seen within the $CD8^+$ T cell compartment, although influenza-specific $CD8^+$ T cells (and $CD4^+$ T cells) were augmented by intrinsic Nrf2 deficiency. Interestingly, this suggests that Nrf2 might have differential effects in influenza-specific $CD8^+$ T cells and bystander T cells, a phenomenon that was recently described in alveolar macrophages during *Mycobacterium tuberculosis* infection.[418] The augmented $CD4^+$ counts within the lungs of mice with Nrf2-null T cells also translated to an increase in activated $CD4^+$ T cells, evidenced by increased expression of CD25, CD69, and CD44. These animals also had an increase in IFNγ-producing $CD4^+$ T cells, consistent with what we observed *ex vivo*.[296] The findings for $CD8^+$ T cells tell an opposite story, as the Nrf2-deficient $CD8^+$ T cells appeared to be less activated and had diminished effector function compared to wildtype $CD8^+$ T cells.

Another perplexing finding in this study was that the Nrf2 activator, tBHQ, did not suppress the $CD8^+$ T cell response to influenza infection, a stark juxtaposition compared to what we had seen in wildtype mice in previous studies. Several possible experimental conditions could explain this finding. First, due to the time gap between

adoptive transfer and beginning of diets, mice in this study were of greater age than mice in our previous studies. Induction of Nrf2 by xenobiotics declines with age which could be one factor explaining why tBHQ effects were largely absent from this study.[259,419–421] It could also be that in the studies in wildtype mice, tBHQ may have affected T cells before they emigrated from the thymus. Thymic output increases during measles virus infections, providing a source of T cells to combat infection.[422] While alterations in thymic output during influenza infection have not been reported, a recent study demonstrated that influenza A(H1N1)pdm09 – the strain responsible for the 2009 pandemic, infected the thymus and induced T cell-mediated thymic atrophy.[423] Additionally, tBHQ was demonstrated to be cytotoxic to rat thymocytes, albeit at doses unlikely to have been achieved in the present studies.[424] In light of these reports, it is possible that tBHQ modulates the development and release of T cells during influenza infection. As B6 SCID mice have smaller thymuses without functional T cells, that could be why tBHQ effects were not seen in the present study.[410] Further studies are warranted to determine exactly how tBHQ modulates T cell function during influenza infection.

To our knowledge, this was the first study to directly assess the role of Nrf2 specifically in T cells during primary influenza infection. Two striking patterns emerged in this study: mice with Nrf2-deficient T cells had an enhanced $CD4^+$ T cell response and a concurrently diminished effector $CD8^+$ T cell response. The lack of cytotoxic T cell response did not impact viral clearance; however, it did protect the host from severe immunopathology within the lungs suggesting Nrf2 within T cells contributes to

immunopathology during influenza infection. As Nrf2 was associated with reduced a $CD4^+$ T cell response and $CD4^+$ T cell responses are important for the formation of memory to influenza viruses, it is tempting to speculate that Nrf2 might suppress memory formation and impair host responses to secondary infection.[37,38] Future studies in our lab will aim to address that question.

CHAPTER 5

Role of Nrf2 in tBHQ-mediated Suppression of the T cell Response to Influenza Virus Infection in Mice with a T Cell-specific Nrf2 Deletion

Abstract

Tert-butylhydroquinone (tBHQ) is a food additive widely used to prevent rancidification of fats in human food products, and it was first used commercially in 1972. Previous studies from our lab have shown immunomodulatory effects of tBHQ at low micromolar concentrations *ex vivo*, including skewing murine $CD4^+$ T cell polarization toward a T_H2 phenotype and impairing primary and Jurkat human T cell differentiation. Moreover, we recently demonstrated that tBHQ consumed through the diet at doses relevant to human exposure produces immunotoxic effects in mice, though the mechanism for these effects remains unknown. We previously utilized an adoptive transfer model with SCID mice to test whether tBHQ elicited its effects through activation of the stress-activated transcription factor, Nrf2. However, tBHQ had no effect on wildtype T cells in that model. To further elucidate the potential mechanism by which tBHQ suppresses T cell responses to primary influenza virus infection, we generated conditional Nrf2 knockout mice using Cre recombinase under the CD4 promoter. These mice and their "wildtype" counterparts were fed mice standard AIN-93G diet which is 0.0014% tBHQ or AIN-93G with the tBHQ removed and then infected the mice with a sublethal titer of influenza A/PR/8/34 (H1N1). Ten days later, various parameters associated with the T cell response to influenza infection were assessed. It was found that mice on the tBHQ diet had a subtle reduction of $CD8^+$ T cells in the lungs as well as diminished effector function. However, these effects were restricted to mice with in-tact Nrf2 within T cells. These results suggest that tBHQ suppresses the T cell response to influenza infection through T cell intrinsic activation of Nrf2.

Introduction

T cell-mediated immunity is vital in antiviral immune responses, and *in vivo* exposures to toxicants hinder both $CD4^+$ and $CD8^+$ T cell responses to IAV infection through various mechanisms.[425–430] While many toxicants such as arsenic, cadmium, TCDD, cannabinoids, and other environmental contaminants have been studied in the context of anti-influenza immunity, many xenobiotics remain uncharacterized. Among those is the widely used, synthetic food additive, *tert*-butylhydroquinone (tBHQ). Results from our lab show that tBHQ has immunomodulatory activity in a variety of immune cells including T cells from mice and humans.[291,293,296,300,301,371,372] In addition to our published studies, we observed that in mature female wildtype mice that dietary tBHQ at doses relevant to human exposure impair the primary immune response to influenza virus leading to diminished memory formation. These effects culminated in enhanced morbidity to heterosubtypic infection. These findings suggest that tBHQ could be a hindrance in the development of long-lasting T cell memory to influenza virus infections and vaccinations, and this could have broad societal impacts as universal influenza vaccines that are reliant on T cells are developed in the near future.

Notably, the mechanism by which tBHQ suppresses T cell responses to influenza infection *in vivo* remain unknown. tBHQ is well known for its ability to activate the transcription factor, Nrf2, through modification of cysteine residues on Keap1.[247,248] Indeed, our lab previously showed that Nrf2 activation by tBHQ impaired T_H1 cell differentiation *ex vivo*.[296] However, other effects of tBHQ on T cell function occur independently of Nrf2 as seen in T cells from Nrf2-deficient mice and Jurkat T cells harboring a CRISPR/Cas9-mediated deletion of Nrf2.[300,371] We previously sought to

identify the mechanism by which tBHQ suppresses T cell responses to influenza infection utilizing an adoptive transfer model with SCID mice receiving either wildtype or Nrf2-deficient T cells prior to influenza infection. However, tBHQ had no effect on T wildtype T cells in this model, potentially due to the increased age of the mice and/or lack of thymic T cells. Accordingly, we sought to develop another model to investigate the role of Nrf2 activation by tBHQ on the immune response to influenza infection *in vivo*. To do this, we bred mice containing flanking LoxP sites (floxed) on either side of exon 5 of Nrf2, which encodes the DNA-binding region of Nrf2 (Neh1), with mice expressing Cre recombinase under the CD4 promoter.[343] This resulted in mice which were homozygous for the floxed Nrf2 allele and hemizygous for CD4-Cre which resulted in ablation of Nrf2 in $CD4^+$ and $CD8^+$ T cells. These mice were then fed diets with or without tBHQ and infected with influenza A virus. The results of this study correlated well with our original studies in wildtype mice exposed to tBHQ, suggesting that tBHQ reduces the effector $CD8^+$ T cell response to influenza infection, and the effects appeared to be largely dependent on Nrf2 within T cells.

Materials and Methods

Animals and Viruses

Mice homozygous for the floxed exon 5 of Nrf2 on a C57BL/6J background were generated as previously described and generously gifted from Dr. Shyam Biswal at Johns Hopkins University.[343] B6.Cg-Tg(Cd4-cre)1Cwi/BfluJ (hereon referred to as CD4-Cre) breeding pairs were purchased from Jackson Laboratories (Bar Harbor, Maine). The mice were housed under specific pathogen-free conditions within the

clinical center vivarium at Michigan State University. Mice homozygous for the floxed Nrf2 allele were bred with mice hemizygous for CD4-Cre to create mice heterozygous for both the floxed Nrf2-allele and CD4-Cre. These heterozygotes were then bred with mice homozygous for the floxed Nrf2 allele, resulting in mice with homozygous floxed Nrf2 and hemizygous CD4-Cre or wildtype CD4. From this point forward, only mice that were homozygous for the floxed Nrf2 allele were used for breeding. For influenza infections, mice harboring homozygous floxed Nrf2 and hemizygous CD4-Cre (referred to as Nrf2-flox^{Cre}) or wildtype CD4 were used (referred to as Nrf2-flox). All animal studies were conducted in accordance with the Guide for Care and Use of Animals as adopted by the National Institutes of Health and were approved by the Institutional Animal Care and Use Committee at Michigan State University.

An aliquot of influenza A/PR/8/34 (H1N1) was generously gifted by Dr. Kymberly Gowdy at East Carolina University in Greenville, North Carolina. The virus was then propagated and quantified following a published protocol.[378] Briefly, the virus was injected into the allantoic fluid of specific pathogen-free, embryonated chicken eggs (Charles River Laboratories, Wilmington, MA). The infected eggs were incubated for 48 hours at 37.5 ˚C, followed by another 24 hours at 4 ˚C. Following incubation, allantoic fluid was collected, centrifuged, and supernatant was divided into single-use aliquots. Aliquots were stored at -80 ˚C until used for experiments. The propagated virus stock was quantified by tissue culture infectious dose 50 ($TCID_{50}$) and hemagglutination methods. For the $TCID_{50}$, the virus was serially diluted across a 96-well plate containing confluent monolayers of MDCK cells (ATCC, Manassas, VA). Cells were observed daily for cytopathic effect, at which point the titer was determined using the Reed-

Muench method.[379] The hemagglutination assay was performed by serially diluting the virus across a 96 well plate containing 0.5% chicken red blood cells and incubating the cells for 30 minutes at room temperature, at which point agglutination was recorded. The virus stock was determined to be 2.5 x 10^5 $TCID_{50}$/mL and 7260 HAU/mL.

Mouse Genotyping

Protocols for genotyping were obtained from Jackson Laboratories.[431,432] Genomic DNA was extracted from tail snips or ear punches and amplified using the KAPA Mouse Genotyping Kit (Kapa Biosystems, Wilmington, MA). For detection of CD4-Cre, wildtype forward, wildtype reverse, and mutant reverse primers were used. For detection of floxed Nrf2, forward and reverse primers flanking exon 5 were used, resulting in a differently sized band dependent upon inclusion of the LoxP sites. Sequences for the primers are included in Table 9. Amplification of genomic DNA utilized a 2 minute start at 94 ºC; 10 cycles of 94 ºC for 20 seconds, 65 ºC for 15 seconds (decreasing temperature by 0.5 ºC per cycle), and 68 ºC for 10 seconds; 28 cycles of 94 ºC for 15 seconds, 60 ºC for 15 seconds, and 72 ºC for 10 seconds; 72 ºC for 2 minutes; and a 10 ºC hold. Following amplification, DNA gel electrophoresis was performed using a 2% agarose gel with a 100 bp ladder included for identification of bands. Bands were visualized with ethidium bromide and a UV light. Wildtype CD4 was 153 bp, CD4-Cre was at 336 bp, wildtype Nrf2 was at 272 bp, and floxed Nrf2 was at 310 bp.

Table 9: qPCR and Genotyping Primer Sequences

Gene	Forward Primer Sequence	Reverse Primer Sequence
Influenza M1	CAAAGCGTCTACGCTGCAGTCC	AAGACCAATCCTGTCACCTCTGA
RPL13a	GTTGATGCCTTCACAGCGTA	AGATGGCGGAGGTGCAG
Nrf2 Exon 5	AGCCAGCTGACCTCCTTAGA	AGTGACTGACTGATGGCAGC
Nrf2 Flox for Genotyping	TCATGAGAGCTTCCCAGACTC	CAGCCAGCTGCTTGTTTTC
CD4-Cre for Genotyping	GTTCTTTGTATATATTGAATGTTAGCC	WT CD4: TATGCTCTAAGGACAAGAATTGACA CD4-Cre: CTTTGCAGAGGGCTAACAGC

Diets and Influenza Infection

Age-matched (8-24wks), female littermates were housed in cages in groups of up to 5 animals per cage and given AIN-93G purified rodent diet containing 0 or 0.0014% tBHQ (Dyets, Inc, Bethlehem, PA) and water *ad libitum*. Food consumption was monitored daily. After 2 weeks of acclimation to the diets, mice were anesthetized with 2,2,2-tribromoethanol (avertin; Alfa Aesar, Ward Hill, MA) via intraperitoneal injection. Mice were intranasally instilled with 30 µL of influenza A/PR/8/34 (H1N1) at a titer of 7.5 $TCID_{50}$/mL (0.22 HAU/mL). This resulted in a total amount of 0.23 $TCID_{50}$ per mouse (0.0066 HAU per mouse). Upon recovery from anesthesia, mice were returned to their cages and monitored daily for changes in food consumption and body weight. Three mice on each diet were intranasally instilled with 30 µL of sterile saline instead of virus as experimental controls. The timeline for this experiment can be seen in Figure 6.

Blinding

Upon weaning, mice were assigned an identity (X2 - #). For all parameters, these numbers were used in the absence of identifying information related to treatment, and a separate log was kept denoting which experimental groups animals belonged to. Animals were re-identified following completion of assays. The key can be seen in Table 10.

Tissue Collection and Cell Separation

Ten days after primary infection, mice were anesthetized with avertin and euthanized via cardiac puncture. Mice were euthanized via cardiac puncture, at which point blood was collected into heparinized tubes. Bronchoalveolar lavage fluid (BALF) was collected by cannulating the trachea and flushing the lungs with 1 mL of sterile saline. Lungs were excised and placed in 5 mL of DMEM containing 1 mg/mL collagenase D and subsequently dissociated with the gentleMACS dissociator (Miltenyi Biotec, Auburn, CA). After dissociation, 1 mL of lung homogenate was centrifuged and resuspended in TRIzol reagent RNA analysis. The remaining lung homogenate was used for FACS analysis. Spleens of some mice were collected to assess Nrf2 knockdown within $CD4^+$ and $CD8^+$ T cells. Spleens were gently disrupted using the plunger of a 10 mL syringe and the remaining cells were passed through a 40 μm strainer. Cells were washed in DMEM, and then $CD4^+$ and $CD8^+$ T cells were separately isolated using negative selection kits (Miltenyi Biotec, Auburn, CA).

Immunophenotyping

After dissociation, lung cells were washed in FACS buffer (1% FBS in dPBS). Cells were incubated with Fc block (BD Pharmingen, San Diego, CA) prior to labeling with antibodies against CD4, CD8α, CD25, CD69, CD44, CD62L, FasL, CD107a, IL-12 receptor β2, CTLA4, and the H-2D(b) Influenza A $PA_{224-233}$ SSLENFRAYV (Alexa 647-labeled MHC-I Tetramer) and I-A(b) Influenza A $NP_{311-325}$ QVYSLIRPNENPAHK (PE-labeled MHC-II Tetramer) tetramers (Table 6). Cell viability was assessed by labeling cells with the Zombie Aqua Fixable Viability Kit (BioLegend, San Diego, CA) prior to labeling with antibodies, per the manufacturer's protocol.

Ex Vivo Stimulation and Intracellular Labeling

24 hours before collection, splenic $CD11c^+$ dendritic cells were isolated from untreated C57BL/6J mice using positive selection (Miltenyi Biotec, Auburn, CA). Dendritic cells were plated at a density of 4×10^5 cells/mL in RPMI 1640 supplemented with 10% fetal bovine serum, 25 mM HEPES, 1 mM sodium pyruvate, 1x nonessential amino acids, and 100 U/mL penicillin and streptomycin. Influenza A $NP_{366-374}$ (ASNENMETM) and influenza A $NP_{311-325}$ (QVYSLIRPNENPAHK) peptides were synthesized (New England Peptide, Inc., Gardner, MA) and added to dendritic cells. 24 hours later, single-cell suspensions from the lungs of infected mice were co-cultured with the dendritic cells for 5 hours in the presence of monensin (BioLegend). Cells were labeled with the Zombie Aqua kit prior to Fc blocking and labeling with fluorescent antibodies against CD4, CD8α, IL-12 receptor β2, FasL, CD107a, and the H-2D(b)-restricted and I-A(b)-restricted influenza A tetramers. After surface labeling, cells were permeabilized

Table 10: Cre/Flox Blinding Key

Mouse ID	Genotype	Diet		Mouse ID	Genotype	Diet
X2-026	FL/FL	Control		X2-178	FL/FL	Control
X2-027	FL/FL	Control		X2-179	Cre+ FL/FL	Control
X2-028	Cre+ FL/FL	Control		X2-180	FL/FL	Control
X2-029	FL/FL	tBHQ		X2-186	FL/FL	tBHQ
X2-030	FL/FL	tBHQ		X2-187	Cre+ FL/FL	tBHQ
X2-031	FL/FL	tBHQ		X2-188	FL/FL	tBHQ
X2-035	FL/FL	tBHQ		X2-189	Cre+ FL/FL	tBHQ
X2-036	Cre+ FL/FL	tBHQ		X2-190	FL/FL	tBHQ
X2-037	FL/FL	tBHQ		X2-191	Cre+ FL/FL	tBHQ
X2-038	Cre+ FL/FL	tBHQ		X2-192	Cre+ FL/FL	tBHQ
X2-043	FL/FL	Control		X2-197	Cre+ FL/FL	tBHQ
X2-044	Cre+ FL/FL	Control		X2-198	Cre+ FL/FL	Control
X2-127	Cre+ FL/FL	tBHQ		X2-207a	Cre+ FL/FL	Control
X2-128	FL/FL	tBHQ		X2-207b	FL/FL	Control
X2-131	FL/FL	Control		X2-216	FL/FL	tBHQ
X2-132	Cre+ FL/FL	Control		X2-226	Cre+ FL/FL	Control
X2-133	Cre+ FL/FL	Control		X2-228	Cre+ FL/FL	Control
X2-138	FL/FL	tBHQ		X2-232	Cre+ FL/FL	Control
X2-142	Cre+ FL/FL	tBHQ		X2-241	Cre+ FL/FL	tBHQ
X2-143	FL/FL	Control		X2-255	Cre+ FL/FL	Control
X2-149	FL/FL	Control		X2-256	Cre+ FL/FL	Control
X2-150	Cre+ FL/FL	Control		X2-257	FL/FL	tBHQ
X2-151	FL/FL	Control		X2-259	Cre+ FL/FL	tBHQ
X2-154	Cre+ FL/FL	Control		X2-265	FL/FL	Control
X2-155	Cre+ FL/FL	Control		X2-267	Cre+ FL/FL	tBHQ
X2-156	Cre+ FL/FL	tBHQ		X2-280	Cre+ FL/FL	Control
X2-157	FL/FL	tBHQ		X2-291	Cre+ FL/FL	tBHQ
X2-164	Cre+ FL/FL	tBHQ		X2-292	FL/FL	tBHQ
X2-171	FL/FL	Control		X2-293	FL/FL	Control
X2-172	FL/FL	Control		X2-294	FL/FL	tBHQ
X2-173	Cre+ FL/FL	Control		X2-309	Cre+ FL/FL	Control
X2-177	Cre+ FL/FL	Control		X2-311	FL/FL	Control

with the FoxP3/transcription factor staining buffer set (eBioscience). After permeabilization, cells were labeled with antibodies against IFNγ, T-bet, and Granzyme B (GZMB) (Table 6). After labelling, cells were immediately analyzed on the Attune NxT.

RNA Isolation and Quantitative PCR

RNA was isolated from lung homogenate or isolated T cells using TRIzol reagent per the manufacturer's protocol (Life Technologies, Grand Island, NY). RNA was quantified with the Nanodrop 2000c spectrophotometer (Thermo Fisher Scientific, Waltham, MA). Following reverse transcription, cDNA was quantified with real-time PCR SYBR green analysis using the QuantStudio 7 Flex Real-Time PCR System (Applied Biosystems, Foster City, CA). Ribosomal protein L13A (RPL13A) served as the endogenous control and relative mRNA expression was calculated using the ΔΔCt method. Primer sequences are listed in Table 9.

Statistical Analysis

The mean ± SEM was determined for each treatment group in individual experiments. Homogenous data were analyzed by two-way parametric ANOVA with Prism8 (GraphPad Software, San Diego, CA). When significant differences were observed, Tukey's post-hoc analysis was used to compare treatment groups. Animals which showed no signs of infection were excluded from statistical analyses.

Results

Generation of Mice Harboring a T Cell-specific Nrf2 Deletion

Previous studies utilized mice with a floxed exon 5 within the Nrf2 gene to knock out Nrf2 in a cell-specific manner.[323,341,343,433–435] Accordingly, we utilized these mice to ablate Nrf2 within T cells. We utilized mice expressing Cre under the CD4 promoter, as during T cell development, immature T cells express $CD4^+$ and $CD8^+$ simultaneously before committing to either the $CD4^+$ or $CD8^+$ lineage, thus allowing Cre expression to occur in all conventional T cells.[436] Additionally, we chose to use mice with hemizygous Cre expression, as Cre toxicity has been observed within $CD4^+$ T cells; notably, CD4 expression occurs later than other T cell-specific genes during development, making this the most likely driver of Cre expression to not affect T cell development.[437] Utilizing this strategy, T cells from mice with hemizygous Cre expression and homozygous for floxed Nrf2 showed substantial reduction of Nrf2 exon 5 mRNA expression (Figure 39). While some Nrf2 exon 5 mRNA was detected in T cells from Cre^+ mice, this is likely due to residual non-T cells in the sample following negative selection which typically yields 95% pure T cell populations.

A)

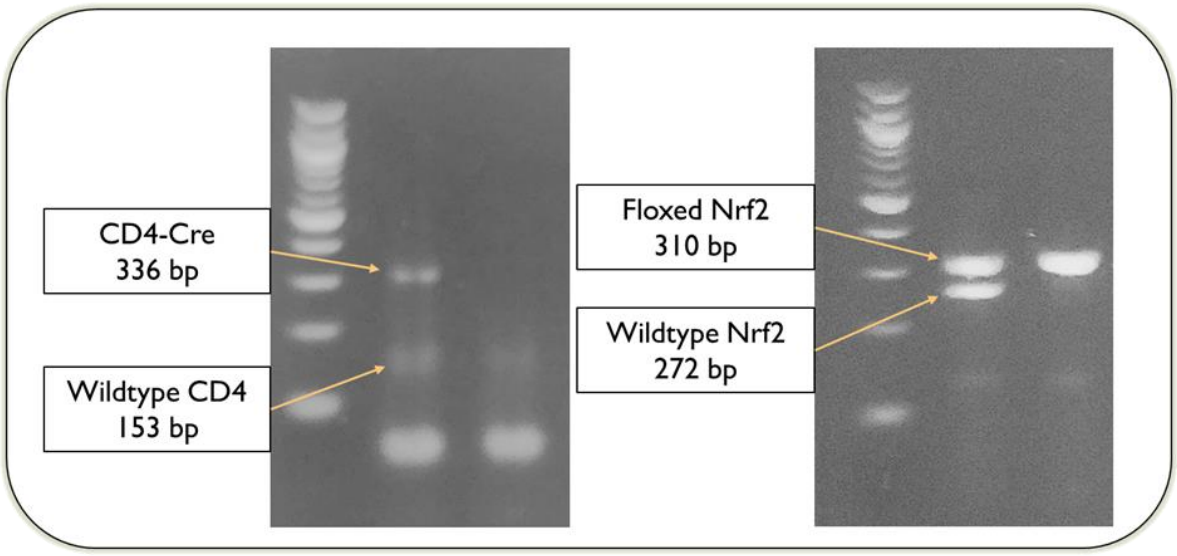

B)

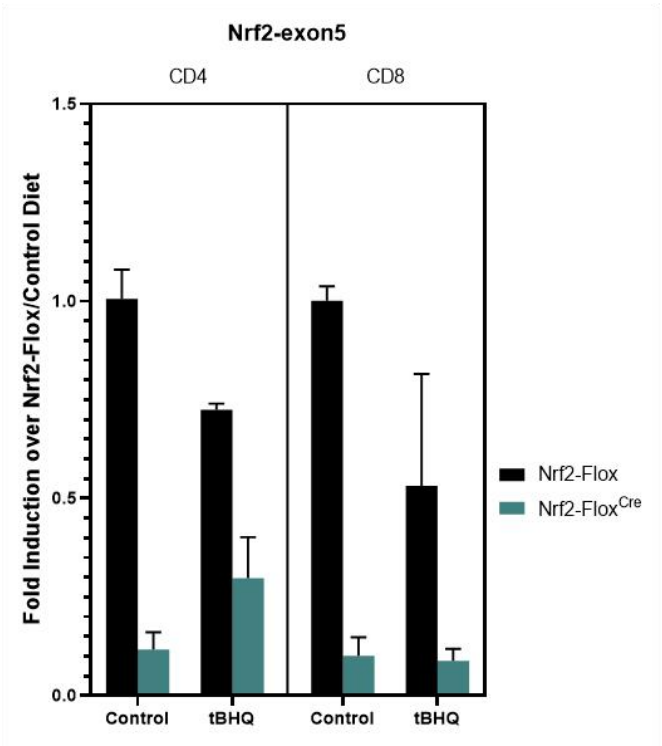

Figure 39: Cre recombinase expression driven under the CD4 promoter drives Nrf2 ablation in both CD4$^+$ and CD8$^+$ T cells. (A) Genomic DNA was isolated from tissues of mice collected at weaning. Wildtype/mutant CD4 and Nrf2 were visualized by gel electrophoresis following DNA amplification. (B) Nrf2-flox mice with or without hemizygous Cre expression under the CD4 promoter were fed diets with or without 0.0014% tBHQ for 14 days prior to infection with influenza virus. Ten days post-infection, spleens were removed and splenic CD4$^+$ and CD8$^+$ T cells were magnetically isolated. RNA was isolated from the purified cell populations, and Nrf2 exon 5 mRNA

Figure 39: (cont'd) was quantified by qRT-PCR and normalized to the housekeeper gene RPL13a. Mean ± SEM is shown for n = 3 mice per group.

Dietary Exposure to tBHQ is Associated with a Modest Decrease in Lung CD8$^+$ T cells

Following influenza infection, T cell populations within the lung were assessed. Lungs were removed and homogenized, and the resulting single-cell suspension was labeled with antibodies against CD8α and CD4 in addition to influenza peptide-loaded tetramers. Viable CD4$^+$ and CD8$^+$ T cells (Figure 40A) and influenza specific CD4$^+$ (Figure 40B) and CD8$^+$ (Figure 40C) T cells were detected via flow cytometry. Similar to what was observed in wildtype mice exposed to tBHQ, Nrf2-flox mice exposed to tBHQ tended to have fewer CD8$^+$ T cells in their lungs, and this effect was not seen in mice lacking functional Nrf2 in T cells (Figure 40E). Additionally, Nrf2-flox mice exposed to tBHQ had a subtle reduction in influenza-specific CD4$^+$ and CD8$^+$ T cells (Figure 40F, G).

tBHQ Reduced Effector T Cell Populations within the Lung and Impaired Effector Function

We previously observed a strong effect of tBHQ on effector T cell function in wildtype mice. To determine whether those effects were mediated by Nrf2, we examined effector function in mice with a conditional Nrf2 deletion. While less pronounced than in the original experiments, a similar trend was seen in the current studies whereby tBHQ reduced the number of effector (CD44^{hi}) T cells in the lungs of infected mice (Figure 41). Additionally, granzyme B and CD107a, two markers of cytotoxic function, were reduced in CD8$^+$ T cells in a Nrf2-dependent manner (Figure

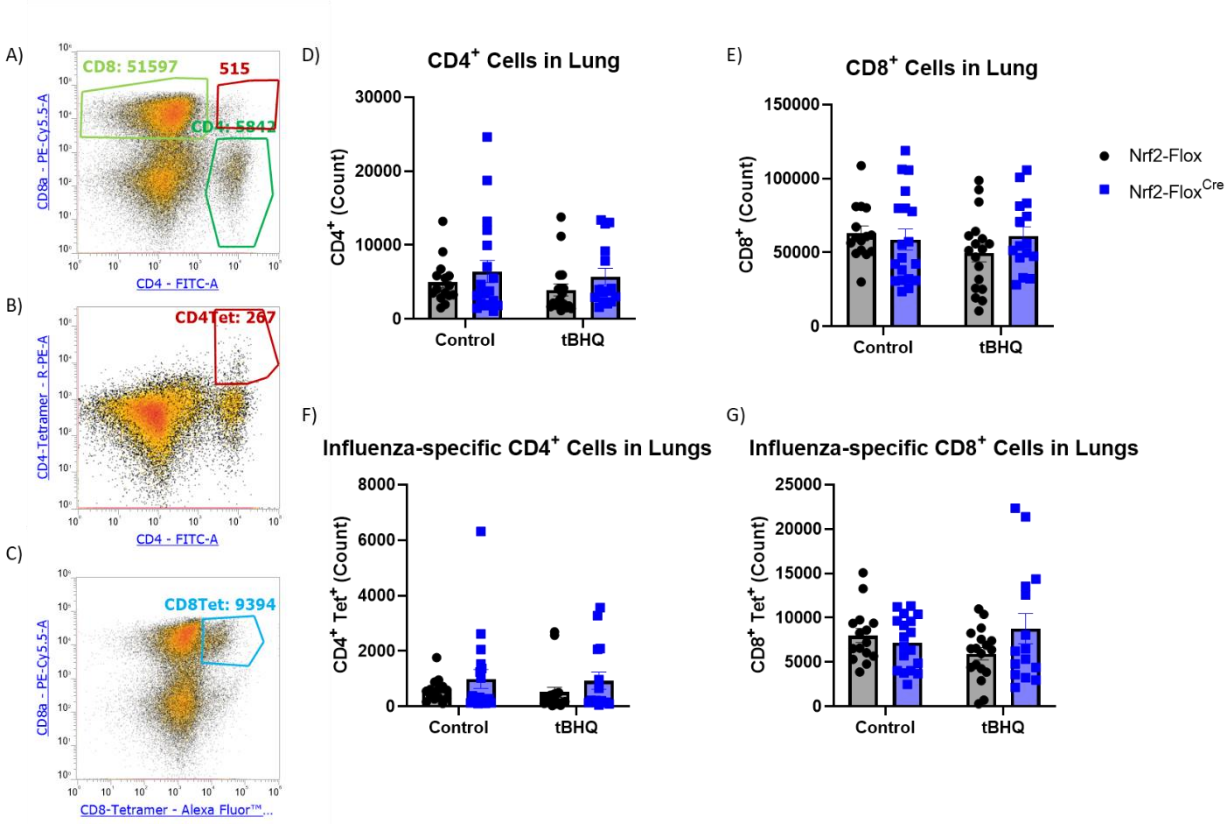

Figure 40: Dietary tBHQ is associated with a Nrf2-dependent reduction in lung CD8⁺ T cells following influenza infection. Mice were put on a diet with or without 0.0014% tBHQ 14 days prior to intranasal instillation with influenza A/PR/8/34 (H1N1). Ten days post-infection, lungs were removed and homogenized. Lung homogenates were labeled with fluorescent antibodies against CD4 and CD8α and influenza peptide-loaded tetramers. Cells were quantified via flow cytometry. (A-C) Representative density plots of $CD4^+$/$CD8^+$ T cells, influenza-specific $CD4^+$ T cells, and influenza-specific $CD8^+$ T cells, respectively, within the lungs of infected mice. (D-E) Quantification of lung $CD4^+$ and $CD8^+$ T cells. (F-G) Quantification of influenza-specific $CD4^+$ T cells and $CD8^+$ T cells within the lungs of infected mice. Graphs show combined data from five independent experiments with similar results.

42). Taken together, these data suggest that tBHQ activates Nrf2 within T cells leading to suppressed effector responses during influenza infection. Notably, these effects were not seen in Nrf2-flox^{Cre} mice, suggesting Nrf2 activation within T cells by tBHQ contributes to the reduced effector function during infection.

tBHQ Exposure Correlated with Reduced T-bet but not IFNγ Expression in CD8$^+$ T cells.

We previously showed *ex vivo* that Nrf2 activation by tBHQ impaired T_H1 cell polarization, evidenced by diminished IFNγ secretion and T-bet DNA-binding activity.[296] Accordingly, we identified T_H1 cells and the CD8$^+$ correlate, Tc1 cells, using intracellular antibodies to detect IFNγ and T-bet (Figure 43A, B). tBHQ exposure caused a Nrf2-dependent reduction in the number of T-bet$^+$ CD8$^+$ cells but had no effect on the number of IFNγ$^+$ cells (Figure 43F, G). Accordingly, no difference was observed in Tc1 cells (Figure 43H). In contrast, tBHQ appeared to have no effect within CD4$^+$ T cells with regard to T_H1 numbers (Figure 43C-E). This downward trend was not observed in Nrf2-flox^{Cre} mice, suggesting Nrf2 within T cells could modulate T-bet expression following activation by tBHQ.

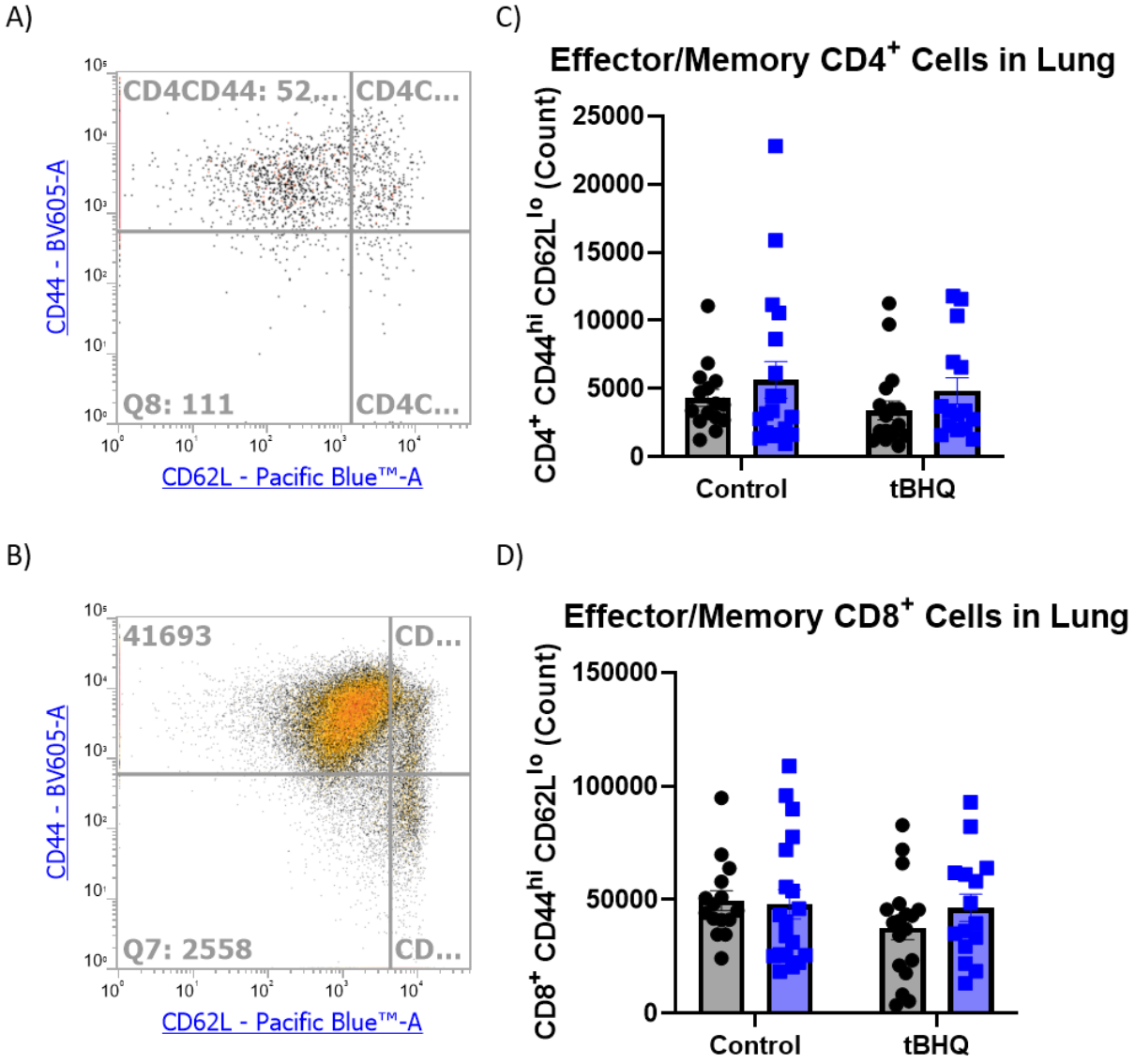

Figure 41: tBHQ exposure was associated with a reduced number of effector ($CD44^{hi}CD62L^{lo}$) CD8 T cells in the lungs of infected mice. Mice were put on a diet with or without 0.0014% tBHQ 14 days prior to intranasal instillation with influenza A/PR/8/34 (H1N1). Ten days post-infection, lungs were removed and homogenized. Lung homogenates were labeled with fluorescent antibodies against CD4 and CD8α and influenza peptide-loaded tetramers. Cells were quantified via flow cytometry. (A-B) Representative density plots of CD44 and CD62L expression on $CD4^+$ and $CD8^+$ T cells (C-D) Quantification of effector $CD4^+$ and $CD8^+$ T cells. Graphs show combined data from five independent experiments with similar results.

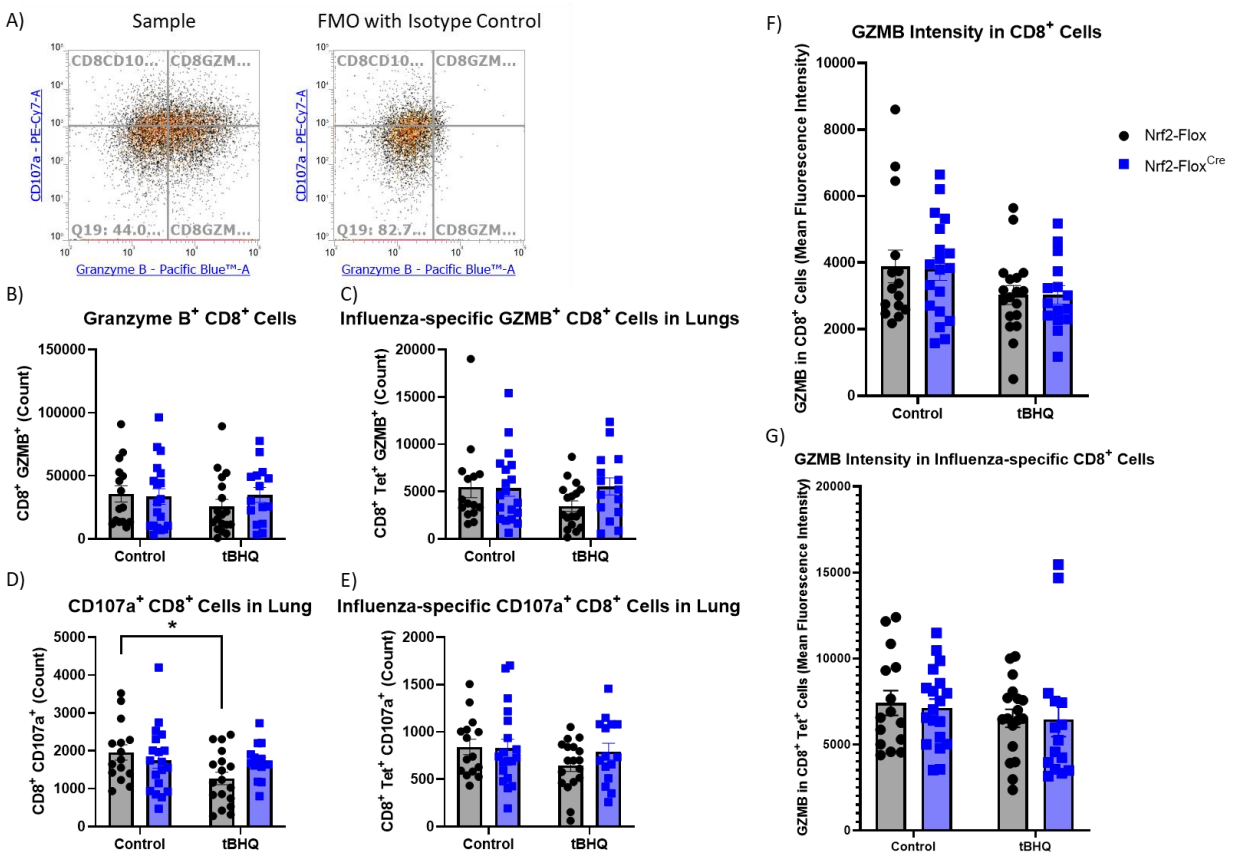

Figure 42: tBHQ exposure was associated with effector function in CD8$^+$ T cells.
Mice were put on a diet with or without 0.0014% tBHQ 14 days prior to intranasal instillation with influenza A/PR/8/34 (H1N1). Ten days post-infection, lungs were removed and homogenized. The resulting single-cell suspension was co-cultured with influenza-peptide-pulsed dendritic cells in the presence of monensin. 5 hours later, cells were labeled with antibodies against CD4, CD8α, CD107a, and granzyme B (GZMB) in addition to tetramers to identify influenza-specific cells. Cells were quantified with the Attune NxT flow cytometer. (A) Density plots showing positive staining of GZMB with a targeted antibody (left) compared to an FMO with an isotype control. (B-C) Quantification of GZMB$^+$ CD8$^+$ and influenza specific CD8$^+$ cells. (D-E) Quantification of CD107a$^+$ CD8$^+$ and influenza specific CD8$^+$ cells. (F-G) Mean GZMB fluorescence intensity within CD8$^+$ and influenza-specific CD8$^+$ cells. * $p < 0.05$ between the indicated groups (2-way ANOVA with Tukey's post-test).

tBHQ Exposure Correlated with Reduced Viral Clearance in a Nrf2-dependent Manner

We next assessed viral clearance. Ten days post-infection, we analyzed viral RNA levels in the lung using primers to amplify viral M1 RNA. We saw a 2-fold increase in viral RNA in animals fed tBHQ, though there was a lot of variability and therefore the effect was not statistically significant (Figure 44). Notably, this variability was largely absent in Nrf2-flox^{Cre} mice exposed to tBHQ.

The Absence of Nrf2 in T Cells Reduced Morbidity in Mice Exposed to tBHQ

Following sublethal infection with influenza A virus, body weight was monitored daily (Figure 45). Mice lacking Nrf2 in the T cell compartment showed substantially lower morbidity during infection compared to mice with wildtype T cells, though this oddly only occurred in mice exposed to tBHQ. Presently, it is unclear why this was the case as Nrf2-flox^{Cre} mice had similar immunological profiles on both the control and tBHQ-containing diets. Similar with our previous findings, tBHQ was not associated with increased morbidity in Nrf2-flox animals (correlated with wildtype mice previously).

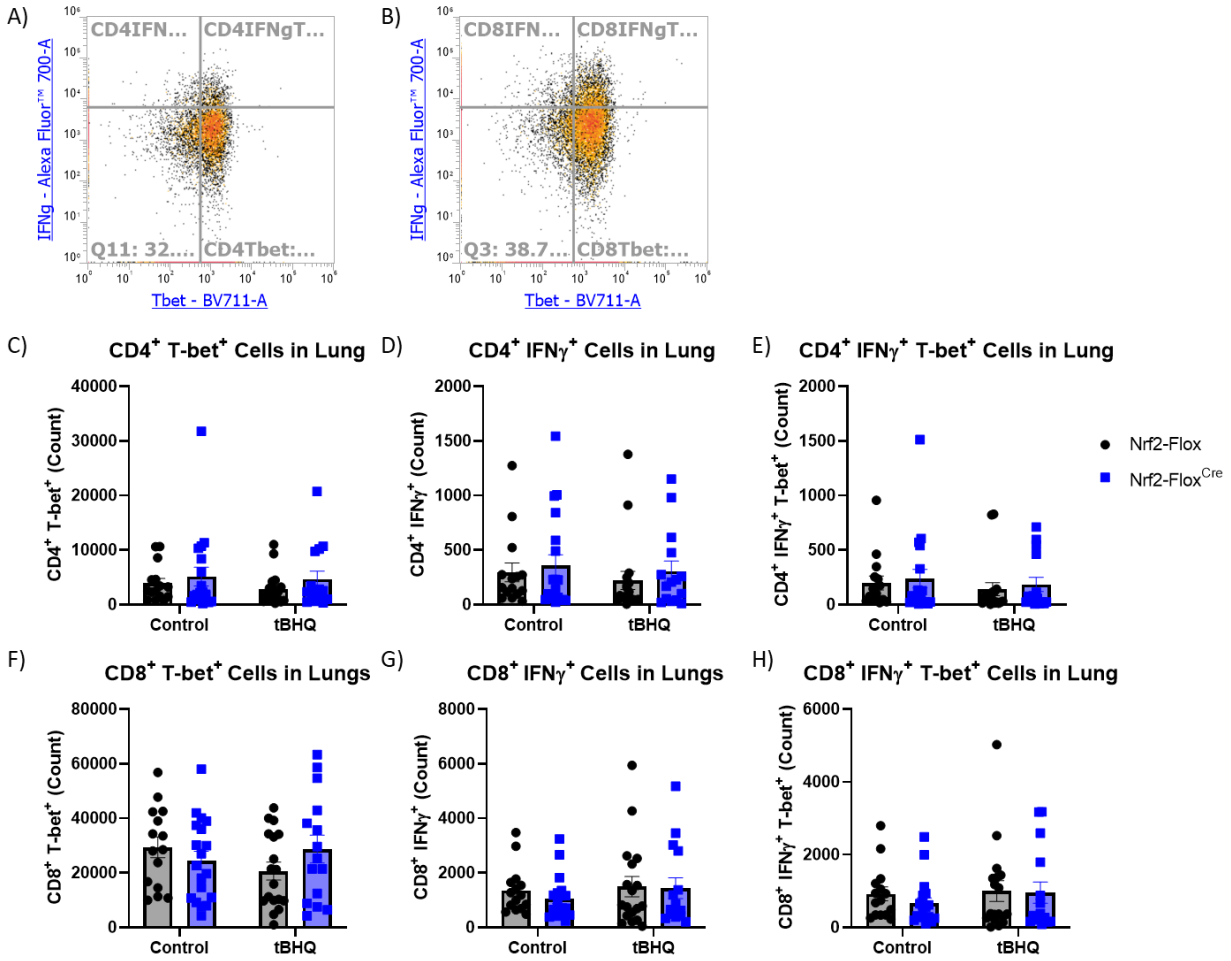

Figure 43: tBHQ exposure was associated with diminished T-bet in CD8⁺ T cells.
Mice were put on a diet with or without 0.0014% tBHQ 14 days prior to intranasal instillation with influenza A/PR/8/34 (H1N1). Ten days post-infection, lungs were removed and homogenized. The resulting single-cell suspension was co-cultured with influenza-peptide-pulsed dendritic cells in the presence of monensin. 5 hours later, cells were labeled with antibodies against CD4, CD8α, IFNγ, and T-bet. Cells were quantified with the Attune NxT flow cytometer. (A-B) Density plots showing positive staining of IFNγ and T-bet within $CD4^+$ (A) and $CD8^+$ (B) T cells. (C-E) Number of $CD4^+$ T cells with intracellular T-bet, IFNγ, or both. (F-H) Number of $CD8^+$ T cells with intracellular T-bet. IFNγ, or both.

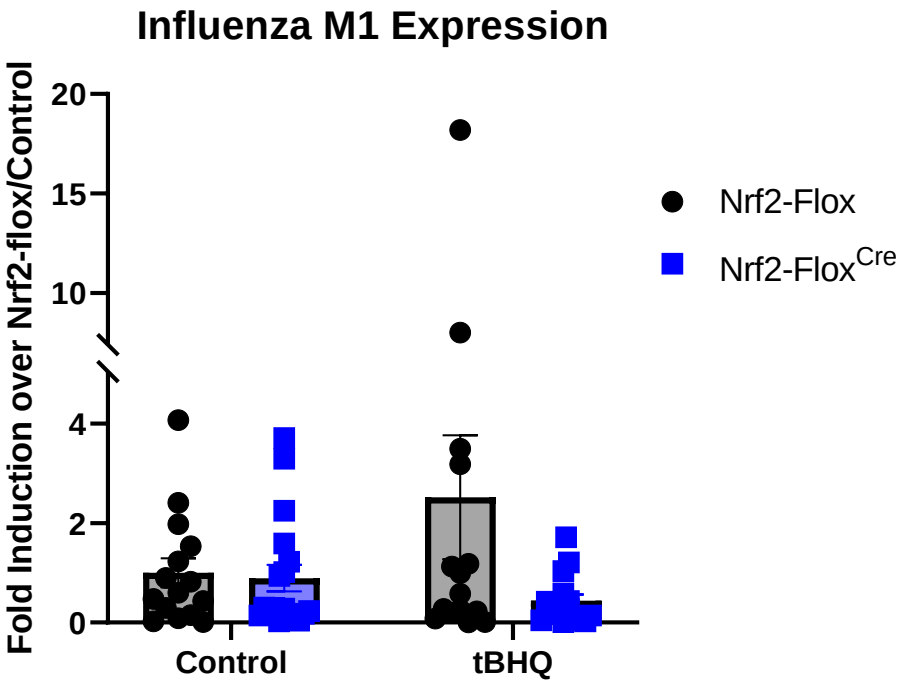

Figure 44: tBHQ associated with increased viral titer in the lungs of infected mice. Mice were put on a diet with or without 0.0014% tBHQ 2 weeks prior to intranasal instillation with either sterile saline or influenza A/PR/8/34 (H1N1). Ten days post-infection, lungs were removed and homogenized. Real-time PCR was used to quantify viral RNA from the lung homogenate. The viral matrix protein, M1, was used for viral quantification and was normalized to the housekeeper gene RPL13a.

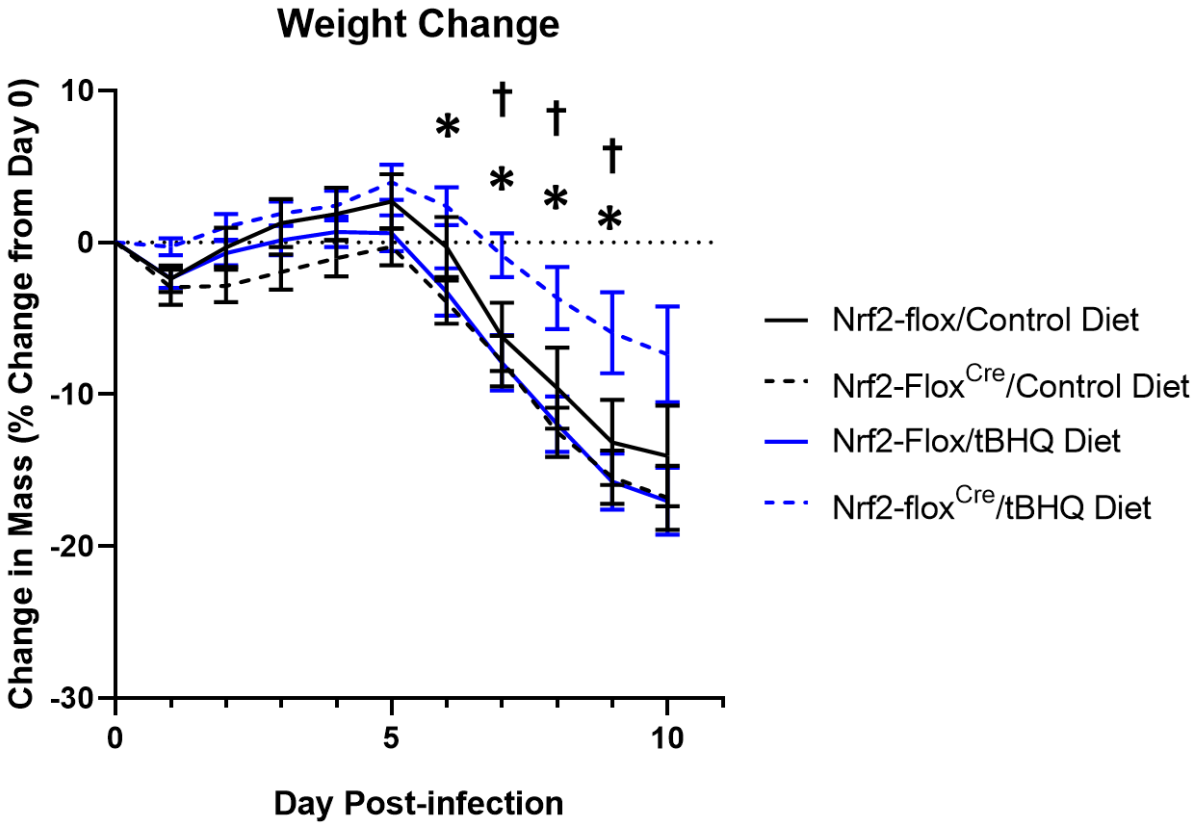

Figure 45: The absence of Nrf2 in T cells protected tBHQ-exposed mice against influenza-associated weight loss. Nrf2-flox and Nrf2-flox^{Cre} mice were placed on diets with or without 0.0014% tBHQ. 2 weeks after starting the diets, mice were infected with 0.23 $TCID_{50}$ of influenza A/PR/8/34 (H1N1) and their body weights were monitored daily. * denotes $p < 0.05$ between control and tBHQ-exposed animals within the Nrf2-flox^{Cre} mice. † denotes $p < 0.05$ between Nrf2-flox and Nrf2-flox^{Cre} animals on tBHQ diet.

Discussion

tBHQ is a ubiquitous food additive in the Western diet, though it is severely understudied in the context of immune responses and potential immunotoxicities. We previously showed tBHQ could suppress $CD4^+$ T cell activation and skew polarization.[296,301,371,372] Additionally, we observed *in vivo* that tBHQ suppressed the T cell response to influenza A virus infection. We initially hypothesized that these effects *in vivo* were due to Nrf2 activation, as tBHQ is a potent Nrf2 activator.[248] Our first

mechanistic studies utilized SCID mice which were reconstituted with T cells from either wildtype or Nrf2-null animals. However, tBHQ had no effect on wildtype T cells in that model, though Nrf2 indeed had detrimental effects on influenza-associated immunopathology. Consequently, we sought to utilize a different genetic model to interrogate the potential Nrf2-dependent effects of tBHQ on T cells during influenza infection. We did this by creating a conditional knockout mouse lacking Nrf2 specifically within T cells. Notably, the findings of these studies were mostly statistically insignificant due to variability between batches used for experiments, though the trends remained consistent batch-to-batch and were largely consistent with our previous statistically-powered experiments in wildtype animals.

Our previous studies in wildtype animals revealed that tBHQ abrogated the $CD8^+$ T cell response to influenza infection by suppressing T cell infiltration to the lung and impairing effector function within the $CD8^+$ T cells. These effects correlated with increased viral RNA within the lungs of tBHQ-exposed mice. The current studies yielded similar results, though the effects were less substantial than in the initial experiments. Nonetheless, subtle reductions in $CD8^+$ and influenza-specific $CD8^+$ T cells were observed in mice on a tBHQ diet, though these effects were absent in mice lacking Nrf2 in T cells. Furthermore, the number of effector T cells was reduced by tBHQ, and effector function as measured by granzyme B and CD107a expression was diminished by tBHQ in a T cell-intrinsic Nrf2-dependent fashion, ultimately suggesting that dietary tBHQ activates Nrf2 within T cells to suppress antiviral immune responses. These effects were associated with an increase in viral RNA in mice on the tBHQ diet, and this effect was also absent in the conditional knockout animals. An unexpected

finding in these experiments was the protection elicited by tBHQ in mice with a conditional deletion of Nrf2. Interestingly, these mice had 50% less weight loss compared to their counterparts on a control diet, and tBHQ was not protective in mice with in-tact Nrf2 within T cells. Nrf2 was previously demonstrated to confer benefits to epithelial cells during influenza infection, including preventing viral entry and cell death.[357,363] In light of these new findings, it is possible that *in vivo* activation of Nrf2 by dietary tBHQ diminishes T cell-mediated immunity to infection while concurrently protecting airway epithelial cells. In the absence of Nrf2 in T cells, immune function and viral clearance are restored, and tBHQ could elicit beneficial effects within the airway epithelium in the absence of detrimental immunomodulatory effects, thereby leading to the protection seen here. Notably, mice with a conditional knockout of Nrf2 in the alveolar type II cells demonstrated the ability of Nrf2 to protect these cells against toxic insult.[341] Future studies could begin to explore the balance between Nrf2 protection in airway epithelial cells and immune suppression in T cells by employing airway epithelium-specific deletion of Nrf2 expressing Cre recombinase under the Club cell secretory protein promoter.[438]

In contrast to our studies that utilized an adoptive transfer model, the current studies revealed no genotype differences beyond weight loss. In SCID mice, transfer of Nrf2-null T cells was associated with an increase of influenza-specific T cells responding to infection, an enhancement of $IFN\gamma^+$ $CD4^+$ T cells, and diminished effector function that ameliorated lung damage. Several differences could contribute to these discrepancies. First, thymic development of T cells is absent in SCID mice.[410] Accordingly, if thymic output is important during influenza infection – something that

remains to be explored – this represents one major difference between the two models. Additionally, SCID mice lack natural killer T (NKT) cells, and it was recently shown that Nrf2 modulates NKT cell maturation, homeostasis, and effector function.[292] Similar to $CD4^+$ T cells, NKT cells produce IFNγ and stimulate T cells during influenza infection; the absence of this cell type in the SCID adoptive transfer model could therefore explain the difference observed in T cell responses.[439] Future studies incorporating adoptive transfer of NKT cells could provide insight into their importance in modulating T cell responses during influenza infection in the presence or absence of Nrf2. Another difference could be harbored within the microbiota of the mice in these studies. The SCID mice were housed under stricter pathogen-free conditions than Nrf2-flox mice, and therefore are extremely likely to have distinct microbiomes. Emerging evidence has revealed the importance of the intestinal and respiratory microbiota in modulating host immunity including T cell-mediated immunity to influenza infection and could be a contributing factor to the differences observed in these studies.[440–444] Further studies are warranted to clarify the role of Nrf2 within T cells during influenza infection.

CHAPTER 6
Summary, Significance, and Future Directions

Summary of Findings

Previous studies from our lab utilized *ex vivo* studies to assess the role of tBHQ and concurrent Nrf2 activation on T cell function. These studies revealed that tBHQ impaired $CD4^+$ T cell activation and polarization, and some of these effects required Nrf2. However, it was unclear if tBHQ could elicit these effects *in vivo* settings in which tBHQ can be metabolized and may not reach tissue concentrations high enough to achieve immunomodulatory effects. We hypothesized that tBHQ, through activation of Nrf2 in T cells, would diminish the T cell response to influenza infection in mice. To begin exploring the effects of tBHQ on T cells *in vivo*, an influenza model was established in which mice were fed diets with or without tBHQ at a dose relevant to human exposure, and the T cell responses to influenza infection were assessed. Initial findings in wildtype mice revealed that tBHQ suppressed $CD4^+$ and $CD8^+$ T cell responses to primary influenza infection, evidenced by fewer $CD8^+$ T cells in the lung and reduced surface expression of effector molecules on both $CD4^+$ and $CD8^+$ T cells. This led to enhanced viral RNA detected within the lungs. While direct evidence of impaired T_H1 polarization was not observed, mice on a tBHQ diet were prone to an inflammatory type 2 immune response characterized by eosinophilic inflammation and mucus hypersecretion compared to mice on a control diet. Notably, the tBHQ-mediated immune suppression resulted in a reduced capacity for memory formation which led to an insufficient memory response to heterosubtypic infection.

As we hypothesized that tBHQ would elicit its effects on T cells through intrinsic Nrf2 activation, we utilized two distinct models to assess the role of Nrf2 on tBHQ-mediated suppression of antiviral T cell responses. The first model utilized SCID mice

which lack functional T cells. The T cell compartments of these mice were reconstituted with T cells from either wildtype or Nrf2-null mice. After allowing ample time for establishment of the T cell populations, mice were exposed to tBHQ and infected with influenza A virus. This study revealed that T cell-specific Nrf2 exacerbates immunopathology during influenza infection. Notably, IFNγ production was augmented in Nrf2-deficient T cells *in vivo*, consistent with our previous findings *ex vivo*.[296] Despite this increase in IFNγ production, effector function was diminished in Nrf2-deficient T cells which suggests Nrf2 contributes to effector function. Additionally, tBHQ had virtually no effect on T cell function in this model. These findings come in stark contrast to the findings of our other model utilizing Cre recombinase to delete Nrf2 within T cells. In this model, the only consistent finding with the adoptive transfer model was that Nrf2-deficient T cells correlated with reduced morbidity, albeit only in the presence of tBHQ. Furthermore, utilizing a conditional knockout of Nrf2 revealed that the immunomodulatory effects of tBHQ required Nrf2 in T cells. While the findings of the two models are quite distinct, they both indicate that Nrf2 modulates the T cell response to influenza virus and worsens host outcomes.

Significance of Findings

tBHQ can be found in a vast array of foods as it is used to prevent rancidification of fats.[367] It was first approved for use in food in the 1970's, decades before immunotoxicology assessment for food additives became utilized.[370] The allowable daily intake, based on toxicity findings in dogs, was established as 0.7 mg/kg/day, though expert estimates suggest consumers likely exceed this value, up to 7.7

mg/kg/day.[369] To this day, no risk assessment is publicly available on potential immunotoxicities elicited by tBHQ. To our knowledge, the current studies are the first to demonstrate that tBHQ consumed through the diet at doses relevant to human exposure hamper T cell-mediated immunity to viral infection. These findings come at a time in which the role of T cell-mediated immunity is greatly appreciated, especially in response to heterosubtypic infection. In the 2009 influenza pandemic, heterosubtypic immunity conferred by T cells provided protection to the elderly population, while healthy adults – usually not at risk of severe infection – were the primary sufferers of severe H1N1 infection.[74] Additionally, T cells were recently identified which could provide heterosubtypic protection against SARS-CoV-2, the causative agent for the COVID-19 pandemic.[445] Accordingly, heterosubtypic immunity elicited by T cells is a vital weapon for global health against certain viral infections. Moreover, universal influenza vaccines designed to protect against all strains, including novel strains with pandemic potential, will need to elicit long-lived T cell memory.[122,399] Accordingly, it is imperative to identify mechanisms which impair the formation of heterosubtypic immunity and ways to improve the development of long-lived T cell memory pools. The current findings suggest that tBHQ impairs the formation of heterosubtypic memory by ablating T cell responses to primary influenza infection. By performing further risk assessment studies and evaluation of tBHQ-mediated immunotoxicities, it may be possible to overcome one hurdle to the generation of an efficacious T cell-targeting influenza vaccine.

In addition to the toxicological importance of these studies, valuable insight was gained into the role of Nrf2 in T cells *in vivo*. Nrf2 activation by tBHQ within T cells led

to a type 2 inflammatory response in wildtype mice, and follow-up studies using conditional knockout of Nrf2 in T cells suggest that this effect required Nrf2 in a T cell-dependent manner. Notably, other studies demonstrated that Nrf2 suppressed T_H2-mediated pathologies within the lung.[295,339] However, the data presented here suggest Nrf2 activation promoted a type 2 immune response. It is entirely possible that Nrf2 can modulate both T_H1 and T_H2 responses *in vivo* depending on various environmental factors. Additionally, $CD4^+$ T cells exhibit a degree of plasticity, and the cytokine milieu during influenza infection can convert T_H2 cells to T_H1 cells.[446] Of note, childhood respiratory viral infections are associated with the development of airway hyperresponsiveness and asthma later in life.[447] However, influenza virus was shown to prevent the development of asthma in a mouse model in which T_H1 cells prevented the recruitment of T_H2 cells and eosinophils to the airways.[448] In the context of these studies, Nrf2 activation by tBHQ resulted in eosinophilia within the lungs, and thus tBHQ exposure may contribute to the development of T_H2-mediated airway disease following influenza infection.

Future Directions

While the current studies demonstrated that tBHQ, through activation of Nrf2 in T cells, impairs the T cell response to influenza infection, much work remains to determine how these effects occur. For all of the presented experiments, tBHQ was fed to the mice for the duration of the studies, beginning two weeks prior to initial infection up through terminal collection. However, it is unclear at which point(s) in the immune response to infection tBHQ may impact T cell function. In the context of primary

influenza infection, influenza-specific T cells can be readily detected in the mediastinal lymph node 4 days post-infection and T cell levels peak in the lungs 10 days post-infection.[449–451] However, mice infected with influenza have decreased appetite and therefore reduced exposure to tBHQ late in infection, suggesting the observed changes in T cell function likely occur early during the priming and expansion phase of the T cell response to infection. Additionally, it is unclear from these studies if initial exposure to tBHQ is sufficient to abrogate memory T cell responses to infection or if continued tBHQ exposure is required. Future studies should address these questions. For instance, in both primary and heterosubtypic infection models, mice could be exposed to tBHQ for the first 5 days post-infection, then switched to a control diet devoid of tBHQ. This would provide vital information on whether tBHQ causes persistent changes within influenza-specific T cells leading to suppressed memory formation. It would be reassuring to know if tBHQ exposure during primary infection, or vaccination, is sufficient to dampen memory formation. Conversely, it would be concerning to know tBHQ causes lasting effects on T cell populations.

Another pitfall of the current studies was the failure to thoroughly investigate the immunosuppressive features of $CD8^+$ T cells and $FoxP3^+$ Tregs known to be important in limiting anti-influenza immune responses.[58,59,382] While IL-10 is known to be an immunosuppressive cytokine and limits inflammation during influenza infection, we were unable to detect IL-10 in lung cells by flow cytometry as well as secreted cytokine within bronchoalveolar lavage fluid. Due to the hyperinflammatory nature of this model, it is likely that IL-10-producing cells are rare within the lung and thus hard to detect with the current methodologies. Additionally, IL-10-producing $CD4^+$ T cells are highly

heterogenous, and not all IL-10-producing T cell populations possess immunosuppressive activity.[452] To explore the role of tBHQ/Nrf2 on immunosuppressive T cell functions during influenza infection, further studies must be conducted. A challenge to these studies will be tying findings within regulatory T cell populations to effector populations, as FoxP3^{+} Tregs peak in the lung several days ahead of the effector T cell peak.[54,59] Additionally, the function of FoxP3^{+} Tregs and IL-10 during influenza is complex, as these limit memory responses while promoting memory formation and have disparate effects depending on the timing of their responses during primary infection.[54,57,59,125,127,382] Future studies could explore the effects of tBHQ on IL-10 deficient mice to determine if tBHQ modulates the T cell response to influenza infection through an IL-10-dependent manner. Notably, tBHQ was shown to induce IL-10 production in astroglia.[387] More nuanced studies could also utilize IL-10 reporter mice to determine if tBHQ augments the number of IL-10-producing cells in lungs and lymph nodes during influenza infection. For these studies, it will be critical to establish a time course to capture the kinetics of IL-10 production and subsequent immune suppression. Further studies could utilize single-cell RNA sequencing on purified T cell populations from the lung to identify cells with transcriptomic profiles correlating with immune suppression. Notably, this could identify a role for FoxP3^{-} regulatory T cells, such as Tr1 cells, which have so far been unexplored in the context of influenza infection.[453]

Another oversight in these studies was the potential role of Nrf2 activation on chemokine signaling. Chemokines are known to be important in trafficking of T cells to the lungs during infection, and it was just recently revealed that the CXCL16/CXCR6

signaling pathway recruited precursor memory $CD8^+$ T cells to the airways during IAV infection, promoting the development of heterosubtypic immunity.[115] mRNA expression analysis revealed that tBHQ significantly downregulated both CXCL16 and CXCR6 in the lungs of infected mice (data not shown). Additionally, *in silico* analysis revealed several putative ARE sequences in each gene, and microarray data from liver revealed that Nrf2-null mice had 4-fold induction of CXCR6 expression.[454] Future studies should begin to explore the role of Nrf2 on chemokine signaling.

Lastly, human relevance of the current findings must be assessed. At present, exposure data about tBHQ is largely absent from the literature making it impossible to identify an epidemiological link between tBHQ exposure and influenza infections. Additionally, human studies to assess this link would be difficult as tBHQ is often unlabeled on food packaging, and even when it is labeled the amount is not included. To overcome these challenges, the use of humanized SCID mice could be beneficial. The Hu-SRC-SCID mouse model allows for the engraftment of human hematopoietic stem cells isolated from cord blood and results in the development of a humanized immune system in the mice, including T cells, B cells, NK cells, antigen presenting cells, and myeloid cells.[455] The caveat is that the resulting T cells develop within the mouse thymus and therefore have T cell receptors reminiscent of murine T cells instead of human T cell receptors. However, this is a small disadvantage in comparison to the benefit of using this model to interrogate effects of tBHQ on the human immune response to influenza infection.

Ultimately, the presented studies provide a solid framework to begin interrogating the potential immunotoxicity of tBHQ on antiviral immune responses *in vivo* and provide initial insight into the ability of Nrf2 to regulate the T cell response to influenza infection.

WORKS CITED

WORKS CITED

1. Nayak, D. P., Balogun, R. A., Yamada, H., Zhou, Z. H. & Barman, S. Influenza virus morphogenesis and budding. *Virus Res.* **143**, 147–161 (2009).

2. Gamblin, S. J. & Skehel, J. J. Influenza hemagglutinin and neuraminidase membrane glycoproteins. *J. Biol. Chem.* **285**, 28403–28409 (2010).

3. Grambas, S. & Hay, A. J. Maturation of influenza a virus hemagglutinin-Estimates of the pH encountered during transport and its regulation by the M2 protein. *Virology* **190**, 11–18 (1992).

4. Honda, A., Ueda, K., Nagata, K. & Ishihama, A. RNA polymerase of influenza virus: Role of NP in RNA chain elongation. *J. Biochem.* **104**, 1021–1026 (1988).

5. Tong, S. *et al.* A distinct lineage of influenza A virus from bats. *Proc. Natl. Acad. Sci. U. S. A.* **109**, 4269–4274 (2012).

6. Zhu, X. *et al.* Crystal structures of two subtype N10 neuraminidase-like proteins from bat influenza A viruses reveal a diverged putative active site. *Proc. Natl. Acad. Sci. U. S. A.* **109**, 18903–18908 (2012).

7. Types of Influenza Viruses | CDC. https://www.cdc.gov/flu/about/viruses/types.htm.

8. Russell, R. J., Gamblin, S. J. & Skehel, J. J. Influenza glycoproteins: Hemagglutinin and neuraminidase. in *Textbook of Influenza* vol. 2 67–100 (2013).

9. Sellers, S. A., Hagan, R. S., Hayden, F. G. & Fischer, W. A. The hidden burden of influenza: A review of the extra-pulmonary complications of influenza infection. *Influenza Other Respi. Viruses* **11**, 372–393 (2017).

10. World Health Organization. Influenza (Seasonal). https://www.who.int/news-room/fact-sheets/detail/influenza-(seasonal) (2018).

11. Iuliano, A. D. *et al.* Estimates of global seasonal influenza-associated respiratory mortality: a modelling study. *Lancet* **391**, 1285–1300 (2018).

12. Paget, J. *et al.* Global mortality associated with seasonal influenza epidemics: New burden estimates and predictors from the GLaMOR Project. *J. Glob. Health* **9**, 1–12 (2019).

13. Lee, V. J. *et al.* Advances in measuring influenza burden of disease. *Influenza Other Respi. Viruses* **12**, 3–9 (2018).

14. Hensley, S. E. *et al.* Hemagglutinin receptor binding avidity drives influenza a

virus antigenic drift. *Science (80-.).* **326**, 734–736 (2009).

15. López-Labrador, F. X. *et al.* Genetic characterization of influenza viruses from influenza-related hospital admissions in the St. Petersburg and Valencia sites of the Global Influenza Hospital Surveillance Network during the 2013/14 influenza season. *J. Clin. Virol.* **84**, 32–38 (2016).

16. Bender, B. S., Croghan, T., Zhang, L. & Small, Jr, P. A. Transgenic Mice Lacking Class I Major Histocompatibility Complex-restricted T Cells Have Delayed Viral Clearance and Increased Mortality after Influenza Virus Challenge. *J. Exp. Med.* **175**, 1143–1145 (1992).

17. Rangel-Moreno, J. *et al.* B Cells Promote Resistance to Heterosubtypic Strains of Influenza via Multiple Mechanisms. *J. Immunol.* **180**, 454–463 (2008).

18. Tamura, S. & Kurata, T. Defense mechanisms against influenza virus infection in the respiratory tract mucosa. *Jpn. J. Infect. Dis.* **57**, 236–47 (2004).

19. Iwasaki, T. & Nozima, T. Defense mechanisms against primary influenza virus infection in mice: I. The roles of interferon and neutralizing antibodies and thymus dependence of interferon and antibody production. *J. Immunol.* **118**, 256–263 (1977).

20. Lv, J. *et al.* Kinetics of pulmonary immune cells, antibody responses and their correlations with the viral clearance of influenza A fatal infection in mice. *Virol. J.* **11**, (2014).

21. Chen, X. *et al.* Host immune Response to influenza A virus infection. *Front. Immunol.* **9**, (2018).

22. Keating, R. *et al.* The kinase mTOR modulates the antibody response to provide cross-protective immunity to lethal infection with influenza virus. *Nat. Immunol.* **14**, 1266–1276 (2013).

23. LaMere, M. W. *et al.* Contributions of Antinucleoprotein IgG to Heterosubtypic Immunity against Influenza Virus. *J. Immunol.* **186**, 4331–4339 (2011).

24. Nguyen, H. H., van Ginkel, F. W., Vu, H. L., McGhee, J. R. & Mestecky, J. Heterosubtypic Immunity to Influenza A Virus Infection Requires B Cells but Not CD8 + Cytotoxic T Lymphocytes. *J. Infect. Dis.* **183**, 368–76 (2001).

25. Epstein, S. L. *et al.* Mechanisms of heterosubtypic immunity to lethal influenza A virus infection in fully immunocompetent, T cell-depleted, beta2-microglobulin-deficient, and J chain-deficient mice. *J. Immunol.* **158**, 1222–1230 (1997).

26. Kim, Y. J. *et al.* Roles of antibodies to influenza A virus hemagglutinin, neuraminidase, and M2e in conferring cross protection. *Biochem. Biophys. Res. Commun.* **493**, 393–398 (2017).

27. Park, J. K. *et al.* Pre-existing immunity to influenza virus hemagglutinin stalk might drive selection for antibody-escape mutant viruses in a human challenge model. *Nat. Med.* **26**, 1240–1246 (2020).

28. Lorenzo, M. E. *et al.* Antibody responses and cross protection against lethal influenza A viruses differ between the sexes in C57BL/6 mice. *Vaccine* **29**, 9246–9255 (2011).

29. Chen, Q. *et al.* Human Vγ9Vδ2-T cells synergize CD4+ T follicular helper cells to produce influenza virus-specific antibody. *Front. Immunol.* **9**, 1–12 (2018).

30. Dong, P. *et al.* γδ T Cells Provide Protective Function in Highly Pathogenic Avian H5N1 Influenza A Virus Infection. *Front. Immunol.* **9**, 1–11 (2018).

31. Guo, X. zhi J. *et al.* Lung γδ T Cells Mediate Protective Responses during Neonatal Influenza Infection that Are Associated with Type 2 Immunity. *Immunity* **49**, 531-544.e6 (2018).

32. Goldberg, E. L. *et al.* Ketogenic diet activates protective gd T cell responses against influenza virus infection. *Sci. Immunol.* **4**, (2019).

33. Topham, D. J., Tripp, R. a & Doherty, P. C. CD8+ T cells clear influenza virus by perforin or Fas-dependent processes. *J. Immunol.* **159**, 5197–5200 (1997).

34. Swain, S. L., McKinstry, K. K. & Strutt, T. M. Expanding roles for CD4+ T cells in immunity to viruses. *Nat. Rev. Immunol.* **12**, 136–148 (2012).

35. Terhune, Julia; Berk, Erik; Czerniecki, B. J. Dendritic Cell-Induced Th1 and Th17 Cell Differentiation for Cancer Therapy. *Vaccines* **1**, 527–549 (2013).

36. Bossie, A. & Vitetta, E. S. IFN-gamma enhances secretion of IgG2a from IgG2a-committed LPS-stimulated murine B cells: implications for the role of IFN-gamma in class switching. *Cell. Immunol.* **135**, 95–104 (1991).

37. Sun, J. C. & Bevan, M. J. Defective CD8 T cell memory following acute infection without CD4 T cell help. *Science* **300**, 339–42 (2003).

38. Shedlock, D. J. Requirement for CD4 T Cell Help in Generating Functional CD8 T Cell Memory. *Science* **300**, 337–339 (2003).

39. Murray, H. W. Interferon-gamma, the activated macrophage, and host defense against microbial challenge. *Ann. Intern. Med.* **108**, 595–608 (1988).

40. Staitieh, B. S. *et al.* Activation of Alveolar Macrophages with Interferon-gamma Promotes Antioxidant Defenses via the Nrf2-ARE Pathway. *J Clin Cell Immunol* **6**, 1–17 (2015).

41. McKinstry, K. K. *et al.* IL-10 Deficiency Unleashes an Influenza-Specific Th17

Response and Enhances Survival against High-Dose Challenge. *J. Immunol.* **182**, 7353–7363 (2009).

42. Maroof, A., Yorgensen, Y. M., Li, Y. & Evans, J. T. Intranasal Vaccination Promotes Detrimental Th17-Mediated Immunity against Influenza Infection. *PLoS Pathog.* **10**, (2014).

43. Wang, J. *et al.* Respiratory influenza virus infection induces intestinal immune injury via microbiotamediated Th17 cell-dependent inflammation. *J. Exp. Med.* **211**, 2397–2410 (2014).

44. Gopal, R. *et al.* Mucosal pre-exposure to Th17-inducing adjuvants exacerbates pathology after influenza infection. *Am. J. Pathol.* **184**, 55–63 (2014).

45. Er, J. Z., Koean, R. A. G. & Ding, J. L. Loss of T-bet confers survival advantage to influenza–bacterial superinfection. *EMBO J.* **38**, 1–16 (2019).

46. Graham, M. B., Braciale, V. L. & Braciale, T. J. Influenza virus-specific CD4+ T helper type 2 T lymphocytes do not promote recovery from experimental virus infection. *J. Exp. Med.* **180**, 1273–82 (1994).

47. McMaster, S. R., Wilson, J. J., Wang, H. & Kohlmeier, J. E. Airway-Resident Memory CD8 T Cells Provide Antigen-Specific Protection against Respiratory Virus Challenge through Rapid IFN-γ Production. *J. Immunol.* **195**, 203–9 (2015).

48. Brunner, T. *et al.* Expression of Fas ligand in activated T cells is regulated by c-Myc. *J. Biol. Chem.* **275**, 9767–9772 (2000).

49. Waring, P. & Müllbacher, A. Cell death induced by the Fas/Fas ligand pathway and its role in pathology. *Immunol. Cell Biol.* **77**, 312–317 (1999).

50. Bálint *et al.* Supramolecular attack particles are autonomous killing entities released from cytotoxic T cells. *Science (80-.).* **368**, 897–901 (2020).

51. Johnson, B. J. *et al.* Single-cell perforin and granzyme expression reveals the anatomical localization of effector CD8+ T cells in influenza virus-infected mice. *Proc. Natl. Acad. Sci. U. S. A.* **100**, 2657–2662 (2003).

52. Voskoboinik, I., Whisstock, J. C. & Trapani, J. A. Perforin and granzymes: Function, dysfunction and human pathology. *Nat. Rev. Immunol.* **15**, 388–400 (2015).

53. Chiusolo, V. *et al.* Granzyme B enters the mitochondria in a Sam50-, Tim22- and mtHsp70-dependent manner to induce apoptosis. *Cell Death Differ.* **24**, 747–758 (2017).

54. Betts, R. J. *et al.* Influenza A Virus Infection Results in a Robust, Antigen-Responsive, and Widely Disseminated Foxp3+ Regulatory T Cell Response. *J.*

Virol. **86**, 2817–2825 (2012).

55. Egarnes, B. & Gosselin, J. Contribution of Regulatory T Cells in Nucleotide-Binding Oligomerization Domain 2 Response to Influenza Virus Infection. *Front. Immunol.* **9**, (2018).

56. Brincks, E. L. *et al.* Antigen-Specific Memory Regulatory CD4 + Foxp3 + T Cells Control Memory Responses to Influenza Virus Infection. *J. Immunol.* **190**, 3438–3446 (2013).

57. Chappert, P. *et al.* Antigen-specific Treg impair CD8+ T-cell priming by blocking early T-cell expansion. *Eur. J. Immunol.* **40**, 339–350 (2010).

58. Bennink, J. R. *et al.* Regulatory T Cells Suppress CD8 + T Cell Responses Induced by Direct Priming and Cross-Priming and Moderate Immunodominance Disparities. *J. Immunol.* **174**, 3344–51 (2005).

59. Rogers, M. C. *et al.* CD4 + Regulatory T Cells Exert Differential Functions during Early and Late Stages of the Immune Response to Respiratory Viruses. *J. Immunol.* **201**, 1253–1266 (2018).

60. Betts, R. J., Ho, A. W. S. & Kemeny, D. M. Partial depletion of natural CD4 +CD25 + regulatory T cells with anti-CD25 antibody does not alter the course of acute influenza a virus infection. *PLoS One* **6**, (2011).

61. Moser, E. K., Hufford, M. M. & Braciale, T. J. Late Engagement of CD86 after Influenza Virus Clearance Promotes Recovery in a FoxP3 + Regulatory T Cell Dependent Manner. *PLoS Pathog.* **10**, e1004315 (2014).

62. Sell, S. *et al.* Intraepithelial T-cell cytotoxicity, induced bronchus-associated lymphoid tissue, and proliferation of pneumocytes in experimental mouse models of influenza. *Viral Immunol.* **27**, 484–496 (2014).

63. Sell, S., Mckinstry, K. K. & Strutt, T. M. Mouse Models Reveal Role of T-Cytotoxic and T-Reg Cells in Immune Response to Influenza : Implications for Vaccine Design. *Viruses* **11**, (2019).

64. Lukacher, A. E., Morrison, L. A., Braciale, V. L., Malissen, B. & Brachiale, T. J. Expression of specific cytolytic activity by H2-I region-restricted, influenza virus-specific T lymphocyte clones. *J. Exp. Med.* **162**, 171–187 (1985).

65. Zaunders, J. J. *et al.* Identification of circulating antigen-specific CD4+ T lymphocytes with a CCR5+, cytotoxic phenotype in an HIV-1 long-term nonprogressor and in CMV infection. *Blood* **103**, 2238–2247 (2004).

66. van Leeuwen, E. M. M. *et al.* Emergence of a CD4+CD28- Granzyme B+, Cytomegalovirus-Specific T Cell Subset after Recovery of Primary Cytomegalovirus Infection. *J. Immunol.* **173**, 1834–1841 (2004).

67. Thewissen, M. *et al.* CD4+CD28null T Cells in Autoimmune Disease: Pathogenic Features and Decreased Susceptibility to Immunoregulation. *J. Immunol.* **179**, 6514–6523 (2007).

68. Brien, J. D., Uhrlaub, J. L. & Nikolich-Zugich, J. West Nile Virus-Specific CD4 T Cells Exhibit Direct Antiviral Cytokine Secretion and Cytotoxicity and Are Sufficient for Antiviral Protection. *J. Immunol.* **181**, 8568–8575 (2008).

69. Stuller, K. A. & Flano, E. CD4 T Cells Mediate Killing during Persistent Gammaherpesvirus 68 Infection. *J. Virol.* **83**, 4700–4703 (2009).

70. Quezada, S. A. *et al.* Tumor-reactive CD4 $^{+}$ T cells develop cytotoxic activity and eradicate large established melanoma after transfer into lymphopenic hosts. *J. Exp. Med.* **207**, 637–650 (2010).

71. Xie, Y. *et al.* Naive tumor-specific CD4 $^{+}$ T cells differentiated in vivo eradicate established melanoma. *J. Exp. Med.* **207**, 651–667 (2010).

72. Weiskopf, D. *et al.* Dengue virus infection elicits highly polarized CX3CR1 + cytotoxic CD4 + T cells associated with protective immunity. *Proc. Natl. Acad. Sci.* 4–11 (2015) doi:10.1073/pnas.1505956112.

73. Brown, D. M., Dilzer, A. M., Meents, D. L. & Swain, S. L. CD4 T Cell-Mediated Protection from Lethal Influenza: Perforin and Antibody-mediated Mechanisms Give a One-Two Punch. *J. Immunol.* **177**, 2888–2898 (2006).

74. Wilkinson, T. M. a. *et al.* Preexisting influenza-specific CD4+ T cells correlate with disease protection against influenza challenge in humans. *Nat. Med.* **18**, 276–282 (2012).

75. Brown, D. M., Kamperschroer, C., Dilzer, A. M., Roberts, D. M. & Swain, S. L. IL-2 and antigen dose differentially regulate perforin- and FasL-mediated cytolytic activity in antigen specific CD4+ T cells. *Cell. Immunol.* **257**, 69–79 (2009).

76. Hua, L. *et al.* Cytokine-dependent induction of CD4+ T cells with cytotoxic potential during influenza virus infection. *J. Virol.* **87**, 11884–93 (2013).

77. Workman, A. M., Jacobs, A. K., Vogel, A. J., Condon, S. & Brown, D. M. Inflammation enhances IL-2 driven differentiation of cytolytic CD4 T cells. *PLoS One* **9**, 1–12 (2014).

78. Maimone, M. M. & Morrison, L. A. Features of target cell lysis by class I and class II MHC-restricted cytolytic T lymphocytes. *J. Immunol.* **137**, 3639–3643 (1986).

79. Brown, D. M., Lee, S., Garcia-Hernandez, M. de la L. & Swain, S. L. Multifunctional CD4 cells expressing gamma interferon and perforin mediate protection against lethal influenza virus infection. *J. Virol.* **86**, 6792–803 (2012).

80. Marshall, N. B. *et al.* NKG2C/E Marks the Unique Cytotoxic CD4 T Cell Subset, ThCTL, Generated by Influenza Infection. *J. Immunol.* **198**, 1142–1155 (2017).

81. Jellison, E. R., Kim, S.-K. & Welsh, R. M. Cutting Edge: MHC Class II-Restricted Killing In Vivo during Viral Infection. *J. Immunol.* **174**, 614–618 (2005).

82. Oja, A. E. *et al.* The transcription factor hobit identifies human cytotoxic CD4+ T cells. *Front. Immunol.* **8**, 1–11 (2017).

83. Takeuchi, A. *et al.* CRTAM determines the CD4+ cytotoxic T lymphocyte lineage. *J. Exp. Med.* **213**, 123–38 (2016).

84. Yap, K. L. & Ada, G. L. The Recovery of Mice from Influenza A Virus Infection: Adoptive Transfer of Immunity with Influenza Virus-specific Cytotoxic T Lymphocytes Recognizing a Common Virion Antigen. *Scand. J. Immunol.* **8**, 413–420 (1978).

85. Ennis, F. A., Yi-Hua, Q. & Schild, G. C. Antibody and cytotoxic T lymphocyte responses of humans to live and inactivated influenza vaccines. *J. Gen. Virol.* **58**, 273–281 (1982).

86. Trieu, M.-C. *et al.* Long-term maintenance of the influenza-specific cross-reactive memory CD4+ T-cell responses following repeated annual influenza vaccination. *J. Infect. Dis.* jiw619 (2016) doi:10.1093/infdis/jiw619.

87. Lu, L. Y. & Askonas, B. A. Cross-reactivity for different type A influenza viruses of a cloned T-killer cell line. *Nature* **288**, 164–165 (1980).

88. Sridhar, S. *et al.* Predominance of heterosubtypic IFN-γ-only-secreting effector memory T cells in pandemic H1N1 naive adults. *Eur. J. Immunol.* **42**, 2913–2924 (2012).

89. Wiersma, L. C. M. *et al.* Heterosubtypic immunity to H7N9 influenza virus in isogenic guinea pigs after infection with pandemic H1N1 virus. *Vaccine* **33**, 6977–6982 (2015).

90. Koutsakos, M. *et al.* Human CD8+ T cell cross-reactivity across influenza A, B and C viruses. *Nat. Immunol.* **20**, 613–25 (2019).

91. Roti, M. *et al.* Healthy human subjects have CD4+ T cells directed against H5N1 influenza virus. *J. Immunol. (Baltimore, Md 1950)* **180**, 1758–1768 (2008).

92. Reber, A. J. *et al.* Extensive T cell cross-reactivity between diverse seasonal influenza strains in the ferret model. *Sci. Rep.* **8**, (2018).

93. Benton, K. A. *et al.* Heterosubtypic Immunity to Influenza A Virus in Mice Lacking IgA, All Ig, NKT Cells, or gdT Cells. *J. Immunol.* **166**, 7437–7445 (2001).

94. Teijaro, J. R., Verhoeven, D., Page, C. A., Turner, D. & Farber, D. L. Memory CD4 T cells direct protective responses to influenza virus in the lungs through helper-independent mechanisms. *J. Virol.* **84**, 9217–9226 (2010).

95. Liang, S., Mozdzanowska, K., Palladino, G. & Gerhard, W. Heterosubtypic immunity to influenza type A virus in mice. Effector mechanisms and their longevity. *J. Immunol.* **152**, 1653–1661 (1994).

96. Laidlaw, B. J. *et al.* CD4+ T Cell Help Guides Formation of CD103+ Lung-Resident Memory CD8+ T Cells during Influenza Viral Infection. *Immunity* **41**, 633–645 (2014).

97. Cullen, J. G. *et al.* CD4 + T help promotes influenza virus-specific CD8 + T cell memory by limiting metabolic dysfunction. *Proc. Natl. Acad. Sci. U. S. A.* **116**, 4481–4488 (2019).

98. McKinstry, K. K. *et al.* Memory CD4 + T cells protect against influenza through multiple synergizing mechanisms. *J. Clin. Invest.* **122**, 2847–2856 (2012).

99. Laidlaw, B. J. *et al.* Cooperativity Between CD8+ T Cells, Non-Neutralizing Antibodies, and Alveolar Macrophages Is Important for Heterosubtypic Influenza Virus Immunity. *PLoS Pathog.* **9**, (2013).

100. Guo, H., Santiago, F., Lambert, K., Takimoto, T. & Topham, D. J. T Cell-Mediated Protection against Lethal 2009 Pandemic H1N1 Influenza Virus Infection in a Mouse Model. *J. Virol.* **85**, 448–455 (2011).

101. Hillaire, M. L. B. *et al.* Cross-protective immunity against influenza pH1N1 2009 viruses induced by seasonal influenza A (H3N2) virus is mediated by virus-specific T-cells. *J. Gen. Virol.* **92**, 2339–2349 (2011).

102. Braeckel-Budimir, N. Van *et al.* Antigen exposure history defines CD8 T cell dynamics and protection during localized pulmonary infections. *Front. Immunol.* **8**, Article 40 (2017).

103. Richards, K. A. *et al.* Direct Ex Vivo Analyses of HLA-DR1 Transgenic Mice Reveal an Exceptionally Broad Pattern of Immunodominance in the Primary HLA-DR1-Restricted CD4 T-Cell Response to Influenza Virus Hemagglutinin. *J. Virol.* **81**, 7608–7619 (2007).

104. Richards, K. a, Chaves, F. a & Sant, A. J. Infection of HLA-DR1 transgenic mice with a human isolate of influenza a virus (H1N1) primes a diverse CD4 T-cell repertoire that includes CD4 T cells with heterosubtypic cross-reactivity to avian (H5N1) influenza virus. *J. Virol.* **83**, 6566–77 (2009).

105. Kandasamy, M. *et al.* RIG-I Signaling Is Critical for Efficient Polyfunctional T Cell Responses during Influenza Virus Infection. *PLoS Pathog.* **12**, 1–24 (2016).

106. Nguyen, H. H. *et al.* Gamma interferon is not required for mucosal cytotoxic T-lymphocyte responses or hetero- subtypic immunity to influenza A virus infection in mice. *J. Virol.* **74**, 5495–5501 (2000).

107. Price, G. E., Gaszewska-Mastarlarz, a & Moskophidis, D. The role of alpha/beta and gamma interferons in development of immunity to influenza A virus in mice. *J. Virol.* **74**, 3996–4003 (2000).

108. Kohlmeier, J. E., Ely, K. H., Roberts, A. D., Blackman, M. A. & Woodland, D. L. T-cell memory and recall responses to respiratory virus infections. *Immunol. Rev.* **211**, 119–132 (2006).

109. Mueller, S. N., Gebhardt, T., Carbone, F. R. & Heath, W. R. Memory T Cell Subsets , Migration Patterns , and Tissue Residence. *Annu. Rev. Immunol.* **31**, 137–61 (2013).

110. Herndler-Brandstetter, D. *et al.* KLRG1+ Effector CD8+ T Cells Lose KLRG1, Differentiate into All Memory T Cell Lineages, and Convey Enhanced Protective Immunity. *Immunity* **48**, 716-729.e8 (2018).

111. Böttcher, J. P. *et al.* Functional classification of memory CD8 + T cells by CX3CR1 expression. *Nat. Commun.* **6**, (2015).

112. Gerlach, C. *et al.* The Chemokine Receptor CX3CR1 Defines Three Antigen-Experienced CD8 T Cell Subsets with Distinct Roles in Immune Surveillance and Homeostasis. *Immunity* **45**, 1270–1284 (2016).

113. Pizzolla, A. *et al.* Influenza-specific lung-resident memory T cells are proliferative and polyfunctional and maintain diverse TCR profiles. *J. Clin. Invest.* **128**, 721–733 (2018).

114. Wu, T. *et al.* Lung-resident memory CD8 T cells (T RM) are indispensable for optimal cross-protection against pulmonary virus infection. *J. Leukoc. Biol.* **95**, 215–224 (2014).

115. Wein, A. N. *et al.* CXCR6 regulates localization of tissue-resident memory CD8 T cells to the airways. *J. Exp. Med.* (2019).

116. Braeckel-budimir, N. Van *et al.* Repeated Antigen Exposure Extends the Durability of Cells and Heterosubtypic Immunity Repeated Antigen Exposure Extends the Durability of Influenza-Specific Lung-Resident Memory CD8 + T Cells and Heterosubtypic Immunity. *Cell Rep.* **24**, 3374–3382 (2018).

117. Olson, J. A., McDonald-Hyman, C., Jameson, S. C. & Hamilton, S. E. Effector-like CD8+ T Cells in the Memory Population Mediate Potent Protective Immunity. *Immunity* **38**, 1250–1260 (2013).

118. Cox, M. A., Barnum, S. R., Bullard, D. C. & Zajac, A. J. ICAM-1 – dependent

tuning of memory CD8 T-cell responses following acute infection. *Proc Natl Acad Sci U S A* **110**, 1416–1421 (2013).

119. Lee, Y.-N., Lee, Y.-T., Kim, M.-C., Gewirtz, A. T. & Kang, S.-M. A Novel Vaccination Strategy Mediating the Induction of Lung-Resident Memory CD8 T Cells Confers Heterosubtypic Immunity against Future Pandemic Influenza Virus. *J. Immunol.* **196**, 2637–2645 (2016).

120. Zens, K. D., Chen, J. K. & Farber, D. L. Vaccine-generated lung tissue–resident memory T cells provide heterosubtypic protection to influenza infection. *JCI Insight* **1**, e85832 (2016).

121. Kinjyo, I. *et al.* Real-time tracking of cell cycle progression during CD8+ effector and memory T-cell differentiation. *Nat. Commun.* **6**, (2015).

122. Valkenburg, S. A. *et al.* Protection by universal influenza vaccine is mediated by memory CD4 T cells. *Vaccine* **36**, 4198–4206 (2018).

123. Bot, A., Bot, S. & Bona, C. A. Protective role of gamma interferon during the recall response to influenza virus. *J. Virol.* **72**, 6637–6645 (1998).

124. Longhi, M. P. *et al.* Interleukin-6 is crucial for recall of influenza-specific memory CD4+T cells. *PLoS Pathog.* **4**, 2–9 (2008).

125. Surls, J., Nazarov-Stoica, C., Kehl, M., Casares, S. & Brumeanu, T. D. Differential effect of CD4+Foxp3+ T-regulatory cells on the B and T helper cell responses to influenza virus vaccination. *Vaccine* **28**, 7319–7330 (2010).

126. Lin, P. *et al.* Vaccine-induced antigen-specific regulatory T cells attenuate the antiviral immunity against acute influenza virus infection. *Mucosal Immunol.* **11**, 1239–1253 (2018).

127. Tian, Y., Mollo, S. B., Harrington, L. E. & Zajac, J. IL-10 Regulates Memory T Cell Development and the Balance between Th1 and Follicular Th Cell Responses during an Acute Viral Infection. *J. Immunol.* **197**, 1308–21 (2016).

128. Zhirnov, O. P. Solubilization of matrix protein M1/M from virions occurs at different pH for orthomyxo- and paramyxoviruses. *Virology* **176**, 274–279 (1990).

129. Jing, X. *et al.* Functional studies indicate amantadine binds to the pore of the influenza A virus M2 proton-selective ion channel. *Proc. Natl. Acad. Sci. U. S. A.* **105**, 10967–10972 (2008).

130. Suzuki, H. *et al.* Emergence of amantadine-resistant influenza A viruses: Epidemiological study. *J. Infect. Chemother.* **9**, 195–200 (2003).

131. Influenza Antiviral Medications: Summary for Clinicians. *Centers for Disease Control and Prevention, National Center for Immunization and Respiratory*

Diseases (NCIRD) https://www.cdc.gov/flu/professionals/antivirals/summary-clinicians.htm (2020).

132. Mckimm-Breschkin, J. L. Influenza neuraminidase inhibitors: Antiviral action and mechanisms of resistance. *Influenza Other Respi. Viruses* **7**, 25–36 (2012).

133. Toots, M. & Plemper, R. K. Next-generation direct-acting influenza therapeutics. *Transl. Res.* **00**, (2020).

134. Oboho, I. K. *et al.* Benefit of early initiation of influenza antiviral treatment to pregnant women hospitalized with laboratory-confirmed influenza. *J. Infect. Dis.* **214**, 507–515 (2016).

135. Aoki, F. Y. *et al.* Early administration of oral oseltamivir increases the benefits of influenza treatment. *J. Antimicrob. Chemother.* **51**, 123–129 (2003).

136. Ma, W., Huo, X. & Zhou, M. The healthcare seeking rate of individuals with influenza like illness: a meta-analysis. *Infect. Dis. (Auckl).* **50**, 728–735 (2018).

137. Tai, C. Y. *et al.* Characterization of human influenza virus variants selected in vitro in the presence of the neuraminidase inhibitor GS 4071. *Antimicrob. Agents Chemother.* **42**, 3234–3241 (1998).

138. Choi, W.-S. *et al.* Screening for Neuraminidase Inhibitor Resistance Markers among Avian Influenza Viruses of the N4, N5, N6, and N8 Neuraminidase Subtypes. *J. Virol.* **92**, e01580-17 (2018).

139. Lee, N. & Hurt, A. C. Neuraminidase inhibitor resistance in influenza: a clinical perspective. *Curr. Opin. Infect. Dis.* **31**, 520–526 (2018).

140. Lackenby, A. *et al.* Global update on the susceptibility of human influenza viruses to neuraminidase inhibitors and status of novel antivirals, 2016–2017. *Antiviral Res.* **157**, 38–46 (2018).

141. Drug Trial Snapshot: XOFLUZA. *U.S. Food and Drug Administration* https://www.fda.gov/drugs/drug-approvals-and-databases/drug-trial-snapshot-xofluza (2019).

142. Noshi, T. *et al.* In vitro characterization of baloxavir acid, a first-in-class cap-dependent endonuclease inhibitor of the influenza virus polymerase PA subunit. *Antiviral Res.* **160**, 109–117 (2018).

143. Hayden, F. G. *et al.* Baloxavir marboxil for uncomplicated influenza in adults and adolescents. *N. Engl. J. Med.* **379**, 913–923 (2018).

144. Phase III Study Showed XOFLUZA (Baloxavir Marboxil) is Effective at Preventing Influenza Infection. *Genentech* https://www.gene.com/media/press-releases/14793/2019-06-03/phase-iii-study-showed-xofluza-baloxavir (2019).

145. Taniguchi, K. *et al.* Inhibition of avian-origin influenza A(H7N9) virus by the novel cap-dependent endonuclease inhibitor baloxavir marboxil. *Sci. Rep.* **9**, 1–12 (2019).

146. Mishin, V. P. *et al.* Susceptibility of Influenza A, B, C, and D Viruses to Baloxavir. *Emerg. Infect. Dis.* **25**, 1969–1972 (2019).

147. Chesnokov, A. *et al.* Replicative Fitness of Seasonal Influenza A Viruses With Decreased Susceptibility to Baloxavir. *J. Infect. Dis.* **221**, 367–371 (2020).

148. Checkmahomed, L. *et al.* Impact of the Baloxavir-Resistant Polymerase Acid I38T Substitution on the Fitness of Contemporary Influenza A(H1N1)pdm09 and A(H3N2) Strains. *J. Infect. Dis.* **221**, 63–70 (2020).

149. Imai, M. *et al.* Influenza A variants with reduced susceptibility to baloxavir isolated from Japanese patients are fit and transmit through respiratory droplets. *Nat. Microbiol.* **5**, 27–33 (2020).

150. Corti, D. *et al.* Tackling influenza with broadly neutralizing antibodies. *Curr. Opin. Virol.* **24**, 60–69 (2017).

151. Laursen, N. S. & Wilson, I. A. Broadly neutralizing antibodies against influenza viruses. *Antiviral Res.* **98**, 476–483 (2013).

152. Inc., V. B. Study of VIR-2482 in Healthy Volunteers. *ClinicalTrials.gov* https://clinicaltrials.gov/ct2/show/NCT04033406?recrs=ad&type=Intr&cond=influenza&draw=2&rank=62 (2019).

153. Wollacott, A. M. *et al.* Safety and Upper Respiratory Pharmacokinetics of the Hemagglutinin Stalk-Binding Antibody VIS410 Support Treatment and Prophylaxis Based on Population Modeling of Seasonal Influenza A Outbreaks. *EBioMedicine* **5**, 147–155 (2016).

154. Laursen, N. S. *et al.* Universal protection against influenza infection by a multidomain antibody to influenza hemagglutinin. *Science* **362**, 598–602 (2018).

155. Kadam, R. U. *et al.* Potent peptidic fusion inhibitors of influenza virus. *Science (80-.).* **358**, 496–502 (2017).

156. Kadam, R. U. & Wilson, I. A. A small-molecule fragment that emulates binding of receptor and broadly neutralizing antibodies to influenza A hemagglutinin. *Proc. Natl. Acad. Sci. U. S. A.* **115**, 4240–4245 (2018).

157. Smallwood, H. S. *et al.* Targeting Metabolic Reprogramming by Influenza Infection for Therapeutic Intervention. *Cell Rep.* **19**, 1640–1653 (2017).

158. Toots, M. *et al.* Characterization of orally efficacious influenza drug with high resistance barrier in ferrets and human airway epithelia. *Sci. Transl. Med.* **11**,

eaax5866 (2019).

159. McCaffrey, S. FDA: Human trials can begin for Emory COVID-19 antiviral. *Emory News Center* https://news.emory.edu/stories/2020/04/covid_eidd2801_fda/index.html (2020).

160. Hayden, F. G. & De Jong, M. D. Human influenza: Pathogenesis, clinical features, and management. in *Textbook of Influenza* (eds. Webster, R. G. & Monto, A. S.) 373–391 (Wiley-Blackwell, 2013).

161. McCullers, J. A. Preventing and treating secondary bacterial infections with antiviral agents. *Antivir. Ther.* **16**, 123–135 (2011).

162. Newton, A. H., Cardani, A. & Braciale, T. J. The host immune response in respiratory virus infection: balancing virus clearance and immunopathology. *Semin. Immunopathol.* **38**, 471–482 (2016).

163. Liu, Q., Zhou, Y. & Yang, Z. The cytokine storm of severe influenza and development of immunomodulatory therapy. *Cell. Mol. Immunol.* **13**, 3–10 (2016).

164. Krammer, F. The human antibody response to influenza A virus infection and vaccination. *Nat. Rev. Immunol.* **19**, 383–397 (2019).

165. Webby, R. Understanding immune responses to the influenza vaccine. *Nat. Med.* **22**, 1387–1388 (2016).

166. Grohskopf, L. A. *et al.* Prevention and Control of Seasonal Influenza With Vaccines: Recommendations of the Advisory Committee on Immunization Practices—United States, 2019–20 Influenza Season. *MMWR Recomm. Reports* **68**, (2019).

167. Choi, A., García-sastre, A. & Schotsaert, M. Host immune response-inspired development of the influenza vaccine. *Ann. Allergy, Asthma Immunol.* (2020) doi:10.1016/j.anai.2020.04.008.

168. Shasha, D. *et al.* Quadrivalent versus trivalent influenza vaccine: clinical outcomes in two influenza seasons, historical cohort study. *Clin. Microbiol. Infect.* **26**, 101–106 (2020).

169. Kissling, E. *et al.* Effectiveness of influenza vaccine against influenza A in Europe in seasons of different A(H1N1)pdm09 and the same A(H3N2) vaccine components (2016–17 and 2017–18). *Vaccine X* **3**, 100042 (2019).

170. Diallo, A. *et al.* Effectiveness of Seasonal Influenza Vaccination in Children in Senegal During a Year of Vaccine Mismatch: A Cluster-randomized Trial. *Clin. Infect. Dis.* **69**, 1780–1788 (2019).

171. Rose, A. M. C. *et al.* Vaccine effectiveness against influenza A(H3N2) and B

among laboratory-confirmed, hospitalised older adults, Europe, 2017-18: A season of B lineage mismatched to the trivalent vaccine. *Influenza Other Respi. Viruses* 302–310 (2020) doi:10.1111/irv.12714.

172. Tricco, A. C. *et al.* Comparing influenza vaccine efficacy against mismatched and matched strains: A systematic review and meta-analysis. *BMC Med.* **11**, (2013).

173. Zost, S. J. *et al.* Contemporary H3N2 influenza viruses have a glycosylation site that alters binding of antibodies elicited by egg-adapted vaccine strains. *Proc. Natl. Acad. Sci. U. S. A.* **114**, 12578–12583 (2017).

174. Wu, N. C. *et al.* A structural explanation for the low effectiveness of the seasonal influenza H3N2 vaccine. *PLoS Pathog.* **13**, 1–17 (2017).

175. Couch, R. B. *et al.* Randomized comparative study of the serum antihemagglutinin and antineuraminidase antibody responses to six licensed trivalent influenza vaccines. *Vaccine* **31**, 190–195 (2012).

176. Johnson, P. R., Feldman, S., Thompson, J. M., Mahoney, J. D. & Wright, P. F. Comparison of long-term systemic and secretory antibody responses in children given live, attenuated, or inactivated influenza A vaccine. *J. Med. Virol.* **17**, 325–335 (1985).

177. Hoft, D. F. *et al.* Live and inactivated influenza vaccines induce similar humoral responses, but only live vaccines induce diverse T-cell responses in young children. *J. Infect. Dis.* **204**, 845–853 (2011).

178. Uddback, I. E. M. *et al.* Combined local and systemic immunization is essential for durable T-cell mediated heterosubtypic immunity against influenza A virus. *Sci. Rep.* **6**, (2016).

179. Quan, F., Compans, R. W., Nguyen, H. H. & Kang, S.-M. Induction of Heterosubtypic Immunity to Influenza Virus by Intranasal Immunization. *J. Virol.* **82**, 1350–1359 (2008).

180. Takada, A., Matsushita, S., Ninomiya, A., Kawaoka, Y. & Kida, H. Intranasal immunization with formalin-inactivated virus vaccine induces a broad spectrum of heterosubtypic immunity against influenza virus infection in mice. *Vaccine* **21**, 3212–3218 (2003).

181. Fislová, T. *et al.* Differences in Antibody Responses of Mice to Intranasal or Intraperitoneal Immunization with Influenza A Virus and Vaccination with Subunit Influenza Vaccine. *Acta Virol.* **49**, 243–250 (2005).

182. Allie, S. R. *et al.* The establishment of resident memory B cells in the lung requires local antigen encounter. *Nat. Immunol.* **20**, 97–108 (2019).

183. Tables on clinical evaluation of influenza vaccines. *World Health Organization*

https://www.who.int/immunization/diseases/influenza/clinical_evaluation_tables/en/ (2020).

184. Clemens, E. B., Van de Sandt, C., Wong, S. S., Wakim, L. M. & Valkenburg, S. A. Harnessing the power of T cells: The promising hope for a universal influenza vaccine. *Vaccines* **6**, 1–30 (2018).

185. Antrobus, R. D. *et al.* Coadministration of seasonal influenza vaccine and MVA-NP+M1 simultaneously achieves potent humoral and cell-mediated responses. *Mol. Ther.* **22**, 233–238 (2014).

186. Vries, R. D. De *et al.* Induction of Cross-Clade Antibody and T-Cell Responses by a Modified Vaccinia Virus Ankara – Based Influenza A (H5N1) Vaccine in a Randomized Phase 1 / 2a Clinical Trial. *J. Infect. Dis.* **218**, 614–23 (2018).

187. Vogel, A. J. & Brown, D. M. Single-Dose CpG Immunization Protects Against a Heterosubtypic Challenge and Generates Antigen-Specific Memory T Cells. *Front. Immunol.* **6**, (2015).

188. Pizzolla, A. & Wakim, L. M. Memory T Cell Dynamics in the Lung during Influenza Virus Infection. *J. Immunol.* **202**, 374–381 (2019).

189. Pizzolla, A. *et al.* Resident memory CD8+ T cells in the upper respiratory tract prevent pulmonary influenza virus infection. *Sci. Immunol.* **2**, eaam6970 (2017).

190. Akondy, R. S. *et al.* Origin and differentiation of human memory CD8 T cells after vaccination. *Nature* **552**, 362–367 (2017).

191. Van De Sandt, C. E. *et al.* Human Influenza A Virus-Specific CD8+ T-Cell Response is Long-Lived. *J. Infect. Dis.* **212**, 81–85 (2015).

192. Moi, P., Chan, K., Asunis, I., Cao, A. & Kan, Y. W. Isolation of NF-E2-related factor 2 (Nrf2), a NF-E2-like basic leucine zipper transcriptional activator that binds to the tandem NF-E2/AP1 repeat of the beta-globin locus control region. *Proc. Natl. Acad. Sci.* **91**, 9926–9930 (1994).

193. Chan, K., Lu, R., Chang, J. C. & Kan, Y. W. NRF2, a member of the NFE2 family of transcription factors, is not essential for murine erythropoiesis, growth, and development. *Proc. Natl. Acad. Sci. U. S. A.* **93**, 13943–8 (1996).

194. Lacher, S. E. *et al.* Beyond antioxidant genes in the ancient Nrf2 regulatory network. *Free Radic. Biol. Med.* **88**, 452–465 (2015).

195. Iso, T., Suzuki, T., Baird, L. & Yamamoto, M. Absolute Amounts and Status of Nrf2-Keap1-Cul3 Complex within Cells. *Mol. Cell. Biol.* **36**, MCB.00389-16 (2016).

196. Venugopal, R., Jaiswal, A. K. & Kan, Y. W. Nrf1 and Nrf2 positively and c-Fos and Fra1 negatively regulate the human antioxidant response element-mediated

expression of NAD(P)H:quinone oxidoreductase 1 gene. *Proc. Natl. Acad. Sci.* **93**, 14960–14965 (1996).

197. Itoh, K. *et al.* An Nrf2/Small Maf Heterodimer Mediates the Induction of Phase II Detoxifying Enzyme Genes through Antioxidant Response Elements. *Biochem. Biophys. Res. Commun.* **236**, 313–322 (1997).

198. Itoh, K. *et al.* Cloning and characterization of a novel erythroid cell-derived CNC family transcription factor heterodimerizing with the small Maf family proteins. *Mol. Cell. Biol.* **15**, 4184–4193 (1995).

199. Wasserman, W. W. & Fahl, W. E. Functional antioxidant responsive elements. *Proc. Natl. Acad. Sci. U. S. A.* **94**, 5361–5366 (1997).

200. Thimmulappa, R. K. *et al.* Identification of Nrf2-regulated Genes Induced by the Chemopreventive Agent Sulforaphane by Oligonucleotide Microarray Identification of Nrf2-regulated Genes Induced by the Chemopreventive Agent. *Cancer Res.* **62**, 5196–5203 (2002).

201. Lee, J. M., Calkins, M. J., Chan, K., Kan, Y. W. & Johnson, J. A. Identification of the NF-E2-related factor-2-dependent genes conferring protection against oxidative stress in primary cortical astrocytes using oligonucleotide microarray analysis. *J. Biol. Chem.* **278**, 12029–12038 (2003).

202. Malhotra, D. *et al.* Global mapping of binding sites for Nrf2 identifies novel targets in cell survival response through chip-seq profiling and network analysis. *Nucleic Acids Res.* **38**, 5718–5734 (2010).

203. Katsuoka, F., Otsuki, A., Takahashi, M., Ito, S. & Yamamoto, M. Direct and Specific Functional Evaluation of the Nrf2 and MafG Heterodimer by Introducing a Tethered Dimer into Small Maf-Deficient Cells. *Mol. Cell. Biol.* **39**, e00273-19 (2019).

204. Venugopal, R. & Jaiswal, A. K. Nrf2 and Nrf1 in association with Jun proteins regulate antioxidant response element-mediated expression and coordinated induction of genes encoding detoxifying enzymes. *Oncogene* **17**, 3145–3156 (1998).

205. Yamamoto, T. *et al.* Identification of polymorphisms in the promoter region of the human NRF2 gene. *Biochem. Biophys. Res. Commun.* **321**, 72–79 (2004).

206. Itoh, K. *et al.* Keap1 represses nuclear activation of antioxidant responsive elements by Nrf2 through binding to the amino-terminal Neh2 domain. *Genes Dev.* **13**, 76–86 (1999).

207. McMahon, M., Itoh, K., Yamamoto, M. & Hayes, J. D. Keap1-dependent proteasomal degradation of transcription factor Nrf2 contributes to the negative regulation of antioxidant response element-driven gene expression. *J. Biol. Chem.*

278, 21592–600 (2003).

208. Stewart, D., Killeen, E., Naquin, R., Alam, S. & Alam, J. Degradation of transcription factor Nrf2 via the ubiquitin-proteasome pathway and stabilization by cadmium. *J. Biol. Chem.* **278**, 2396–402 (2003).

209. Kobayashi, A. *et al.* Oxidative Stress Sensor Keap1 Functions as an Adaptor for Cul3-Based E3 Ligase To Regulate Proteasomal Degradation of Nrf2. *Mol. Cell. Biol.* **24**, 7130–7139 (2004).

210. McMahon, M., Thomas, N., Itoh, K., Yamamoto, M. & Hayes, J. D. Redox-regulated turnover of Nrf2 is determined by at least two separate protein domains, the redox-sensitive Neh2 degron and the redox-insensitive Neh6 degron. *J. Biol. Chem.* **279**, 31556–31567 (2004).

211. Zhang, D. D., Lo, S., Cross, J. V, Templeton, D. J. & Hannink, M. Keap1 is a Redox-Regulated Substrate Adaptor Protein for a Cul3-Dependent Ubiquitin Ligase Complex. *Mol. Cell. Biol.* **24**, 10941–10953 (2004).

212. McMahon, M., Thomas, N., Itoh, K., Yamamoto, M. & Hayes, J. D. Dimerization of substrate adaptors can facilitate Cullin-mediated ubiquitylation of proteins by a 'tethering' mechanism: A two-site interaction model for the Nrf2-Keap1 complex. *J. Biol. Chem.* **281**, 24756–24768 (2006).

213. Ishii, T. *et al.* Transcription factor Nrf2 coordinately regulates a group of oxidative stress-inducible genes in macrophages. *J. Biol. Chem.* **275**, 16023–16029 (2000).

214. Dinkova-Kostova, A. T. *et al.* Direct evidence that sulfhydryl groups of Keap1 are the sensors regulating induction of phase 2 enzymes that protect against carcinogens and oxidants. *Proc. Natl. Acad. Sci. U. S. A.* **99**, 11908–13 (2002).

215. Tong, K. I., Kobayashi, A., Katsuoka, F. & Yamamoto, M. Two-site substrate recognition model for the Keap1-Nrf2 system: A hinge and latch mechanism. *Biol. Chem.* **387**, 1311–1320 (2006).

216. Tong, K. I. *et al.* Different Electrostatic Potentials Define ETGE and DLG Motifs as Hinge and Latch in Oxidative Stress Response. *Mol. Cell. Biol.* **27**, 7511–7521 (2007).

217. Baird, L., Lleres, D., Swift, S. & Dinkova-Kostova, A. T. Regulatory flexibility in the Nrf2-mediated stress response is conferred by conformational cycling of the Keap1-Nrf2 protein complex. *Proc. Natl. Acad. Sci.* **110**, 15259–15264 (2013).

218. Liu, Y. *et al.* A genomic screen for activators of the antioxidant response element. *Proc. Natl. Acad. Sci.* **104**, 5205–5210 (2007).

219. Lau, A. *et al.* A Noncanonical Mechanism of Nrf2 Activation by Autophagy Deficiency: Direct Interaction between Keap1 and p62. *Mol. Cell. Biol.* **30**, 3275–

3285 (2010).

220. Copple, I. M. *et al.* Physical and functional interaction of sequestosome 1 with Keap1 regulates the Keap1-Nrf2 cell defense pathway. *J. Biol. Chem.* **285**, 16782–16788 (2010).

221. Fan, W. *et al.* Keap1 facilitates p62-mediated ubiquitin aggregate clearance via autophagy. *Autophagy* **6**, 614–621 (2010).

222. Jain, A. *et al.* p62/SQSTM1 is a target gene for transcription factor NRF2 and creates a positive feedback loop by inducing antioxidant response element-driven gene transcription. *J. Biol. Chem.* **285**, 22576–22591 (2010).

223. Fujita, K. -i., Maeda, D., Xiao, Q. & Srinivasula, S. M. Nrf2-mediated induction of p62 controls Toll-like receptor-4-driven aggresome-like induced structure formation and autophagic degradation. *Proc. Natl. Acad. Sci.* **108**, 1427–1432 (2011).

224. Yin, S. & Cao, W. Toll-Like Receptor Signaling Induces Nrf2 Pathway Activation through p62-Triggered Keap1 Degradation. *Mol. Cell. Biol.* **35**, 2673–2683 (2015).

225. Huang, H.-C., Nguyen, T. & Pickett, C. B. Regulation of the antioxidant response element by protein kinase C-mediated phosphorylation of NF-E2-related factor 2. *Proc. Natl. Acad. Sci.* **97**, 12475–12480 (2000).

226. Huang, H. C., Nguyen, T. & Pickett, C. B. Phosphorylation of Nrf2 at Ser-40 by protein kinase C regulates antioxidant response element-mediated transcription. *J. Biol. Chem.* **277**, 42769–42774 (2002).

227. Apopa, P. L., He, X. & Ma, Q. Phosphorylation of Nrf2 in the transcription activation domain by casein kinase 2 (CK2) is critical for the nuclear translocation and transcription activation function of Nrf2 in IMR-32 neuroblastoma cells. *J. Biochem. Mol. Toxicol.* **22**, 63–76 (2008).

228. Pi, J. *et al.* Molecular mechanism of human Nrf2 activation and degradation: Role of sequential phosphorylation by protein kinase CK2. *Free Radic. Biol. Med.* **42**, 1797–1806 (2007).

229. Cullinan, S. B. *et al.* Nrf2 Is a Direct PERK Substrate and Effector of PERK-Dependent Cell Survival. *Mol. Cell. Biol.* **23**, 7198–7209 (2003).

230. Zimmermann, K. *et al.* Activated AMPK boosts the Nrf2/HO-1 signaling axis - A role for the unfolded protein response. *Free Radic. Biol. Med.* **88**, 417–426 (2015).

231. Kawai, Y., Garduño, L., Theodore, M., Yang, J. & Arinze, I. J. Acetylation-deacetylation of the transcription factor Nrf2 (nuclear factor erythroid 2-related factor 2) regulates its transcriptional activity and nucleocytoplasmic localization. *J.*

Biol. Chem. **286**, 7629–7640 (2011).

232. Rada, P. *et al.* SCF/ B-TrCP Promotes Glycogen Synthase Kinase 3-Dependent Degradation of the Nrf2 Transcription Factor in a Keap1-Independent Manner. *Mol. Cell. Biol.* **31**, 1121–1133 (2011).

233. Chowdhry, S. *et al.* Nrf2 is controlled by two distinct β-TrCP recognition motifs in its Neh6 domain, one of which can be modulated by GSK-3 activity. *Oncogene* **32**, 3765–81 (2013).

234. Hayes, J. D., Chowdhry, S., Dinkova-Kostova, A. T. & Sutherland, C. Dual regulation of transcription factor Nrf2 by Keap1 and by the combined actions of β-TrCP and GSK-3. *Biochem. Soc. Trans.* **43**, 611–620 (2015).

235. Nioi, P., Nguyen, T., Sherratt, P. J. & Pickett, C. B. The Carboxy-Terminal Neh3 Domain of Nrf2 Is Required for Transcriptional Activation. *Mol. Cell. Biol.* **25**, 10895–10906 (2005).

236. Katoh, Y. *et al.* Two domains of Nrf2 cooperatively bind CBP, a CREB binding protein, and synergistically activate transcription. *Genes to Cells* **6**, 857–868 (2001).

237. Sun, Z., Chin, Y. E. & Zhang, D. D. Acetylation of Nrf2 by p300/CBP Augments Promoter-Specific DNA Binding of Nrf2 during the Antioxidant Response. *Mol. Cell. Biol.* **29**, 2658–2672 (2009).

238. Tanigawa, S. *et al.* Jun dimerization protein 2 is a critical component of the Nrf2/MafK complex regulating the response to ROS homeostasis. *Cell Death Dis.* **4**, e921 (2013).

239. Wu, T. *et al.* Poly(ADP-ribose) polymerase-1 modulates Nrf2-dependent transcription. *Free Radic. Biol. Med.* **67**, 69–80 (2014).

240. Baba, K., Morimoto, H. & Imaoka, S. Seven in absentia homolog 2 (Siah2) protein is a regulator of NF-E2-related factor 2 (Nrf2). *J. Biol. Chem.* **288**, 18393–18405 (2013).

241. Lo, J. Y., Spatola, B. N. & Curran, S. P. WDR23 regulates NRF2 independently of KEAP1. *PLoS Genet.* **13**, 1–26 (2017).

242. Kim, J.-H., Yu, S., Chen, J. D. & Kong, A. N. The nuclear cofactor RAC3/AIB1/SRC-3 enhances Nrf2 signaling by interacting with transactivation domains. *Oncogene* **32**, 514–527 (2013).

243. Zhang, Y. *et al.* Identification of an adaptor protein that facilitates Nrf2-Keap1 complex formation and modulates antioxidant response. *Free Radic. Biol. Med.* **97**, 38–49 (2016).

244. Wu, T. *et al.* Hrd1 suppresses Nrf2-mediated cellular protection during liver cirrhosis. *Genes Dev.* **28**, 708–722 (2014).

245. Malloy, M. T. *et al.* Trafficking of the transcription factor Nrf2 to promyelocytic leukemia-nuclear bodies: Implications for degradation of nrf2 in the nucleus. *J. Biol. Chem.* **288**, 14569–14583 (2013).

246. Komaravelli, N., Ansar, M., Garofalo, R. P. & Casola, A. Respiratory syncytial virus induces NRF2 degradation through a promyelocytic leukemia protein - ring finger protein 4 dependent pathway. *Free Radic. Biol. Med.* **113**, 494–504 (2017).

247. Takaya, K. *et al.* Validation of the multiple sensor mechanism of the Keap1-Nrf2 system. *Free Radic. Biol. Med.* **53**, 817–827 (2012).

248. Kobayashi, M. *et al.* The Antioxidant Defense System Keap1-Nrf2 Comprises a Multiple Sensing Mechanism for Responding to a Wide Range of Chemical Compounds. *Mol. Cell. Biol.* **29**, 493–502 (2009).

249. Saito, R. *et al.* Characterizations of Three Major Cysteine Sensors of Keap1 in Stress Response. *Mol. Cell. Biol.* **36**, MCB.00868-15 (2015).

250. Pi, J., Qu, W., Reece, J. M., Kumagai, Y. & Waalkes, M. P. Transcription factor Nrf2 activation by inorganic arsenic in cultured keratinocytes: involvement of hydrogen peroxide. *Exp. Cell Res.* **290**, 234–245 (2003).

251. Aono, J. *et al.* Activation of Nrf2 and accumulation of ubiquitinated A170 by arsenic in osteoblasts. *Biochem. Biophys. Res. Commun.* **305**, 271–277 (2003).

252. He, X., Chen, M. G., Lin, G. X. & Ma, Q. Arsenic induces NAD(P)H-quinone oxidoreductase I by disrupting the Nrf2-Keap1-Cul3 complex and recruiting Nrf2-Maf to the antioxidant response element enhancer. *J. Biol. Chem.* **281**, 23620–23631 (2006).

253. Wang, X. J., Hayes, J. D., Higgins, L. G., Wolf, C. R. & Dinkova-Kostova, A. T. Activation of the NRF2 Signaling Pathway by Copper-Mediated Redox Cycling of Para- and Ortho-Hydroquinones. *Chem. Biol.* **17**, 75–85 (2010).

254. Imhoff, B. R. & Hansen, J. M. Tert-butylhydroquinone induces mitochondrial oxidative stress causing Nrf2 activation. *Cell Biol. Toxicol.* **26**, 541–551 (2010).

255. Itoh, K. *et al.* Transcription Factor Nrf2 Regulates Inflammation by Mediating the Effect of 15-Deoxy- □ 12 , 14 -Prostaglandin J 2. *Mol. Cell. Biol.* **24**, 36–45 (2004).

256. McMahon, M., Swift, S. R. & Hayes, J. D. Zinc-binding triggers a conformational-switch in the cullin-3 substrate adaptor protein KEAP1 that controls transcription factor NRF2. *Toxicol. Appl. Pharmacol.* **360**, 45–57 (2018).

257. Bergström, P. *et al.* Repeated transient sulforaphane stimulation in astrocytes leads to prolonged Nrf2-mediated gene expression and protection from superoxide-induced damage. *Neuropharmacology* **60**, 343–353 (2011).

258. Mathew, S. T., Bergström, P. & Hammarsten, O. Repeated Nrf2 stimulation using sulforaphane protects fibroblasts from ionizing radiation. *Toxicol. Appl. Pharmacol.* **276**, 188–194 (2014).

259. Zhang, H. *et al.* Nrf2-regulated phase II enzymes are induced by chronic ambient nanoparticle exposure in young mice with age-related impairments. *Free Radic. Biol. Med.* **52**, 2038–2046 (2012).

260. Bischoff, L. J. M., Kuijper, I. A., Schimming, J. P. & Wolters, L. A systematic analysis of Nrf2 pathway activation dynamics during repeated xenobiotic exposure. *Arch. Toxicol.* **93**, 435–451 (2019).

261. Kobayashi, E. H. *et al.* Nrf2 suppresses macrophage inflammatory response by blocking proinflammatory cytokine transcription. *Nat. Commun.* **7**, (2016).

262. Liu, P. *et al.* RPA1 binding to NRF2 switches ARE-dependent transcriptional activation to ARE-NRE–dependent repression. *Proc. Natl. Acad. Sci.* **115**, 201812125 (2018).

263. Thangasamy, A., Rogge, J., Krishnegowda, N. K., Freeman, J. W. & Ammanamanchi, S. Novel function of transcription factor Nrf2 as an inhibitor of RON tyrosine kinase receptor-mediated cancer cell invasion. *J. Biol. Chem.* **286**, 32115–32122 (2011).

264. Bahn, G. *et al.* NRF2/ARE pathway negatively regulates BACE1 expression and ameliorates cognitive deficits in mouse Alzheimer's models. *Proc. Natl. Acad. Sci. U. S. A.* **116**, 12516–12523 (2019).

265. Gjyshi, O. *et al.* Activated Nrf2 Interacts with Kaposi's Sarcoma-Associated Herpesvirus Latency Protein LANA-1 and Host Protein KAP1 To Mediate Global Lytic Gene Repression. *J. Virol.* **89**, 7874–7892 (2015).

266. Ma, Q., Kinneer, K., Bi, Y., Chan, J. Y. & Kan, Y. W. Induction of murine NAD(P)H:quinone oxidoreductase by 2,3,7,8-tetrachlorodibenzo-p-dioxin requires the CNC (cap 'n' collar) basic leucine zipper transcription factor Nrf2 (nuclear factor erythroid 2-related factor 2): cross-interaction between AhR (aryl h. *Biochem. J.* **377**, 205–13 (2004).

267. Yang, H. *et al.* Nrf1 and Nrf2 regulate rat glutamate-cysteine ligase catalytic subunit transcription indirectly via NF-kappaB and AP-1. *Mol. Cell. Biol.* **25**, 5933–46 (2005).

268. Vaz, M. *et al.* Oxidant-Induced Cell Death and Nrf2-Dependent Antioxidative Response Are Controlled by Fra-1/AP-1. *Mol. Cell. Biol.* **32**, 1694–1709 (2012).

269. Pronk, T. E. *et al.* Comparison of the molecular topologies of stress-activated transcription factors HSF1, AP-1, NRF2, and NF-κB in their induction kinetics of HMOX1. *BioSystems* **124**, 75–85 (2014).

270. Cuadrado, A., Martin-Moldes, Z., Ye, J. & Lastres-becker, I. Transcription Factors NRF2 and NF-kB Are Coordinated Effectors of the Rho Family , GTP-binding Protein RAC1 during. *J. Biol. Chem.* **289**, 15244–15258 (2014).

271. Rössler, O. G. & Thiel, G. Specificity of Stress-Responsive Transcription Factors Nrf2, ATF4, and AP-1. *J. Cell. Biochem.* **118**, 127–140 (2017).

272. Levy, S. & Forman, H. J. c-Myc is a Nrf2-interacting protein that negatively regulates phase II genes through their electrophile responsive elements. *IUBMB Life* **62**, 237–246 (2010).

273. Tsai, J. J. *et al.* Nrf2 regulates haematopoietic stem cell function. *Nat. Cell Biol.* **15**, 309–316 (2013).

274. Murakami, S., Shimizu, R., Romeo, P.-H., Yamamoto, M. & Motohashi, H. Keap1-Nrf2 system regulates cell fate determination of hematopoietic stem cells. *Genes to Cells* **19**, 239–53 (2014).

275. Cho, H.-Y. *et al.* Role of Nrf2 in protection against hyperoxic lung injury in mice. *Am. J. Respir. Cell Mol. Biol.* **26**, 175–182 (2002).

276. Kim, K. H. *et al.* MyD88 is a mediator for the activation of Nrf2. *Biochem. Biophys. Res. Commun.* **404**, 46–51 (2011).

277. Ruotsalainen, A. K. *et al.* The absence of macrophage Nrf2 promotes early atherogenesis. *Cardiovasc. Res.* **98**, 107–115 (2013).

278. Sha, L. K. *et al.* Loss of Nrf2 in bone marrow-derived macrophages impairs antigen-driven $CD8^+$ T cell function by limiting GSH and Cys availability. *Free Radic. Biol. Med.* **83**, 77–88 (2015).

279. Harvey, C. J. *et al.* Targeting Nrf2 Signaling Improves Bacterial Clearance by Alveolar Macrophages in Patients with COPD and in a Mouse Model. *Sci. Transl. Med.* **3**, 78ra32 (2011).

280. Reddy, N. M. *et al.* Innate Immunity against Bacterial Infection following Hyperoxia Exposure Is Impaired in NRF2-Deficient Mice. *J. Immunol.* **183**, 4601–4608 (2009).

281. Wang, Z. *et al.* Tim-3 inhibits macrophage control of Listeria monocytogenes by inhibiting Nrf2. *Sci. Rep.* **7**, (2017).

282. Williams, M. A. *et al.* Disruption of the Transcription Factor Nrf2 Promotes Pro-Oxidative Dendritic Cells That Stimulate Th2-Like Immunoresponsiveness upon

Activation by Ambient Particulate Matter. *J. Immunol.* **181**, 4545–4559 (2008).

283. Yeang, H. X. A. *et al.* Loss of transcription factor nuclear factor-erythroid 2 (NF-E2) p45-related factor-2 (Nrf2) leads to dysregulation of immune functions, redox homeostasis, and intracellular signaling in dendritic cells. *J. Biol. Chem.* **287**, 10556–10564 (2012).

284. Li, N. *et al.* Nrf2 deficiency in dendritic cells enhances the adjuvant effect of ambient ultrafine particles on allergic sensitization. *J. Innate Immun.* **5**, 543–554 (2013).

285. Rangasamy, T. *et al.* Nuclear erythroid 2 p45-related factor 2 inhibits the maturation of murine dendritic cells by ragweed extract. *Am. J. Respir. Cell Mol. Biol.* **43**, 276–285 (2010).

286. Macoch, M. *et al.* Nrf2-dependent repression of interleukin-12 expression in human dendritic cells exposed to inorganic arsenic. *Free Radic. Biol. Med.* **88**, 381–390 (2015).

287. Wang, J., Liu, P., Xin, S., Wang, Z. & Li, J. Nrf2 suppresses the function of dendritic cells to facilitate the immune escape of glioma cells. *Exp. Cell Res.* **360**, 66–73 (2017).

288. Wei, H. J. *et al.* Nrf2-mediated metabolic reprogramming of tolerogenic dendritic cells is protective against aplastic anemia. *J. Autoimmun.* **94**, 33–44 (2018).

289. Saddawi-Konefka, R. *et al.* Nrf2 Induces IL-17D to Mediate Tumor and Virus Surveillance. *Cell Rep.* **16**, 2348–2358 (2016).

290. Seelige, R. *et al.* Interleukin-17D and Nrf2 mediate initial innate immune cell recruitment and restrict MCMV infection. *Sci. Rep.* **8**, (2018).

291. Boss, A. P. *et al.* The Nrf2 activator tBHQ inhibits the activation of primary murine natural killer cells. *Food Chem. Toxicol.* **121**, 231–236 (2018).

292. Pyaram, K. *et al.* Keap1-Nrf2 System Plays an Important Role in Invariant Natural Killer T Cell Development and Homeostasis. *Cell Rep.* **27**, 699–707 (2019).

293. Bursley, J. K. & Rockwell, C. E. Nrf2-dependent and -independent effects of tBHQ in activated murine B cells. *Food Chem. Toxicol.* (2020) doi:10.1016/j.fct.2020.111595.

294. Lugade, A. A. *et al.* Nrf2 regulates chronic lung inflammation and B-cell responses to nontypeable Haemophilus influenzae. *Am. J. Respir. Cell Mol. Biol.* **45**, 557–565 (2011).

295. Kikuchi, N. *et al.* Nrf2 protects against pulmonary fibrosis by regulating the lung oxidant level and Th1/Th2 balance. *Respir. Res.* **11**, (2010).

296. Rockwell, C. E., Zhang, M., Fields, P. E. & Klaassen, C. D. Th2 skewing by activation of Nrf2 in CD4(+) T cells. *J. Immunol.* **188**, 1630–7 (2012).

297. Chorley, B. N. *et al.* Identification of novel NRF2-regulated genes by ChiP-Seq: Influence on retinoid X receptor alpha. *Nucleic Acids Res.* **40**, 7416–7429 (2012).

298. Noel, S. *et al.* T Lymphocyte-specific Activation of Nrf2 Protects from AKI. *J. Am. Soc. Nephrol.* **26**, (2015).

299. Noel, S., Lee, S. A., Sadasivam, M., Hamad, A. R. A. & Rabb, H. KEAP1 Editing Using CRISPR/Cas9 for Therapeutic NRF2 Activation in Primary Human T Lymphocytes. *J. Immunol.* **200**, 1929–1936 (2018).

300. Zagorski, J. W., Maser, T. P., LIby, K. T. & Rockwell, C. E. Nrf2-dependent and -independent effects of tBHQ, CDDO-Im, and H2O2 in human Jurkat T cells as determined by CRISPR/Cas9 gene editing. *J. Pharmacol. Exp. Ther.* **9**, 259–267 (2017).

301. Turley, A. E., Zagorski, J. W. & Rockwell, C. E. The Nrf2 activator tBHQ inhibits T cell activation of primary human CD4 T cells. *Cytokine* **71**, 289–295 (2015).

302. Klemm, P. *et al.* Nrf2 expression driven by Foxp3 specific deletion of Keap1 results in loss of immune tolerance in mice. *Eur. J. Immunol.* **00**, 1–10 (2019).

303. Marzec, J. M. *et al.* Functional polymorphisms in the transcription factor NRF2 in humans increase the risk of acute lung injury. *FASEB J.* **21**, 2237–2246 (2007).

304. Suzuki, T. *et al.* Regulatory Nexus of Synthesis and Degradation Deciphers Cellular Nrf2 Expression Levels. *Mol. Cell. Biol.* **33**, 2402–2412 (2013).

305. Córdova, E. J., Velázquez-Cruz, R., Centeno, F., Baca, V. & Orozco, L. The NRF2 gene variant, -653G/A, is associated with nephritis in childhood-onset systemic lupus erythematosus. *Lupus* **19**, 1237–1242 (2010).

306. Huppke, P. *et al.* Activating de novo mutations in NFE2L2 encoding NRF2 cause a multisystem disorder. *Nat. Commun.* **8**, (2017).

307. Yoh, K. *et al.* Nrf2-deficient female mice develop lupus-like autoimmune nephritis. *Kidney Int.* **60**, 1343–1353 (2001).

308. Li, J., Stein, T. D. & Johnson, J. A. Genetic dissection of systemic autoimmune disease in Nrf2-deficient mice. *Physiol Genomics* **18**, 261–272 (2004).

309. Ma, Q., Battelli, L. & Hubbs, A. F. Multiorgan Autoimmune Inflammation, Enhanced Lymphoproliferation, and Impaired Homeostasis of Reactive Oxygen Species in Mice Lacking the Antioxidant-Activated Transcription Factor Nrf2. *Am. J. Pathol.* **168**, 1960–1974 (2006).

310. Jiang, T. *et al.* Nrf2 suppresses lupus nephritis through inhibition of oxidative injury and the NF-κB-mediated inflammatory response. *Kidney Int.* **85**, 333–343 (2014).

311. Zhao, M. *et al.* Nuclear Factor Erythroid 2-related Factor 2 Deficiency Exacerbates Lupus Nephritis in B6/lpr mice by Regulating Th17 Cell Function. *Sci. Rep.* **6**, (2016).

312. Yang, L., Fan, X., Cui, T., Dang, E. & Wang, G. Nrf2 Promotes Keratinocyte Proliferation in Psoriasis through Up-Regulation of Keratin 6, Keratin 16, and Keratin 17. *J. Invest. Dermatol.* **137**, 2168–2176 (2017).

313. Ogawa, T. *et al.* Nuclear Factor Erythroid 2-Related Factor 2 (Nrf2) Regulates Epidermal Keratinization under Psoriatic Skin Inflammation. *Am. J. Pathol.* **190**, 577–585 (2020).

314. Johnson, D. A., Amirahmadi, S., Ward, C., Fabry, Z. & Johnson, J. A. The absence of the pro-antioxidant transcription factor Nrf2 exacerbates experimental autoimmune encephalomyelitis. *Toxicol. Sci.* **114**, 237–46 (2010).

315. Hayashi, M. *et al.* Whole-Body In Vivo Monitoring of Inflammatory Diseases Exploiting Human Interleukin 6-Luciferase Transgenic Mice. *Mol. Cell. Biol.* **35**, 3590–3601 (2015).

316. Hubbs, A. F. *et al.* Vacuolar leukoencephalopathy with widespread astrogliosis in mice lacking transcription factor Nrf2. *Am. J. Pathol.* **170**, 2068–2076 (2007).

317. Wheeler, M. A. *et al.* MAFG-driven astrocytes promote CNS inflammation. *Nature* **578**, 593–599 (2020).

318. Morales Pantoja, I. E., Hu, C. L., Perrone-Bizzozero, N. I., Zheng, J. & Bizzozero, O. A. Nrf2-dysregulation correlates with reduced synthesis and low glutathione levels in experimental autoimmune encephalomyelitis. *J. Neurochem.* **139**, 640–650 (2016).

319. Larabee, C. M. *et al.* Loss of Nrf2 exacerbates the visual deficits and optic neuritis elicited by experimental autoimmune encephalomyelitis. *Mol. Vis.* **22**, 1503–1513 (2016).

320. McDougald, D. S., Dine, K. E., Zezulin, A. U., Bennett, J. & Shindler, K. S. SIRT1 and NRF2 gene transfer mediate distinct neuroprotective effects upon retinal ganglion cell survival and function in experimental optic neuritis. *Investig. Ophthalmol. Vis. Sci.* **59**, 1212–1220 (2018).

321. Linker, R. A. *et al.* Fumaric acid esters exert neuroprotective effects in neuroinflammation via activation of the Nrf2 antioxidant pathway. *Brain* **134**, 678–692 (2011).

322. Scannevin, R. H. *et al.* Fumarates promote cytoprotection of central nervous system cells against oxidative stress via the nuclear factor (erythroid-derived 2)-like 2 pathway. *J. Pharmacol. Exp. Ther.* **341**, 274–284 (2012).

323. Hammer, A. *et al.* Role of nuclear factor (Erythroid-derived 2)-like 2 signaling for effects of fumaric acid esters on dendritic cells. *Front. Immunol.* **8**, (2017).

324. Hu, X., Li, L., Yan, S. & Li, Z. Arsenic trioxide suppresses acute graft-versus-host disease by activating the Nrf2/HO-1 pathway in mice. *Br. J. Haematol.* **186**, e145–e148 (2019).

325. Wruck, C. J. *et al.* Role of oxidative stress in rheumatoid arthritis: Insights from the Nrf2-knockout mice. *Ann. Rheum. Dis.* **70**, 844–850 (2011).

326. Wu, W. J. *et al.* S-propargyl-cysteine attenuates inflammatory response in rheumatoid arthritis by modulating the Nrf2-ARE signaling pathway. *Redox Biol.* **10**, 157–167 (2016).

327. Yagishita, Y., Uruno, A., Chartoumpekis, D. V., Kensler, T. W. & Yamamoto, M. Nrf2 represses the onset of type 1 diabetes in non-obese diabetic mice. *J. Endocrinol.* **240**, 403–416 (2019).

328. Dong, W. *et al.* Sodium butyrate activates NRF2 to ameliorate diabetic nephropathy possibly via inhibition of HDAC. *J. Endocrinol.* **232**, 71–83 (2017).

329. Suzuki, T. *et al.* Systemic Activation of NRF2 Alleviates Lethal Autoimmune Inflammation in Scurfy Mice. *Mol. Cell. Biol.* **37**, e00063-17 (2017).

330. Kavian, N. *et al.* The Nrf2-antioxidant response element signaling pathway controls fibrosis and autoimmunity in scleroderma. *Front. Immunol.* **9**, (2018).

331. Liu, Y. *et al.* Nrf2/ARE pathway inhibits inflammatory infiltration by macrophage in rats with autoimmune myositis. *Mol. Immunol.* **105**, 165–172 (2019).

332. Chan, K. & Kan, Y. W. Nrf2 is essential for protection against acute pulmonary injury in mice. *Proc. Natl. Acad. Sci. U. S. A.* **96**, 12731–12736 (1999).

333. Cho, H. Y., Reddy, S. P., DeBiase, A., Yamamoto, M. & Kleeberger, S. R. Gene expression profiling of NRF2-mediated protection against oxidative injury. *Free Radic. Biol. Med.* **38**, 325–343 (2005).

334. Cho, H. Y. *et al.* Nrf2-regulated PPARγ expression is critical to protection against acute lung injury in mice. *Am. J. Respir. Crit. Care Med.* **182**, 170–182 (2010).

335. Reddy, N. M., Potteti, H. R., Mariani, T. J., Biswal, S. & Reddy, S. P. Conditional Deletion of Nrf2 in Airway Epithelium Exacerbates Acute Lung Injury and Impairs the Resolution of Inflammation. *Am. J. Respir. Cell Mol. Biol.* **45**, 1161–1168 (2011).

336. Ishii, Y. *et al.* Transcription Factor Nrf2 Plays a Pivotal Role in Protection against Elastase-Induced Pulmonary Inflammation and Emphysema. *J. Immunol.* **175**, 6968–6975 (2005).

337. Rangasamy, T. *et al.* Disruption of Nrf2 enhances susceptibility to severe airway inflammation and asthma in mice. *J. Exp. Med.* **202**, 47–59 (2005).

338. Chen, J. S. *et al.* Mouse model of membranous nephropathy induced by cationic bovine serum albumin: Antigen dose-response relations and strain differences. *Nephrol. Dial. Transplant.* **19**, 2721–2728 (2004).

339. Sussan, T. E. *et al.* Nrf2 reduces allergic asthma in mice through enhanced airway epithelial cytoprotective function. *Am. J. Physiol. Lung Cell. Mol. Physiol.* **309**, L27–L36 (2015).

340. Shintani, Y. *et al.* Nuclear factor erythroid 2-related factor 2 (Nrf2) regulates airway epithelial barrier integrity. *Allergol. Int.* **64**, S54–S63 (2015).

341. Traver, G. *et al.* Loss of Nrf2 promotes alveolar type 2 cell loss in irradiated, fibrotic lung. *Free Radic. Biol. Med.* **112**, 578–586 (2017).

342. Chang, A. L., Ulrich, A., Suliman, H. B. & Piantadosi, C. A. Redox regulation of mitophagy in the lung during murine Staphylococcus aureus sepsis. *Free Radic. Biol. Med.* **78**, 179–189 (2015).

343. Kong, X. *et al.* Enhancing Nrf2 pathway by disruption of Keap1 in myeloid leukocytes protects against sepsis. *Am. J. Respir. Crit. Care Med.* **184**, 928–938 (2011).

344. Thimmulappa, R. K. *et al.* Nrf2-dependent protection from LPS induced inflammatory response and mortality by CDDO-Imidazolide. *Biochem. Biophys. Res. Commun.* **351**, 883–889 (2006).

345. Thimmulappa, R. K. *et al.* Nrf2 is a critical regulator of the innate immune response and survival during experimental sepsis. *J. Clin. Invest.* **116**, 984–95 (2006).

346. Athale, J. *et al.* Nrf2 promotes alveolar mitochondrial biogenesis and resolution of lung injury in Staphylococcus aureus pneumonia in mice. *Free Radic. Biol. Med.* **53**, 1584–1594 (2012).

347. Gomez, J. C., Dang, H., Martin, J. R. & Doerschuk, C. M. Nrf2 Modulates Host Defense during Streptococcus pneumoniae Pneumonia in Mice. *J. Immunol.* **197**, 2867–79 (2016).

348. Schaedler, S. *et al.* Hepatitis B virus induces expression of antioxidant response element-regulated genes by activation of Nrf2. *J. Biol. Chem.* **285**, 41074–41086 (2010).

349. Ivanov, A. V. *et al.* Hepatitis C virus proteins activate NRF2/ARE pathway by distinct ROS-dependent and independent mechanisms in HUH7 cells. *PLoS One* **6**, e24957 (2011).

350. Sugiyama, K. *et al.* Prominent steatosis with hypermetabolism of the cell line permissive for years of infection with hepatitis C virus. *PLoS One* **9**, e94460 (2014).

351. Murakami, Y. *et al.* Dual effects of the Nrf2 inhibitor for inhibition of hepatitis C virus and hepatic cancer cells. *BMC Cancer* **18**, (2018).

352. Olagnier, D. *et al.* Nrf2 negatively regulates STING indicating a link between antiviral sensing and metabolic reprogramming. *Nat. Commun.* **9**, (2018).

353. Gunderstofte, C. *et al.* Nrf2 Negatively Regulates Type I Interferon Responses and Increases Susceptibility to Herpes Genital Infection in Mice. *Front. Immunol.* **10**, 2101 (2019).

354. Page, A. *et al.* Marburgvirus Hijacks Nrf2-Dependent Pathway by Targeting Nrf2-Negative Regulator Keap1. *Cell Rep.* **6**, 1026–1036 (2014).

355. Cho, H.-Y. *et al.* Antiviral activity of Nrf2 in a murine model of respiratory syncytial virus disease. *Am. J. Respir. Crit. Care Med.* **179**, 138–50 (2009).

356. Ivanciuc, T., Sbrana, E., Casola, A. & Garofalo, R. P. Protective role of nuclear factor erythroid 2-related factor 2 against respiratory syncytial virus and human metapneumovirus infections. *Front. Immunol.* **9**, (2018).

357. Kosmider, B. *et al.* Nrf2 protects human alveolar epithelial cells against injury induced by influenza A virus. *Respir. Res.* **13**, (2012).

358. Huang, H., Falgout, B., Takeda, K., Yamada, K. M. & Dhawan, S. Nrf2-dependent induction of innate host defense via heme oxygenase-1 inhibits Zika virus replication. *Virology* **503**, 1–5 (2017).

359. Olagnier, D. *et al.* Cellular Oxidative Stress Response Controls the Antiviral and Apoptotic Programs in Dengue Virus-Infected Dendritic Cells. *PLoS Pathog.* **10**, e1004566 (2014).

360. Zhang, H. S., Li, H. Y., Zhou, Y., Wu, M. R. & Zhou, H. Sen. Nrf2 is involved in inhibiting Tat-induced HIV-1 long terminal repeat transactivation. *Free Radic. Biol. Med.* **47**, 261–268 (2009).

361. Bai, Z., Zhao, X., Li, C., Sheng, C. & Li, H. EV71 virus reduces Nrf2 activation to promote production of reactive oxygen species in infected cells. *Gut Pathog.* **12**, (2020).

362. Patra, U., Mukhopadhyay, U., Sarkar, R., Mukherjee, A. & Chawla-Sarkar, M. RA-

839, a selective agonist of Nrf2/ARE pathway, exerts potent anti-rotaviral efficacy in vitro. *Antiviral Res.* **161**, 53–62 (2019).

363. Kesic, M. J., Simmons, S. O., Bauer, R. & Jaspers, I. Nrf2 expression modifies influenza A entry and replication in nasal epithelial cells. *Free Radic. Biol. Med.* **51**, 444–453 (2011).

364. Cheng, Y. L. *et al.* Activation of Nrf2 by the dengue virus causes an increase in CLEC5A, which enhances TNF-α production by mononuclear phagocytes. *Sci. Rep.* **6**, (2016).

365. Yageta, Y. *et al.* Role of Nrf2 in Host Defense against Influenza Virus in Cigarette Smoke-Exposed Mice. *J. Virol.* **85**, 4679–4690 (2011).

366. Yageta, Y. *et al.* Carbocisteine reduces virus-induced pulmonary inflammation in mice exposed to cigarette smoke. *Am. J. Respir. Cell Mol. Biol.* **50**, 963–973 (2014).

367. Shahidi, F. Antioxidants in food and food antioxidants. *Mol. Nutr. Food Res.* **44**, 158–163 (2000).

368. FAO/WHO. *49th JECFA Meeting. Evaluation of certain food additives and contaminants.* http://apps.who.int/iris/bitstream/10665/42142/1/WHO_TRS_884.pdf (1999).

369. FAO/WHO. *51st JECFA Meeting. Evaluation of National Assessments of Intake of tert-Butylhydroquinone.* http://www.inchem.org/documents/jecfa/jecmono/v042je26.htm (1999).

370. House, R. Regulatory Guidance in Immunotoxicology. *Encyclopedia of Immunotoxicology* 551–555 (2005) doi:10.1007/978-3-642-54596-2_1248.

371. Zagorski, J. W. *et al.* Differential Effects of the Nrf2 Activators tBHQ and CDDO-Im on the Early Events of T Cell Activation. *Biochem. Pharmacol.* **147**, 67–76 (2018).

372. Zagorski, J. W. *et al.* The Nrf2 activator, tBHQ, differentially affects early events following stimulation of Jurkat cells. *Toxicol. Sci.* **136**, 63–71 (2013).

373. Rolfes, M. *et al.* Estimated Influenza Illnesses, Medical Visits, Hospitalizations, and Deaths Averted by Vaccination in the United States | Seasonal Influenza (Flu) | CDC. https://www.cdc.gov/flu/about/disease/2015-16.htm#table1 (2016).

374. Molinari, N. A. M. *et al.* The annual impact of seasonal influenza in the US: Measuring disease burden and costs. *Vaccine* **25**, 5086–5096 (2007).

375. Lu, P. J., Singleton, J. A., Euler, G. L., Williams, W. W. & Bridges, C. B. Seasonal influenza vaccination coverage among adult populations in the United States,

2005-2011. *Am. J. Epidemiol.* **178**, 1478–1487 (2013).

376. Tian, C., Wang, H., Wang, W. & Luo, X. Characteristics associated with influenza vaccination uptake among adults. *J. Public Health (Bangkok).* 1–7 (2018) doi:10.1093/pubmed/fdy189.

377. Kensler, T. W., Wakabayashi, N. & Biswal, S. Cell survival responses to environmental stresses via the Keap1-Nrf2-ARE pathway. *Annu. Rev. Pharmacol. Toxicol.* **47**, 89–116 (2007).

378. Balish, A. L., Katz, J. M. & Klimov, A. I. Influenza: Propagation, Quantification, and Storage. *Curr. Protoc. Microbiol.* 15G.1.1-15G.1.24 (2013) doi:10.1002/9780471729259.mc15g01s29.

379. Matsuoka, Y., Lamirande, E. W. & Subbaran, K. The mouse model for influenza. *Curr. Protoc. Microbiol.* 1–30 (2009) doi:10.1002/9780471729259.mc15g03s13.

380. Gauger, P. C., Loving, C. L. & Vincent, A. L. Enzyme-Linked Immunosorbent Assay for Detection of Serum or Mucosal Isotype-Specific IgG and IgA Whole-Virus Antibody to Influenza A Virus in Swine. in *Animal Influenza Virus* (ed. Spackman, E.) 303–312 (Springer New York, 2014). doi:10.1007/978-1-4939-0758-8_25.

381. Román, E. *et al.* CD4 effector T cell subsets in the response to influenza: Heterogeneity, migration, and function. *J. Exp. Med.* **196**, 957–968 (2002).

382. Sun, J., Madan, R., Karp, C. L. & Braciale, T. J. Effector T cells control lung inflammation during acute influenza virus infection by producing IL-10. *Nat. Med.* **15**, 277–284 (2009).

383. Seah, S. G. K. *et al.* Unlike CD4+T-cell help, CD28 costimulation is necessary for effective primary CD8+T-cell influenza-specific immunity. *Eur. J. Immunol.* **42**, 1744–1754 (2012).

384. Ikeda, G. J., Sapienza, P. P. & Ross, I. A. Distribution and excretion of radiolabelled tert-butylhydroquinone in Fischer 344 rats. *Food Chem. Toxicol.* **36**, 907–914 (1998).

385. FAO/WHO. *19th JECFA Meeting. Toxicological Evaluation of Some Food Colours, Thickening Agents, and Certain Other Substancse*. http://www.inchem.org/documents/jecfa/jecmono/v08je11.htm (1975).

386. Huang, W., Gu, Y. & Mu, H. Determination of tertiary-butylhydroquinone and its metabolites in rat serum by liquid chromatography-ion trap mass spectrometry. *Lipids* **43**, 281–288 (2008).

387. Segev-Amzaleg, N., Trudler, D. & Frenkel, D. Preconditioning to mild oxidative stress mediates astroglial neuroprotection in an IL-10-dependent manner. *Brain.*

Behav. Immun. **30**, 176–185 (2013).

388. Han, R., Xiao, J., Zhai, H. & Hao, J. Dimethyl fumarate attenuates experimental autoimmune neuritis through the nuclear factor erythroid-derived 2-related factor 2/hemoxygenase-1 pathway by altering the balance of M1/M2 macrophages. *J. Neuroinflammation* **13**, (2016).

389. Motamedi, M., Xu, L. & Elahi, S. Correlation of transferrin receptor (CD71) with Ki67 expression on stimulated human and mouse T cells: The kinetics of expression of T cell activation markers. *J. Immunol. Methods* **437**, 43–52 (2016).

390. Betts, M. R. & Koup, R. A. Detection of T-Cell Degranulation: CD107a and b. in *Methods in Cell Biology* vol. 75 497–512 (2004).

391. Han, J. *et al.* Inhibition of acute graft-versus-host disease with retention of graft-versus-tumor effects by dimethyl fumarate. *Front. Immunol.* **8**, (2017).

392. Zou, Q. *et al.* CD8+Treg cells suppress CD8+T cell-responses by IL-10-dependent mechanism during H5N1 influenza virus infection. *Eur. J. Immunol.* **44**, 103–114 (2014).

393. Dutta, A. *et al.* IL-10 inhibits neuraminidase-activated TGF-β and facilitates Th1 phenotype during early phase of infection. *Nat. Commun.* **6**, 1–11 (2015).

394. Kawaguchi, A. *et al.* Impacts of allergic airway inflammation on lung pathology in a mouse model of influenza A virus infection. *PLoS One* **12**, e0173008 (2017).

395. Estimated Influenza Illnesses, Medical visits, Hospitalizations, and Deaths in the United States — 2017–2018 influenza season | Seasonal Influenza (Flu) | CDC. https://www.cdc.gov/flu/about/burden/estimates.htm (2018).

396. Osterholm, M. T., Kelley, N. S., Sommer, A. & Belongia, E. A. Efficacy and effectiveness of influenza vaccines: A systematic review and meta-analysis. *Lancet Infect. Dis.* **12**, 36–44 (2012).

397. Nüssing, S. *et al.* Innate and adaptive T cells in influenza disease. *Front. Med.* **12**, 34–47 (2018).

398. Davis, C. W. *et al.* Influenza vaccine-induced human bone marrow plasma cells decline within a year after vaccination. *Science (80-.).* (2020) doi:10.1126/science.aaz8432.

399. Sridhar, S. Heterosubtypic T-cell immunity to influenza in humans: Challenges for universal T-cell influenza vaccines. *Front. Immunol.* **7**, 1–12 (2016).

400. Bodewes, R. *et al.* Infection of the upper respiratory tract with seasonal influenza A(H3N2) virus induces protective immunity in ferrets against infection with A(H1N1)pdm09 virus after intranasal, but not intratracheal, inoculation. *J. Virol.*

87, 4293–301 (2013).

401. Ma, Q. Role of nrf2 in oxidative stress and toxicity. *Annu. Rev. Pharmacol. Toxicol.* **53**, 401–26 (2013).

402. Guan, Y. *et al.* NF-E2-Related Factor 2 Suppresses Intestinal Fibrosis by Inhibiting Reactive Oxygen Species-Dependent TGF-β1/SMADs Pathway. *Dig. Dis. Sci.* (2017) doi:10.1007/s10620-017-4710-z.

403. Wu, K. C., Liu, J. J. & Klaassen, C. D. Nrf2 activation prevents cadmium-induced acute liver injury. *Toxicol. Appl. Pharmacol.* **263**, 14–20 (2012).

404. Osburn, W. O. *et al.* Genetic or pharmacologic amplification of nrf2 signaling inhibits acute inflammatory liver injury in mice. *Toxicol. Sci.* **104**, 218–27 (2008).

405. Lu, C. *et al.* Memory regulatory T cells home to the lung and control influenza A virus infection. *Immunol. Cell Biol.* **97**, 774–786 (2019).

406. Wirth, T. C., Martin, M. D., Starbeck-Miller, G., Harty, J. T. & Badovinac, V. P. Secondary CD8+ T-cell responses are controlled by systemic inflammation. *Eur. J. Immunol.* **41**, 1321–1333 (2011).

407. Elbahesh, H., Saletti, G., Gerlach, T. & Rimmelzwaan, G. F. Broadly protective influenza vaccines: design and production platforms. *Curr. Opin. Virol.* **34**, 1–9 (2018).

408. Furuya, A. K. M. *et al.* Sulforaphane Inhibits HIV Infection of Macrophages through Nrf2. *PLOS Pathog.* **12**, e1005581 (2016).

409. Nio, Y. *et al.* Bardoxolone methyl as a novel potent antiviral agent against hepatitis B and C viruses in human hepatocyte cell culture systems. *Antiviral Res.* **169**, 104537 (2019).

410. Bosma, M. J. & Carroll, A. M. The scid mouse mutant: Definition, characterization, and potential uses. *Annu. Rev. Immunol.* **9**, 323–350 (1991).

411. Christianson, S. W. *et al.* Role of natural killer cells on engraftment of human lymphoid cells and on metastasis of human T-lymphoblastoid leukemia cells in C57BL/6J-scid mice and in C57BL/6J-scid bg mice. *Cell. Immunol.* **171**, 186–199 (1996).

412. Nema, S. & Avis, K. Freeze-thaw studies of a model protein, lactate dehydrogenase, in the presence of cryoprotectants. *J. Parenter. Sci. Technol.* **47**, 76–83 (1993).

413. Su, X., Looney, M., Robriquet, L., Fang, X. & Matthay, M. A. Direct visual instillation as a method for efficient delivery of fluid into the distal airspaces of anesthetized mice. *Exp. Lung Res.* **30**, 479–493 (2004).

414. Revelli, D. A., Boylan, J. A. & Gherardini, F. C. A non-invasive intratracheal inoculation method for the study of pulmonary melioidosis. *Front. Cell. Infect. Microbiol.* **2**, (2012).

415. Morales-Nebreda, L. *et al.* Intratracheal administration of influenza virus is superior to intranasal administration as a model of acute lung injury. *J. Virol. Methods* **209**, 116–120 (2014).

416. Rao, G. V. S. *et al.* Efficacy of a technique for exposing the mouse lung to particles aspirated from the pharynx. *J. Toxicol. Environ. Heal. Part A* **66**, 1441–1452 (2003).

417. McGrath-Morrow, S. A. *et al.* Immune response to intrapharyngeal LPS in neonatal and juvenile mice. *Am. J. Respir. Cell Mol. Biol.* **52**, 323–331 (2015).

418. Rothchild, A. C. *et al.* Alveolar macrophages generate a noncanonical NRF2-driven transcriptional response to Mycobacterium tuberculosis in vivo. *Sci. Immunol.* **4**, (2019).

419. Pomatto, L. C. D. & Davies, K. J. A. The role of declining adaptive homeostasis in ageing. *J. Physiol.* **595**, 7275–7309 (2017).

420. Zhang, H., Davies, K. J. A. & Forman, H. J. Oxidative stress response and Nrf2 signaling in aging. *Free Radic. Biol. Med.* **88**, 314–336 (2015).

421. Zhou, L., Zhang, H., Davies, K. J. A. & Forman, H. J. Aging-related decline in the induction of Nrf2-regulated antioxidant genes in human bronchial epithelial cells. *Redox Biol.* **14**, 35–40 (2018).

422. Permar, S. R. *et al.* Increased Thymic Output during Acute Measles Virus Infection. *J. Virol.* **77**, 7872–7879 (2003).

423. Liu, B. *et al.* Severe influenza A(H1N1)pdm09 infection induces thymic atrophy through activating innate CD8+CD44hi T cells by upregulating IFN-gamma. *Cell Death Dis.* **5**, (2014).

424. Kamemura, N., Oyama, K., Kanemaru, K., Yokoigawa, K. & Oyama, Y. Diverse cellular actions of tert-butylhydroquinone, a food additive, on rat thymocytes. *Toxicol. Res. (Camb).* **6**, 922–929 (2017).

425. Boule, L. A., Burke, C. G., Jin, G. B. & Lawrence, B. P. Aryl hydrocarbon receptor signaling modulates antiviral immune responses: Ligand metabolism rather than chemical source is the stronger predictor of outcome. *Sci. Rep.* **8**, (2018).

426. Boulé, L. A. *et al.* Developmental exposure to a mixture of 23 chemicals associated with unconventional oil and gas operations alters the immune system of mice. *Toxicol. Sci.* **163**, 639–654 (2018).

427. Ehrlich, A. K., Pennington, J. M., Bisson, W. H., Kolluri, S. K. & Kerkvliet, N. I. TCDD, FICZ, and other high affinity AhR ligands dose-dependently determine the fate of CD4+T cell differentiation. *Toxicol. Sci.* **161**, 310–320 (2018).

428. Kozul, C. D., Ely, K. H., Enelow, R. I. & Hamilton, J. W. Low-dose arsenic compromises the immune response to influenza A infection in vivo. *Environ. Health Perspect.* **117**, 1441–1447 (2009).

429. Karmaus, P. W. F., Chen, W., Crawford, R., Kaplan, B. L. F. & Kaminski, N. E. δ9-tetrahydrocannabinol impairs the inflammatory response to influenza infection: Role of antigen-presenting cells and the cannabinoid receptors 1 and 2. *Toxicol. Sci.* **131**, 419–433 (2013).

430. Warren, T. K., Mitchell, K. A. & Lawrence, B. P. Exposure to 2,3,7,8-Tetrachlorodibenzo-p-dioxin (TCDD) Suppresses the Humoral and Cell-Mediated Immune Responses to Influenza A Virus without Affecting Cytolytic Activity in the Lung. *Toxicol. Sci.* **56**, 114–123 (2000).

431. B6.Cg-Tg(Cd4-cre)1Cwi/BfluJ. https://www.jax.org/Protocol?stockNumber=022071&protocolID=21365.

432. C57BL/6-Nfe2l2tm1.1Sred/SbisJ. https://www.jax.org/Protocol?stockNumber=025433&protocolID=20272.

433. Xue, P. *et al.* Adipose deficiency of Nrf2 in ob/ob mice results in severe metabolic syndrome. *Diabetes* **62**, 845–854 (2013).

434. Zhang, L., Dasuri, K., Fernandez-Kim, S. O., Bruce-Keller, A. J. & Keller, J. N. Adipose-specific ablation of Nrf2 transiently delayed high-fat diet-induced obesity by altering glucose, lipid and energy metabolism of male mice. *Am. J. Transl. Res.* **8**, 5309–5319 (2016).

435. Taguchi, K., Masui, S., Itoh, T., Miyajima, A. & Yamamoto, M. Nrf2 activation ameliorates hepatotoxicity induced by a heme synthesis inhibitor. *Toxicol. Sci.* **167**, 126–137 (2019).

436. Taniuchi, I. CD4 Helper and CD8 Cytotoxic T Cell Differentiation. *Annu. Rev. Immunol.* **36**, 579–601 (2018).

437. Shi, J. & Petrie, H. T. Activation Kinetics and Off-Target Effects of Thymus-Initiated Cre Transgenes. *PLoS One* **7**, (2012).

438. Mall, M., Grubb, B. R., Harkema, J. R., Neal, W. K. O. & Boucher, R. C. Increased airway epithelial Na+ absorption produces cystic fibrosis-like lung disease in mice. *Nat. Med.* **10**, 487–493 (2004).

439. Kulkarni, R. R., Haeryfar, S. M. & Sharif, S. The invariant NKT cell subset in anti-viral defenses: a dark horse in anti-influenza immunity? *J. Leukoc. Biol.* **88**, 635–

643 (2010).

440. Steed, A. L. *et al.* The Microbial Metabolite Desaminotyrosine Protects from Influenza through Type I Interferon. *Science* **357**, 498–502 (2017).

441. Yu, B. *et al.* Dysbiosis of gut microbiota induced the disorder of helper T cells in influenza virus-infected mice. *Hum. Vaccines Immunother.* **11**, 1140–1146 (2015).

442. Pang, P. *et al.* Alteration of intestinal flora stimulates pulmonary microRNAs to interfere with host antiviral immunity in influenza. *Molecules* **23**, (2018).

443. Tsang, T. K. *et al.* Association Between the Respiratory Microbiome and Susceptibility to Influenza Virus Infection. *Clin. Infect. Dis.* **71**, 1195–1203 (2020).

444. Kaul, D. *et al.* Microbiome disturbance and resilience dynamics of the upper respiratory tract during influenza A virus infection. *Nat. Commun.* **11**, (2020).

445. Mateus, J. *et al.* Selective and cross-reactive SARS-CoV-2 T cell epitopes in unexposed humans. *Science (80-.).* (2020) doi:10.1126/science.abd3871.

446. Kostense, S. *et al.* Interleukin 12 administration enhances Th1 activity but delays recovery from influenza A virus infection in mice. *Antiviral Res.* **38**, 117–130 (1998).

447. Dulek, D. E. & Peebles, R. S. Viruses and asthma. *Biochim. Biophys. Acta - Gen. Subj.* **1810**, 1080–1090 (2011).

448. Wohlleben, G. *et al.* Influenza A Virus Infection Inhibits the Efficient Recruitment of Th2 Cells into the Airways and the Development of Airway Eosinophilia. *J. Immunol. (Baltimore, Md 1950)* **170**, 4601–4611 (2003).

449. Lawrence, C. W. & Braciale, T. J. Activation, Differentiation, and Migration of Naive Virus-Specific CD8+ T Cells during Pulmonary Influenza Virus Infection. *J. Immunol.* **173**, 1209–1218 (2004).

450. Buchweitz, J. P., Harkema, J. R. & Kaminski, N. E. Time-Dependent Airway Epithelial and Inflammatory Cell Responses Induced by Influenza Virus A/PR/8/34 in C57BL/6 Mice. *Toxicol. Pathol.* **35**, 424–435 (2007).

451. Po, J. L. Z., Gardner, E. M., Anaraki, F., Katsikis, P. D. & Murasko, D. M. Age-associated decrease in virus-specific CD8+ T lymphocytes during primary influenza infection. *Mech. Ageing Dev.* **123**, 1167–1181 (2002).

452. Brockmann, L. *et al.* Molecular and functional heterogeneity of IL-10-producing CD4 + T cells. *Nat. Commun.* **9**, (2018).

453. Groux, H. *et al.* A CD4+ T-cell subset inhibits antigen-specific T-cell responses and prevents colitis. *Nature* **389**, 737–742 (1997).

454. Chartoumpekis, D. V *et al.* Hepatic Gene Expression Profiling in Nrf2 Knockout Mice after Long-Term High-Fat Diet-Induced Obesity. **2013**, (2013).

455. Shultz, L. D., Brehm, M. A., Victor Garcia-Martinez, J. & Greiner, D. L. Humanized mice for immune system investigation: progress, promise and challenges. *Nat. Rev. Immunol.* **12**, 786–798 (2012).